WYDZIAŁ GEOINŻYNIERII

Dziedzina nauk inżynieryjno-technicznych

Dyscyplina: inżynieria środowiska, górnictwo i energetyka

mgr inż. Dawid Nosek

Rozprawa doktorska

Wpływ modyfikacji anody na wytwarzanie energii elektrycznej w mikrobiologicznych ogniwach paliwowych

Effect of anode modification on the electricity generation in microbial fuel cell

Praca wykonana w Katedrze Biotechnologii w Ochronie Środowiska

Promotor pracy: prof. dr hab. inż. Agnieszka Cydzik-Kwiatkowska

Katedra Biotechnologii w Ochronie Środowiska

Uniwersytet Warmińsko-Mazurski w Olsztynie

Olsztyn, 2024

1:3482154069

Wykaz artykułów naukowych wchodzących w skład cyklu powiązanych tematycznie artykułów składających się na rozprawę doktorską:

[P1] **Nosek D.**, Jachimowicz P., Cydzik-Kwiatkowska A. (2020). Anode modification as an alternative approach to improve electricity generation in microbial fuel cells. Energies 13(24), 6596. **(MNiSW$_{2020}$ = 140 pkt, IF = 3,004)**

[P2] **Nosek D.**, Cydzik-Kwiatkowska A. (2020). Microbial structure and energy generation in microbial fuel cells powered with waste anaerobic digestate. Energies 13(18), 4712. **(MNiSW$_{2020}$ = 140 pkt, IF = 3,004)**

[P3] **Nosek D.**, Samsel O., Pokój T., Cydzik-Kwiatkowska A. (2023). Waste volatile fatty acids as a good electron donor in microbial fuel cell with iron-modified anode. International Journal of Environmental Science and Technology 20, 13021–13032. **(MNiSW$_{2023}$ = 70 pkt, IF = 3,100)**

[P4] **Nosek D.**, Mikołajczyk T., Cydzik-Kwiatkowska A. (2023). Anode modification with Fe_2O_3 affects the anode microbiome and improves energy generation in microbial fuel cells powered by wastewater. International Journal of Environmental Research and Public Health 20(3), 2580. **(MNiSW$_{2023}$ = 140 pkt, IF = 4,614)**.

[P5] **Nosek D.**, Mikołajczyk T., Cydzik-Kwiatkowska A. (2024). Enhancing microbial fuel cell performance: anode modification with reduced graphene oxide and iron(III) for improved electricity generation. Clean Technology and Environmental Policy. doi.org/10.1007/s10098-024-02820-3. **(MNiSW$_{2023}$ = 100 pkt, IF = 4,300)**.

Sumaryczny Impact Factor opublikowanych wyżej wymienionych publikacji zgodnie z bazą JCR: **18,022**

Sumaryczna liczba punktów MNiSW opublikowanych ww. publikacji: **590.**

Impact Factor i sumaryczna liczba punktów MNiSW zostały obliczone uwzględniając punktację z dnia publikacji.

Pełne teksty wymienionych powyżej prac (wraz z oświadczeniami współautorów publikacji) stanowią załączniki do prezentowanej pracy.

3:8887602329

mgr inż. Dawid Nosek

nr albumu: 1476

dyscyplina: inżynieria środowiska,

górnictwo i energetyka

Katedra Biotechnologii w Ochronie Środowiska

Wydział Geoinżynierii

Olsztyn, dnia 02.09.2024

Przewodniczący Rady Naukowej Dyscypliny

Inżynieria Środowiska, Górnictwo i Energetyka

prof. dr hab. inż. Marcin Dębowski

Uniwersytetu Warmińsko-Mazurskiego w Olsztynie

OŚWIADCZENIE

o samodzielnym napisaniu rozprawy doktorskiej

Świadoma(-y) odpowiedzialności prawnej oświadczam, że rozprawa doktorska pod tytułem „Wpływ modyfikacji anody na wytwarzanie energii elektrycznej w mikrobiologicznych ogniwach paliwowych" została napisana przeze mnie samodzielnie i nie zawiera treści uzyskanych w sposób niezgodny z obowiązującymi przepisami.

Oświadczam również, że przedstawiona rozprawa nie jest i nie była wcześniej podstawą do ubiegania się o nadanie stopnia naukowego doktora. Ponadto oświadczam, że treść rozprawy doktorskiej przedstawionej przez mnie do obrony, zawarta na przekazywanym nośniku elektronicznym, jest identyczna z jej wersją drukowaną.

W związku z powyższym oświadczam, że wyrażam zgodę na poddanie rozprawy doktorskiej procedurze antyplagiatowej.

Dawid Nosek

(podpis kandydata)

4:1377154559

Prof. dr hab. inż. Agnieszka Cydzik-Kwiatkowska   Olsztyn, 02.09.2024

Katedra Biotechnologii w Ochronie Środowiska

Wydział Geoinżynierii

<div align="right">
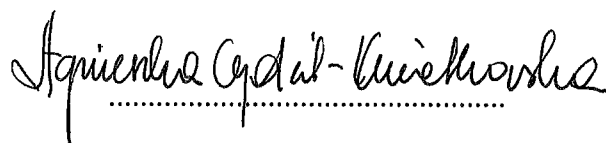
Przewodniczący Rady Naukowej Dyscypliny

Inżynieria Środowiska, Górnictwo i Energetyka

prof. dr hab. inż. Marcin Dębowski

Uniwersytetu Warmińsko-Mazurskiego w Olsztynie

</div>

OŚWIADCZENIE

promotora rozprawy doktorskiej

Oświadczam, że rozprawa doktorska mgr inż. Dawida Noska pod tytułem „Wpływ modyfikacji anody na wytwarzanie energii elektrycznej w mikrobiologicznych ogniwach paliwowych" została przygotowana pod moim kierunkiem i stwierdzam, że spełnia ona warunki do przedstawienia jej w postępowaniu o nadanie stopnia naukowego.

(podpis promotora)

Spis treści

Streszczenie w języku polskim

Zużycie paliw kopalnych w globalnej gospodarce negatywnie wpływa na zasoby naturalne, przyczyniając się do ich zmniejszenia oraz zanieczyszczenia środowiska. W obliczu tych problemów badania nad alternatywnymi źródłami energii nabierają coraz większego znaczenia. Jedną z obiecujących technologii są mikrobiologiczne ogniwa paliwowe (ang. Microbial Fuel Cell, MFC), które wykorzystują mikrobiologiczne procesy konwersji substratów organicznych w energię elektryczną. Wykorzystanie tej technologii w praktyce może nie tylko redukować emisję szkodliwych gazów cieplarnianych, ale także zminimalizować zależność od paliw kopalnych. Czynniki ograniczające pełnoskalowe stosowanie MFC, takie jak niska moc wyjściowa, wysoki opór wewnętrzny czy luki w wiedzy na temat zależności między mikroorganizmami a generowaniem mocy elektrycznej, skłaniają do badań nad rozwojem i doskonaleniem MFC. Celem pracy było określenie wpływu wielkości anody, modyfikacji anody Fe_2O_3 oraz kompozytem zredukowanego tlenku grafenu (ang. reduced graphene oxide, rGO) i Fe na wydajność MFC, skład mikrobiomu anodowego oraz potencjał metaboliczny błony biologicznej.

Początkowo w badaniach testowano wpływ wielkości anody na pracę MFC. Do MFC wprowadzano krótkołańcuchowe kwasy tłuszczowe (KKT) z beztlenowej fermentacji wstępnych osadów ściekowych. W MFC o powierzchni anody 600 cm^2 eksploatowanym przy obciążeniu 69,12 mg ChZT/(g s.m.·d) uzyskano moc ogniwa wynoszącą 15,3 mW/m^2. Zwiększenie powierzchni anody do 1200 cm^2 (obciążenie 36,21 mg ChZT/(g s.m.·d)) nie zwiększyło gęstości mocy, ale poprawiło efektywność usuwania związków organicznych. W błonie biologicznej anody podczas fazy wpracowania MFC licznie występowały *Deftia* sp. i *Methanobacterium* sp. W fazie stabilnej pracy MFC w błonie biologicznej zwiększył się udział egzoelektrogenów z rodzaju *Rhodopseudomonas* sp., co przyczyniło się do bardziej efektywnej i stabilnej produkcji energii elektrycznej. W MFC o większej powierzchni anody w błonie biologicznej licznie występowały *Leucobacter* sp., *Frigoribacterium* sp. i *Phenylobacterium* sp., co skutkowało wysokim i stabilnym usuwaniem ChZT (ponad 85%). W kolejnym etapie badań w MFC zasilanym odpadowymi KKT anodę modyfikowano Fe_2O_3 w dawce 2,5 g/m^2 anody. Modyfikacja spowodowała poprawę transferu elektronów do anody, zwiększając gęstość mocy, gęstość prądu i napięcie, odpowiednio 3,6-krotnie, 1,8-krotnie i 1,4-krotnie w stosunku do MFC z anodą niemodyfikowaną. Dodatek Fe_2O_3 znacząco

wpłynął na mikrobiom błony biologicznej, przyczyniając się do rozwoju *Pseudomonas* sp. i *Geothrix* sp. o wysokim potencjale produkcji energii elektrycznej. To dowodzi, że modyfikacja anody Fe_2O_3 może korzystnie wpływać na skład mikrobiologiczny błony biologicznej na anodzie, co przekłada się na efektywność pracy MFC. Aby zbadać wpływ dawki Fe_2O_3 na wydajność MFC, anodę modyfikowano Fe_2O_3 w dawce 1,25, 2,5, 5 i 10 g/m^2 powierzchni anody. Fe_2O_3 w dawce od 1,25 do 5 g/m^2 poprawiło wytwarzanie energii elektrycznej, przy czym najwyższą gęstość mocy (1,39 mW/m^2) uzyskano w MFC z anodami modyfikowanymi 2,5 oraz 5 g Fe_2O_3/m^2. Moc ogniw z 2,5 oraz 5 g Fe_2O_3/m^2 anody była 2,8 razy wyższa, a rezystancja odpowiednio 5,6 i 4,7 razy niższa niż w reaktorze kontrolnym. Z badań wynika, że dawka 10 g Fe_2O_3/m^2 anody skutkowała dwukrotnym obniżeniem gęstości mocy w stosunku do anody niemodyfikowanej. Usuwanie substancji organicznych ze ścieków było bardziej stabilne w MFC z anodami modyfikowanymi niższymi dawkami Fe_2O_3. Chociaż głównym źródłem węgla w ściekach był octan, wśród KKT w ściekach odprowadzanych z MFC dominowały kwasy propionowy i walerianowy; proporcja kwasu propionowego do innych KKT zwiększała się ze wzrostem dawki Fe_2O_3 wykorzystanej do modyfikacji anody. Modyfikacja anody Fe_2O_3 stymulowała wzrost mikroorganizmów produkujących polimery zewnątrzkomórkowe z rodzajów *Zoogloea* i *Acidovorax*, co sprzyjało tworzeniu błony biologicznej. W mikrobiomach anod modyfikowanych dawkami 1,25 i 2,5 g Fe_2O_3/m^2 dominującymi bakteriami, potencjalnie odpowiedzialnymi za produkcję energii elektrycznej, były *Pseudomonas* sp., *Oscillochloris* sp. i *Rhizobium* sp., natomiast przy 5 i 10 g Fe_2O_3/m^2 – egzoelektrogeny *Dechloromonas* sp. i *Desulfobacter* sp. W ostatnim etapie badań anody modyfikowano jonami Fe(III) (w dawkach 34 i 68 mg na powierzchnię anody, co odpowiada 0,85 i 1,7 g Fe/m^2 anody) oraz rGO (stała dawka: 200 mg na powierzchnię anody). Najwyższą gęstość mocy (8,55 mW/m^2) oraz napięcie (342,7 ± 72,8 mV) osiągnięto w MFC z anodą zmodyfikowaną kompozytem rGO/68 mg Fe. Całkowite opory wewnętrzne i opór przenoszenia ładunku w tym MFC były odpowiednio około 4 i 2 razy niższe niż w kontrolnym MFC. Poziomy pojemności dwuwarstwowej, czyli zdolności do magazynowania ładunku na styku powierzchni elektrolitu i elektrod przewodzących zmodyfikowanych anod, mierzone przy potencjale 900 mV, były do 3,7 razy wyższe (MFC z anodą zmodyfikowaną rGO/68 mg Fe) niż w kontrolnym MFC. Sekwencjonowanie mikrobiomu anodowego i analiza statystyczna wskazały, że udział procentowy *Pseudoxanthomonas* sp. *Themomonas* sp., *Dechloromonas* sp., *Microcystis* sp., *Sphingopyxis* sp. i *Paracoccus* sp. w błonie biologicznej pozytywnie korelował

z wytwarzaniem energii elektrycznej w MFC. Analiza potencjału metabolicznego mikrobiomów anodowych wykazała, że produkcja energii elektrycznej była głównie związana z odwrotnym cyklem kwasu cytrynowego. W MFC z anodą zmodyfikowaną kompozytem rGO/34 mg Fe stwierdzono najwyższy potencjał metaboliczny produkcji i konwersji energii, obrony komórek bakteryjnych przed niekorzystnymi warunkami środowiskowymi (np. stresem oksydacyjnym), replikacji, rekombinacji oraz naprawy DNA.

W badaniach dowiedziono, że modyfikacja anody zarówno związkami żelaza, jak i kompozytem rGO/Fe, pozwala zwiększyć gęstość mocy generowanej przez ogniwo MFC, poprawiając właściwości pojemnościowe elektrody oraz zmniejszając opór wewnętrzny ogniwa. Mikroorganizmy odgrywały kluczową rolę w produkcji energii elektrycznej, a ich skład i potencjał metaboliczny zależały od sposobu modyfikacji anody. Modyfikacja anod kompozytem rGO/Fe zwiększyła potencjał metaboliczny mikrobiomu w zakresie produkcji i konwersji energii, co podkreśla znaczenie inżynierii materiałowej w optymalizacji eksploatacji MFC. Uzyskane wyniki wskazują na możliwość poprawy produkcji energii elektrycznej z odpadów i ścieków w MFC przez modyfikację anod i wnoszą nową wiedzę, która może być wykorzystana do zrównoważonej produkcji energii elektrycznej, promując ekologiczne i efektywne wykorzystanie zasobów naturalnych.

Słowa kluczowe: mikrobiologiczne ogniwa paliwowe, krótkołańcuchowe kwasy tłuszczowe, żelazo, zredukowany tlenek grafenu, zbiorowiska mikrobiologiczne

9:9288028525

Streszczenie w języku angielskim

The use of fossil fuels in the global economy damages natural resources and contributes to their depletion and environmental pollution. In view of these problems, research into alternative energy sources is becoming increasingly important. One of the promising technologies is microbial fuel cells (MFCs), which use microbial processes to convert organic substrates into electrical energy. The practical use of this technology can not only reduce the emission of harmful greenhouse gases, but also reduce dependence on fossil fuels. Factors limiting the large-scale use of MFCs, such as low output power, high internal resistance, or the lack of knowledge about the relationship between microorganisms and electrical energy production, are prompting research into the development and improvement of MFCs. This work aimed to determine the effects of anode size, anode modification Fe_2O_3, reduced graphene oxide (rGO), and rGO-Fe composite on MFC efficiency, anode microbiome composition, and biofilm metabolic potential.

Initially, the study tested the effect of anode size on MFC operation. Volatile fatty acids (VFA) from anaerobic fermentation of primary sewage sludge were introduced into the MFC. In the MFC with an anode surface of 600 cm^2 operated at a load of 69.12 mg COD/(g d.m.·d), a cell power of 15.3 mW/m^2 was obtained. Increasing the anode surface to 1200 cm^2 (load of 36.21 mg COD/(g d.m. ·d)) did not increase the power density, but improved the efficiency of organic compound removal. *Deftia* sp. and *Methanobacterium* sp. were abundant in the anode biofilm during the MFC development phase. In the stable phase of MFC operation, the share of exoelectrogens of the genus *Rhodopseudomonas* sp. increased in the biofilm, contributing to more efficient and stable electricity production. In the MFC with a larger anode surface, *Leucobacter* sp., *Frigoribacterium* sp., and *Phenylobacterium* sp. were abundant in the biofilm, which resulted in high and stable COD removal (over 85%). In the next stage of the study, in the MFC powered by waste VFA, the anode was modified with Fe_2O_3 at a dose of 2.5 g/m^2 of anode. The modification improved electron transfer to the anode, increasing power density, current density, and voltage, respectively, 3.6-fold, 1.8-fold, and 1.4-fold compared to the MFC with an unmodified anode. The addition of Fe_2O_3 significantly affected the microbiome of the biofilm, contributing to the development of *Pseudomonas* sp. and *Geothrix* sp. with high potential for electricity production. This proves that the modification of the Fe_2O_3 anode can have a beneficial effect on the microbiological composition of the biofilm on

the anode, which translates into the efficiency of the MFC. To investigate the effect of the Fe_2O_3 dose on the MFC efficiency, the anode was modified with Fe_2O_3 at a dose of 1.25, 2.5, 5.0, and 10 g/m^2 of the anode surface. Fe_2O_3 at a dose from 1.25 to 5.0 g/m^2 improved the electricity generation, with the highest power density (1.39 mW/m^2) obtained in the MFC with anodes modified with 2.5 and 5.0 g Fe_2O_3/m^2. The power of the cells with 2.5 and 5.0 g Fe_2O_3/m^2 of the anode was 2.8 times higher, and the resistance was 5.6 and 4.7 times lower, respectively, than in the control reactor. The study showed that the dose of 10 g Fe_2O_3/m^2 of the anode resulted in a twofold reduction in power density compared to the unmodified anode. The removal of organic substances from wastewater was more stable in the MFC with anodes modified with lower doses of Fe_2O_3. Although acetate was the main source of carbon in the wastewater, propionic and valeric acids dominated among the VFA in the wastewater discharged from the MFC; the proportion of propionic acid to other VFA increased with the increase in the dose of Fe_2O_3 used for anode modification. Fe_2O_3 anode modification stimulated the growth of microorganisms producing extracellular polymers from the genera *Zoogloea* and *Acidovorax*, which promoted the formation of a biofilm. In the microbiomes of anodes modified with doses of 1.25 and 2.5 g Fe_2O_3/m^2, the dominant bacteria, potentially responsible for electricity production, were *Pseudomonas* sp., *Oscillochloris* sp., and *Rhizobium* sp., while at 5 and 10 g Fe_2O_3/m^2 – the exoelectrogens *Dechloromonas* sp. and *Desulfobacter* sp. In the last stage of the study, the anodes were modified with Fe(III) ions (in doses of 34 and 68 mg per anode surface, corresponding to 0.85 and 1.7 g Fe/m^2 of anode) and rGO (fixed dose: 200 mg per anode surface). The highest power density (8.55 mW/m^2) and voltage (342.7 ± 72.8 mV) were achieved in the MFC with an anode modified with rGO/68 mg Fe composite. Total internal resistances and charge transfer resistance in this MFC were approximately 4 and 2 times lower, respectively, than in the control MFC. The levels of double-layer capacitance, i.e. the ability to store charge at the interface of the electrolyte and conductive electrode surfaces of the modified anodes, measured at a potential of 900 mV, were up to 3.7 times higher (MFC with an anode modified with rGO/68 mg Fe) than in the control MFC. Anodic microbiome sequencing and statistical analysis indicated that the percentage of *Pseudoxanthomonas* sp. *Themomonas* sp., *Dechloromonas* sp., *Microcystis* sp., *Sphingopyxis* sp., and *Paracoccus* sp. in the biofilm positively correlated with electricity production in MFC. Analysis of the metabolic potential of anodic microbiomes showed that electricity production was mainly related to the reverse citric acid cycle. The highest metabolic potential of energy production and conversion, bacterial

cell defense against adverse environmental conditions (e.g. oxidative stress), DNA replication, recombination, and repair was found in MFC with rGO/34 mg Fe composite modified anode.

The study has shown that modifying the anode with both iron compounds and rGO-Fe composite allows an increase in the power density generated by the MFC cell by improving the capacitive properties of the electrode and reducing the internal resistance of the cell. The microorganisms played a key role in power generation, and their composition and metabolic potential depended on the method of anode modification. Modifying the anodes with an rGO-Fe composite increased the metabolic potential of the microbiome in terms of energy production and conversion, highlighting the importance of materials engineering in optimizing the operation of MFCs. The results obtained indicate the possibility of improving power generation from waste and wastewater in MFCs by modifying the anodes and gaining new insights that can be used for sustainable electricity production, promoting ecological and efficient use of natural resources.

Keywords: microbial fuel cells, volatile fatty acids, iron, reduced graphene oxide, microbial communities

Wstęp

Najważniejszym wyzwaniem dla współczesnego świata jest bezpieczeństwo energetyczne i czyste środowisko, które umożliwiają zrównoważony rozwój społeczny i gospodarczy na świecie. Niewystarczające zasoby paliw kopalnych i emisja gazów cieplarnianych inspirują naukowców do badań nad metodami wykorzystania alternatywnych źródeł energii, które nie będą emitować zanieczyszczeń do środowiska (Kober i in. 2020). Ilość wytworzonej mocy elektrycznej z odnawialnych źródeł energii (OZE) w 2023 r. w Polsce wyniosła ponad 4 tys. GWh. Jest to energia pochodząca głównie z małych instalacji OZE wykorzystujących energię słoneczną (73%) i energię wiatrową (12%) (dane na dzień 07.05.2024; Urząd Regulacji Energetyki 2024).

Ze względu na postępującą urbanizację i zwiększającą się produkcję ścieków i odpadów zaczęto postrzegać je jako nośniki energii (Siddiqi i in. 2019), wykorzystywane np. do wytwarzania zawierającego metan biogazu, ale również wodoru czy energii elektrycznej. Wiele z tych procesów jest oparte o metabolizm mikroorganizmów. W ostatnich 20 latach nastąpił szybki rozwój systemów elektrochemicznych, wśród których można wyróżnić mikrobiologiczne ogniwa elektrolityczne do produkcji wodoru oraz mikrobiologiczne ogniwa paliwowe. MFC są to urządzenia, w których metabolizm mikroorganizmów jest wykorzystywany do wytwarzania energii elektrycznej (Logan i in. 2009). W porównaniu z tradycyjnymi źródłami energii (paliwa kopalne), MFC mają wiele zalet. Mogą być wykorzystywane do wytwarzania energii elektrycznej z szerokiej gamy substancji organicznych, w tym odpadów spożywczych, odpadów rolniczych lub ścieków, co może przyczynić się do zmniejszenia ilości materii organicznej w odpadach (Li i in. 2014; Pandey i in. 2016). W przeciwieństwie do innych form fermentacji beztlenowej, które wymagają określonych warunków temperaturowych do wydajnego działania, MFC mogą działać w szerokim zakresie temperatur, w tym zarówno w warunkach mezofilnych, jak i termofilnych (Li i in. 2013). MFC nie wytwarzają znacznych ilości osadu ani gazów cieplarnianych, co czyni je bardziej zrównoważoną i przyjazną dla środowiska opcją wytwarzania energii elektrycznej ze ścieków w porównaniu do wytwarzania energii ze źródeł konwencjonalnych (Kurniawan i in. 2022).

Budowa i zasada działania MFC

Proces konwersji substancji organicznych w elektryczność może być prowadzony w reaktorach MFC o różnej konfiguracji: dwukomorowym MFC lub jednokomorowym MFC. W dwukomorowym MFC występują dwie komory (oddzielone membraną umożliwiającą wymianę protonów): anodowa, w której panują warunki beztlenowe, i katodowa, w której utrzymuje się warunki tlenowe. W jednokomorowym MFC komora beztlenowa jest oddzielona od katody membraną. W tym przypadku brak jest oddzielnej komory katodowej, a sama katoda ma styczność z powietrzem. Oba typy MFC wykorzystują tę samą zasadę działania. Elektrody są połączone obwodem zewnętrznym z przyłożoną zewnętrzną rezystancją. Komorę anodową zaszczepia się osadem czynnym, najczęściej beztlenowym, bądź różnego rodzaju ściekami zawierającymi mikroorganizmy. W ten sposób dochodzi do rozwoju błony biologicznej na anodzie, a w niej bakterii elektroaktywnych. Mikroorganizmy rozkładają materię organiczną do CO_2 oraz H^+, jednocześnie uwalniając elektrony, których końcowym akceptorem jest anoda. Protony migrują przez membranę protonowymienną do komory katodowej. Elektrony są przenoszone obwodem zewnętrznym na katodę, gdzie w wyniku połączenia tlenu i H^+ powstaje woda (Logan i in. 2009).

Ze względu na procesy elektrochemiczne zachodzące na powierzchni elektrod jednym z ważniejszych czynników wpływających na wydajne działanie MFC jest materiał elektrody. Do produkcji anod najczęściej wykorzystuje się materiały węglowe bądź grafitowe, tj. filc węglowy/grafitowy, tkaninę węglową, papier węglowy czy pręty grafitowe. Zaletami tych materiałów jest niski koszt produkcji, dobra przewodność elektryczna i duża powierzchnia czynna, co sprzyja osadzaniu baterii, oraz odporność na korozję i trwałość (Fan i in. 2021). Anody mogą być też wykonane z metali, takich jak nikiel lub platyna, co zwiększa jednak ryzyko korozji.

Transfer elektronów

Podstawową reakcją w MFC jest przenoszenie elektronów z komórek bakteryjnych na anodę. Sprzężenie metabolizmu drobnoustrojów z zewnętrzną stałą powierzchnią prowadzi do zewnątrzkomórkowego transferu elektronów (ang. Extracellular Electron Transfer, EET). Bakterie posiadające zdolność przenoszenia elektronów są uznawane za elektroaktywne. W zależności od mechanizmów przenoszenia ładunku wyróżnia się zazwyczaj dwa rodzaje EET – bezpośredni (ang.

14

Direct Electron Transfer, DET) i pośredni transfer elektronów (ang. Mediated Electron Transfer, MET) (Pankratova i in. 2019). DET występuje, gdy bakterie mają bezpośredni kontakt z elektrodą. Przeniesienie elektronów następuje bezpośrednio na anodę przez białka aktywne, występujące w zewnętrznej błonie komórkowej, takie jak flawoproteiny, białka wielomiedziowe czy cytochromy (Light i in. 2018; Holmes i in. 2008; Carlson i in. 2012). MET jest promowany przez zastosowanie syntetycznych mediatorów chemicznych lub wydzielanych przez mikroorganizmy związków redoks, umożliwiających przeniesienie elektronów z wewnątrzkomórkowych centrów redoks na powierzchnię elektrody (Schröder 2007). Mediatory wydzielane przez określone mikroorganizmy mogą wspierać EET innych gatunków bakterii, zwiększając wydajność przenoszenia ładunku w konsorcjach drobnoustrojów (Rabaey i in. 2004). Zastosowanie sztucznych mediatorów redoks może skutkować cytotoksycznością (Hassan i in. 2017), hamować wzrost elektrogenów i zwiększać koszt eksploatacji MFC (Das i in. 2022). Z tego powodu w ostatnich latach prowadzono szereg badań w celu poprawy przenoszenia ładunku przez modyfikację powierzchni anody, mającą za zadanie zwiększenie powierzchni właściwej do rozwoju błony biologicznej oraz poprawy przewodności i biokompatybilności powierzchni.

Modyfikacja elektrod

Modyfikacje anody mają na celu zwiększenie jej pola powierzchni przez zwiększenie chropowatości, co sprzyja adhezji mikroorganizmów i tworzeniu błony biologicznej, a tym samym poprawia szybkość przenoszenia ładunku i aktywność drobnoustrojów (Barenjee i in. 2022). Typowe modyfikacje elektrod obejmują powlekanie elektrod materiałami przewodzącymi, takimi jak tlenki metali czy polimery, ale również trawienie czy obróbkę powierzchni anod np. kwasami nieorganicznymi (Nosek i in. 2020). Liu i in. (2014) zmodyfikowali anodę przez trawienie tkaniny węglowej w roztworze kwasu mrówkowego o procencie masowym 44% i 88%. Analiza elektrochemiczna dowiodła, że zmodyfikowane anody wykazywały 2,2–2,4 razy wyższy pik prądu utleniania niż anoda niemodyfikowana, co wskazywało na większą aktywność mediatorów redoks oraz szybkość przenoszenia elektronów do anody. Maksymalna gęstość mocy, czyli ilość mocy wytworzona z 1 m^2 anody, była o 38,1% do 43,6% wyższa niż w MFC z elektrodą niemodyfikowaną.

Innym podejściem do poprawy wydajności MFC było tworzenie anod kompozytowych, które polegało na wytworzeniu anody z kilkoma modyfikatorami, poprawiającymi przenoszenie ładunku i zwiększającymi gęstości prądu i gęstości mocy. Yellappa i in. (2021) wykazali, że anoda ze stali nierdzewnej modyfikowana polianiliną i węglem aktywnym (SSM/PANi/AC) zapewniała maksymalną powierzchnię do produkcji energii i zmniejszała straty omowe oraz rezystancję przenoszenia ładunku. Moc wyjściowa i skuteczność usuwania ChZT w MFC z kompozytową anodą wyniosła odpowiednio 322 mW/m^2 i 88% w porównaniu do 169 mW/m^2 oraz 54%, uzyskanych w MFC z anodą z siatki ze stali nierdzewnej. Maksymalna pojemność właściwa elektrody kompozytowej była 2,8 razy wyższa niż w MFC z anodą SSM-PANi. MFC SSM/PANi/AC wykazywało mniejszą rezystancję przeniesienia ładunku (29,9 Ω) niż SSM-PANi (206,8 Ω) i SSM (678 Ω).

Rozwój nanotechnologii umożliwił naukowcom zastosowanie do modyfikacji anody takich materiałów jak grafen. Grafen jest krystaliczną, alotropową odmiana węgla, w której każdy atom węgla jest mocno powiązany z sąsiednimi atomami leżącymi w odległości C-C 0,142 nm przez unikalną chmurę elektronową. W ciągu ostatniej dekady grafen i jego pochodne były stosowane z wysoką wydajnością w inżynierii biomedycznej, medycynie oraz badaniach dotyczących kosmosu i zrównoważonej produkcji energii (Tiwari i in. 2018). Dwuwymiarowa struktura, duża powierzchnia i wysoka przewodność elektryczna grafenu sprawiają, że dobrze przechowuje ładunki elektryczne (Wang i in. 2015). Modyfikacja anody grafenem może skutkować poprawą wydajności ogniw, ponieważ ma on dużą powierzchnię właściwą i wysokie przewodnictwo, co może ułatwiać przenoszenie elektronów z komórek drobnoustrojów na anodę. Zhang i in. (2011) po raz pierwszy zmodyfikowali grafenem anodę z siatki ze stali nierdzewnej w dwukomorowym MFC. Zmodyfikowana elektroda wykazywała wyższą odpowiedź prądową i odwracalną reakcję przenoszenia elektronów w stosunku do elektrody niemodyfikowanej. Maksymalna moc uzyskana w MFC ze zmodyfikowaną anodą była 18 razy wyższa niż w kontroli. Pomimo osiągniętych sukcesów produkcja taniego grafenu o wysokiej jakości na skalę przemysłową pozostaje dużym wyzwaniem. Z tego względu podjęto badania nad tlenkiem grafenu (GO), który można produkować w dużych ilościach przy niższych kosztach. Stosowane w procesie produkcji silne utleniacze powodują występowanie licznych defektów w sieci GO, które skutkują mniejszą przewodnością elektryczną. Dobrym kompromisem pomiędzy tymi dwiema formami węgla jest zredukowany tlenek grafenu (rGO), który wykazuje podobne

właściwości do grafenu przy niższych kosztach produkcji (Tarcan i in. 2020). Mahmoud i in. (2021) wykazali, że w MFC z anodą z pasty węglowej zmodyfikowanej rGO uzyskano 5,8 razy większe napięcie wyjściowe oraz około 20-krotnie wyższą moc ogniwa w porównaniu do kontroli. W innym badaniu modyfikacja papieru węglowego z użyciem rGO poprawiła gęstość mocy ponad 2-krotnie, jednocześnie zwiększając napięcie wyjściowe z 546,2 do 633,4 mV. Dodatkową zaletą było zwiększenie trwałości elektrody po modyfikacji oraz praca MFC przy wysokim napięciu – napięcie w kolejnych cyklach pracy MFC utrzymywało się na poziomie 71,2% pierwotnego napięcia (Ma i in. 2020).

Ze względu na koszty, dostępność oraz właściwości elektryczne dużym zainteresowaniem w modyfikacjach elektrod w MFC cieszą się metale i ich tlenki, w szczególności żelazo. Żelazo jest dobrym modyfikatorem anody, ponieważ ma wysoką przewodność elektryczną. Żelazo jest aktywnym metalem redoks, co oznacza, że może ulegać reakcjom utleniania i redukcji. Ta właściwość sprawia, że jest skutecznym mediatorem między komórkami drobnoustrojów a anodą, zwiększając szybkość przenoszenia elektronów (Huang i in. 2021). Dodatkowo żelazo promuje występowanie bakterii elektroaktywnych w układach MFC (Xu i in. 2017). Wykazano, że użycie żelaza jako mediatora zwiększa moc wyjściową i poprawia stabilność pracy ogniw. Żelazo może również działać jako katalizator reakcji elektrochemicznych na anodzie, zwiększając gęstość prądu i gęstość mocy MFC, a także zmniejszając nadpotencjał, czyli wartość potencjału elektrody wymaganą do przenoszenia elektronów (Zheng i in. 2022; Wang i in. 2022). Dostępność i przystępna cena związków żelaza sprawiają, że jest to praktyczna opcja dla zastosowań technologii MFC na dużą skalę, co czyni z tego obiecującą strategię rozwoju zrównoważonych systemów energetycznych.

Stężenie i rodzaj substratu

Ważnym aspektem wpływającym na wydajność MFC jest rodzaj i stężenie substratu (Prathiba i in. 2022). Do tej pory w MFC wykorzystano wiele różnego rodzaju czystych substratów, tj. kwasów organicznych (kwas octowy, propionowy, masłowy itp.), węglowodanów (glukoza, fruktoza, sacharoza) czy białek (albumina) (Jafary i in. 2013; Chen i in. 2014; Rosales-Sierra i in. 2017; Tariq i in. 2021). W badaniach często wykorzystywano pożywki z octanem, który jako prosty związek chemiczny indukuje wzrost bakterii egzoelektrogennych, a także sprzyja metabolizmowi drobnoustrojów

17:2343110693

nakierowanemu na produkcję bioenergii w MFC. Ponadto octan jest głównym produktem końcowym w wielu szlakach metabolicznych (Aelterman 2009; Sonawane i in. 2022).

You i in. (2021) przetestowali kilka rodzajów ścieków powstających w gospodarstwach domowych jako substraty w MFC – ścieki ze zlewu kuchennego, ze zmywarki, pralki, wanny i toalety (wyłącznie mocz). Najwyższy poziom mocy wynoszący 3,91 ± 0,27 mW uzyskano, gdy użyto moczu. Największą skuteczność usuwania ChZT osiągnięto w MFC zasilanym ściekami ze zlewu kuchennego – 84,6 ± 3,0%. Dla porównania MFC zasilane moczem osiągnęło skuteczność usuwania ChZT na poziomie 39%. Większość materii organicznej w ściekach pochodzących ze zlewu kuchennego została rozłożona przez organizmy inne niż egzoelektrogenne. Wyższa moc osiągnięta w MFC z moczem mogła natomiast wynikać z najwyższej przewodności substratu w porównaniu do innych substratów. Zastosowanie rozcieńczenia moczu wodą z kąpieli lub z kranu, co stanowi realistyczny scenariusz, wykazało, że moc wyjściowa MFC spadała wraz ze wzrostem rozcieńczenia. Co ciekawe, po dodaniu komercyjnego wybielacza w pełnym stężeniu po początkowym spadku mocy ogniwa wydajność powróciła do poprzedniego poziomu w ciągu 48 godzin po zastąpieniu go świeżym moczem. Sugeruje to, że systemy MFC są dość wytrzymałe i mogą być odporne na krótkotrwałe narażenie na chemikalia domowe. W innym badaniu wykorzystano ścieki komunalne z oczyszczalni ścieków w dwukomorowym MFC z anodą z siatki węglowej pokrytej proszkiem grafitowym. Maksymalne napięcie i gęstość mocy wyniosły odpowiednio 595 mV i 205,87 mW/m^2. Stężenie ChZT w ściekach zostało obniżone z 451 do 361 mg/dm^3 (Akçay i Ar 2023). Ścieki z fermy świń zostały wykorzystane w stosie MFC z przepływem ciągłym (kilka reaktorów MFC lub anod połączonych ze sobą równolegle bądź szeregowo). Przy obciążeniu ładunkiem związków organicznych (ŁZO) wynoszącym 4,9 kg ChZT/(m^3·d) i połączeniu równoległym, ogniwo osiągnęło maksymalną gęstość mocy 175,7 W/m^2 przy 0,38 V i 42,8 mA oraz efektywność usuwania ChZT na poziomie 77,1% i azotu amonowego na poziomie 80,7%. Przy ŁZO 1,2 kg ChZT/(m^3·d) MFC generowały stosunkowo mniejszą moc (54,4 W/m^2 przy 0,36 V i 14,3 mA), ale uzyskiwano wyższą efektywność oczyszczania ścieków (83,4% dla ChZT i 90,8% dla NH$_4$-N) (Zhuang i in. 2012).

Idealnym rozwiązaniem pod względem ekonomicznym i środowiskowym jest wykorzystanie w MFC substancji odpadowych, zawierających wysokie stężenia materii organicznej, którą można przekonwertować do energii elektrycznej. KKT są pożądanymi substratami ze względu na ich biodegradowalny charakter, przystępną cenę oraz

18:5538352369

możliwość wykorzystania do produkcji związków o wartości dodanej, takich jak polihydroksyalkaniany (PHA), paliw pochodzenia mikrobiologicznego (wodór, biogaz i energia elektryczna) oraz innych cennych związków (kwas bursztynowy, kwas cytrynowy i butanol) (Sekoai i in. 2021). Badania wskazują również, że odpadowe KKT można skutecznie wykorzystać do produkcji energii elektrycznej oraz że połączenie MFC i fermentacji beztlenowej może zapewnić dobre wyniki produkcji bioenergii, wspierając rozwój gospodarki o obiegu zamkniętym.

Mohanakrishna i in. (2010) wykorzystali ścieki bogate w KKT uzyskane w wyniku ciemnej fermentacji odpadów roślinnych jako substrat w jednokomorowym MFC z katodą powietrzną. Początkowo MFC zasilano ściekami syntetycznymi na bazie glukozy przy ŁZO wynoszącym 0,98 kg ChZT/(m^3·d) przez trzy kolejne cykle karmienia (każdy cykl trwał 96 h). Poprawę wydajności zaobserwowano przy każdym kolejnym karmieniu. Po 264 h zarejestrowano maksymalne napięcie obwodu otwartego wynoszące 288 mV i gęstość prądu 328,57 mA/m^2. Od czwartego cyklu do układu dozowano odpadowe KKT, uzyskując ŁZO 3,13 kg ChZT/(m^3·d). Bezpośrednio po wymianie substratu napięcie obwodu otwartego wyniosło 108 mV, a gęstość prądu 111 mA/m^2. W kolejnych trzech cyklach pracy MFC zaobserwowano poprawę gęstości prądu (do około 220 mA/m^2). Od 7. cyklu karmienia zastosowano niższy ŁZO, wynoszący 1,91 kg ChZT/(m^3·d), i zaobserwowano znaczną poprawę wydajności MFC. Maksymalną wydajność MFC zarejestrowano w 9. cyklu zasilania (296 mV; 317,14 mW/m^2). W kolejnym etapie obniżono ŁZO do 0,93 kg ChZT/(m^3·d). Zaobserwowano zwiększenie napięcia obwodu otwartego i gęstości prądu, które ustabilizowały się w kolejnych dwóch cyklach i wynosiły odpowiednio 308 mV i 362,86 mA/m^2. Gęstość mocy była odwrotnie proporcjonalna do spadku ŁZO w ogniwie, co mogło wynikać z efektywnego transferu elektronów w systemie MFC. Choi i in. (2011) wykorzystali KKT z fermentacji odpadów żywnościowych w dwukomorowym MFC. Produkty fermentacji obejmowały głównie octan, propionian, maślan i walerianian w stosunku 2:1:6:1,5. Przez pierwsze 100 h ogniwo generowało stabilne, niskie napięcie przy użyciu świeżej mieszanki KKT jako paliwa (maksymalna gęstość mocy 15,3 mW/m^2 i napięcie 175 mV). Octan i propionian były szybciej zużywane niż długołańcuchowe KKT. Szybkość degradacji maślanu wzrosła, gdy w komorze anodowej nie było krótkich KKT, co wskazuje, że obecność łatwo degradowalnych związków organicznych o krótkich łańcuchach spowalnia rozkład KKT o dłuższych łańcuchach. Po wyczerpaniu mieszaniny KKT dodano świeży octan i propionian, co spowodowało znaczący wzrost wydajności ogniwa w kolejnym cyklu

19:3724705333

(maksymalna gęstość mocy 240 mW/m^2 i napięcie 533 mV). Po 200 godzinach, gdy jako substraty zastosowano jedynie maślan i walerianian, napięcie stopniowo spadało do 390 mV; spadek ten wskazywał na wolniejszą degradację, a zatem mniejszą sumę elektronów akceptowanych przez elektrodę niż obserwowano w przypadku KKT o krótszych łańcuchach. Po wyczerpaniu wszystkich KKT (około 800 h) dodano świeży octan, uzyskując gęstość mocy około 50 mW/m^2. Dodany octan został usunięty szybciej niż octan z mieszaniny KKT, co sugeruje, że inne KKT hamowały wykorzystanie octanu.

Mikroorganizmy w MFC

Wiele mikroorganizmów może wytwarzać prąd elektryczny i przenosić elektrony na anody w różnych typach układów bioelektrochemicznych. Zazwyczaj są to bakterie redukujące żelazo czy siarkę, zdolne do wytwarzania dużej gęstości mocy w umiarkowanych temperaturach. Zastosowanie odpowiednich pożywek i warunków do wzrostu powoduje, że wiele innych mikroorganizmów, od zwykłych drożdży po ekstremofile, może również generować wysokie gęstości prądu (Logan i in. 2019). Bakterie elektroaktywne występują w naturalnych ekosystemach: w glebie, wodzie, osadach dennych jezior i rzek (Chabert i in. 2015; Lu i in. 2021). W układach elektrochemicznych stosowano różne grupy mikroorganizmów o odmiennych preferencjach środowiskowych i potencjale metabolicznym (Thapa i in. 2022).

Moc elektryczna wytwarzana w MFC zależy w dużym stopniu od rodzaju mikroorganizmów wykorzystanych do zaszczepienia komory anodowej. Wydajność produkcji energii przez mieszane zbiorowiska mikroogranizmów jest znacznie wyższa niż w przypadku czystych kultur (Wang i in. 2021). W takich zbiorowiskach mikroorganizmy mogą współdziałać synergicznie – bakterie niezdolne do transportu elektronów mogą współdziałać z mikroorganizmami egzoelektrogennymi i ułatwiać im wytwarzanie prądu przez usuwanie substancji chemicznych hamujących proces lub wytwarzanie substratów wykorzystywanych przez egzoelektrogeny (Logan i in. 2019).

Fatemi i in. (2012) zbadali wytwarzanie energii elektrycznej w dwukomorowych MFC zasilanych pożywką zawierającą glukozę, w których do zaszczepienia ogniw wykorzystano czystą kulturę *Saccharomyces cerevisiae*, osad beztlenowy z reaktorów zasilanych ściekami mleczarskimi oraz ścieki z oczyszczalni beztlenowej. Najwyższą gęstość mocy uzyskano w MFC zaszczepionym ściekami beztlenowymi, co było spowodowane obecnością bakterii egzoelektrogennych. Bakterie metanogenne oraz

denitryfikacyjne w mieszanych kulturach zużywają substraty organiczne bez wytwarzania prądu. Bakterie egzoelektrogenne występujące w mieszanych kulturach mają większą aktywność elektrochemiczną niż czyste kultury (*S. cerevisiae*), co prowadzi do zwiększenia wytwarzania energii w MFC. Sprawność usuwania ChZT w kulturach mieszanych wynosiła ponad 70%, natomiast w MFC z *S. cerevisiae* – jedynie 54%. Gęstość mocy wytworzona przez kultury mieszane była 2,5–3,0-krotnie wyższa niż w MFC z *S. cerevisiae*. Islam i in. (2020) zbadali wpływ wzajemnych interakcji drobnoustrojów na wytwarzanie energii w MFC zasilanym ściekami z tłoczni oleju palmowego. Spośród różnych inokulów najwyższą gęstość mocy wynoszącą 14,8 W/m^3 osiągnięto w MFC zaszczepionym współhodowlą *Pseudomonas aeruginosa i Klebsiella variicola*. Było to efektem reakcji synergistycznych między oboma gatunkami – *K. variicola* wytwarzał 1,3-propanodiol, który z kolei stymulował wytwarzanie przez *P. aeruginosa* piocyjaniny, która jest mediatorem redox. Uzyskana moc była 3 razy wyższa niż w przypadku czystej kultury *P. aeruginosa*. Wykorzystanie jako inokulum *K. variicola* i *Bacillus cereus* pozytywnie wpłynęło na wytwarzanie energii, skutkując maksymalną gęstością mocy wynoszącą 11,8 W/m^3, podczas gdy antagonistyczne oddziaływania między *B. cereus* i *P. aeruginosa* skutkowały obniżeniem wytwarzania mocy do 1,9 W/m^3. Powiązania synergistyczne między bakteriami zwiększały wytwarzanie energii przez produkcję mediatorów przenoszących elektrony (takich jak 2,5-di-tert-butylo-1,4-benzochinon) i wydajne tworzenie błony biologicznej. Antagonistyczna zależność między mikroorganizmami skutkowała wytwarzaniem metabolitów hamujących wzrost i aktywność komórek, co prowadziło do spadku aktywności metabolicznej mikrobiomu na elektrodach.

Zdolność mikroorganizmów do wytwarzania prądu elektrycznego lub przyjmowania i wykorzystywania elektronów pozostaje fascynującym i szybko rozwijającym się zagadnieniem. Odkrywane są nowe mikroorganizmy o elektroaktywności zewnątrzkomórkowej, a rozważane mechanizmy przenoszenia elektronów poszerzyły się wraz z odkryciem bakterii wytwarzających pilusy (rodzaj fimbrii, czyli wypustek białkowych), które mogą przenosić elektrony wzdłuż włókien białkowych (Logan i in. 2019). Znajomość składu gatunkowego mikrobiomów anodowych oraz powiązanie go z wydajnością ogniw jest bardzo ważnym aspektem działania MFC w celu identyfikacji gatunków, które są bezpośrednio i pośrednio odpowiedzialne za metabolizm substratów i wytwarzanie prądu elektrycznego.

Podsumowując, rozwój technologii MFC ma istotne znaczenie w inżynierii środowiska poprzez opracowanie bardziej efektywnych i zrównoważonych technologii oczyszczania ścieków oraz produkcji energii elektrycznej. Badania nad modyfikacją anody mają na celu poprawę wydajności ogniw w odniesieniu do usuwania zanieczyszczeń i generacji energii elektrycznej oraz zwiększenie stabilności i trwałości pracy MFC. Identyfikacja zbiorowisk zasiedlających anodę pozwala na wyselekcjonowanie gatunków bakterii zdolnych do EET, które można w przyszłości wykorzystać do bioaugumentacji MFC w pełnej skali. Istniejące problemy z przeniesieniem technologii MFC na pełną skalę, dotyczące wysokiego oporu wewnętrznego i niskiej mocy wyjściowej, spowodowały potrzebę modyfikacji materiałów elektrodowych w celu zwiększenia powierzchni do rozwoju błony biologicznej i powstania bardziej biokompatybilnych elektrod, a także zwiększenia liczby miejsc aktywnych elektrochemicznie. Zagadnienie modyfikacji elektrod anodowych, wady i zalety poszczególnych materiałów elektrodowych oraz możliwości ich wykorzystania do przyjaznej dla środowiska produkcji energii elektrycznej w MFC opisano w **P1**, stanowiącej załącznik do dysertacji.

Cel i zakres badań

Celem badań było określenie wpływu modyfikacji anody na produkcję energii elektrycznej i skład mikrobiologiczny błony biologicznej na anodzie w MFC, zasilanym ściekami komunalnymi oraz odpadowymi KKT z fermentacji beztlenowej osadów wstępnych.

Zakres badań obejmował:

1. ocenę wpływu wielkości anody, skutkującej różnym ŁZO, na wytarzanie energii elektrycznej oraz skład gatunkowy mikrobiomu anodowego w MFC (**P2**),
2. wpływ modyfikacji anody Fe_2O_3 na wytwarzanie energii elektrycznej, usuwanie związków organicznych i skład gatunkowy mikrobiomu anodowego w MFC (**P3**, **P4**),
3. wpływ modyfikacji anody rGO i kompozytem rGO/Fe na wytwarzanie energii elektrycznej, usuwanie związków organicznych i skład gatunkowy mikrobiomu anodowego w MFC (**P5**).

Hipotezy badawcze

W badaniach weryfikowano następujące hipotezy badawcze:

H1: wielkość anody wpływa na wytwarzanie energii elektrycznej,

H2: odpadowe KKT mogą być wykorzystane do produkcji energii w MFC;

H3: modyfikacja anody Fe_2O_3 wpływa na moc elektryczną generowaną w MFC oraz efektywność usuwania substancji organicznych i skład gatunkowy mikrobiomu anodowego;

H4: modyfikacja anody rGO i kompozytem rGO-Fe wpływa na moc elektryczną generowaną w MFC oraz efektywność usuwania substancji organicznych i skład gatunkowy mikrobiomu anodowego.

23:2793691509

Metodyka i wyniki badań

Zrównoważona produkcja energii elektrycznej ze źródeł odnawialnych przez mikroorganizmy uznawana jest za atrakcyjną alternatywę dla wytwarzania energii z paliw kopalnych. Ze względu na niską moc wyjściową i dość wysoki opór wewnętrzny ogniw istnieje potrzeba modyfikacji materiałów elektrodowych w celu poprawy wydajności MFC. W pracy pt. „Anode modification as an alternative approach to improve electricity generation in microbial fuel cells" (**P1**), stanowiącej załącznik 1 do dysertacji, dokonano przeglądu literatury dotyczący modyfikacji anod w układach MFC. Przeanalizowano materiały wykorzystywane do tworzenia anod, takie jak metale czy materiały węglowe. Oceniono skuteczność modyfikacji elektrod za pomocą tlenków metali, nanomateriałów węglowych czy polimerów. Z przeglądu literatury wynika, że najbardziej obiecującymi rozwiązaniami w MFC jest modyfikacja anod wysoko przewodzącymi nanomateriałami węglowymi z polimerami (np. polidopamina czy polianilina) oraz materiałami węglopochodnymi (np. GO czy nanorurki węglowe). Takie modyfikacje zwiększyły hydrofilowość i powierzchnię właściwą anod, co wpłynęło na wyższą produkcję energii elektrycznej. Wykazano, że takie modyfikacje anod wpływają na skład zbiorowiska bakterii egzoelektrogennych w błonie biologicznej anody, a bakterie redukujące siarkę uważane są za mikroorganizmy w największym stopniu odpowiedzialne za wydajną produkcję energii elektrycznej. W oparciu o przegląd literaturowy w poszczególnych etapach badań w pracy doktorskiej przeanalizowano możliwość modyfikacji anod. W pierwszym etapie zastosowano modyfikację polegającą na zwiększeniu powierzchni anody i wykorzystaniu odpadowych KKT, a w drugim etapie wykorzystano łatwo dostępny Fe_2O_3 w różnych dawkach i przy różnej konfiguracji reaktora MFC, poddając ocenie efektywność usuwania zanieczyszczeń, wydajność wytwarzania energii oraz analizując skład mikrobiomu anodowego. W trzecim etapie przeprowadzono badania, w których anody MFC modyfikowano z wykorzystaniem rGO oraz kompozytu rGO/Fe w celu określenia wydajności wytwarzania energii, usuwania zanieczyszczeń oraz zbadania składu mikrobiomów anodowych.

I etap badań

Badania przeprowadzono w dwukomorowym MFC z membraną protonowymienną (PEM) o powierzchni 8,5 cm^2. Anodę i katodę wykonano z filcu grafitowego (GF; we wszystkich kolejnych etapach elektrody były wykonane z tego

materiału), natomiast obwód zewnętrzny łączący anodę i katodę wykonano z drutu miedzianego połączonego opornikiem 1 kΩ. Komorę zaszczepiono tlenowym osadem granulowanym z oczyszczalni ścieków w Lubawie. Jako substrat wykorzystano mieszaninę KKT z fermentacji beztlenowej osadów wstępnych z oczyszczalni ścieków „Łyna" w Olsztynie. Badanie prowadzono w dwóch MFC o tej samej konfiguracji, różniących się wielkością anody. W MFC1 całkowita powierzchnia anody wynosiła 600 cm^2, natomiast w MFC2 – 1200 cm^2. Obciążenie komory anodowej ładunkiem zanieczyszczeń w obu reaktorach wynosiło 700 mg ChZT/(dm^3·d), co odpowiadało 69,12 i 36,21 mg ChZT/(g s.m.·d), odpowiednio w MFC1 i MFC2. W odpływie z komór anodowych oznaczano stężenia ChZT, KKT oraz pH. Wykonano badanie polaryzacji anod w celu wykreślenia krzywych gęstości mocy i krzywych polaryzacji oraz przeanalizowano strukturę mikrobiomu anodowego z wykorzystaniem wysokosprawnego sekwencjonowania (gen 16S rDNA, platforma MiSeq Illumina). Zarówno w tym, jak i kolejnych etapach badań, wyniki zostały przeanalizowane statystycznie (pakiet Statistica 13.3, StatSoft), przy założeniu $p < 0.05$. Wyniki eksperymentu przedstawiono w artykule naukowym pt. „Microbial structure and energy generation in microbial fuel cells powered with waste anaerobic digestate" (**P2**), stanowiącym załącznik 2 do dysertacji.

W badaniach wykazano, że pomimo większej powierzchni anody w MFC2 nie uzyskano bardziej efektywnej generacji energii. Początkowo napięcia w MFC2 były wyższe niż w MFC1, ale po osiągnięciu plateau były na podobnym poziomie (około 30 mV). Gęstość prądu po ustabilizowaniu napięcia była około 2,6 razy wyższa w MFC1 niż w MFC2. Najwyższą moc uzyskano w MFC1 (15,2 mW/m^2) przy gęstości prądu 0,54 mA/m^2 i oporze zewnętrznym 10 kΩ. Podczas normalnej pracy ogniwo działało przy niższym oporze zewnętrznym 1 kΩ, a gęstość mocy wynosiła 3,5 mW/m^2. Oba MFC charakteryzowały się wysokimi oporami wewnętrznymi, które wynosiły 10,72 kΩ w MFC1 i 9,12 kΩ w MFC2. Wysoki opór wewnętrzny mógł być spowodowany konfiguracją MFC, tj. stosunkowo małą powierzchnią membrany w stosunku do objętości reaktora, co ograniczało przepływ protonów, oraz długim dystansem między anodą a katodą. Istotnym problemem eksploatacyjnym było zarastanie membrany PEM błoną biologiczną, co mogło wpływać na niższą wydajność produkcji energii w MFC ze względu na zmniejszony transport protonów. Niższy ŁZO w MFC2, pomimo niższej produkcji energii, przyczynił się do bardziej wydajnego i stabilnego usuwania związków

25:1117645841

organicznych. Sprawność usuwania ChZT w czasie stabilnej pracy ogniwa wyniosła 85% i była istotnie wyższa niż w MFC1.

Analiza danych sekwencjonowania genu 16S rDNA mikrobiomów błony biologicznej z obu reaktorów pokazała, że skład gatunkowy na anodach w MFC zmieniał się w czasie, co znacząco wpływało na efektywność degradacji substancji organicznych. Większość mikroorganizmów obecnych w badanych MFC należała do rodzajów *Rhodopseudomonas*, *Acidovorax*, *Acinetobacter*, *Clostridium*, *Methanobacterium* i *Leucobacter*. W błonie biologicznej anody podczas fazy wpracowania MFC licznie występowały *Deftia* sp., *Methanobacterium* sp. i *Rhodopseudomonas* sp. Wyższy ŁZO w MFC1 przyczynił się do wytworzenia stabilnego zbiorowiska mikroorganizmów zdominowanego przez *Rhodopseudomonas* sp., który mógł odgrywać kluczową rolę w generacji energii. Przy niższym ŁZO w MFC2 wzrosła liczebność mikroorganizmów z rodzajów *Leucobacter*, *Frigoribacterium* i *Phenylobacterium*, co z kolei skutkowało wydajnym rozkładem substancji organicznych. Niezależnie od wielkości anody *Clostridium* sp. i egzoelektrogeny należące do rodzajów *Desulfobulbus* i *Acinetobacter* występowały licznie w obu MFC zasilanych odpadowymi KKT.

Badania wskazują, że zwiększenie powierzchni anody, mimo że wspiera rozwój mikroorganizmów i stabilny rozkład złożonych substancji organicznych, nie przekłada się na wyższą generację energii elektrycznej. Duże powierzchnie anodowe mogą powodować znaczne rozproszenie elektronów, z których część jest wykorzystywana w innych procesach metabolicznych, co prowadzi do większych strat elektronów. Kluczowe dla zwiększenia efektywności i stabilności produkcji energii elektrycznej w MFC mogą być optymalizacja składu mikroorganizmów oraz kontrola obciążenia układu ładunkiem związków organicznych.

II etap badań

W II. etapie badań anody modyfikowano Fe_2O_3. Początkowo do zasilania MFC wykorzystano KKT, a anodę modyfikowano 2,5 g Fe_2O_3/m^2 (**P3**). Następnie wykorzystano ścieki syntetyczne o składzie zbliżonym do ścieków komunalnych, a anody modyfikowano Fe_2O_3 w dawkach: 1,25, 2,5, 5, 10 g Fe_2O_3/m^2 anody (**P4**).

W **P3** badania przeprowadzono w reaktorach o tej samej geometrii co w I etapie, przy czym powierzchnia anody i katody wynosiła 200 cm^2, a opór zewnętrzny – 4,7 kΩ. W eksperymencie wykorzystano odpadowe KKT z oczyszczalni ścieków „Łyna"

w Olsztynie, które rozcieńczano do stężenia 400 mg ChZT/dm^3. Modyfikacja anody polegała na zanurzeniu elektrody anodowej w zawiesinie 0,05 g Fe$_2$O$_3$ w 100 cm^3 wody destylowanej, autoklawowaniu anody przez 1 h i suszeniu w 80°C. Reaktor ze zmodyfikowaną anodą oznaczono jako MFC$_{Fe}$. Fragment zmodyfikowanej anody poddano analizie SEM/EDS w celu identyfikacji Fe na anodzie. Reaktor z anodą niemodyfikowaną stanowił MFC kontrolny. W odpływie z obu MFC analizowano stężenia ChZT, KKT, NH$_4$-N oraz pH. Dodatkowym aspektem pracy była analiza chromatograficzna odpływu z MFC pod kątem składu KKT. Wyznaczono krzywe gęstości mocy i krzywe polaryzacji. Woltamperometrię cykliczną (ang. cyclic voltammetry, CV) przeprowadzono w układzie trójelektrodowym z anodą jako elektrodą pracującą. Na koniec eksperymentu pobrano próbki biomasy celem zidentyfikowania gatunków bakterii dominujących w mikrobiomie anodowym. Próbki błony biologicznej anod analizowano tak jak w etapie I.

Analiza SEM/EDS wykazała, że Fe$_2$O$_3$ został zdeponowany na anodzie z efektywnością osadzania na poziomie 99,1%. Napięcia zarejestrowane w MFC$_{Fe}$ były istotnie statystycznie wyższe niż w MFC kontrolnym, a obecność Fe(III) na anodzie nie tylko poprawiła wytwarzanie energii elektrycznej, ale także spowodowała bardziej stabilne wytwarzanie napięcia. W MFC kontrolnym moc maksymalna, wyznaczona z krzywych gęstości, była prawie 4-krotnie mniejsza od mocy uzyskanej w MFC$_{Fe}$. Modyfikacja spowodowała poprawę transferu elektronów do anody, zwiększając gęstość mocy, gęstość prądu i napięcie odpowiednio 3,6-krotnie, 1,8-krotnie i 1,4-krotnie w stosunku do MFC z anodą niemodyfikowaną. W okresie stabilnej pracy MFC skuteczność usuwania ChZT wyniosła 54,3 ± 9,8% i 48,8 ± 9,5%, odpowiednio dla MFC kontrolnego i MFC$_{Fe}$, i nie różniła się istotnie statystycznie między reaktorami. Stężenia NH$_4$-N w odpływie z MFC$_{Fe}$ były istotnie niższe niż w kontroli MFC, wykazując pozytywny wpływ obecności Fe(III) na metabolizm azotu amonowego. Skuteczność usuwania KKT kształtowała się na poziomie 60,4 ± 16,9% i 50,2 ± 26,3% odpowiednio w MFC kontrolnym i MFC$_{Fe}$. Analiza chromatograficzna wykazała, że w substracie dodawanym do MFC dominowały kwasy propionowy, enantowy i izokapronowy (odpowiednio 60%, 15% i 13% wszystkich KKT), natomiast KKT z odpływu składały się głównie z kwasu propionowego (71%) i walerianowego (17%).

Modyfikacja anody Fe$_2$O$_3$ zmniejszyła różnorodność mikrobiomu anodowego o ponad 20% w porównaniu z kontrolą. Obecność Fe(III) w dawce 2,5 g Fe$_2$O$_3$/m^2 anody pozytywnie wpłynęła na liczebność Burkholderiales i Pseudomonadales w mikrobiomie,

która była około 2-krotnie wyższa w MFC_{Fe} niż w MFC kontrolnym, natomiast 10-krotnie i 5-krotnie obniżyła udział procentowy bakterii z rzędu Rhodocyclales i Clostridiales w błonie biologicznej. Osadzenie Fe(III) na anodzie skutkowało zwiększeniem udziału w mikrobiomie elektrogenów *Pseudomonas* sp. i *Geothrix* sp. oraz bakterii biorących udział w degradacji KKT, takich jak *Acidovorax* sp., *Brevundimonas* sp. i *Leucobacter* sp., w porównaniu do MFC kontrolnego.

W kolejnym badaniu (**P4**) analizowano wpływ dawki Fe_2O_3 osadzonego na anodzie na wytwarzanie energii elektrycznej, usuwanie związków organicznych oraz zbiorowisko mikroorganizmów. Eksperyment został przeprowadzony w dwukomorowym MFC wykonanym z pleksiglasu o objętości komór anodowej i katodowej 2 dm^3. Jako separator między komorami zastosowano PEM o wymiarach 8 × 8 cm. W badaniu zastosowano reaktor z większą powierzchnią membrany, by zwiększyć pole przepływu protonów. Anody wykonano z filcu węglowego (10 cm × 20 cm × 0,3 cm) połączonego z drutem ze stali nierdzewnej, jak w poprzednich etapach. Jako kontrolę zastosowano MFC z niezmodyfikowaną anodą. W pozostałych MFC na anodzie osadzono Fe_2O_3 w dawkach 0,05 g ($MFC_{0,05Fe}$; 1,25 g Fe_2O_3/m^2), 0,1 g ($MFC_{0,1Fe}$; 2,5 g Fe_2O_3/m^2), 0,2 g ($MFC_{0,2Fe}$, 5 g Fe_2O_3/m^2) i 0,4 g ($MFC_{0,4Fe}$, 10 g Fe_2O_3/m^2). Fe_2O_3 osadzono na elektrodach w ten sam sposób jak w **P3**. Jako anolit zastosowano pożywkę syntetyczną zbliżoną składem do ścieków komunalnych z octanem sodu jako źródłem węgla organicznego (400 mg $ChZT/dm^3$). Zawartość komór anodowych stale mieszano na mieszadle magnetycznym. Analiza odcieków obejmowała stężenia ChZT, NH_4-N i KKT. Odcieki poddano także analizie chromatograficznej w celu identyfikacji i określenia zawartości poszczególnych KKT. Przeprowadzono również analizy elektrochemiczne, obejmujące wyznaczenie krzywych polaryzacji i mocy, oraz woltamperometrię cykliczną, wykonaną za pomocą potencjostatu (Gammry Instrument Interface 1010E) w układzie trójelektrodowym. Próbki błony biologicznej poddano wysokosprawnemu sekwencjonowaniu.

Analiza SEM/EDX powierzchni zmodyfikowanych elektrod pokazała, że udziały masowe Fe na elektrodach anodowych wynosiły 5,5%, 6,9%, 10,7% i 14,2% odpowiednio dla dawek Fe_2O_3 0,05, 0,1, 0,2 i 0,4 g. Osadzanie Fe_2O_3 zwiększyło chropowatość powierzchni elektrod, a tym samym ich powierzchnię właściwą.

Fe_2O_3 w dawce od 1,25 do 5 g/m^2 poprawił wytwarzanie energii elektrycznej, przy czym najwyższą gęstość mocy (1,39 mW/m^2) uzyskano w MFC z dawkami 2,5 oraz 5 g Fe_2O_3/m^2 anody. Moc ogniw z 2,5 oraz 5 g Fe_2O_3/m^2 anody była 2,8 razy wyższa,

a rezystancja odpowiednio 5,6 i 4,7 razy niższa niż w kontroli. Z badań wynika, że dawka 10 g Fe_2O_3/m^2 anody skutkowała dwukrotnym obniżeniem gęstości mocy w stosunku do anody niemodyfikowanej. Krzywe polaryzacji wykazały, że modyfikacja anody Fe_2O_3 zmniejsza rezystancję wewnętrzną ogniwa najprawdopodobniej przez lepszy transfer elektronów ze względu na obecność cząstek Fe. Największą rezystancję wewnętrzną, wynoszącą 1029 Ω, zanotowano w MFC kontrolnym, natomiast najniższą rezystancję wewnętrzną (184,9 Ω) w MFC z 2,5 g Fe_2O_3/m^2 anody. Cykliczna woltamperometria pokazała zwiększoną gęstość prądu na elektrodach z błoną biologiczną wraz ze wzrostem ilości osadzonego Fe_2O_3. Profil CV elektrod z 5 i 10 g Fe_2O_3/m^2 wykazywał dwa szerokie odwracalne piki związane z procesem utleniania i redukcji Fe. Obszary pod krzywymi CV dla tych anod były większe niż dla pozostałych anod, co mogło wskazywać na większą pojemność w stosunku do ładunku elektrycznego.

Średnia efektywność usuwania ChZT we wszystkich reaktorach wyniosła ponad 70%, co wskazuje, że beztlenowa błona biologiczna na anodzie była dobrze rozwinięta i aktywna. Niższe dawki Fe_2O_3 sprzyjały bardziej stabilnemu i skutecznemu usuwaniu ChZT w porównaniu z MFC kontrolnym. W MFC z 1,25 i 2,5 g Fe_2O_3/m^2 anody ChZT został usunięty z efektywnością odpowiednio 83,96 ± 10,1% i 85,5 ± 14%. Średnie stężenia ChZT w ściekach oczyszczonych z tych ogniw wynosiły odpowiednio 29,5 ± 14,9 i 30,8 ± 7,6 mg $ChZT/dm^3$ i były istotnie niższe niż w pozostałych MFC. Skuteczność usuwania NH_4-N we wszystkich MFC wyniosła około 37%, a stężenia NH_4-N w ściekach oczyszczonych nie różniły się istotnie. Analiza chromatograficzna ścieków doprowadzonych i odpływu pokazała, że kwas octowy stanowił największą część KKT w substracie (86%), podczas gdy pozostałe 14% stanowiły inne kwasy, głównie kwas propionowy (7%). W odpływie z MFC kontrolnego kwas propionowy i walerianowy stanowiły odpowiednio 58% i 23% KKT, natomiast kwas heksanowy i izoheksanowy łącznie 12%. W miarę zwiększania dawki Fe_2O_3 użytej do modyfikacji zwiększał się udział kwasu propionowego, natomiast zmniejszał się udział kwasu walerianowego, kapronowego i izokapronowego. W ściekach oczyszczonych kwas octowy występował w odpływie w niewielkich ilościach (od 0,2% w $MFC_{0.1Fe}$ do 3,0% wszystkich wykrytych KKT w MFC kontrolnym).

W trakcie eksperymentu w mikrobiomach poszczególnych MFC dominowały Proteobacteria. Drugą najliczniejszą grupą były Bacteroidetes (do 11% w MFC z 1,25 g Fe_2O_3/m^2). Wysoki odsetek niesklasyfikowanych bakterii (do 44% w MFC z 1,25 g Fe_2O_3/m^2) wskazywał, że wiele jeszcze niezidentyfikowanych bakterii odgrywało

ważną rolę w produkcji energii w MFC. Modyfikacja anody Fe_2O_3 stymulowała wzrost mikroorganizmów produkujących polimery zewnątrzkomórkowe z rodzajów *Zoogloea* i *Acidovorax*, co sprzyjało tworzeniu błony biologicznej. W mikrobiomach anod modyfikowanych dawkami 1,25 i 2,5 g Fe_2O_3/m^2 dominującymi bakteriami potencjalnie odpowiedzialnymi za produkcję energii elektrycznej były *Pseudomonas* sp., *Oscillochloris* sp. i *Rhizobium* sp., natomiast przy 5 i 10 g Fe_2O_3/m^2 – elektrogeny *Dechloromonas* sp. i *Desulfobacter* sp. Obserwowane zmiany składu gatunkowego egzoelektrogenów wskazują na złożone interakcje pomiędzy modyfikacją elektrod i ekologią mikroorganizmów a procesami metabolicznymi w MFC.

Wyniki wskazują, że obecność Fe(III) na anodzie zwiększa produkcję energii elektrycznej o około 280–360% przez szybszy transfer elektronów i zmniejszenie oporu wewnętrznego oraz może zwiększać właściwości pojemnościowe elektrody. Niższe dawki Fe_2O_3 skutkują stabilnym usuwaniem ChZT z efektywnością powyżej 80%. Osadzenie Fe(III) na anodzie może zmniejszać zróżnicowanie gatunkowe mikrobiomów anodowych, powodując jednocześnie wzrost w błonie biologicznej mikroorganizmów zdolnych do produkcji energii elektrycznej z rodzajów *Oscillochloris, Pseudomonas, Dechloromonas* czy *Desulfobacter*.

III etap badań

Ostatni etap badań polegał na analizie wpływu modyfikacji anody rGO w stałej dawce (200 mg) oraz kompozytem rGO/Fe w dwóch dawkach Fe – 34 i 68 mg Fe (0,85 i 1,7 g/m^2 anody) na powierzchnię anody (**P5**). Eksperyment przeprowadzono w reaktorach o konfiguracji jak w etapie II (**P4**), stosując jako źródło węgla ścieki syntetyczne z octanem sodu, przy czym stężenie ChZT wynosiło 180 mg/dm^3. GF modyfikowano galwanicznie w atmosferze argonu. Proces obejmował 15 cykli woltamperometrii w zakresie od –1,5 do 0,8 V względem elektrody Ag/AgCl (3 M) z szybkością skanowania 50 mV/s. Jako elektrodę roboczą zastosowano GF, natomiast jako przeciwelektrodę wykorzystano platynowaną siatkę tytanową (10 cm × 15 cm, Goodfellow, Wielka Brytania). Następnie przeprowadzono elektrochemiczne osadzanie Fe na rGO/GF przy użyciu kąpieli elektrolitycznej zawierającej następujące składniki: 240 g $FeSO_4 \cdot 7H_2O/dm^3$ (czystość 99%, Sigma-Aldrich) oraz 40 g NaCl/dm^3 ($\geq$ 99,5%, Sigma-Aldrich). Osadzanie prowadzono przy katodowej gęstości prądu 1 mA/cm^2 w temperaturze pokojowej przez 2 i 4 minuty, co dało osadzenie Fe odpowiednio około 34 mg ($rGO-Fe_{34}$) i 68 mg ($rGO-Fe_{68}$).

W trakcie eksperymentu przeprowadzono analizę elektrochemiczną obejmującą wyznaczenie krzywych polaryzacji i mocy, wolamperometrię cykliczną oraz dodatkowo elektrochemiczną spektroskopię impedancyjną (ang. Electrochemical Impedance Spectroscopy, EIS). Aby scharakteryzować powierzchnię czystego GF po sonikacji w łaźni ultradźwiękowej oraz GF modyfikowanych rGO i rGO-Fe, zastosowano skaningowy mikroskop elektronowy Quanta FEG 250 (SEM/EDX, Quanta FEG 250, FEI). Do identyfikacji rGO na elektrodzie zastosowano spektrometr w podczerwieni z transformacją Fouriera IRSpirit-T (Shimadzu) wyposażony w kryształ diamentu z osłabionym całkowitym odbiciem (ATR-FTIR).

Analogicznie do poprzednich etapów przeprowadzono analizę składu mikrobiomów błony biologicznej na każdej z testowanych anod oraz analizę statystyczną wyników. Dodatkowym aspektem tego etapu była analiza potencjału metabolicznego mikrobiomów. Do określenia potencjału metabolicznego mikrobiomów wykorzystano bazę danych KEGG oraz Cluster of Orthologous Groups (COG) w programie PICRUSt.

Średnie efektywności usuwania ChZT w MFC wynosiły od $49,9 \pm 16,5\%$ do $65,6 \pm 5,4\%$; nie obserwowano istotnych różnic między reaktorami. Średnie stężenie azotu amonowego w ściekach surowych wynosiło $25,3 \pm 2,3$ mg/dm^3. Skuteczność usuwania NH_4-N była podobna we wszystkich reaktorach (61–65%). Stężenia azotu azotanowego(V) w ściekach oczyszczonych nie różniły się między reaktorami i wynosiły średnio $1,8 \pm 1,2$; $3,4 \pm 1,1$; $1,4 \pm 1,5$ i $2,01 \pm 1,2$ mg/dm^3 odpowiednio w MFC kontrolnym, MFC-rGO, MFC-rGO-Fe$_{34}$ i MFC-rGO-Fe$_{68}$. Najwyższe stężenie azotu azotanowego(III) uzyskano w odpływie z MFC-rGO-Fe$_{34}$ ($2,04 \pm 2,09$ mg/dm^3).

Najwyższe napięcia uzyskano w MFC-rGO-Fe$_{68}$ – w stabilnej fazie cyklu (od 17. do 105. godziny) wynosiły średnio $342,7 \pm 72,8$ mV i były istotnie wyższe niż w pozostałych MFC. Największą moc ogniwa, wynoszącą $8,55$ mW/m^2, uzyskano w MFC-rGO-Fe$_{68}$ przy gęstości prądu $46,25$ mA/m^2. Gęstość mocy ogniwa MFC-rGO-Fe$_{68}$ była 42,2-, 3,0- i 7,9-krotnie wyższa niż w przypadku odpowiednio MFC kontrolnego, MFC-rGO i MFC-rGO-Fe$_{34}$. Modyfikowanie anod za pomocą rGO i Fe zmniejszyło rezystancję wewnętrzną, która wynosiła 540 Ω w MFC kontrolnym, 260 Ω w MFC-rGO, 390 Ω w MFC-rGO-Fe$_{34}$ i 132 Ω w MFC-rGO-Fe$_{68}$. Po modyfikacji anody z wykorzystaniem rGO elektroda wykazywała znaczny wzrost gęstości prądu w porównaniu z elektrodą kontrolną. Osadzenie Fe na anodzie w dawkach 34 mg i 68 mg dodatkowo zwiększyło gęstości prądu odpowiednio do 82 i 136 mA przy 1,35 V. Rezystancja przenoszenia ładunku dla niezmodyfikowanej elektrody GF mieściła się

w zakresie od około 9,0 Ω do około 7,7 Ω w obrębie testowanych potencjałów. Modyfikacja elektrod spowodowała całkowite zmniejszenie rezystancji przenoszenia ładunku o około 1,2 razy dla elektrody rGO, 1,5 raza dla elektrody rGO-Fe$_{34}$ i 2 razy dla elektrody rGO-Fe$_{68}$ przy testowanym potencjale roboczym 900 mV w porównaniu do elektrody kontrolnej (8,12 Ω). W przypadku MFC kontrolnego wartości zarejestrowane dla pojemności dwuwarstwowej (ang. double layer capacitance, Cdl) spadły z 263 µF przy potencjale 400 mV do 88 µF przy potencjale 900 mV. Modyfikacja elektrody z użyciem rGO spowodowała znaczny wzrost Cdl, niemniej jednak zmniejszał się on wraz ze wzrostem potencjału z 420 µF przy 500 mV do 95 µF przy 900 mV. Osadzanie Fe spowodowało nieznaczny wzrost wartości Cdl w porównaniu z MFC-rGO, ale nadal był on 2,5 razy i 4,6 razy większy dla potencjału 400 mV niż obserwowany dla elektrody kontrolnej, co wskazuje na lepsze gromadzenie ładunku na powierzchni styku elektrody z elektrolitem.

Analiza mikrobiologiczna pokazała, że zróżnicowanie mikroorganizmów było nieco wyższe we wszystkich MFC w początkowej fazie działania w stosunku do inokulum co wskazuje, że mikroorganizmy w błonie biologicznej konkurowały ze sobą. W miarę stabilizacji pracy MFC wartości wskaźnika Shannona stopniowo malały i osiągały wartości 2,9–3,8 w zależności od reaktora, co sugeruje, że w mikrobiomach zaczęły dominować mikroorganizmy najlepiej przystosowane do określonych warunków eksploatacyjnych. We wszystkich próbkach przeważały mikroorganizmy należące do Proteobacteria. Ich odsetek wzrósł z 14,8% w inokulum do 74,0% w błonie w MFC-rGO-Fe$_{68}$. Dominującymi klasami były β-Proteobacteria i ϒ-Proteobacteria. MFC-rGO-Fe$_{68}$ (dzień 30.) charakteryzował się najwyższym udziałem Verrucomicrobia. Bacteroidetes najliczniej występowały w MFC-rGO-Fe$_{34}$, stanowiąc pod koniec badań 47,7% wszystkich zidentyfikowanych organizmów. Na początku doświadczenia udział Bacteroidetes był podobny w obu reaktorach z anodą modyfikowaną rGO-Fe (około 15%). W MFC-rGO-Fe$_{68}$ przez cały okres badań nie zidentyfikowano mikroorganizmów należących do rzędu Sphingobacteriales, należącego do Bacteroidetes, natomiast w MFC-rGO-Fe$_{34}$ niesklasyfikowane bakterie z tego rzędu stanowiły na koniec eksperymentu 31,6% wszystkich uzyskanych sekwencji. Firmicutes były wskaźnikiem dynamicznych zmian gatunkowych we wczesnych stadiach tworzenia błony biologicznej anody. W kontrolnym MFC, MFC-rGO i MFC-rGO-Fe$_{68}$ Firmicutes stanowiły 5,5%, 9,2% i 11,2% mikrobiomu na początku eksperymentu, jednak ich liczba malała z czasem.

Najliczniejszym gatunkiem w MFC-rGO i MFC-rGO-Fe$_{68}$ był *Lysobacter daecheongensis*, który stanowił ostatecznie odpowiednio 20,71% i 27,02% mikrobiomu. Mikroorganizmy z rodzaju *Acidovorax* występowały licznie w MFC kontrolnym (2,48–3,62%) i MFC-rGO-Fe34 (2,33–6,65%). Ich udział procentowy w MFC-rGO-Fe$_{68}$ wahał się w granicach 0,21–0,63%, co wskazywało na niską tolerancję na obecność Fe w środowisku. W MFC kontrolnym *Pseudoxathomonas* sp. stanowiły ponad 7% wszystkich zidentyfikowanych sekwencji, natomiast wraz ze wzrostem dawki Fe ich udział w mikrobiomie spadł odpowiednio do 3,59% i 0,73% w MFC-rGO-Fe$_{34}$ i MFC-rGO-Fe$_{68}$. Liczebność *Dechloromonas* sp. i *Zooglea* sp., posiadających potencjał do przenoszenia elektronów na anodę, była wyższa w MFC ze zmodyfikowanymi anodami niż w kontroli.

Analiza statystyczna pozwoliła wskazać gatunki potencjalnie odpowiedzialne za wytwarzanie energii elektrycznej. Udział procentowy w mikrobiomie anodowym *Pseudoxanthomonas* sp., *Stenomorphomonas* sp. i *Thermomonas brevis* dodatnio korelował z produkcją energii w MFC kontrolnym. Udział procentowy *Dechloromonas* sp. w błonie biologicznej korelował dodatnio z produkcją energii w MFC-rGO. Najwięcej bakterii, których liczebność pozytywnie korelowała z produkcją energii, zidentyfikowano w MFC-rGO-Fe$_{34}$ (*Opitutus* sp., *Fluviicola taffensis*, *Magnetospirillum* sp., Candidatus *Halomonas fosfatis*, *Turneriella parva* i niesklasyfikowane Sphingobacteriales). W przypadku MFC-rGO-Fe$_{68}$ analiza statystyczna wykazała dodatnią istotną korelację między liczebnością *Microcystis* sp., *Sphingopyxis* sp. i *Paracoccus* sp. a gęstością prądu.

Analiza potencjału metabolicznego mikrobiomu błony biologicznej anod wykazała, że ponad 8% wszystkich szlaków metabolicznych w MFC-rGO-Fe$_{34}$ było odpowiedzialnych za produkcję i konwersję energii a 1% za obronę przed niekorzystnymi warunkami środowiskowymi i wartości te były znacząco wyższe w porównaniu do pozostałych reaktorów z modyfikowanymi anodami. Mikrobiom z MFC-rGO-Fe$_{34}$ charakteryzował również najlepszy potencjał replikacji, rekombinacji i naprawy DNA spośród wszystkich MFC. Uzyskane dane sugerują, że modyfikacja anody rGO i niższa dawka Fe zapewniają mikrobiomowi błony biologicznej anody najszerszy zakres potencjalnych szlaków metabolicznych produkcji energii oraz najlepszy potencjał obrony przed niekorzystnymi warunkami środowiskowymi. Fakt, że w przypadku rGO-Fe$_{68}$ nie zaobserwowano tak szerokiego zakresu szlaków metabolicznych może świadczyć o większej specjalizacji społeczności mikroorganizmów przy wyższym stężeniu Fe w środowisku, co mogło wyeliminować z błony część mikroorganizmów wrażliwych na

Fe. Mobilność komórek, mogąca mieć z wiązek z wytwarzaniem wici i rzęsek, we wszystkich MFC wzrosła średnio 2,9-krotnie w porównaniu z inokulum. Najczęściej identyfikowane szlaki metaboliczne we wszystkich reaktorach były związane z biosyntezą aminokwasów, metabolizmem węgla, metabolizmem metanu oraz puryn i pirymidyn. Metabolizm węgla obejmował głównie cykl kwasu cytrynowego, glikolizę węglowodanów (szlak Embdena-Meyerhofa), utlenianie pirogronianu i w mniejszym stopniu fotooddychanie. Natomiast metabolizm węgla powiązany z metabolizmem energetycznym zachodził głównie w redukcyjnym cyklu kwasu cytrynowego, cyklu dikarboksylanowo-hydroksymaślanowym, niepełnym redukcyjnym cyklu kwasu cytrynowego, redukcyjnym cyklu pentozowym oraz cyklu fosforanowym.

Weryfikacja hipotez badawczych

Eksperymenty przeprowadzone w poszczególnych etapach badań wskazują, że większa powierzchnia anody, choć sprzyja rozwojowi mikroorganizmów i bardziej efektywnemu oraz stabilnemu rozkładowi złożonych substancji organicznych, nie zwiększa generacji energii elektrycznej (**H1**). Większe powierzchnie anodowe mogą prowadzić do dużej dyspersji elektronów, z których niektóre są zużywane w innych procesach metabolicznych, co zwiększa straty elektronów. Materia organiczna zawarta w odpadowych KKT jest efektywnie przekształcana w prąd elektryczny w układach MFC, co potwierdza hipotezę 2 **(H2; P2 i P3)**. Optymalizacja składu mikrobiologicznego w MFC oraz kontrola obciążenia organicznego mogą być kluczowe dla zwiększenia efektywności i stabilności produkcji energii elektrycznej w tego typu systemach.

Modyfikacja anody Fe_2O_3 wpływa na moc elektryczną generowaną w MFC oraz efektywność usuwania substancji organicznych i skład gatunkowy mikrobiomu anodowego. W **P3** dowiedziono, że napięcia w MFC z 2,5 g Fe_2O_3/m^2 anody były istotnie wyższe niż w MFC z anodą niemodyfikowaną, co wskazuje, że obecność Fe(III) pozytywnie wpływa na wytwarzanie energii elektrycznej, powoduje bardziej stabilne wytwarzanie napięcia oraz 4-krotnie zwiększa moc ogniwa. Modyfikacja anody 2,5 g Fe_2O_3/m^2 zwiększyła gęstość prądu i napięcie odpowiednio 1,8-krotnie i 1,4-krotnie. W okresie stabilnej pracy MFC efektywność usuwania ChZT wyniosła w obu reaktorach około 50%. Obecność Fe(III) istotnie obniżyła stężenia NH_4-N w odpływie z MFC_{Fe} w porównaniu do kontroli. Sekwencjonowanie wykazało ponad 20-procentowe zmniejszenie różnorodności gatunkowej mikrobiomu anodowego w MFC_{Fe} w porównaniu do kontroli. Fe(III) na anodzie dwukrotnie zwiększyło udział procentowy *Burkholderiales* i *Pseudomonadales* w mikrobiomie, natomiast 10-krotnie i 5-krotnie obniżyło liczebność bakterii z rzędów *Rhodocyclales* i *Clostridiales*. Udział w mikrobiomie elektrogenów takich jak *Pseudomonas* sp. i *Geothrix* sp. był wyższy w MFC_{Fe}. W badaniu z optymalizacją dawki Fe_2O_3 na anodzie (**P4**) wykazano, że najwyższą gęstość mocy (1,39 mW/m²) uzyskano w MFC z dawką 2,5 i 5 g Fe_2O_3/m^2 anody – była ona 2,8 razy wyższa niż w MFC z anodą niemodyfikowaną i 5,8 razy wyższa niż w MFC z 10 g Fe_2O_3/m^2 anody. Modyfikacja anod Fe(III) powodowała zmniejszenie rezystancji wewnętrznej ogniwa. Średnia skuteczność usuwania ChZT we wszystkich reaktorach wyniosła ponad 70%. Niskie dawki Fe_2O_3 sprzyjały bardziej stabilnemu i skutecznemu usuwaniu ChZT w porównaniu z kontrolą MFC. Osadzenie Fe(III)

35:1097803618

zmniejszyło zróżnicowanie gatunkowe mikrobiomów anodowych, powodując jednocześnie wzrost w błonie biologicznej rodzajów mikroorganizmów zdolnych do produkcji energii elektrycznej, takich jak *Oscillochloris, Pseudomonas, Dechloromonas, Desulfobacter*. Powyższe badania pozwoliły zweryfikować **H3 (P4)**.

Modyfikacja elektrod za pomocą rGO i rGO-Fe spowodowała zmniejszenie rezystancji przenoszenia ładunku w stosunku do kontroli MFC, natomiast wzrost pojemności zmodyfikowanych elektrod wskazywał na poprawę przechowywania ładunku na granicy faz elektroda-elektrolit. Napięcie MFC (342,7 ± 72,8 mV) i moc ogniwa (8,55 mW/m^2) były istotnie wyższe w przypadku osadzania kompozytu rGO-Fe$_{68}$ niż w pozostałych wariantach. Zastosowanie kompozytu rGO-Fe$_{68}$ spowodowało, że całkowity opór wewnętrzny ogniwa był około 4 razy mniejszy, a opór przenoszenia ładunku 2 razy mniejszy niż w reaktorze kontrolnym. Dominującymi bakteriami egzoelektrogennymi w MFC były *Pseudoxanthomonas* sp., *Zoogloea* sp. i *Dechloromonas* sp. Produkcja energii elektrycznej była głównie związana z odwrotnym cyklem cytrynianowym, a MFC-rGO-Fe$_{34}$ posiadał najszerszy zakres potencjalnych szlaków metabolicznych umożliwiających wydajne wytwarzanie energii. **P5** pozwoliła pozytywnie zweryfikować **H4**.

Podsumowanie i wnioski

Przeprowadzone badania pozwoliły zweryfikować postawione hipotezy badawcze i wykazały, że:

- powlekanie anody Fe_2O_3 zwiększa gęstość mocy elektrycznej i pozwala nawet 6-krotnie zmniejszyć opór wewnętrzny ogniwa,

- dawka Fe_2O_3 wpływa na stabilność i efektywność usuwania ChZT; dawki na poziomie 1,25 i 2,5 g/m^2 anody pozwoliły stabilnie usuwać ChZT z efektywnością do 85%,

- osadzenie Fe_2O_3 na anodzie może zmniejszać zróżnicowanie gatunkowe mikrobiomów anodowych, powodując jednocześnie wyższy udział egzoelektrogenów w mikrobiomie,

- kompozyt rGO/Fe zwiększa moc elektryczną MFC przez zmniejszenie rezystancji przenoszenia ładunku elektrycznego oraz zwiększenie pojemności dwuwarstwowej elektrody, a także zwiększenie liczby miejsc aktywnych na anodzie,

- kompozyt rGO/Fe pozwala na zwiększenie udziału egzoelektrogenów w błonie biologicznej na anodzie,

- odpadowe KKT z fermentacji osadów wstępnych mogą być wykorzystywane w MFC do efektywnej produkcji energii elektrycznej,

- główne szlaki metaboliczne prowadzące do usuwania substancji organicznych oraz produkcji energii elektrycznej w MFC były związane z odwrotnym cyklem cytrynianowym,

- zwiększenie powierzchni anody wspomaga stabilne i skuteczne usuwanie ChZT, jednak nie przekłada się na wyższą generację energii elektrycznej,

Spis literatury

1. Aelterman, P., Rabaey, K., Pham, H.T., Boon, N., & Verstraete, W. (2006). Continuous electricity generation at high voltages and currents using stacked microbial fuel cells. Environmental Science & Technology, 40(10), 3388–3394.

2. Akçay, G.H., & Ar, İ. (2023). Investigation of domestic wastewater treatment and electricity generation using a two chambered microbial fuel cell with composite anode electrode. Afyon Kocatepe Üniversitesi Fen Ve Mühendislik Bilimleri Dergisi, 23(1), 177–185.

3. Banerjee, A., Calay, R.K., & Mustafa, M. (2022). Review on material and design of anode for microbial fuel cell. Energies, 15(6), 2283.

4. Carlson, H.K., Iavarone, A.T., Gorur, A., Yeo, B.S., Tran, R., Melnyk, R.A., Mathies, R.A., Auer, M., & Coates, J.D. (2012). Surface multiheme *c*-type cytochromes from *Thermincola potens* and implications for respiratory metal reduction by Gram-positive bacteria. Proceedings of the National Academy of Sciences, 109(5), 1702–1707.

5. Chabert, N., Ali, O.A., & Achouak, W. (2015). All ecosystems potentially host electrogenic bacteria. Bioelectrochemistry, 106, 88–96.

6. Chen, C.Y., Chen, T.Y., & Chung, Y.C. (2014). A comparison of bioelectricity in microbial fuel cells with aerobic and anaerobic anodes. Environmental Technology, 35(3), 286–293.

7. Choi, J.D.R., Chang, H.N., & Han, J.I. (2011). Performance of microbial fuel cell with volatile fatty acids from food wastes. Biotechnology Letters, 33, 705–714.

8. Das, S., Das, S., & Ghangrekar, M.M. (2022). Bacterial signalling mechanism: an innovative microbial intervention with multifaceted applications in microbial electrochemical technologies: a review. Bioresource Technology, 344, 126218.

9. Fan, X., Zhou, Y., Jin, X., Song, R.B., Li, Z., & Zhang, Q. (2021). Carbon material-based anodes in the microbial fuel cells. Carbon Energy, 3(3), 449–472.

10. Fatemi, S., Ghoreyshi, A.A., Najafpour, G., & Rahimnejad, M. (2012). Bioelectricity generation in mediator-less microbial fuel cell: application of pure and mixed cultures. Iranica Journal of Energy & Environment, 3(2), 104–108.

11. Geim, A.K., & Novoselov, K.S. (2007). The rise of graphene. Nature Materials, 6(3), 183–191.

12. Hassan, R.Y., Mekawy, M.M., Ramnani, P., & Mulchandani, A. (2017). Monitoring of microbial cell viability using nanostructured electrodes modified with Graphene/Alumina nanocomposite. Biosensors and Bioelectronics, 91, 857–862.

13. Holmes, D.E., Mester, T., O'Neil, R.A., Perpetua, L.A., Larrahondo, M.J., Glaven, R., Sharma, M.L., Ward J.E., Nevin, P.K. & Lovley, D.R. (2008). Genes for two multicopper proteins required for Fe (III) oxide reduction in *Geobacter sulfurreducens* have different expression patterns both in the subsurface and on energy-harvesting electrodes. Microbiology, 154(5), 1422–1435.

14. Huang, J., Jones, A., Waite, T.D., Chen, Y., Huang, X., Rosso, K.M., Kappler, A., Mansor, M., Tratnyek, P.G., & Zhang, H. (2021). Fe (II) redox chemistry in the environment. Chemical Reviews, 121(13), 8161–8233.

15. Jafary, T., Rahimnejad, M., Ghoreyshi, A.A., Najafpour, G., Hghparast, F., & Daud, W.R.W. (2013). Assessment of bioelectricity production in microbial fuel cells through series and parallel connections. Energy Conversion and Management, 75, 256–262.

16. Kober, T., Schiffer, H.W., Densing, M., & Panos, E. (2020). Global energy perspectives to 2060–WEC's World Energy Scenarios 2019. Energy Strategy Reviews, 31, 100523.

17. Kurniawan, T.A., Othman, M.H.D., Liang, X., Ayub, M., Goh, H.H., Kusworo, T.D., Mohyuddin, A., & Chew, K.W. (2022). Microbial fuel cells (MFC): a potential game-changer in renewable energy development. Sustainability, 14(24), 16847.

18. Li, L.H., Sun, Y.M., Yuan, Z.H., Kong, X.Y., & Li, Y.L. (2013). Effect of temperature change on power generation of microbial fuel cell. Environmental Technology, 34(13–14), 1929–1934.

19. Li, W.W., Yu, H.Q., & He, Z. (2014). Towards sustainable wastewater treatment by using microbial fuel cells-centered technologies. Energy & Environmental Science, 7(3), 911–924.

20. Light, S.H., Su, L., Rivera-Lugo, R., Cornejo, J.A., Louie, A., Iavarone, A.T., Ajo-Franklin, C.M., & Portnoy, D.A. (2018). A flavin-based extracellular electron transfer mechanism in diverse Gram-positive bacteria. Nature, 562(7725), 140–144.

21. Liu, W., Cheng, S., & Guo, J. (2014). Anode modification with formic acid: A simple and effective method to improve the power generation of microbial fuel cells. Applied Surface Science, 320, 281–286.

22. Logan, B.E., Rossi, R., Ragab, A.A., & Saikaly, P.E. (2019). Electroactive microorganisms in bioelectrochemical systems. Nature Reviews Microbiology, 17(5), 307–319.

23. Lu, X., von Haxthausen, K.A., Brock, A.L., & Trapp, S. (2021). Turnover of lake sediments treated with sediment microbial fuel cells: a long-term study in a eutrophic lake. Science of the Total Environment, 796, 148880.

24. Ma, J., Shi, N., Zhang, Y., Zhang, J., Hu, T., Xiao, H., Tang, T., & Jia, J. (2020). Facile preparation of polyelectrolyte-functionalized reduced graphene oxide for significantly improving the performance of microbial fuel cells. Journal of Power Sources, 450, 227628.

25. Mahmoud, R.H., Samhan, F.A., Ibrahim, M.K., Ali, G.H., & Hassan, R.Y. (2021). Formation of electroactive biofilms derived by nanostructured anodes surfaces. Bioprocess and Biosystems Engineering, 44, 759–768.

26. Mohanakrishna, G., Mohan, S.V., & Sarma, P.N. (2010). Utilizing acid-rich effluents of fermentative hydrogen production process as substrate for harnessing bioelectricity: an integrative approach. International Journal of Hydrogen Energy, 35(8), 3440–3449.

27. Mohanakrishna, G., Mohan, S.V., & Sarma, P.N. (2010). Utilizing acid-rich effluents of fermentative hydrogen production process as substrate for harnessing bioelectricity: an integrative approach. International Journal of Hydrogen Energy, 35(8), 3440–3449.

28. Nosek, D., Jachimowicz, P., & Cydzik-Kwiatkowska, A. (2020). Anode modification as an alternative approach to improve electricity generation in microbial fuel cells. Energies, 13(24), 6596.

29. Pandey, P., Shinde, V.N., Deopurkar, R.L., Kale, S.P., Patil, S.A., & Pant, D. (2016). Recent advances in the use of different substrates in microbial fuel cells toward wastewater treatment and simultaneous energy recovery. Applied Energy, 168, 706–723.

30. Pankratova, G., Hederstedt, L., & Gorton, L. (2019). Extracellular electron transfer features of Gram-positive bacteria. Analytica Chimica Acta, 1076, 32–47.

31. Prathiba, S., Kumar, P.S., & Vo, D.V.N. (2022). Recent advancements in microbial fuel cells: A review on its electron transfer mechanisms, microbial community, types of substrates and design for bio-electrochemical treatment. Chemosphere, 286, 131856.

32. Rabaey, K., Boon, N., Siciliano, S.D., Verhaege, M., & Verstraete, W. (2004). Biofuel cells select for microbial consortia that self-mediate electron transfer. Applied and Environmental Microbiology, 70(9), 5373–5382.

33. Rosales-Sierra, A., Rosales-Mendoza, S., Monreal-Escalante, E., Celis, L.B., Razo-Flores, E., & Cercado, B. (2017). Acclimation strategy using complex volatile fatty acid mixtures increases the microbial fuel cell (MFC) potential. ChemistrySelect, 2(22), 6277–6285.

34. Schröder, U. (2007). Anodic electron transfer mechanisms in microbial fuel cells and their energy efficiency. Physical Chemistry Chemical Physics, 9(21), 2619–2629.

35. Sekoai, P.T., Ghimire, A., Ezeokoli, O.T., Rao, S., Ngan, W.Y., Habimana, O., Yao, Y., Yang, P., Fung, A.H.Y., Yoro, K.O., Daramola, M.O., & Hung, C.H. (2021). Valorization of volatile fatty acids from the dark fermentation waste Streams-A promising pathway for a biorefinery concept. Renewable and Sustainable Energy Reviews, 143, 110971.

36. Siddiqi, M.M., Naseer, M.N., Abdul Wahab, Y., Hamizi, N.A., Badruddin, I.A., Chowdhury, Z.Z., Akbarzedech, O., Johan, M.R., Khan, T.M.Y., & Kamangar, S. (2019). Evaluation of municipal solid wastes based energy potential in urban Pakistan. Processes, 7(11), 848.

37. Sonawane, J.M., Mahadevan, R., Pandey, A., & Greener, J. (2022). Recent progress in microbial fuel cells using substrates from diverse sources. Heliyon, 8(12).

38. Tarcan, R., Todor-Boer, O., Petrovai, I., Leordean, C., Astilean, S., & Botiz, I. (2020). Reduced graphene oxide today. Journal of Materials Chemistry C, 8(4), 1198–1224.

39. Tariq, M., Wang, J., Bhatti, Z.A., Bilal, M., Malik, A.J., Akhter, M.S., Mahmood, Q., Hussain, S., Ghfar, A., Al-Anazy, M.M., & Ouladsmane, M. (2021). Bioenergy potential of albumin, acetic acid, sucrose, and blood in microbial fuel cells treating synthetic wastewater. Processes, 9(8), 1289.

40. Thapa, B.S., Kim, T., Pandit, S., Song, Y.E., Afsharian, Y.P., Rahimnejad, M., Kim, J. R., & Oh, S.E. (2022). Overview of electroactive microorganisms and electron transfer mechanisms in microbial electrochemistry. Bioresource Technology, 347, 126579.

41. Tiwari, S.K., Mishra, R.K., Ha, S.K., & Huczko, A. (2018). Evolution of graphene oxide and graphene: from imagination to industrialization. ChemNanoMat, 4(7), 598–620.

42. Wang, T., Huang, D., Yang, Z., Xu, S., He, G., Li, X., Hu, N., Yin, G., He, D., & Zhang, L. (2016). A review on graphene-based gas/vapor sensors with unique properties and potential applications. Nanomicro Letters, 8(2), 95–119.

43. Wang, J., Li, B., Wang, S., Liu, T., Jia, B., Liu, W., & Dong, P. (2022). Metal-organic framework-derived iron oxide modified carbon cloth as a high-power density microbial fuel cell anode. Journal of Cleaner Production, 341, 130725.

44. Wang, S., Adekunle, A., Tartakovsky, B., & Raghavan, V. (2021). Synthesizing developments in the usage of solid organic matter in microbial fuel cells: A review. Chemical Engineering Journal Advances, 8, 100140.

45. Xu, X., Zhao, Q., Wu, M., Ding, J., & Zhang, W. (2017). Biodegradation of organic matter and anodic microbial communities analysis in sediment microbial fuel cells with/without Fe (III) oxide addition. Bioresource Technology, 225, 402–408.

46. Yellappa, M., Modestra, J.A., Reddy, Y.R., & Mohan, S.V. (2021). Functionalized conductive activated carbon-polyaniline composite anode for augmented energy recovery in microbial fuel cells. Bioresource Technology, 320, 124340.

47. You, J., Greenman, J., & Ieropoulos, I.A. (2021). Microbial fuel cells in the house: A study on real household wastewater samples for treatment and power. Sustainable Energy Technologies and Assessments, 48, 101618.

48. Zheng, X., Hou, S., Amanze, C., Zeng, Z., & Zeng, W. (2022). Enhancing microbial fuel cell performance using anode modified with Fe_3O_4 nanoparticles. Bioprocess and Biosystems Engineering, 45(5), 877–890.

49. Zhuang, L., Zheng, Y., Zhou, S., Yuan, Y., Yuan, H., & Chen, Y. (2012). Scalable microbial fuel cell (MFC) stack for continuous real wastewater treatment. Bioresource Technology, 106, 82–88.

Praca nr 1

Nosek D., Jachimowicz P., Cydzik-Kwiatkowska A.

Anode modification as an alternative approach to improve electricity generation in microbial fuel cells

Energies

2020

Anode Modification as an Alternative Approach to Improve Electricity Generation in Microbial Fuel Cells

Dawid Nosek *, Piotr Jachimowicz and Agnieszka Cydzik-Kwiatkowska *

Department of Environmental Biotechnology, University of Warmia and Mazury in Olsztyn, Słoneczna 45g, 10-709 Olsztyn, Poland; piotr.jachimowicz@uwm.edu.pl

* Correspondence: dawid.nosek@uwm.edu.pl (D.N.); agnieszka.cydzik@uwm.edu.pl (A.C.-K.);
   Tel.: +48-89-523-4144 (D.N.)

Abstract: Sustainable production of electricity from renewable sources by microorganisms is considered an attractive alternative to energy production from fossil fuels. In recent years, research on microbial fuel cells (MFCs) technology for electricity production has increased. However, there are problems with up-scaling MFCs due to the fairly low power output and high operational costs. One of the approaches to improving energy generation in MFCs is by modifying the existing anode materials to provide more electrochemically active sites and improve the adhesion of microorganisms. The aim of this review is to present the effect of anode modification with carbon compounds, metallic nanomaterials, and polymers and the effect that these modifications have on the structure of the microbiological community inhabiting the anode surface. This review summarizes the advantages and disadvantages of individual materials as well as possibilities for using them for environmentally friendly production of electricity in MFCs.

Keywords: microbial fuel cells; anode modification; electrode materials; nanomaterials; polymers; microbial community; exoelectrogens

1. Introduction

In view of the growing demand for electricity, there is a need to develop environmentally friendly technologies. In the European Union, there is a trend towards production of energy from renewable resources, particularly by using waste from biomass management [1]. The sustainable production of electricity from renewable sources by microorganisms is considered an attractive alternative to producing energy from fossil fuels. One of the trialed solutions are microbial fuel cells (MFCs), in which the metabolic activity of microorganisms is utilized to produce electricity by oxidation of organic substances on the anode and transfer of electrons to the cathode [2]. Electrochemically active biofilms in MFCs can be also successfully used for the synthesis of nanoparticles and band gap narrowing of metal oxides [3,4].

In recent years, research on MFCs technology for sustainable electricity production has increased (Figure 1).
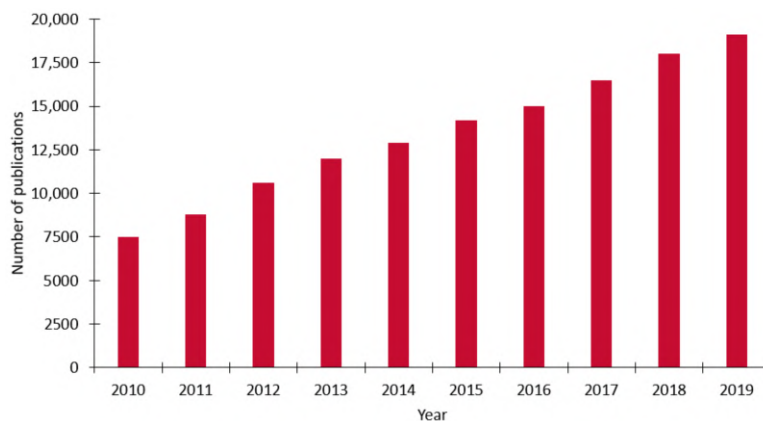
Figure 1. Number of publications per year found in the Google Scholar database using the search term "microbial fuel cells" (MFCs); (data acquired on 29 October 2020).

Wastewater contains large amounts of organic compounds that can be used as a potential carbon source in MFCs [5,6]. Current economic trends and legal regulations require that facilities such as wastewater treatment plants should be modernized to not only remove nutrients but also produce bioproducts and energy [5–7]. The use of MFCs in wastewater treatment systems can bring many benefits at the environmental, economic, operational stability, and energy management levels (Figure 2).
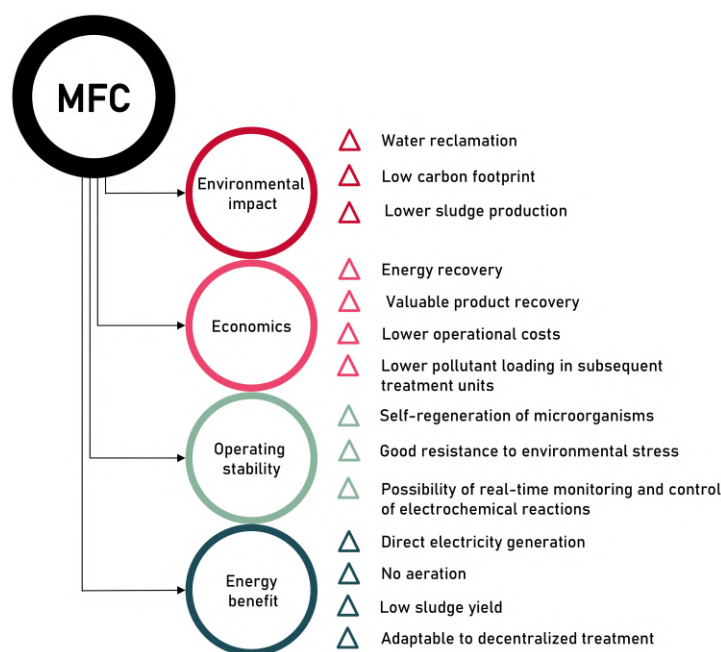
Figure 2. Potential benefits of MFCs for energy, environmental, operational, and economic sustainability.

Usually, MFCs are designed as single- or two-chamber systems [8,9]. A two-chamber MFCs has one chamber with an anode and one with a cathode, separated from each other by a proton exchange membrane (PEM). Single-chamber MFCs are more economical because the cathode is constantly exposed to air (so-called air cathodes), and there is no need to aerate the cathode chamber. Another advantage of one-chamber MFCs is the smaller distance between the anode and the cathode, which favors the efficient production of electricity [10]. The activity of microorganisms in the anode biofilm causes the decomposition of organic substances into electrons and protons. The electrons are transferred to the cathode by the external circuit, while the protons are transferred through the PEM to the cathode compartment (Figure 3). Some species, instead of transporting electrons to the exogenous acceptor, pass them directly to the anode. Such a phenomenon is called electrogenesis,

and the groups of electrochemically active microorganisms capable of carrying out this process are exoelectrogens [11]. Some bacteria are capable of producing secondary metabolites, which can act as redox shuttles [12]. Bacteria such as *Shewanella* sp. or *Escherichia coli* produce flavins, while *Pseudomonas* sp. produce phenazines (e.g., pyocyanin, pyorubin or oxychlororaphin)—these metabolites take part in an extracellular electron transfer. Other organisms (e.g., *Enterococcus faecalis* or *Faecalibacterium prausnitzii*) can use them, and as a result, electron transfer can take place over longer distances [13–16]. Biofilm formation by bacteria on the anode electrode is by far the most important mode of electrode–microbe interaction. To avoid competition between oxygen and electron carriers (mediators), anaerobic conditions should be ensured for the operation of the anodes of most MFCs [17]. The presence of oxygen, which is a terminal electron acceptor, in the anode compartment resulted in a lower power generation [18].
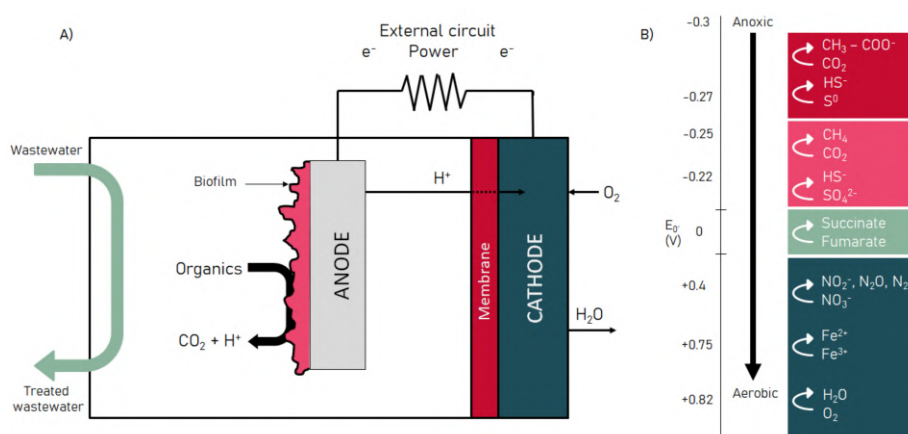
Figure 3. Diagram of an MFC reactor (**A**) and chemical changes in an MFCs depending on the oxygen conditions (**B**).

In MFCs, both pure bacterial cultures and mixed microbial consortia [19,20] are used, but pure cultures generate lower electrical voltage than diverse microbial consortia [21,22]. The advantage of using complex microbial consortia is that they can utilize complex substrates more efficiently due to syntrophic interactions between fermentative bacteria and exoelectrogens; such cooperation may enhance exoelectrogenic activity [23,24]. Syntrophic interactions are also observed between the exoelectrogens themselves [23]. However, pure bacterial cultures are important in elucidation of the electron transfer mechanisms in the biofilm [25].

Anaerobic respiration and fermentation are the main metabolic pathways of oxidation of organics by bacteria. Complex organic compounds are initially hydrolyzed into simpler chemical compounds such as fatty acids, sugars, amino acids, or aromatic compounds (Figure 4). Then, these simple organics can be either fermented or completely oxidized to CO_2, which results in the transfer of electrons to the anode. The ideal conditions for effective oxidation with maximum electron generation can be achieved if the exoelectrogens oxidize the organic matter completely to CO_2. The extracellular electron transfer can take place directly through cytochromes (redox proteins) because their outer cell membrane with exposed *c*-type cytochromes is in a direct or indirect (pili) contact with the electrode surface. Type IV pili are the conductive nanowires that transport the electrons from cell to cell inside the biofilm as well as from cells to the electrode surface. In addition to direct electron transport, microorganisms can also donate electrons indirectly via soluble electron shuttles [25]. Electron transfer from bacteria to the anode is facilitated by extracellular heteropolysaccharides as well as the cytochrome-*c* protein complexes present on bacteria cell walls [26].
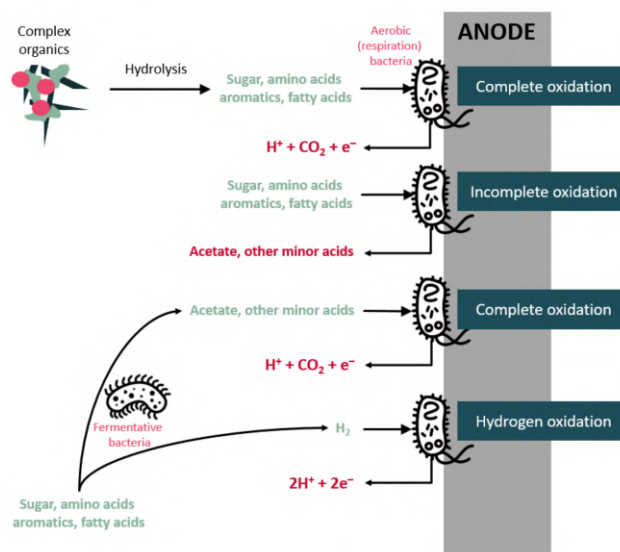
Figure 4. Conceptual representation of electricity generation from organic waste on the anode biofilm.

The diversity of the microbial community in the MFCs is determined not only by the origin of the inoculum, but also by the type of fuel used to power the cell, the presence of redox mediators, the oxygen conditions in the bioreactor, and the type of anode [27]. Studies by Eyiuche et al. [28] showed that, in an acetate-fed community on stainless steel (SS) anodes, *Desulfuromonas* sp. was abundant (15.4%) and *Geobacter* sp. was markedly less abundant (0.7%). On a carbon cloth (CC) anode, both genera were present in similar amounts (6.0–9.8%), indicating that an anode material affected exoelectrogenic genus enrichment in biofilms. In MFCs with an SS anode modified with carbon nanotubes (SS/CNTs), in the biofilm, such fermenting bacteria as *Chlorofexi* sp. and *Rhodanobacter lindaniclasticus* predominated, which resulted from the fact that the MFC was powered with the filtrate from fermentation of primary sludge. Exolectrogenic bacteria such as *Desulfovibro* sp., *Geobacter* sp., *Desulfobulbus* sp., and *Rhodopseudomonas* sp. occurred with a share of less than 1% [29]. *Geobacter* sp. was able to actively inhibit other microorganisms in the biofilm by production of extracellular proteins [30]. *Geobacter* sp. may have a competitive advantage over other genera in MFCs, due to this inhibitory activity as well as its robust capabilities for anaerobic respiration and flagellar chemotaxis, which allows it to gain proximity to the anode surface.

The studies have shown that the performance of MFCs increased with the increase in an anode's potential. Positive potential selected for, e.g., *Shewanella putrefaciens* biofilm [31], while negative anode potential promoted the growth of electrochemically active anode-respiring *Geobacter* sp. [32]. Bacteria such as *Geobacter sulfurreducens* and *Thermincola ferriacetica* that form thick multilayer biofilms of 38–50 µm at anodes can produce higher current density than bacteria that form thin biofilms [33,34]. On the other hand, thick biofilm can also hinder electron transfer. Since the anode surface plays a significant role in promoting and maintaining bio-catalytic activity, this surface can be modified to become a more favorable habitat for microorganisms enhancing electron transfer from the bacteria to the anode surface. Generally, greater bacterial adhesion enables the generation of more power with minimum electricity loss [35].

The aim of the literature review is to present possible methods of increasing the efficiency of electricity production by modifying the anode materials, and the effect that these modifications have on the structure of the microbiological community inhabiting the anode surface. This review summarizes the advantages and disadvantages of individual materials and the possibilities for their use in the production of environmentally friendly electricity in MFCs.

2. Electrode Materials

The anode material and its structure can directly affect bacteria attachment, electron transfer, and substrate oxidation. Anode materials must be corrosion-resistant, have a high specific surface area and electrical conductivity, and have a low electrical resistance and a low cost. The anode must also be made of a chemically stable material that can operate in an environment where highly diverse organic and inorganic constituents are present, which can react with some anode materials and reduce MFCs performance [36]. To ensure electron transfer, the anode material should be biocompatible [37]. In this review, the most frequently used electrode materials are presented, along with possible methods of modifying them, which can change the structure of the microbial communities on the anode and improve electricity generation in the MFCs.

2.1. Carbon Electrodes

Carbon-based electrodes are commonly used in various types of MFCs (Table 1) because they are chemically stable, resistant to environmental conditions in MFCs, have a high electrical conductivity, and a high specific surface area, which creates good conditions for biofilm development [38]. Carbon-based electrodes can be made of carbon/graphite felt (CF/GF), CC, carbon paper (CP), graphite paper (GP), and activated carbon (AC) [2,39]. The most commonly used CF and CC are characterized by a high porosity, electrical conductivity, and a specific surface area; however, CF shows better chemical and mechanical stability and is cheaper [40]. Despite the many advantages of carbon materials, they also have some disadvantages, such as a high hydrophobicity, which does not favor the adhesion of microorganisms and thus translates to a lower electron transfer capacity [41]. For hydrophilic surfaces, an instantaneous bacterial attachment is observed—the planktonic bacterial cells simultaneously attach and form colonies that increase and cover the whole surface. For hydrophobic surfaces, a progressive bacterial attachment is observed—only a limited number of bacteria attach to the surface and form colonies decreasing the surface hydrophobicity. Decreased surface hydrophobicity allows for immobilization of new bacteria [42]. On the other hand, a hydrophobic surface will be easily colonized by bacteria with a high cell surface hydrophobicity or bacteria that switched from hydrophilic to hydrophobic phenotypes in response to environmental conditions [43].

Although carbon materials generally exhibit good electrical conductivity, MFCs power generation efficiency can differ depending on which material is used. For example, cell voltage was higher when CF was used as the anode in a dual-chamber MFC than when CC or CP were used. For CF, the maximum power density of MFC was 420 mW/m^2, while for CC and CP, the power density was two log units (0.76 mW/m^2) and three log units (8.37·10^{-6} mW/m^2) lower, respectively, than that of CF [44]. Similar results were obtained by using anodes of various carbon-based materials in the soil MFC. The highest voltage and power were obtained in the MFC with a GF anode (346 ± 5 mV and 24.0 mW/m^2, respectively). The values obtained for GP were much lower (130 ± 5 mV and 4.5 mW/m^2, respectively). The type of carbon material affects also the charge transfer resistance (Rct). After a comparison of anodes made of aluminum sheet, GF and CC showed that the lowest Rct was observed for GF [45].

Table 1. Summary of carbon anode properties.

Anode (Non-Modification)	Reactor Configuration	Substrate	Power Density	Anode Surface Characterization	Reference
GF	dual chamber	sodium acetate trihydrate	0.48 A/m^2	disorganized web of fibers with a diameter of 10 to 14 μm	[46]
Porous graphite	single chamber	glucose	2.6 W/m^2	large number of pores with a diameter of 0 to 300 nm	[47]

Table 1. *Cont.*

Anode (Non-Modification)	Reactor Configuration	Substrate	Power Density	Anode Surface Characterization	Reference
CP	dual chamber	distillery wastewater	110 mW/m^2	water contact angle 126° (medium hydrophobicity)	[48]
GF	dual chamber	glucose	388 mW/m^2	water contact angle >120° (medium hydrophobicity)	[49]
CC	single chamber	wastewater	40 mW/m^2	smooth fibers of around 7 μm diameter	[50]
CF	singe chamber	glucose	680 mW/m^2	smooth surface	[51]
Graphitized mesophase pitch-based carbon foam			1800 mW/m^2	a well-developed macropore structure with a single hole diameter of around 300 μm	
Mesophase pitch-based carbon brush (CBr)			1350 mW/m^2	smooth surface	

The surface morphology of anode materials should be improved with respect to anode-bacteria interactions [52]. To increase the surface area of an anode, electrochemical oxidation [53,54], chemical [55], and heat treatment can be used [56], increasing the adhesion of microorganisms and the output power of the cell. In recent years, carbon microfiber (CMF) paper and carbon nanofiber (CNF) mats have been tested as anode materials in MFC. The use of thinner carbon materials for CNF electrodes resulted in a larger specific surface area and a better morphology of the electrode surface, which promoted adhesion of bacteria and formation of a dense and stable biofilm, increasing energy production. Compared to CMF, CNF showed a 10-fold increase in current [57], better electron transfer kinetics, and high electrical conductivity [58–60]. Activation of CNF in a tube furnace (creating activated carbon nanofiber nonwoven, ACNFN) increased the specific surface area of CNF from 25.31 to 1158.75 m^2/g [61]. The porous structure of ACNFN favored the active colonization of the anode by bacteria, resulting in a high and stable energy production. Biofilm growth on the ACNFN anode was about 3.2–4.2 times thicker than that on the CC anode. Highly conductive anodes with increased biocompatibility can be obtained using the polymer 3D printing technique and the carbonation process. The obtained materials have over 95% porosity; thus, the surface area (internal and external) for biofilm growth is high. The maximum voltages of the 3D anodes were about 33.7–138.4% higher than the voltage obtained with the CC anode and depended on the pore size in 3D anodes. The maximum power densities decreased in the order: 300 μm > 200 μm > 400 μm > 100 μm > 500 μm > CC. The unexpectedly low maximum power density of 100 μm anode with the largest specific surface area indicated that 3D printing technology can increase the power of the MFC, but the pore size in anodes should be optimized. The solution resistance of the MFC with the 3D anodes averaged 24.2 Ω and was approximately 8.6 Ω lower compared to the CC anode, while the Rct of the CC anode was slightly lower than that of the 3D anodes [62].

The configuration of the electrodes has evolved from a planar to a three-dimensional structure; however, the power generation and cost of the electrode so far discussed have not reached commercial levels. Therefore, in recent years, modifications with the use of carbon compounds and nanostructures have attracted much interest.

2.2. Metal Electrodes

Electrodes made of metals such as silver, SS, aluminum, nickel, molybdenum, titanium, gold, and copper ensure high performance in MFCs due to their good electrical conductivity.

Stainless steel is a commercially available industrial material with a high mechanical and corrosion resistance, high conductivity, and low cost [63], and it is regarded as a good electrode material for MFC anodes [64]. The macroporosity of SS anodes enables attachment of carbon nanoparticles, which improves the anode biocompatibility and also favors internal colonization by bacteria that could enhance electrode reactions [65]. To increase the specific surface area of SS anodes, the surface can be etched with, e.g., sulfuric acid (VI) [65].

When using copper wires, an increase in the anode surface from 2.5 to 20.1 cm^2 increased the maximum power density from 0.3 to 0.67 mW/m^2. It was also shown that an increase in the initial COD concentration from 1000 to 6000 mg COD/L with an anode area of 20.1 cm^2 further increased the maximum power density to 2.9 mW/m^2 [66]. It should be remembered that copper is toxic to microorganisms [2]; therefore, copper is more often used as a cathode in MFCs [67–70]. Baudler et al. [71] tested gold, silver, copper, nickel, cobalt, and titanium as anode materials in comparison to a graphite electrode. On gold, silver, copper, and nickel anodes, a homogeneous and optically dense red biofilm was formed, indicating predominance of *Geobacter* sp. The electrodes made of gold, silver, and copper had a current density higher than that made of graphite. Active biofilm did not form on the cobalt and titanium anodes. In the study, no toxic effects of copper were observed on electrochemically active bacteria.

The use of nickel foam improved electricity generation in a single-chamber MFC. The maximum output power with nickel foam was about 45 mW/m^2 higher than with a CC anode. It was observed that, although nickel foam increased electricity production, it also underwent anodic corrosion to form nickel phosphate [72]. In another study, using nickel foam as an anode in MFC ensured a maximum power density of 8.29 W/m^3, a Coulomb efficiency of 6.95%, and an internal resistance of 116 Ω. Modification of nickel foam using chitosan, polyaniline, and titanium carbide increased the power and Coulomb efficiency more than two-fold and reduced the internal resistance 2.5-fold. Epifluorescence and scanning electron microscope (SEM) analysis of microbial colonies on a nickel foam anode indicated that the adhesion of bacteria was less stable and that the colonies were not firmly attached to the anode surface [73].

These reports indicate that metal anodes, although they are good electron conductors, have low chemical resistance because they dissolve in contact with the anolyte, and their relatively flat surface may have lower biocompatibility than the surface of carbon anodes. Therefore, most experiments in MFCs with metal anodes indicate the necessity of modification of the anode surface.

3. Anode Modification

The main limitations in up-scaling of MFCs include low power density and expensive electrode materials. Power density can be increased by ensuring that the anode is hydrophilic and has a high specific surface area.

The surface roughness is of great importance for energy production in the MFCs as the anode morphology should facilitate the adherence of bacteria and subsequent biofilm formation. Electrochemical oxidation of CC anodes with ammonium bicarbonate, at different voltage densities, contributed to the removal of impurities from the CC surface, and the degree of etching increased with increasing current density, causing the formation of grooves increasing the specific surface of the anode [74]. Electrochemical modification of the surface of the nano-rough gold deposited on silicon wafers showed that at lower current densities, randomly distributed deposits appeared on the anode surface, covering about 50–70% of the surface. The use of higher current densities resulted in the formation of gas bubbles that shaped round micro-craters with a diameter of about 10 μm, increasing the density of the generated current 6.7 times compared to the unmodified anode [75].

Hydrophobicity of surface often determines the adhesion of the biofilm to the anode. Guo et al. [76] modified a glassy carbon anode with different functional groups such as $-OH$, $-CH_3$, $-SO_3^-$, $-N^+(CH_3)_3$. The anode modified with $-OH$ group showed the highest surface hydrophobicity. The best results were achieved for the anode modified by $-N^+(CH_3)_3$—the water contact angle of 15°

was reduced 4 times compared to the unmodified anode, and the amount of biomass produced on the electrode surface was the highest. The percentage of Geobacter sp. on the −CH$_3$-modified anode was about 40% lower than that on the anodes with modified with −N$^+$(CH$_3$)$_3$, −OH, and −SO$_3$$^-$ [76].

The literature indicates that, to overcome the problem of low power density, modification of anode materials, especially with high porosity nano-structured materials, is a good approach.

3.1. Metal Compounds

An improvement in MFC performance can be obtained by modification of the anode with iron compounds. Iron-reducing bacteria such as *Geobacter* sp. and *Shewanella* sp. are important electrogenes in MFCs [77,78]. Due to the insolubility of iron compounds in the pH range of 7 to 8, Fe-reducing bacteria reduce this metal either via direct contact with their outer membrane cytochromes or by using conductive pili [79]. The use of Fe-modified electrodes in a bio-electrochemical coagulation system increases the activity of denitrification enzymes [80]. The addition of iron also prevents methane production under low redox potential [81], which is a common problem in MFCs. In an MFC with a CF anode modified with graphene oxide (GO) and Fe$_2$O$_3$ and powered with pure acetate, the maximum stable voltage was 590 ± 5 mV [82], and the presence of iron stimulated the growth of exoelectrogens belonging to *Desulfovibrio* sp. Fe$_3$O$_4$ and bentonite-Fe were used as GF anode modifiers, significantly decreasing the internal resistance of MFC and increasing the maximum power densities to 18.28 and 29.98 mW/m^2, respectively, compared to 10.6 mW/m^2 obtained in an MFC with a GF anode. Modifications contributed to the enrichment of exoelectrogens from the genera *Proteiniphilum* and *Geobacter* in the anode biofilm [83]. The dose of iron for modification should be carefully chosen, because overdosing may result in lowered energy production [84].

MnO$_2$, Pd, or Fe$_3$O$_4$ nanoparticles mixed with carbon black (CB) were used for the modification of a CC anode in an MFC designed for removal of pharmaceutically active compounds. Nanoparticles of MnO$_2$, Pd, or Fe$_3$O$_4$ were loaded to the anode surface by using 5% Nafion reagent as a binder. In MFCs with modified anodes, efficient removal of carbamazepine (over 80%) and, to a lesser extent, ibuprofen (up to 20%) was noted. The maximum power density increased by 21, 15, and 10%, respectively, in MFCs with Pd−, MnO$_2$−, and Fe$_3$O$_4$−modified CB/CC anodes compared to the MFC with a CB/CC anode. The anodic biofilm on anodes modified with MnO$_2$ and Fe$_3$O$_4$ was enriched with *Geobacter* sp., while modification of the anode with Pd promoted the occurrence of both *Geobacter* sp. and *Sphaerochaeta* sp. [85].

Electricity generation in MFCs can also be increased by co-modification with active substances. Co-modification of MoO$_2$ nanoparticles highly dispersed on nitrogen-doped carbon nanorods with Co increasing the electron conductivity of carbon. The biofilm from an MFC with an anode co-modified with Co had fewer *Geobacter* sp., but it provided a higher power density in comparison to an anode without Co. This indicates that Co is toxic for exoelectrogens but improves electrocatalytic activity and increases power density [86]. Such an observation was confirmed by Alhamadi et al. [87] who showed that Co/cellulose nanocomposites had antibacterial properties regarding both G+ and G- pathogens such as *Staphylococcus aureus*, *Escherichia coli*, *Acinetobacter baumannii*, and *Pseudomonas aeruginosa*. On the other hand, Kooti et al. [88] reported that CoFe$_2$O$_4$ (10 mg/mL) did not affect the growth of *E. coli*, *P. aeruginosa*, *S. aureus*, and *Bacillus subtilis.* In another experiment, Co oxide synthesized from cobalt (II) nitrate increased the voltage in an MFC and electron transfer by almost two-fold compared to an MFC with an unmodified anode [89].

The anode surface can also be modified by adding a modifying substance to the substrate inoculated to an MFCs. The addition of Fe and S to the substrate resulted in the maintenance of a stable voltage in the reactor and reduced the charge-transfer resistance of the anode. The power density curves showed that, in the presence of Fe and S, the maximum power density of the MFC was 1.92 times greater than in the control MFC [90]. Iron sulfides are capable of acting as naturally occurring electrical conductors and electrocatalysts, which, due to their metallic and semiconductor properties, facilitate extracellular electron transfer [34]. Many ferric reducing bacteria and sulfur

reducing bacteria in anode biofilms are classified as exoelectrogens [91]. Sulphur reducing bacteria can transfer electrons through four possible pathways, which are (I) syntrophic interaction with sulfur oxidizing bacteria; (II) via cytochromes when there is a direct contact of the cell with the electrode; (III) synthesis of electron-conducting pili produced by bacteria attached to the electrode surface; and (IV) nanoparticles of metal sulfides, such as FeS, that transfer electrons via the external membrane of the microbial cells [92–95]. The group of microorganisms involved in the biosynthesis of iron sulfide nanoparticles, and thus, in biochemical processes generating electricity, include *Shewanella putrefaciens* [96], *Desulfobulbus* sp. [97] *Desulfovibrio vulgaris*, and *Acidiphilium cryputum* [98]. The increase in the share of sulfur metabolizing microorganisms belonging to *Desulfobulbus* sp. positively correlated with the production of electric current in a powered with waste volatile fatty acids [99]. Modification of the anode with iron sulfide nanomaterials promoted the growth of sulfur reducing bacteria belonging to *Enterobacteriaceae*, *Desulfovibrio* sp., and *Geobacter* sp., which increased the electricity production in MFC [90].

3.2. Carbon Composites

MFCs performance can be improved by anode modifications with allotrope varieties of carbon (e.g., graphene), carbon compounds (e.g., graphene oxide—GO), or other carbon composites (e.g., carbon black—CB or carbon nanotubes—CNT). Carbon modifiers increase the specific surface area of the anode, which creates more space for the attachment of microorganisms and increases the number of electrochemically active sites for the electron transfer. Many of the carbon compounds are also good conductors. For these reasons, carbon modifiers are commonly used in MFCs (Table 2), although the antibacterial activity of some carbon compounds such as, e.g., graphene has been reported [100]. The antimicrobial activity of GO surface coatings increased four-fold when GO sheet area decreased from 0.65 to 0.01 μm^2. The higher antimicrobial effect of smaller GO sheets was attributed to oxidative mechanisms associated with the higher defect density of smaller sheets [101].

Previous studies indicate that an attractive option for anode modification is graphene, made of carbon atoms with sp^2 hybridization, which form a tightly packed crystal lattice resembling a honeycomb [102]. The structure of graphene gives it mechanical strength, flexibility, and excellent electrical conductivity [82,103]. Modification of a CF anode using GO (GO was deposited by immersing CF in a suspension of GO in ethylene glycol and heating at 200 °C) in an MFC powered with sodium acetate increased the maximum stable voltage to about 13% higher than in MFC with an unmodified anode [82]. Even better results were obtained by using reduced GO (rGO). Wu et al. [104] showed that cathode modification with rGO in a membrane-less MFC improved energy recovery due to the improved structure of cathode and electron transfer, and better biocompatibility of functional bacteria related to electron transfer in comparison to a GO-modified anode. The modification of CF with zeolite clay/GO increased the power density and corresponding Coulomb efficiency by 3.6 and 2.75 times compared to an MFC with an unmodified CF anode. The high specific surface area of GO facilitated the coating of the anode with zeolite. Zeolite adheres well to bacterial cells, which increased the anodic biocompatibility [105]. Microbiological studies of biofilm on anodes covered with rGO and GO showed that rGO favored the growth of exoelectrogens from *Geobacter* sp., which predominated in the microbial community. The presence of rGO also promoted the growth of *Ignavibacterium* sp., which both transfer electrons to the anode and degrade organic pollutants [104].

Another type of carbon compounds for anode modifications are CNTs, which are graphene foils rolled into cylindrical nanotubes. The tube diameter can vary considerably and ranges from less than 1 nm to over 100 nm [106]. CNT, depending on the type of arrangement of hexagonal rings, can show metallic or semiconductor properties. CNTs are characterized by high flexibility and excellent thermal conductivity [107]. Liang et al. [108] observed that anode modification with GO, graphene, and CNT increased the electrochemically active surface and the number of microbes in the anode biofilm, and improved electricity generation in MFC. Depending on the modifying factor, after 110

days, from 0.49 to 0.98 kJ of energy was obtained. In an MFC with a CNT-modified anode, the highest phenanthrene removal efficiency (78%) was obtained.

In MFC with a CNT/SS anode, the maximum power density was in the range of 69.8–164.9 W/m^3, and it was 7 to 21 times higher than in the control MFC with a GF anode. The energy recovery was at a level of 0.15–0.60 kWh/kg COD [29]. It was also shown that multi-walled CNT with OH hydroxyl group produced the higher current in comparison with CNT due to surface roughness and looser network dispersion, which allowed for better bacterial adhesion [109]. Modification of GF anode with CNTs increased the abundance of *Deltaproteobacteria*, *Alphaproteobacteria*, and *Geobacter* sp. in comparison to unmodified anode [110]. In another study, similar conclusions were reached, because the abundance of *Desulfomonas* sp. and *Geobacter* sp. on the GF anode modified with nitrogen-doped CNT/polyaniline/MnO$_2$ was 1.33 times higher than in the biofilm of unmodified GF anode [111].

CB is a low-cost conductive nanomaterial, produced in the process of burning petroleum products, that is used in electrochemical devices or sensors [112]. CB showed exceptional mechanical properties, biocompatibility, and good electrochemical properties; therefore, it has been used to produce electrodes with thin layers of composites. CB can be activated with chemical compounds. Study of Zheng et al. [113] indicated that in MFC operated on LS matrix modified with CB with H$_2$O$_2$ treatment produced more power compared to identically operated MFC but with CB with HNO$_3$ treatment and a control MFC without chemical treatment of CB. The integration of conductive coke with a relatively high specific surface area to which microorganisms readily adhere to a conductive CB, which has a low electrical resistance at a ratio of 2:1, increased in power density by a factor of 2.3 in comparison with control. The complementary advantages of both carbon materials enhanced the performance of the MFC [114].

Table 2. Performance of MFCs with an anode modified with carbon nanocomposites.

Anode Modification	Reactor Configuration	Substrate	Power Density	Inoculum	Reference
LS/CB/H$_2$O$_2$	Dual chamber	Sodium acetate	62 W/m^3	MFC effluent	[113]
CVe/ACP	MFC stack	Urine	21 W/m^3	Anaerobic activated sludge	[115]
CC/CB	-	Sodium acetate	12 A/m^2	MFC effluent	[116]
CC/MWCNT-COOH	Single chamber	Glucose	560 mW/m^2	Activated sludge	[117]
Carbon fiber brush/MWCNT	Dual chamber	Wastewater	1278 mW/m^3	Wastewater	[118]
SS/AC SS/CNT SS/SWCNhorns	Single chamber	Acetate	244 mW/m^2 261 mW/m^2 327 mW/m^2	MFC effluent	[119]
Sponge/nitrogen-doped CNT	Dual chamber	Sodium acetate	2.8 W/m^3	-	[120]
3D G/MWCNTs/SS	Dual chamber	Lactate	502 W/m^3	*Shewanella oneidensis*	[121]
GOA-GFB graphite fiber brush/graphene oxide aerogel	Dual chamber	Sodium lactate	54 W/m^3	*Shewanella oneidensis* MR-1	[122]
Nitrogen-doped CNS/CC	Dual chamber	Sodium acetate	1122 mW/m^2	anaerobic sludge	[123]

3.3. Polymers

In recent years, much research has focused on the modification of anodes in MFCs using semiconductor polymers such as polydopamine (PDA), polypyroles (PPy), and polyaniline (PANI). Modification of the anode with polymers increased capacitive properties, biocompatibility, and an

active surface of the anode [124]. Polymers are quite stable and are not quickly consumed in the reactor. The literature review shows that, in MFCs with polymer-modified anodes, the power density was in the range of 17–3317 mW/m^2 (Table 3). The use of polymers and additional modifiers, such as graphene or metal nanoparticles, allows us to obtain more electrochemically active sites on the anode [41].

The use of PANI as a modifier increases the electrochemical activity and roughness of the anode, reduces the anode potential, and also gives higher reproducibility of the results than in the case of unmodified anode [125]. PANI is a hydrophilic compound, therefore PANI coating can enhance the transfer of nutrients to the anode biofilm [126]. For anode modifications, PANI together with nanocomposites, e.g., Au, can be used to increase the low biocompatibility of pure metal nanoparticles. The Au/PANI-modified CC anode showed higher electrochemical activity due to increased specific surface area and electrical conductivity. The power density generated at the Au/PANI/CC anode was 2.42, 1.45, and 3.72 times higher than that of the unmodified anode, PANI-modified, and Au-modified CC anode, respectively [127]. Mashkour et al. [126] investigated the effect of modification of an anode from bacterial cellulose-carbon nanotubes (BC/CNT) with polyaniline (BC/CNT/PANI). Before colonization, Rct for the BC/CNT-modified anode was 14.52 Ω and for the BC/CNT/PANI-modified anode was 41.28 Ω. The higher Rct of BC/CNT/PANI anode compared to the BC/CNT anode can be explained by a low conductivity of PANI in neutral pH. However, after biofilm formation, the Rct of the electrodes demonstrated an opposite trend. Biofilm density on the BC/CNT/PANI-modified anode was higher than on the BC/CNT anode. Image analysis indicated that PANI increased the biocompatibility of the anode and microbial growth—the average diameter of bacteria in biofilm from the BC/CNT/PANI-modified anode was more than two times higher than in the biofilm from the BC/CNT-modified anode.

The method used for anode modification also affects the efficiency of energy generation in the MFC. The use of pulsed electropolymerization allowed to obtain a brush-like structure on the surface of PANI-modified CC anode. The obtained maximum power density of an MFC with an anode modified with pulsed electropolymerization was 36% higher than that of an MFC with an anode modified with PANI at a constant voltage and 58% higher than in an MFC with an unmodified anode. In addition, over 50% reduction in Rct was obtained if pulsed electropolymerization was applied during the anode modification in comparison with other anodes [128].

Modification of an anode with PDA causes that the anode surface is more hydrophilic and a cell power density in MFC is higher [129]. PDA was used to modify Mo_2C/MoO_2 nanoparticles on a CF anode, increasing the current density by 4.96 times compared to the unmodified FC anode and 1.38 times compared to an the MFC with the Mo_2C/MoO_2-modified anode. Modification of nanoparticles with PDA also lowers the Rct of MFC [130]. The promising results were obtained by modifying a CC anode simultaneously with PDA and rGO. The use of both modifications of CC anode increased the power density 2.2 and 1.9 times compared to the PDA-modified and rGO-modified anodes, respectively. The presence of PDA increased hydrophilicity of the anode surface and adhesion of bacterial cells, while the rGO provided more electrochemically active sites on the anode surface [131].

The beneficial effect of a simultaneous modification of an anode with polymer and other substances was also reported for PPy. The modification of CBr with PPy, carboxymethylcellulose and CNTs allowed us to obtain a macroporous 3D structure with a high specific surface area on the anode that promoted adhesion and growth of microorganisms. This modification increased the working time of MFCs due to long-term maintenance of an electrochemical activity of microbial cells. CNTs increased the anode conductivity, and PPy provided a high capacity and biocompatibility of the anode [120]. Modification of SS anode with PPy increased the corrosion resistance, biocompatibility, and power density of the anode compared to an unmodified stainless-steel anode [132]. Modification of anodes with CNT and PPy was reported as an attractive and inexpensive alternative to the use of Pt in MFCs [133]. There are also reports on the use of more niche modifiers, such as poly(3-aminophenylboronic acid). The use of poly(3-aminophenylboronic acid) to modify the CC anode shortened the growth time of the bacterial

biofilm on the electrodes by two times, while the power density was 928 ± 20 mW/m^2 and was about 4.5 times higher than in the MFC with an unmodified anode [134].

In many cases, the modification of anodes with polymers contributed to the improvement of the hydrophilicity and specific surface of the anode. PANI electroplating introduced a rough layer on the graphite fiber. SEM analysis showed that the PANI membrane was rough and loose, containing a lot of nano-cilia. Bare GF had a strongly hydrophobic surface (water contact angle of 113–120°), but after modification with PANI, the water droplet was completely and rapidly adsorbed by the anode [135]

On the other hand, the sponge made of polyvinyl formaldehyde and graphite nanopowder showed a hyperhydrophilic character—regardless of the share of the graphite nanopowder, the anode contact angle was <10° [136]. In another study, the PDA/rGO coating improved biocompatibility of the CC membrane—the water contact angle was close to 0° (superhydrophilicity). Superhydrophilicity contributed to the rapid adherence of microorganisms and increased bacterial stability on the anodes [137]. Polymers also reduce the corrosivity of metals. The bare SS plate was smooth with only some scratches. In contrast, the PPy-coated SS plate surface was covered with particles with a diameter of 1 to 2.5 μm, and the electrode surface was rough and porous. The corrosion potential decreased from −553.6 to −382.2 mV after the modification of the SS plate with PPy [132].

Table 3. Performance of MFCs with anodes modified with polymers.

Anode Modification	Reactor Configuration	Substrate	Power Density	Inoculum	Reference
PPy-CMC-CNTs/CBr	Dual chamber	Sodium acetate	2970 mW/m^2	Mixed culture	[138]
PPy-CMC-TiN/CBr hydrogel anode	Dual chamber	Sodium acetate	14 W/m^3	Anaerobic mixed culture	[139]
SS/PPy-W	Single chamber	Sodium acetate	1870 mW/m^2	Landfill leachate	[140]
PPy/MWNT/graphite rods	Single chamber	Saccharose	201 mW/m^2	Anaerobic sludge	[141]
magnetic PPy/nanofibers/SrFe$_{12}$O$_{19}$/nonwoven textile	Dual chamber	Glucose	3317 mW/m^2	MFC effluent	[142]
PPy/SAC/SS	Dual chamber	Sodium acetate	45 W/m^3	*Geobacter sulfurreducens*	[143]
Ti$_4$O$_7$/GO/PANI	Single chamber	Oil-containing restaurant wastewater	2073 mW/m^2	mixed bacterial culture	[144]
PANI/GF	Dual chamber	Sodium acetate	216 mW/m^2	Anaerobic sludge with *Chaetoceros*	[145]
Au/PANI/CC	Dual chamber	Glucose	804 mW/m^2	*Escherichia coli* ATCC 27325	[127]
TiO$_2$-20 *PANI/CP	Dual chamber	NaHCO$_3$	813 mW/m^2	*Shewanella loihica PV-4*	[146]
rGO/PANI/CBr	Single chamber	Glucose	862 mW/m^2	Sludge	[147]
PANI/Fe/GF	Bentos MFC	Seawater and marine sediment	17 mW/m^2	Marine sediment	[148]
PANI nanoflower/CC	Dual chamber	Mixed medium containing M9 salt medium, 5% LB broth, and 10 mM sodium lactate	389 mW/m^2	*Shewanella oneidensis* MR-1	[149]
PDA/rGO/CC	Dual chamber	Sodium acetate	2047 mW/m^2	Activated anaerobic sludge	[131]
PDA/Mo$_2$C-MoO$_2$/GF	Single chamber	Glucose	1640 mW/m^2	*E. coli*	[130]
PDA **/AC/SS	Single chamber	Wastewater with acetate	803 mW/m^2	Wastewater	[129]

* 20 cycles of cyclic voltammetry polymerization. ** With 50% (wt.) polydopamine (PDA) added.

In research on modifications of the anode with polymers or co-modification with other metal or carbon compounds, pure cultures of microorganisms such as *Escherichia coli* [127] or *Shewanella* sp. [150, 151] are most often used to inoculate the reactors. There are few studies on the influence of anode modifications with polymers on multispecies microbial community of anode. They indicate that the modifications increase the number of *Proteobacteria*, *Deltaproteobacteria*, and the genus *Geobacter* [110,152]. The presence of polydiallyldimethylammonium (PDDA) on the CF electrode accelerated the attachment of exoelectrogens to the surface through electrostatic attraction—*Geobacter* sp. and *Pseudomonas* sp. were about nine and three times higher, respectively, on PDDA-modified CF anode than on the unmodified anode [152]. On the other hand, the share of exoelectrogens from genera *Acinetobacter*, *Brucella*, and *Bacillus* was about 1.4 times lower on PDDA-modified CC anode than on the unmodified anode [153]. Chen and Wang [154] showed that *E. coli* cells grown in PDDA microcarriers had the same viability as those grown in suspension, as evidenced by an increase in optical density and cell number. However, *Chlorella vulgaris* cells showed extremely poor viability inside PDDA microcarriers, possibly due to blockage of nutrient uptake by the diallyldimethylammonium quaternary ammonium cation. At anodes modified with 50% PDA, an approximate twofold increase in the percentage of *Proteobacteria* (up to 33%) and *Firmicutes* (up to 3%) biomass was observed compared to unmodified anode [129]. Modification of the CC anode with PANI stimulated the participation of *Geobacter* sp. in the biofilm, while the simultaneous use of PDA with rGO on the CC anode caused that *Geobacter* sp. accounted for over 80% of the microorganisms identified in the biofilm. The anode modifications could select for the growth of bacteria from the anolyte. Changes in the properties of the anode surface may also affect a transcriptomic profile of microorganisms in MFC; in the cells of microorganisms inhabiting the PDA/rGO modified anode, electrogenesis related to outer-surface octaheme *c*-type cytochrome *omcZ* was highly expressed [155].

4. Conclusions

To increase the production of electricity in MFCs, a holistic approach should be applied that connects operational parameters of the reactor with environmental conditions and microbial structure of the biomass. The literature review shows that the most promising solutions for MFCs are modification of anodes from highly conductive carbon nanomaterials with polymers (e.g., PDA or PANI) and carbon-derived materials (e.g., GO or CNT). Such modifications increased hydrophilicity and the specific surface of anodes, resulting in a higher electricity production. Anode modifications affect the composition of exoelectrogenic bacteria in the anode biofilm, and sulfur-reducing bacteria are regarded as microorganisms mostly responsible for the efficient production of electricity. Although technological research indicates an improvement in the efficiency of energy generation as a result of modification, there is little data showing the effect of modification on microbial metabolism. Therefore, future research should focus on metatranscriptomic analysis to indicate factors that determine the activity of exoelectrogens in MFCs.

Abbreviations

AC	active carbon
ACNFN	activated carbon nanofiber nonwoven
ACP	activated carbon powder
BC	bacterial cellulose
CB	carbon black
CBr	carbon brush
CC	carbon cloth
CF/GF	carbon/graphite felt
CMC	carboxymethylcellulose
CMF	carbon microfiber
CNF	carbon nanofiber
CNS	caron nanosheet
CNT	carbon nanotubes
COD	chemical oxygen demand
CP	carbon paper
CVe	carbon veil
GFB	graphite fiber brush
GO	graphene oxide
GOA	graphene oxide aerogel
GP	graphite paper
kWh	kilowatt hour
LS	loofah sponge
MFC	microbial fuel cell
MWCNT	multi-walled carbon nanotube
PANI	polyaniline
PDA	polydopamine
PDDA	polydiallyldimethylammonium
PEM	proton exchange membrane
PPy	polypyroles
Rct	charge transfer resistance
rGO	reduced graphene oxide
SAC	sargassum activated carbon
SS	stainless-steel
SWCNhorns	single-walled carbon nanohorns
TiN	titanium nanoparticle

References

1. Commisson European. Sustainable and Optimum Use of Biomass for Energy in the EU beyond 2020. Final Report. 2017. Available online: https://ec.europa.eu/energy/studies/sustainable-and-optimal-use-biomass-energy-eu-beyond-2020_en (accessed on 9 September 2020).

2. Logan, B.E.; Hamelers, B.; Rozendal, R.; Schröder, U.; Keller, J.; Freguia, S.; Aelterman, P.; Verstraete, W.; Rabaey, K. Microbial fuel cells: Methodology and technology. *Environ. Sci. Technol.* **2006**, *40*, 5181–5192. [CrossRef]

3. Khan, M.M.; Ansari, A.J.; Lee, J.H.; Lee, J.; Cho, M.C. Mixed culture electrochemically active biofilms and their microscopic and spectroelectrochemical studies. *ACS Sustain. Chem. Eng.* **2014**, *2*, 423–432. [CrossRef]

4. Khan, M.E.; Khan, M.M.; Min, B.K.; Cho, M.H. Microbial fuel cell assisted band gap narrowed TiO2 for visible light-induced photocatalytic activities and power generation. *Sci. Rep.* **2018**, *8*, 1723. [CrossRef]

5. Catal, T.; Li, K.; Bermek, H.; Liu, H. Electricity production from twelve monosaccharides using microbial fuel cells. *J. Power Sources* **2008**, *175*, 196–200. [CrossRef]

6. Jachimowicz, P.; Cydzik-Kwiatkowska, A.; Szklarz, P. Effect of aeration mode on microbial structure and efficiency of treatment of TSS-rich wastewater from meat processing. *Appl. Sci.* **2020**, *10*, 7414. [CrossRef]

7. Capodaglio, A.; Olsson, G. Energy issues in sustainable urban wastewater management: Use, demand reduction and recovery in the urban water cycle. *Sustainability* **2019**, *12*, 266. [CrossRef]

8. Chae, K.J.; Choi, M.J.; Lee, J.W.; Kim, K.Y.; Kim, I.S. Effect of different substrates on the performance, bacterial diversity, and bacterial viability in microbial fuel cells. *Bioresour. Technol.* **2009**, *100*, 3518–3525. [CrossRef]

9. Feng, Y.; Yang, Q.; Wang, X.; Liu, Y.; Lee, H.; Ren, N. Treatment of biodiesel production wastes with simultaneous electricity generation using a single-chamber microbial fuel cell. *Bioresour. Technol.* **2011**, *102*, 411–415. [CrossRef]

10. Lanas, V.; Ahn, Y.; Logan, B.E. Effects of carbon brush anode size and loading on microbial fuel cell performance in batch and continuous mode. *J. Power Sources* **2014**, *247*, 228–234. [CrossRef]

11. Logan, B.E. Exoelectrogenic bacteria that power microbial fuel cells. *Nat. Rev. Microbiol.* **2009**, *7*, 375–381. [CrossRef]

12. Shen, H.B.; Yong, X.Y.; Chen, Y.L.; Liao, Z.H.; Si, R.W.; Zhou, J.; Zheng, T. Enhanced bioelectricity generation by improving pyocyanin production and membrane permeability through sophorolipid addition in *Pseudomonas aeruginosa*-inoculated microbial fuel cells. *Bioresour. Technol.* **2014**, *167*, 490–494. [CrossRef] [PubMed]

13. Von Canstein, H.; Ogawa, J.; Shimizu, S.; Lloyd, J.R. Secretion of flavins by *Shewanella* species and their role in extracellular electron transfer. *Appl. Environ. Microbiol.* **2008**, *74*, 615–623. [CrossRef] [PubMed]

14. McAnulty, M.J.; Wood, T.K. YeeO from *Escherichia coli* exports flavins. *Bioengineered* **2014**, *5*, 386–392. [CrossRef] [PubMed]

15. Khan, M.T.; Browne, W.R.; Van Dijl, J.M.; Harmsen, H.J.M. How can faecalibacterium prausnitzii employ riboflavin for extracellular electron transfer? *Antioxidants Redox. Signal.* **2012**, *17*, 1433–1440. [CrossRef]

16. Zhang, E.; Cai, Y.; Luo, Y.; Piao, Z. Riboflavin-shuttled extracellular electron transfer from *Enterococcus faecalis* to electrodes in microbial fuel cells. *Can. J. Microbiol.* **2014**, *60*, 753–759. [CrossRef]

17. Cornejo, J.A.; Lopez, C.; Babanova, S.; Santoro, C.; Artyushkova, K.; Ista, L.; Schuler, A.J.; Atanassov, P. Surface modification for enhanced biofilm formation and electron transport in shewanella anodes. *J. Electrochem. Soc.* **2015**, *162*, H597–H603. [CrossRef]

18. Kim, B.H.; Park, H.S.; Kim, H.J.; Kim, G.T.; Chang, I.S.; Lee, J.; Phung, N.T. Enrichment of microbial community generating electricity using a fuel-cell-type electrochemical cell. *Appl. Microbiol. Biotechnol.* **2004**, *63*, 672–681. [CrossRef]

19. Jadhav, D.A.; Ghangrekar, M.M. Optimising the proportion of pure and mixed culture in inoculum to enhance the performance of microbial fuel cells. *Int. J. Environ. Technol. Manag.* **2020**, *23*, 50. [CrossRef]

20. Esfandyari, M.; Fanaei, M.A.; Gheshlaghi, R.; Akhavan Mahdavi, M. Dynamic modeling of a continuous two-chamber microbial fuel cell with pure culture of *Shewanella*. *Int. J. Hydrogen Energy* **2017**, *42*, 21198–21202. [CrossRef]

21. Hassan, S.H.A.; Kim, Y.S.; Oh, S.E. Power generation from cellulose using mixed and pure cultures of cellulose-degrading bacteria in a microbial fuel cell. *Enzyme Microb. Technol.* **2012**, *51*, 269–273. [CrossRef]

22. Cao, Y.; Mu, H.; Liu, W.; Zhang, R.; Guo, J.; Xian, M.; Liu, H. Electricigens in the anode of microbial fuel cells: Pure cultures versus mixed communities. *Microb. Cell Fact.* **2019**, *18*, 39. [CrossRef] [PubMed]

23. Kiely, P.D.; Regan, J.M.; Logan, B.E. The electric picnic: Synergistic requirements for exoelectrogenic microbial communities. *Curr. Opin. Biotechnol.* **2011**, *22*, 378–385. [CrossRef] [PubMed]

24. Logan, B.E.; Rossi, R.; Ragab, A.; Saikaly, P.E. Electroactive microorganisms in bioelectrochemical systems. *Nat. Rev. Microbiol.* **2019**, *17*, 307–319. [CrossRef] [PubMed]

25. Kumar, R.; Singh, L.; Zularisam, A.W. Exoelectrogens: Recent advances in molecular drivers involved in extracellular electron transfer and strategies used to improve it for microbial fuel cell applications. *Renew. Sustain. Energy Rev.* **2016**, *56*, 1322–1336. [CrossRef]

26. Li, Y.; Xu, D.; Chen, C.; Li, X.; Jia, R.; Zhang, D.; Sand, W.; Wang, F.; Gu, T. Anaerobic microbiologically influenced corrosion mechanisms interpreted using bioenergetics and bioelectrochemistry: A review. *J. Mater. Sci. Technol.* **2018**, *34*, 1713–1718. [CrossRef]

27. Mitra, P.; Hill, G.A. Continuous microbial fuel cell using a photoautotrophic cathode and a fermentative anode. *Can. J. Chem. Eng.* **2012**, *90*, 1006–1010. [CrossRef]

28. Eyiuche, N.J.; Asakawa, S.; Yamashita, T.; Ikeguchi, A.; Kitamura, Y.; Yokoyama, H. Community analysis of biofilms on flame-oxidized stainless steel anodes in microbial fuel cells fed with different substrates. *BMC Microbiol.* **2017**, *17*, 145. [CrossRef]

29. Kim, H.; Kim, B.; Yu, J. Effect of HRT and external resistances on power generation of sidestream microbial fuel cell with CNT-coated SSM anode treating actual fermentation filtrate of municipal sludge. *Sci. Total Environ.* **2019**, *675*, 390–396. [CrossRef]

30. Chignell, J.F.; De Long, S.K.; Reardon, K.F. Meta-proteomic analysis of protein expression distinctive to electricity-generating biofilm communities in air-cathode microbial fuel cells. *Biotechnol. Biofuels* **2018**, *11*, 121. [CrossRef]

31. Carmona-Martínez, A.A.; Harnisch, F.; Kuhlicke, U.; Neu, T.R.; Schröder, U. Electron transfer and biofilm formation of *Shewanella putrefaciens* as function of anode potential. *Bioelectrochemistry* **2013**, *93*, 23–29. [CrossRef]

32. Wei, J.; Liang, P.; Cao, X.; Huang, X. A new insight into potential regulation on growth and power generation of *Geobacter sulfurreducens* in microbial fuel cells based on energy viewpoint. *Environ. Sci. Technol.* **2010**, *44*, 3187–3191. [CrossRef]

33. Parameswaran, P.; Bry, T.; Popat, S.C.; Lusk, B.G.; Rittmann, B.E.; Torres, C.I. Kinetic, electrochemical, and microscopic characterization of the thermophilic, anode-respiring bacterium *Thermincola ferriacetica*. *Environ. Sci. Technol.* **2013**, *47*, 4934–4940. [CrossRef]

34. Malvankar, N.S.; Lau, J.; Nevin, K.P.; Franks, A.E.; Tuominen, M.T.; Lovley, D.R. Electrical conductivity in a mixed-species biofilm. *Appl. Environ. Microbiol.* **2012**, *78*, 5967–5971. [CrossRef]

35. Kumar, R.; Singh, L.; Wahid, Z.A.; Din, M.F.M. Exoelectrogens in microbial fuel cells toward bioelectricity generation: A review. *Int. J. Energy Res.* **2015**, *39*, 1048–1067. [CrossRef]

36. Zhou, M.; Chi, M.; Luo, J.; He, H.; Jin, T. An overview of electrode materials in microbial fuel cells. *J. Power Sources* **2011**, *196*, 4427–4435. [CrossRef]

37. Narayanasamy, S.; Jayaprakash, J. Application of carbon-polymer based composite electrodes for Microbial fuel cells. *Rev. Environ. Sci. Biotechnol.* **2020**, *19*, 595–620. [CrossRef]

38. Li, S.; Cheng, C.; Thomas, A. Carbon-based microbial-fuel-cell electrodes: From conductive supports to active catalysts. *Adv. Mater.* **2017**, *29*. [CrossRef]

39. Slate, A.J.; Whitehead, K.A.; Brownson, D.A.; Banks, C.E. Microbial fuel cells: An overview of current technology. *Renew. Sustain. Energy Rev.* **2019**, *101*, 60–81. [CrossRef]

40. Yaqoob, A.A.; Ibrahim, M.N.M.; Rodríguez-Couto, S. Development and modification of materials to build cost-effective anodes for microbial fuel cells (MFCs): An overview. *Biochem. Eng. J.* **2020**, *164*, 107779. [CrossRef]

41. Hindatu, Y.; Annuar, M.S.M.; Gumel, A.M. Mini-review: Anode modification for improved performance of microbial fuel cell. *Renew. Sustain. Energy Rev.* **2017**, *73*, 236–248. [CrossRef]

42. Santoro, C.; Guilizzoni, M.; Baena, J.C.; Pasaogullari, U.; Casalegno, A.; Li, B.; Babanova, S.; Artyushova, K.; Atanassov, P. The effects of carbon electrode surface properties on bacteria attachment and start up time of microbial fuel cells. *Carbon* **2014**, *67*, 128–139. [CrossRef]

43. Bujdáková, H.; Didiášová, M.; Drahovská, H.; Černáková, L. Role of cell surface hydrophobicity in *Candida albicans* biofilm. *Open Life Sci.* **2013**, *8*, 259–262. [CrossRef]

44. Penteado, E.D.; Fernandez-Marchante, C.M.; Zaiat, M.; Gonzalez, E.R.; Rodrigo, M.A. Influence of carbon electrode material on energy recovery from winery wastewater using a dual-chamber microbial fuel cell. *Environ. Technol.* **2017**, *38*, 1333–1341. [CrossRef] [PubMed]

45. Yu, B.; Feng, L.; He, Y.; Yang, L.; Xun, Y. Effects of anode materials on the performance and anode microbial community of soil microbial fuel cell. *J. Hazard. Mater.* **2021**, *401*, 123394. [CrossRef] [PubMed]

46. Kang, Y.L.; Pichiah, S.; Ibrahim, S. Facile reconstruction of microbial fuel cell (MFC) anode with enhanced exoelectrogens selection for intensified electricity generation. *Int. J. Hydrog. Energy* **2017**, *42*, 1661–1671. [CrossRef]

47. Xiong, J.; Hu, M.; Li, X.; Li, H.; Li, X.; Liu, X.; Cao, G.; Li, W. Porous graphite: A facile synthesis from ferrous gluconate and excellent performance as anode electrocatalyst of microbial fuel cell. *Biosens. Bioelectron.* **2018**, *109*, 116–122. [CrossRef]

48. Harshiny, M.; Samsudeen, N.; Kameswara, R.J.; Matheswaran, M. Biosynthesized FeO nanoparticles coated carbon anode for improving the performance of microbial fuel cell. *Int. J. Hydrog. Energy* **2017**, *42*, 26488–26495. [CrossRef]

49. Zhao, Y.; Ma, Y.; Li, T.; Dong, Z.; Wang, Y. Modification of carbon felt anodes using double-oxidant HNO_3/H_2O_2 for application in microbial fuel cells. *RSC Adv.* **2018**, *8*, 2059–2064. [CrossRef]

50. Sayed, E.T.; Alawadhi, H.; Elsaid, K.; Olabi, A.G.; Adel Almakrani, M.; Bin Tamim, S.T.; Alafranji, G.H.M.; Abdelkareem, M.A.A. Carbon-cloth anode electroplated with iron nanostructure for microbial fuel cell operated with real wastewater. *Sustainability* **2020**, *12*, 6538. [CrossRef]

51. Zhang, K.; Ma, Z.; Song, H.; Zhang, M.; Xu, H.; Zhao, N. Macroporous carbon foam with high conductivity as an efficient anode for microbial fuel cells. *Int. J. Hydrog. Energy* **2020**, *45*, 12121–12129. [CrossRef]

52. Kou, T.; Yang, Y.; Yao, B.; Li, Y. Interpenetrated bacteria-carbon nanotubes film for microbial fuel cells. *Small Methods* **2018**, *2*, 1800152. [CrossRef]

53. Tang, X.; Guo, K.; Li, H.; Du, Z.; Tian, J. Electrochemical treatment of graphite to enhance electron transfer from bacteria to electrodes. *Bioresour. Technol.* **2011**, *102*, 3558–3560. [CrossRef] [PubMed]

54. Zhou, M.; Chi, M.; Wang, H.; Jin, T. Anode modification by electrochemical oxidation: A new practical method to improve the performance of microbial fuel cells. *Biochem. Eng. J.* **2012**, *60*, 151–155. [CrossRef]

55. Scott, K.; Rimbu, G.A.; Katuri, K.P.; Prasad, K.K.; Head, I.M. Application of modified carbon anodes in microbial fuel cells. *Process Saf. Environ. Prot.* **2007**, *85*, 481–488. [CrossRef]

56. Feng, Y.; Yang, Q.; Wang, X.; Logan, B.E. Treatment of carbon fiber brush anodes for improving power generation in air-cathode microbial fuel cells. *J. Power Sources* **2010**, *195*, 1841–1844. [CrossRef]

57. Sanchez, D.; Jacobs, D.; Gregory, K.; Huang, J.; Hu, Y.; Vidic, R.; Yun, M. Changes in carbon electrode morphology affect microbial fuel cell performance with *Shewanella oneidensis* MR-1. *Energies* **2015**, *8*, 1817–1829. [CrossRef]

58. McDonough, J.R.; Choi, J.W.; Yang, Y.; La Mantia, F.; Zhang, Y.; Cui, Y. Carbon nanofiber supercapacitors with large areal capacitances. *Appl. Phys. Lett.* **2009**, *95*, 243109. [CrossRef]

59. Wu, L.; Zhang, H.; Ju, X. Detection of NADH and ethanol based on catalytic activity of soluble carbon nanofiber with low overpotential. *Anal. Chem.* **2006**, *79*, 453–458. [CrossRef]

60. Ra, E.J.; Raymundo-Piñero, E.; Lee, Y.H.; Béguin, F. High power supercapacitors using polyacrylonitrile-based carbon nanofiber paper. *Carbon N. Y.* **2009**, *47*, 2984–2992. [CrossRef]

61. Manickam, S.S.; Karra, U.; Huang, L.; Bui, N.N.; Li, B.; McCutcheon, J.R. Activated carbon nanofiber anodes for microbial fuel cells. *Carbon N. Y.* **2013**, *53*, 19–28. [CrossRef]

62. Bian, B.; Shi, D.; Cai, X.; Hu, M.; Guo, Q.; Zhang, C.; Wang, Q.; Sun, A.X.; Yang, J. 3D printed porous carbon anode for enhanced power generation in microbial fuel cell. *Nano Energy* **2018**, *44*, 174–180. [CrossRef]

63. Leng, Y.; Ming, P.; Yang, D.; Zhang, C. Stainless steel bipolar plates for proton exchange membrane fuel cells: Materials, flow channel design and forming processes. *J. Power Sources* **2020**, *451*, 227783. [CrossRef]

64. Pocaznoi, D.; Erable, B.; Etcheverry, L.; Delia, M.L.; Bergel, A. Towards an engineering-oriented strategy for building microbial anodes for microbial fuel cells. *Phys. Chem. Chem. Phys.* **2012**, *14*, 13332–13343. [CrossRef] [PubMed]

65. Hou, J.; Liu, Z.; Yang, S.; Zhou, Y. Three-dimensional macroporous anodes based on stainless steel fiber felt for high-performance microbial fuel cells. *J. Power Sources* **2014**, *258*, 204–209. [CrossRef]

66. Zheng, S.; Yang, F.; Chen, S.; Liu, L.; Xiong, Q.; Yu, T.; Zhao, F.; Schröder, U.; Hou, H. Binder-free carbon black/stainless steel mesh composite electrode for high-performance anode in microbial fuel cells. *J. Power Sources* **2015**, *284*, 252–257. [CrossRef]

67. Kargi, F.; Eker, S. Electricity generation with simultaneous wastewater treatment by a microbial fuel cell (MFC) with Cu and Cu–Au electrodes. *J. Chem. Technol. Biotechnol.* **2007**, *82*, 658–662. [CrossRef]

68. Rodenas Motos, P.; ter Heijne, A.; van der Weijden, R.; Saakes, M.; Buisman, C.J.N.; Sleutels, T.H.J.A. High rate copper and energy recovery in microbial fuel cells. *Front. Microbiol.* **2015**, *6*, 527. [CrossRef]

69. Sun, Z.; Cao, R.; Huang, M.; Chen, D.; Zheng, W.; Lin, L. Effect of light irradiation on the photoelectricity performance of microbial fuel cell with a copper oxide nanowire photocathode. *J. Photochem. Photobiol. A Chem.* **2015**, *300*, 38–43. [CrossRef]

70. Myung, J.; Yang, W.; Saikaly, P.E.; Logan, B.E. Copper current collectors reduce long-term fouling of air cathodes in microbial fuel cells. *Environ. Sci. Water Res. Technol.* **2018**, *4*, 513–519. [CrossRef]

71. Baudler, A.; Schmidt, I.; Langner, M.; Greiner, A.; Schröder, U. Does it have to be carbon? Metal anodes in microbial fuel cells and related bioelectrochemical systems. *Energy Environ. Sci.* **2015**, *8*, 2048–2055. [CrossRef]

72. Wang, Y.H.; Xi, H.; Lin, F.J.; Wang, B.S.; Chen, Q.Y. The effect of substrates and anodes on microbial fuel cell performance. In Proceedings of the 2011 International Symposium on Water Resource and Environmental Protection, Xi'an, China, 20–22 May 2011; pp. 1841–1843. [CrossRef]

73. Karthikeyan, R.; Krishnaraj, N.; Selvam, A.; Wong, J.W.C.; Lee, P.K.H.; Leung, M.K.H.; Berchmans, S. Effect of composites based nickel foam anode in microbial fuel cell using *Acetobacter aceti* and *Gluconobacter roseus* as a biocatalysts. *Bioresour. Technol.* **2016**, *217*, 113–120. [CrossRef] [PubMed]

74. Liu, J.; Liu, J.; He, W.; Qu, Y.; Ren, N.; Feng, Y. Enhanced electricity generation for microbial fuel cell by using electrochemical oxidation to modify carbon cloth anode. *J. Power Sources* **2014**, *265*, 391–396. [CrossRef]

75. Champigneux, P.; Renault-Sentenac, C.; Bourrier, D.; Rossi, C.; Délia, M.L.; Bergel, A. Effect of surface roughness, porosity and roughened micro-pillar structures on the early formation of microbial anodes. *Bioelectrochemistry* **2019**, *128*, 17–29. [CrossRef] [PubMed]

76. Guo, K.; Freguia, S.; Dennis, P.G.; Chen, X.; Donose, B.C.; Keller, J.; Gooding, J.J.; Rabaey, K. Effects of surface charge and hydrophobicity on anodic biofilm formation, community composition, and current generation in bioelectrochemical systems. *Environ. Sci. Technol.* **2013**, *47*, 7563–7570. [CrossRef]

77. Engel, C.; Schattenberg, F.; Dohnt, K.; Schröder, U.; Müller, S.; Krull, R. Long-term behavior of defined mixed cultures of *Geobacter sulfurreducens* and *Shewanella oneidensis* in bioelectrochemical systems. *Front. Bioeng. Biotechnol.* **2019**, *7*, 60. [CrossRef]

78. Lovley, D.R. Electromicrobiology. *Annu. Rev. Microbiol.* **2012**, *66*, 391–409. [CrossRef]

79. Ahmed, M.; Lin, O.; Saup, C.M.; Wilkins, M.J.; Lin, L.S. Effects of Fe/S ratio on the kinetics and microbial ecology of an Fe(III)-dosed anaerobic wastewater treatment system. *J. Hazard. Mater.* **2019**, *369*, 593–600. [CrossRef]

80. Qian, G.; Ye, L.; Li, L.; Hu, X.; Jiang, B.; Zhao, X. Influence of electric field and iron on the denitrification process from nitrogen-rich wastewater in a periodic reversal bio-electrocoagulation system. *Bioresour. Technol.* **2018**, *258*, 177–186. [CrossRef]

81. Lovley, D.R.; Phillips, E.J.P. Organic matter mineralization with reduction of ferric iron in anaerobic sediments. *Appl. Environ. Microbiol.* **1986**, *51*, 683–689. [CrossRef]

82. Fu, L.; Wang, H.; Huang, Q.; Song Shun, T.; Xie, J. Modification of carbon felt anode with graphene/Fe$_2$O$_3$ composite for enhancing the performance of microbial fuel cell. *Bioprocess Biosyst. Eng.* **2020**, *43*, 373–381. [CrossRef]

83. Yu, B.; Li, Y.; Feng, L. Enhancing the performance of soil microbial fuel cells by using a bentonite-Fe and Fe3O4 modified anode. *J. Hazard. Mater.* **2019**, *377*, 70–77. [CrossRef]

84. Li, C.; Zhou, K.; He, H.; Cao, J.; Zhou, S. Adding zero-valent iron to enhance electricity generation during MFC start-up. *Int. J. Environ. Res. Public Health* **2020**, *17*. [CrossRef]

85. Xu, H.; Quan, X.; Xiao, Z.; Chen, L. Effect of anodes decoration with metal and metal oxides nanoparticles on pharmaceutically active compounds removal and power generation in microbial fuel cells. *Chem. Eng. J.* **2018**, *335*, 539–547. [CrossRef]

86. Li, X.; Hu, M.; Zeng, L.; Xiong, J.; Tang, B.; Hu, Z.; Xing, L.; Huang, Q.; Li, W. Co-modified MoO$_2$ nanoparticles highly dispersed on N-doped carbon nanorods as anode electrocatalyst of microbial fuel cells. *Biosens. Bioelectron.* **2019**, *145*. [CrossRef]

87. Alahmadi, N.S.; Betts, J.W.; Cheng, F.; Francesconi, M.G.; Kelly, S.M.; Kornherr, A.; Prior, T.J.; Wadhawan, J.D. Synthesis and antibacterial effects of cobalt–cellulose magnetic nanocomposites. *RSC Adv.* **2017**, *7*, 20020–20026. [CrossRef]

88. Kooti, M.; Saiahi, S.; Motamedi, H. Fabrication of silver-coated cobalt ferrite nanocomposite and the study of its antibacterial activity. *J. Magn. Magn. Mater* **2013**, *333*, 138–143. [CrossRef]

89. Veeramani, V.; Rajangam, K.; Nagendran, J. Performance of cobalt oxide/carbon cloth composite electrode in energy generation from dairy wastewater using microbial fuel cells. *Sustain. Environ. Res.* **2020**, *30*, 1–8. [CrossRef]

90. Cui, Y.; Chen, X.; Pan, Z.; Wang, Y.; Xu, Q.; Bai, J.; Jia, H.; Zhou, J.; Yong, X.; Wu, X. Biosynthesized iron sulfide nanoparticles by mixed consortia for enhanced extracellular electron transfer in a microbial fuel cell. *Bioresour. Technol.* **2020**, *318*, 124095. [CrossRef]

91. Deng, X.; Dohmae, N.; Kaksonen, A.H.; Okamoto, A. Biogenic iron sulfide nanoparticles to enable extracellular electron uptake in sulfate-reducing bacteria. *Angew. Chemie* **2020**, *132*, 6051–6055. [CrossRef]

92. Murugan, M.; Miran, W.; Masuda, T.; Lee, D.S.; Okamoto, A. Biosynthesized iron sulfide nanocluster enhanced anodic current generation by sulfate reducing bacteria in microbial fuel cells. *Chem. Electro. Chem.* **2018**, *5*, 4015–4020. [CrossRef]

93. Blázquez, E.; Baeza, J.A.; Gabriel, D.; Guisasola, A. Treatment of real flue gas desulfurization wastewater in an autotrophic biocathode in view of elemental sulfur recovery: Microbial communities involved. *Sci. Total Environ.* **2019**, *657*, 945–952. [CrossRef] [PubMed]

94. Miran, W.; Jang, J.; Nawaz, M.; Shahzad, A.; Lee, D.S. Sulfate-reducing mixed communities with the ability to generate bioelectricity and degrade textile diazo dye in microbial fuel cells. *J. Hazard. Mater.* **2018**, *352*, 70–79. [CrossRef] [PubMed]

95. Rodrigues, I.C.B.; Leão, V.A. Producing electrical energy in microbial fuel cells based on sulphate reduction: A review. *Environ. Sci. Pollut. Res.* **2020**, *27*, 36075–36084. [CrossRef]

96. Huo, Y.C.; Li, W.W.; Chen, C.B.; Li, C.X.; Zeng, R.; Lau, T.C.; Huang, T.Y. Biogenic FeS accelerates reductive dechlorination of carbon tetrachloride by *Shewanella putrefaciens* CN32. *Enzyme Microb. Technol.* **2016**, *95*, 236–241. [CrossRef] [PubMed]

97. Blatter, M.; Furrer, C.; Cachelin, C.P.; Fischer, F. Phosphorus, chemical base and other renewables from wastewater with three 168-L microbial electrolysis cells and other unit operations. *Chem. Eng. J.* **2020**, *390*, 124502. [CrossRef]

98. Zhou, L.; Liu, J.; Dong, F. Spectroscopic study on biological mackinawite (FeS) synthesized by ferric reducing bacteria (FRB) and sulfate reducing bacteria (SRB): Implications for in-situ remediation of acid mine drainage. *Spectrochim. Acta Part A Mol. Biomol. Spectrosc.* **2017**, *173*, 544–548. [CrossRef] [PubMed]

99. Nosek, D.; Cydzik-Kwiatkowska, A. Microbial structure and energy generation in microbial fuel cells powered with waste anaerobic digestate. *Energies* **2020**, *13*, 4712. [CrossRef]

100. Zou, X.; Zhang, L.; Wang, Z.; Luo, Y. Mechanisms of the antimicrobial activities of graphene materials. *J. Am. Chem. Soc.* **2016**, *138*, 2064–2077. [CrossRef]

101. Perreault, F.; De Faria, A.F.; Nejati, S.; Elimelech, M. Antimicrobial properties of graphene oxide nanosheets: Why size matters. *ACS Nano* **2015**, *9*, 7226–7236. [CrossRef]

102. Kim, H.; Abdala, A.A.; MacOsko, C.W. Graphene/polymer nanocomposites. *Macromolecules* **2010**, *43*, 6515–6530. [CrossRef]

103. Lee, C.; Wei, X.; Kysar, J.W.; Hone, J. Measurement of the elastic properties and intrinsic strength of monolayer graphene. *Science* **2008**, *321*, 385–388. [CrossRef] [PubMed]

104. Wu, Y.; Wang, L.; Jin, M.; Kong, F.; Qi, H.; Nan, J. Reduced graphene oxide and biofilms as cathode catalysts to enhance energy and metal recovery in microbial fuel cell. *Bioresour. Technol.* **2019**, *283*, 129–137. [CrossRef] [PubMed]

105. Paul, D.; Noori, M.T.; Rajesh, P.P.; Ghangrekar, M.M.; Mitra, A. Modification of carbon felt anode with graphene oxide-zeolite composite for enhancing the performance of microbial fuel cell. *Sustain. Energy Technol. Assessments* **2018**, *26*, 77–82. [CrossRef]

106. Poland, C.; Hankin, S.; de Brouwere, K.; Holderberke, V.M. *Carbon Nanotubes Criteria Document for the Scientific Committee on Occupational Exposure Limits (SCOEL)*; Finish Raport; European Commission Joint Research Centre: Ispra, Italy, 2012.

107. Lekawa-Raus, A.; Patmore, J.; Kurzepa, L.; Bulmer, J.; Koziol, K. Electrical properties of carbon nanotube based fibers and their future use in electrical wiring. *Adv. Funct. Mater.* **2014**, *24*, 3661–3682. [CrossRef]

108. Liang, Y.; Zhai, H.; Liu, B.; Ji, M.; Li, J. Carbon nanomaterial-modified graphite felt as an anode enhanced the power production and polycyclic aromatic hydrocarbon removal in sediment microbial fuel cells. *Sci. Total Environ.* **2020**, *713*. [CrossRef]

109. Thepsuparungsikul, N.; Ng, T.C.; Lefebvre, O.; Ng, H.Y. Different types of carbon nanotube-based anodes to improve microbial fuel cell performance. *Water Sci. Technol.* **2014**, *69*, 1900–1910. [CrossRef]

110. Zhang, Y.; Chen, X.; Yuan, Y.; Lu, X.; Yang, Z.; Wang, Y.; Sun, J. Long-term effect of carbon nanotubes on electrochemical properties and microbial community of electrochemically active biofilms in microbial fuel cells. *Int. J. Hydrogen Energy* **2018**, *43*, 16240–16247. [CrossRef]

111. Wang, Y.; Chen, Y.; Wen, Q.; Zheng, H.; Xu, H.; Qi, L. Electricity generation, energy storage, and microbial-community analysis in microbial fuel cells with multilayer capacitive anodes. *Energy* **2019**, *189*, 116342. [CrossRef]

112. Silva, T.A.; Moraes, F.C.; Janegitz, B.C.; Fatibello-Filho, O.; Ganta, D. Electrochemical biosensors based on nanostructured carbon black: A review. *J. Nanomater.* **2017**, *4571614*. [CrossRef]

113. Zheng, J.; Cheng, C.; Zhang, J.; Wu, X. Appropriate mechanical strength of carbon black-decorated loofah sponge as anode material in microbial fuel cells. *Int. J. Hydrogen Energy* **2016**, *41*, 23156–23163. [CrossRef]

114. Liu, S.H.; Lai, Y.C.; Lin, C.W. Enhancement of power generation by microbial fuel cells in treating toluene-contaminated groundwater: Developments of composite anodes with various compositions. *Appl. Energy* **2019**, *233–234*, 922–929. [CrossRef]

115. Gajda, I.; Greenman, J.; Ieropoulos, I. Microbial Fuel Cell stack performance enhancement through carbon veil anode modification with activated carbon powder. *Appl. Energy* **2020**, *262*, 114475. [CrossRef] [PubMed]

116. Lan, L.; Li, J.; Feng, Q.; Zhang, L.; Fu, Q.; Zhu, X.; Liao, Q. Enhanced current production of the anode modified by microalgae derived nitrogen-rich biocarbon for microbial fuel cells. *Int. J. Hydrogen Energy* **2020**, *45*, 3833–3839. [CrossRef]

117. Fan, M.; Zhang, W.; Sun, J.; Chen, L.; Li, P.; Chen, Y.; Zhu, S.; Shen, S. Different modified multi-walled carbon nanotube–based anodes to improve the performance of microbial fuel cells. *Int. J. Hydrogen Energy* **2017**, *42*, 22786–22795. [CrossRef]

118. Aryal, R.; Beltran, D.; Liu, J. Effects of Ni nanoparticles, MWCNT, and MWCNT/Ni on the power production and the wastewater treatment of a microbial fuel cell. *Int. J. Green Energy* **2019**, *16*, 1391–1399. [CrossRef]

119. Yang, J.; Cheng, S.; Sun, Y.; Li, C. Improving the power generation of microbial fuel cells by modifying the anode with single-wall carbon nanohorns. *Biotechnol. Lett.* **2017**, *39*, 1515–1520. [CrossRef]

120. Wang, Y.; Pan, X.; Chen, Y.; Wen, Q.; Lin, C.; Zheng, J.; Li, W.; Xu, H.; Qi, L. A 3D porous nitrogen-doped carbon nanotube sponge anode modified with polypyrrole and carboxymethyl cellulose for high-performance microbial fuel cells. *J. Appl. Electrochem.* **2020**, *50*, 1281–1290. [CrossRef]

121. Song, R.B.; Zhao, C.E.; Jiang, L.P.; Abdel-Halim, E.S.; Zhang, J.R.; Zhu, J.J. Bacteria-affinity 3D macroporous graphene/MWCNTs/Fe₃O₄ foams for high-performance microbial fuel cells. *ACS Appl. Mater. Interfaces* **2016**, *8*, 16170–16177. [CrossRef]

122. Yang, X.; Ma, X.; Wang, K.; Wu, D.; Lei, Z.; Feng, C. Eighteen-month assessment of 3D graphene oxide aerogel-modified 3D graphite fiber brush electrode as a high-performance microbial fuel cell anode. *Electrochim. Acta* **2016**, *210*, 846–853. [CrossRef]

123. Xing, X.; Liu, Z.; Chen, W.; Lou, X.; Li, Y.; Liao, Q. Self-nitrogen-doped carbon nanosheets modification of anodes for improving microbial fuel cells' performance. *Catalysts* **2020**, *10*, 381. [CrossRef]

124. Liu, Y.; Zhang, X.; Zhang, Q.; Li, C. Microbial fuel cells: Nanomaterials based on anode and their application. *Energy Technol.* **2020**, *8*, 2000206. [CrossRef]

125. Lai, B.; Tang, X.; Li, H.; Du, Z.; Liu, X.; Zhang, Q. Power production enhancement with a polyaniline modified anode in microbial fuel cells. *Biosens. Bioelectron.* **2011**, *28*, 373–377. [CrossRef] [PubMed]

126. Mashkour, M.; Rahimnejad, M.; Mashkour, M.; Soavi, F. Electro-polymerized polyaniline modified conductive bacterial cellulose anode for supercapacitive microbial fuel cells and studying the role of anodic biofilm in the capacitive behavior. *J. Power Sources* **2020**, *478*, 228822. [CrossRef]

127. Kirubaharan, C.J.; Kumar, G.G.; Sha, C.; Zhou, D.; Yang, H.; Nahm, K.S.; Raj, B.S.; Zhang, Y.; Yong, Y.C. Facile fabrication of Au/polyaniline core-shell nanocomposite as efficient anodic catalyst for microbial fuel cells. *Electrochim. Acta* **2019**, *328*, 135136. [CrossRef]

128. Zhang, W.; Xie, B.; Yang, L.; Liang, D.; Zhu, Y.; Liu, H. Brush-like polyaniline nanoarray modified anode for improvement of power output in microbial fuel cell. *Bioresour. Technol.* **2017**, *233*, 291–295. [CrossRef]

129. Du, Q.; An, J.; Li, J.; Zhou, L.; Li, N.; Wang, X. Polydopamine as a new modification material to accelerate startup and promote anode performance in microbial fuel cells. *J. Power Sources* **2017**, *343*, 477–482. [CrossRef]

130. Zeng, L.; Chen, X.; Li, H.; Xiong, J.; Hu, M.; Li, X.; Li, W. Highly dispersed polydopamine-modified Mo2C/MoO2 nanoparticles as anode electrocatalyst for microbial fuel cells. *Electrochim. Acta* **2018**, *283*, 528–537. [CrossRef]

131. Li, Y.; Liu, J.; Chen, X.; Yuan, X.; Li, N.; He, W.; Feng, Y. Enhanced electricity generation and extracellular electron transfer by polydopamine–reduced graphene oxide (PDA–rGO) modification for high-performance anode in microbial fuel cell. *Chem. Eng. J.* **2020**, *387*, 123408. [CrossRef]

132. Pu, K.B.; Ma, Q.; Cai, W.F.; Chen, Q.Y.; Wang, Y.H.; Li, F.J. Polypyrrole modified stainless steel as high performance anode of microbial fuel cell. *Biochem. Eng. J.* **2018**, *132*, 255–261. [CrossRef]

133. Ghasemi, M.; Wan Daud, W.R.; Hassan, S.H.A.; Jafary, T.; Rahimnejad, M.; Ahmad, A.; Yazdi, M.H. Carbon nanotube/polypyrrole nanocomposite as a novel cathode catalyst and proper alternative for Pt in microbial fuel cell. *Int. J. Hydrogen Energy* **2016**, *41*, 4872–4878. [CrossRef]

134. Zhao, X.; Deng, W.; Tan, Y.; Xie, Q. Promoting electricity generation of *Shewanella putrefaciens* in a microbial fuel cell by modification of porous poly(3-aminophenylboronic acid) film on carbon anode. *Electrochim. Acta* **2020**, *354*, 136715. [CrossRef]

135. Cui, H.F.; Du, L.; Guo, P.B.; Zhu, B.; Luong, J.H. Controlled modification of carbon nanotubes and polyaniline on macroporous graphite felt for high-performance microbial fuel cell anode. *J. Power Sources* **2015**, *283*, 46–53. [CrossRef]

136. Mukherjee, P.; Saravanan, P. Graphite nanopowder functionalized 3-D acrylamide polymeric anode for enhanced performance of microbial fuel cell. *Int. J. Hydrog. Energy* **2020**, *45*, 23411–23421. [CrossRef]

137. Liu, H.; Zhang, Z.; Xu, Y.; Tan, X.; Yue, Z.; Ma, K.; Wang, Y. Reduced graphene oxide@ polydopamine decorated carbon cloth as an anode for a high-performance microbial fuel cell in Congo red/saline wastewater removal. *Bioelectrochemistry* **2020**, *137*, 107675. [CrossRef]

138. Wang, Y.; Zhu, L.; An, L. Electricity generation and storage in microbial fuel cells with porous polypyrrole-base composite modified carbon brush anodes. *Renew. Energy* **2020**, *162*, 2220–2226. [CrossRef]

139. Wang, Y.; Wen, Q.; Chen, Y.; Li, W. Conductive polypyrrole-carboxymethyl cellulose-titanium nitride/carbon brush hydrogels as bioanodes for enhanced energy output in microbial fuel cells. *Energy* **2020**, *204*. [CrossRef]

140. Sonawane, J.M.; Patil, S.A.; Ghosh, P.C.; Adeloju, S.B. Low-cost stainless-steel wool anodes modified with polyaniline and polypyrrole for high-performance microbial fuel cells. *J. Power Sources* **2018**, *379*, 103–114. [CrossRef]

141. Jia, Y.; Ma, D.; Wang, X. Electrochemical preparation and application of PANI/MWNT and PPy/MWNT composite anodes for anaerobic fluidized bed microbial fuel cell. *3 Biotech* **2020**, *10*, 3. [CrossRef]

142. Li, F.; Wang, D.; Liu, Q.; Wang, B.; Zhong, W.; Li, M.; Liu, K.; Lu, Z.; Jiang, H.; Zhao, Q.; et al. The construction of rod-like polypyrrole network on hard magnetic porous textile anodes for microbial fuel cells with ultra-high output power density. *J. Power Sources* **2019**, *412*, 514–519. [CrossRef]

143. Wu, G.; Bao, H.; Xia, Z.; Yang, B.; Lei, L.; Li, Z.; Liu, C. Polypyrrole/sargassum activated carbon modified stainless-steel sponge as high-performance and low-cost bioanode for microbial fuel cells. *J. Power Sources* **2018**, *384*, 86–92. [CrossRef]

144. Li, Z.L.; Yang, S.K.; Song, Y.; Xu, H.Y.; Wang, Z.Z.; Wang, W.K.; Zhao, Y.Q. Performance evaluation of treating oil-containing restaurant wastewater in microbial fuel cell using in situ graphene/polyaniline modified titanium oxide anode. *Environ. Technol.* **2020**, *41*, 420–429. [CrossRef] [PubMed]

145. Rajesh, P.P.; Noori, M.T.; Ghangrekar, M.M. Improving performance of microbial fuel cell by using polyaniline-coated carbon–felt anode. *J. Hazard. Toxic Radioact. Waste* **2020**, *24*, 04020024. [CrossRef]

146. Yin, T.; Zhang, H.; Yang, G.; Wang, L. Polyaniline composite TiO$_2$ nanosheets modified carbon paper electrode as a high performance bioanode for microbial fuel cells. *Synth. Met.* **2019**, *252*, 8–14. [CrossRef]

147. Zhao, N.; Ma, Z.; Song, H.; Wang, D.; Xie, Y. Polyaniline/reduced graphene oxide-modified carbon fiber brush anode for high-performance microbial fuel cells. *Int. J. Hydrogen Energy* **2018**, *43*, 17867–17872. [CrossRef]

148. Jia, Y.H.; Qi, Z.L.; You, H. Power production enhancement with polyaniline composite anode in benthic microbial fuel cells. *J. Cent. South Univ.* **2018**, *25*, 499–505. [CrossRef]

149. Liu, X.; Zhao, X.; Yu, Y.Y.; Wang, Y.Z.; Shi, Y.T.; Cheng, Q.W.; Fang, Z.; Yong, Y.C. Facile fabrication of conductive polyaniline nanoflower modified electrode and its application for microbial energy harvesting. *Electrochim. Acta* **2017**, *255*, 41–47. [CrossRef]

150. Sumisha, A.; Haribabu, K. Modification of graphite felt using nano polypyrrole and polythiophene for microbial fuel cell applications a comparative study. *Int. J. Hydrogen Energy* **2018**, *43*, 3308–3316. [CrossRef]

151. Wang, G.; Feng, C. Electrochemical polymerization of hydroquinone on graphite felt as a pseudocapacitive material for application in a microbial fuel cell. *Polymers* **2017**, *9*, 220. [CrossRef]

152. Zhong, D.; Liao, X.; Liu, Y.; Zhong, N.; Xu, Y. Quick start-up and performance of microbial fuel cell enhanced with a polydiallyldimethylammonium chloride modified carbon felt anode. *Biosens. Bioelectron.* **2018**, *119*, 70–78. [CrossRef]

153. Chen, X.; Li, Y.; Yuan, X.; Li, N.; He, W.; Liu, J. Synergistic effect between poly (diallyldimethylammonium chloride) and reduced graphene oxide for high electrochemically active biofilm in microbial fuel cell. *Electrochim. Acta* **2020**, *359*, 136949. [CrossRef]

154. Chen, Y.Y.; Wang, H.Y. Fabrication and characterization of polyelectrolyte microcarriers for microorganism cultivation through a microfluidic droplet system. *Biomicrofluidics* **2016**, *10*, 014126. [CrossRef]

155. Lin, X.Q.; Li, Z.L.; Liang, B.; Nan, J.; Wang, A.J. Identification of biofilm formation and exoelectrogenic population structure and function with graphene/polyanliline modified anode in microbial fuel cell. *Chemosphere* **2019**, *219*, 358–364. [CrossRef] [PubMed]

Olsztyn, 21.08.2024

(miejscowość, data)

mgr inż. Dawid Nosek

(imię i nazwisko)

Przewodniczący Rady Naukowej Dyscypliny

prof. dr hab. inż. Marcin Dębowski

Uniwersytetu Warmińsko-Mazurskiego w Olsztynie

OŚWIADCZENIE

kandydata

Oświadczam, że w pracy pod tytułem:

Nosek D., Jachimowicz P., Cydzik-Kwiatkowska A. (2020). Anode modification as an alternative approach to improve electricity generation in microbial fuel cells. Energies 13(24), 6596, mój wkład merytoryczny w jej przygotowanie polegał na: zaplanowaniu koncepcji pracy, pozyskaniu i opracowaniu i interpretacji danych literaturowych, graficznym opracowaniu wyników oraz przygotowaniu pierwszej wersji manuskryptu.

Dawid Nosek

(podpis)

66:1024714978

Piotr Jachimowicz

(imię i nazwisko)

Przewodniczący Rady Naukowej Dyscypliny

prof. dr hab. inż. Marcin Dębowski

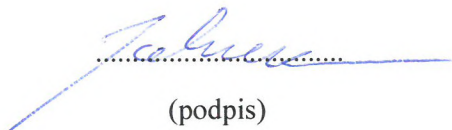**Uniwersytetu Warmińsko-Mazurskiego w Olsztynie**

OŚWIADCZENIE

współautora

Oświadczam, że w pracy pod tytułem:

Nosek D., Jachimowicz P., Cydzik-Kwiatkowska A. (2020). Anode modification as an alternative approach to improve electricity generation in microbial fuel cells. Energies 13(24), 6596, mój wkład merytoryczny w jej przygotowanie polegał na: uczestnictwie w pozyskaniu i opracowaniu danych literaturowych oraz graficznym przedstawieniu zebranych informacji.

Jednocześnie wyrażam zgodę na przedłożenie w/w pracy przez Pana Dawida Noska jako część rozprawy doktorskiej w formie spójnego tematycznie zbioru artykułów naukowych opublikowanych w czasopismach naukowych. Oświadczam, iż samodzielna i możliwa do wyodrębnienia część ww. pracy wykazuje indywidualny wkład kandydata Pana Dawida Noska polegający na:

udziale w zaplanowaniu koncepcji pracy, pozyskaniu i opracowaniu i interpretacji danych literaturowych, graficznym opracowaniu wyników oraz przygotowaniu pierwszej wersji manuskryptu.

(podpis)

prof. zw. dr hab. inż. Agnieszka Cydzik-Kwiatkowska

(imię i nazwisko)

Przewodniczący Rady Naukowej Dyscypliny
prof. dr hab. inż. Marcin Dębowski
Uniwersytetu Warmińsko-Mazurskiego w Olsztynie

OŚWIADCZENIE

współautora

Oświadczam, że w pracy pod tytułem:

Nosek D., Jachimowicz P., Cydzik-Kwiatkowska A. (2020). Anode modification as an alternative approach to improve electricity generation in microbial fuel cells. Energies 13(24), 6596, mój wkład merytoryczny w jej przygotowanie polegał na: udziale w zaplanowaniu koncepcji pracy, recenzowaniu i edycji tekstu, merytorycznym nadzorze pracy i pozyskaniu środków finansowych.

Jednocześnie wyrażam zgodę na przedłożenie w/w pracy przez Pana Dawida Noska jako część rozprawy doktorskiej w formie spójnego tematycznie zbioru artykułów naukowych opublikowanych w czasopismach naukowych. Oświadczam, iż samodzielna i możliwa do wyodrębnienia część ww. pracy wykazuje indywidualny wkład kandydata Pana Dawida Noska polegający na:

udziale w zaplanowaniu koncepcji pracy, pozyskaniu, opracowaniu i interpretacji danych literaturowych, graficznym opracowaniu wyników oraz przygotowaniu pierwszej wersji manuskryptu.

(podpis)

68:1143265700

Praca nr 2

Nosek D., Cydzik-Kwiatkowska A.

Microbial structure and energy generation in microbial fuel cells powered with waste anaerobic digestate.

Energies

2020

Microbial Structure and Energy Generation in Microbial Fuel Cells Powered with Waste Anaerobic Digestate

Dawid Nosek * and Agnieszka Cydzik-Kwiatkowska

Department of Environmental Biotechnology, University of Warmia and Mazury in Olsztyn, Słoneczna 45 G, 10-709 Olsztyn, Poland; agnieszka.cydzik@uwm.edu.pl

* Correspondence: dawid.nosek@uwm.edu.pl; Tel.: +48-89-523-4144; Fax: +48-89-523-4131

Abstract: Development of economical and environment-friendly Microbial Fuel Cells (MFCs) technology should be associated with waste management. However, current knowledge regarding microbiological bases of electricity production from complex waste substrates is insufficient. In the following study, microbial composition and electricity generation were investigated in MFCs powered with waste volatile fatty acids (VFAs) from anaerobic digestion of primary sludge. Two anode sizes were tested, resulting in organic loading rates (OLRs) of 69.12 and 36.21 mg chemical oxygen demand (COD)/(g MLSS·d) in MFC1 and MFC2, respectively. Time of MFC operation affected the microbial structure and the use of waste VFAs promoted microbial diversity. High abundance of *Deftia* sp. and *Methanobacterium* sp. characterized start-up period in MFCs. During stable operation, higher OLR in MFC1 favored growth of exoelectrogens from *Rhodopseudomonas* sp. (13.2%) resulting in a higher and more stable electricity production in comparison with MFC2. At a lower OLR in MFC2, the percentage of exoelectrogens in biomass decreased, while the abundance of genera *Leucobacter, Frigoribacterium* and *Phenylobacterium* increased. In turn, this efficiently decomposed complex organic substances, favoring high and stable COD removal (over 85%). Independent of the anode size, *Clostridium* sp. and exoelectrogens belonging to genera *Desulfobulbus* and *Acinetobacter* were abundant in MFCs powered with waste VFAs.

Keywords: MFC; *Rhodopseudomonas*; anode surface; waste VFA; NGS

1. Introduction

In view of the increasing demand for electricity, sustainable production of electricity from renewable sources by microorganisms is considered an alternative to the generation of energy based on fossil fuels. One of the most attractive solutions are Microbial Fuel Cells (MFCs), which use the metabolism of microorganisms to produce electricity by oxidizing organic substances on the anode and transferring the produced electrons to the cathode without using mediators [1,2].

Most studies on MFCs have been conducted using simple substrates such as glucose or acetate [3,4]. The use of pure acetic acid or its salt in the form of sodium acetate allows for the efficient production of electricity at a high coulombic efficiency [5,6]. Unfortunately, such solution is expensive. To develop economical MFC technology, electricity production should be associated with waste management. The use of complex waste substrates may, however, result in a lower efficiency of electricity generation because microorganisms need time to degrade the complex organic compounds, often present in form of suspensions. To date, waste substances such as molasses, wastewater or food waste have been used to power MFCs [7–9]. The use of wastewater streams rich in short chain fatty acids (volatile fatty acids (VFAs)), which are formed as a result of hydrolysis of organic compounds during acid fermentation,

is an environment-friendly solution. Freguia et al. [10] investigated the use of VFAs in two-chamber MFCs. After about 30 days of operation, they reached a constant current level of 21 ± 2 mA, and mainly acetate and propionate were taken as electron donors. The remaining VFAs, i.e., butyric, valerian and capron acids, were removed at a lower rate. For waste treatment, MFC competes directly with anaerobic digestion (AD), which is already widely practiced and also commercially implemented in large factories, albeit no electricity is directly produced. In comparison with conventional AD, the MFC technology holds specific advantages, such as its applicability for the treatment of substrates with low concentration at temperatures below 20 °C. This provides specific niche applications that do not compete with, but complement, the AD technology.

The conversion of biomass to electricity depends on the composition of the microbial community. Microorganisms in MFC may play different roles. The most important group from the perspective of electricity generation are exoelectrogens, which transfer electrons to the anode [11]. Electrochemically inactive microorganisms are also important because they degrade complex substrates to a simpler one that can be used by exoelectrogens [12,13]. Some microorganisms support defense properties of biofilm and protect other bacteria from unfavorable environmental conditions e.g., a presence of heavy metals [14]. It has been shown that in acetate-based biofilms *Deltaproteobacteria* transfer electrons directly to the anode, while *Clostridia* are responsible for the transformation of complex substrates [15,16]. In MFCs fed with acetate, abundant populations of *Synergistetes*, *Bacteroidetes*, *Proteobacteria* and *Firmicutes* have been observed in anode biofilms [17]. The main groups of anode microorganisms in a two-chamber MFC with graphite electrodes powered with food waste were *Firmicutes*, *Bacteroidetes* and *Proteobacteria* represented by classes *Bacilli*, *Bacteroidia*, *Deltaproteobacteria* and *Gammaproteobacteria* [18]. The predominant exoelectrogen was *Geobacter* sp., that directly transported electrons to the anode using highly conductive type c cytochromes and pili.

The up-scaling of MFCs requires investigations on new materials and reactor configurations because the enlargement of MFCs increases internal electricity losses, which results in a relatively low output power. Peixoto et al. [19] indicated the suitability of compact, flat MFCs for wastewater treatment as a solution for autonomous service in decentralized wastewater treatment systems. A larger active anode surface can increase the MFC output power until the cathode reaction becomes limited, because the large surface provides more space for microorganisms [20]. The impact of anode size on electricity generation in MFCs was investigated by Lanas et al. [21] and Rossi et al. [22]. Lanas et al. [21] used carbon fiber brushes and sodium acetate as a substrate in single-chamber MFCs. In batch mode, the configuration with three larger brushes (25 mm diameter) produced 80% more power than reactors with eight smaller brushes. Rossi et al. [22] used graphite fiber brushes and primary clarifier effluent in single-chamber MFCs. Reducing the diameter of the anode brushes from 5.1 to 2.5 cm did not improve the anode performance, however, the electrode spacing and hydraulic flow were important for MFC performance. Information about the impact of anode size on microorganism and energy production in MFCs powered with complex waste substrates is, however, insufficient and suggests the novelty of the study.

The aim of this study was to examine to the effect of the anode size on the microbiological structure of the anode and the efficiency of energy generation in MFCs fed with waste organics. In the study, volatile fatty acids (VFAs) from AD of primary sludge were used to generate electricity in line with the assumptions of a circular economy.

2. Materials and Methods

2.1. Reactor Set-Up

The experiment was carried out in two identical dual-chamber reactors (H type) made of Plexiglas with cathode and anode chambers, each with a volume of 1L; the active volume of the anode chambers was 700 mL. A Nafion 117 (Alfa Aesar) proton exchange membrane (PEM) with a surface of 8.5 cm^2 was placed between anode and cathode chamber as shown in Figure S1. PEM was treated with 1M

HCl for 30 min and then rinsed with distilled water before use. The electrodes were made of carbon felt (CGT Carbon GmbH, Asbach, Germany) and, without pre-treatment, they were applied to a Zn-Fe wire. In MFC1, the anode was made of 20 carbon felt discs (each disc with a 30 cm^2 surface, total surface area was 600 cm^2). In MFC2, the anode had a surface area of 1200 cm^2 (40 carbon felt discs). In both MFCs the cathode surface was 70 cm^2. The external circuit, connecting the anode and cathode, was made of copper wire connected with a 1-kΩ resistor. The catholyte consisted of 5 g NaCl and 50 mL of phosphate buffer in 1L of distilled water. The catholyte was adjusted to pH 7 with 1M NaOH and 1M HCl.

2.2. Medium and Operation

MFCs were inoculated with 50 mL of aerobic granular sludge from a full-scale wastewater treatment plant in Lubawa (Poland). The microbial characteristics of the inoculum are presented in Świątczak and Cydzik-Kwiatkowska [23]. The process was carried out using a VFAs mixture from AD of primary sludge in a wastewater treatment plant in Olsztyn (Poland) as an electron donor. Characteristics of the VFAs mixture were as follows: 2049 ± 505.5 mg COD/L; 1512.5 ± 164.3 mg BOD_5/L; 648 ± 123.2 mg VFA/L; 192.2 ± 32.1 mg TN/L; 45.4 ± 5.9 mg TP/L; 1750.0 ± 132.0 mg TSS/L. VFAs mixture was sieved through a 2-mm sieve and stored at 4 °C. The anolyte was replaced every 24 h and mixed with crude VFAs in such a ratio that the COD value was about 750 mg COD/L. The pH was adjusted to 7 with 1M NaOH and 1M HCl. The organic loading rate (OLR) in both MFCs was 750 mg COD/(L·d) corresponding to 69.12 and 36.21 mg COD/(g Mixed Liquor Suspended Solids (MLSS·d)) in MFC1 and MFC2, respectively. The MFCs were run for 90 days at room temperature, the OLRs were kept constant throughout the experiment.

2.3. Chemical Analyses

Chemical analyzes of the effluent from the anode chamber included COD concentration, VFA and pH. COD was determined by the cuvette test (Hach Lange, Wrocław, Poland), VFA by distillation according to APHA [24] and pH using TitroLine (Donserv, Warsaw, Poland). Biomass was determined by the weighting method in accordance with APHA [24]. Polarization and power curves were determined according to Watson and Logan [25] using a True-RMS multimeter changing the external resistance of the cell in the range of 30–120,000 Ω. For data collection, the 6600 Counts PC-LINK data acquisition unit was used to record voltage changes every minute. The current was calculated from external resistance using Ohm's law. All calculations were carried out in accordance with Logan et al. [1]. Coulombic efficiency (CE) was determined by using the Equation (1):

$$CE = \frac{M \int_0^{th} I dt}{F \cdot b \cdot v \cdot \Delta COD} \tag{1}$$

where M is molecular weight of oxygen, F is Faraday's constant, b is a number of electron exchanged per mole of oxygen, v is volume of liquid in the anode chamber and ΔCOD is change in COD concentration over time (t_h).

2.4. Microbial Analyses

During the operation of the reactors, samples of inoculum and biomass and supernatant from MFC1 and MFC2 powered with VFAs were collected to analyze microbial composition with next-generation sequencing (NGS). The biomass was collected at 6th, 42th, 61th, 72th, and 87th day of the experiment. The mixture of biomass and supernatant was centrifuged at 13,000 rpm for 10 min. The collected pellets were stored at −20 °C and at the end of the experiment DNA was isolated from all samples using FastDNA® SPIN® Kit For Soil (Q-BIO gene). The quantity and quality of DNA was assessed with the use of NanoDrop spectrophotometer (Thermo Scientific, Waltham, MA, USA) and agarose electrophoresis. The samples were then amplified using primers

515F/806R (GTGCCAGCMGCCGCGGTAA/GGACTACHVGGGTWTCTAAT) targeting the V4 region of the bacterial 16S rDNA gene and sequenced using MiSeq Illumina Platform in Research and Testing Laboratory (USA). Over 400 thousand full sequences were obtained (Table 1). The obtained sequences were analyzed bioinformatically as described in Świątczak and Cydzik-Kwiatkowska [23]. Because the samples were obtained in the same run and characterized by similar amounts of sequences, to avoid loss of data, the data were not normalized. For calculations and visualizations, the ampvis2 package [26] for R version 3.6.2 [27] in the RStudio environment, version 0.99 were used. Diversity of samples was assessed at a genus level using the Shannon index of diversity [28]. A value of $p \leq 0.05$ was defined as significant. The sequences have been deposited in the NCBI Sequence Read Archive (SRA) as the experiment entitled "MFC reactors Raw sequence reads" (Accession: PRJNA646600).

Table 1. Molecular indicators in Microbial Fuel Cell (MFC)1 and MFC2.

Day	MFC1			MFC2		
	Operational Taxonomic Units (OTUs)	Shannon	Reads	OTUs	Shannon	Reads
6	1019	3.963	38,439	1026	4.548	40,590
42	466	2.934	43,939	673	4.044	32,622
61	1026	4.869	57,866	1155	5.423	40,904
72	984	4.808	40,880	1027	5.219	37,040
87	905	4.907	41,054	823	4.906	41,304

The technological and molecular results were statistically analyzed in the Statistica 13.1 (StatSoft) using Student's t-test. The results were considered significant at $p < 0.05$.

3. Results and Discussion

3.1. Electricity Generation

After the addition of a fresh substrate, cell voltage increased rapidly to 50–70 mV (Figure 1a) and 80–90 mV (Figure 1b) in MFC1 and MFC2, respectively, and then gradually decreased to about 20–30 mV.
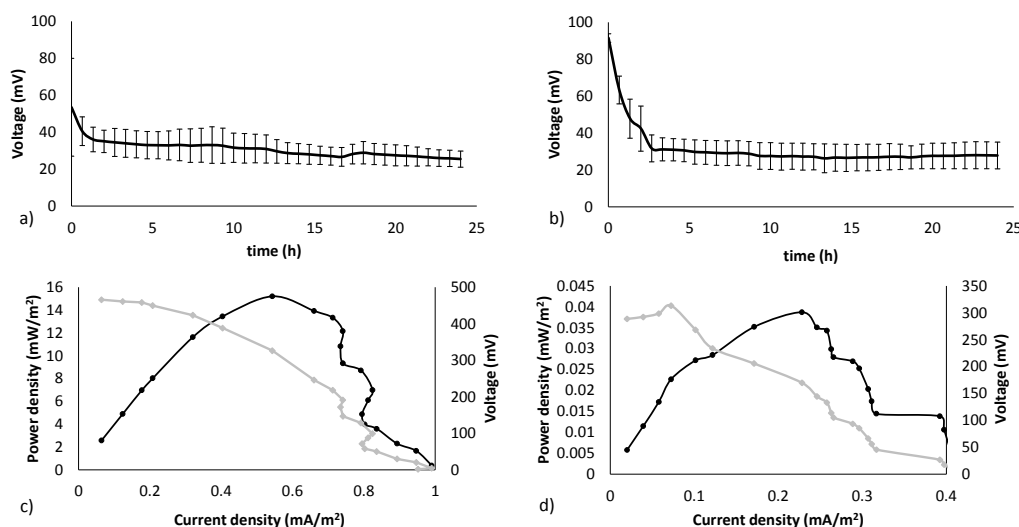

Figure 1. The averaged voltage in an MFC cycle ($n = 7$) in (**a**) MFC1 and (**b**) MFC2 and polarization (grey line) and power curves (black line) in (**c**) MFC1 and (**d**) MFC2; bars represent standard deviation; the arrows show the affiliation of the curve to the axis.

Although the anode in MFC2 was larger, it did not result in a better power generation, because the voltages were only initially higher than in MFC1, and after reaching a plateau they oscillated at a

similar level. The current density after reaching the plateau in MFC1 (836 ± 128 $\mu A/m^2$) was about 2.6 times higher than in MFC2 (316 ± 101 $\mu A/m^2$). The power density was 3.5 mW/m^2 in MFC1 and $1.03 \cdot 10^{-2}$ mW/m^2 in MFC2. In studies of Choi et al. [29], it was observed that for 100 h after feeding of MFC (1 kΩ resistance) with VFAs mixture, a stable, low voltage of 174 mV was generated, and the power density was 15.3 mW/m^2. The higher MFC power than in our study may have resulted from the use of a platinum coating on the cathode: such a coating accelerates the cathode reactions [30].

Power curves show that the power of the cells increased with the increase in external resistance. The highest power obtained in MFC1 was 15.2 mW/m^2 at a current density of 0.54 mA/m^2 (external resistance of 10 kΩ) (Figure 1c). Under normal conditions, the cell worked at a lower external resistance of 1 kΩ, which explains the lower power range (1.3–3.5 mW/m^2). Data indicate that increasing the anode surface did not improve the cell power. In MFC2 at an external resistance of 6.2 kΩ, cell power reached a maximum of 0.038 mW/m^2 and a current density was 0.23 mA/m^2 (Figure 1d). Similar results to those observed in MFC2 were obtained by Revelo Romo et al. [31] in a two-chamber MFC with a biocathode and a salt bridge. The voltage and power density were 8.0 mV and 0.02806 mW/m^2, respectively. The authors observed voltage fluctuations that could have been associated with the activity of exoelectrogenic microorganisms, as well as those that are not able to transfer electrons to the anode, but degrade organic matter. In the present study, internal resistance of the cells was determined from the slope of the polarization curves in the linear region where the ohmic losses predominate. In MFC 1, the internal resistance was 10.72 kΩ, while in the MFC2 it was lower (9.12 kΩ), despite a higher ratio of anode to membrane surface. Such high resistances can be explained by the cell configuration: relatively small area of the membrane in relation to the reactor volume, which limited proton flow [22,32], and the long distance between the anode and the cathode.

Lanas et al. [21] investigated how the diameter of anode brush, an anode number and the distance between electrodes affected MFC performance. In batch mode, the configuration with three larger brushes provided 80% more power than reactors with eight smaller brushes. This was due to the greater negative and stable potential of the anode. After moving the smaller brushes closer to the cathode, the power in the batch mode increased significantly from 690 to 1030 mW/m^2. The distance between the anode and the cathode in our study was much larger (15 cm) than in the studies of Lanas et al. [21] (1.65 cm), which may explain the lower power of the cell. In the present study, PEM fouling was observed (Figure 2) due to the rapid growth of microorganisms fed with waste VFAs. Despite cleaning of the membrane, after several days of operation, a repeated overgrowing effect was observed. Such a phenomenon can a reduce the efficiency of energy production in MFCs, due to reduced proton transport.
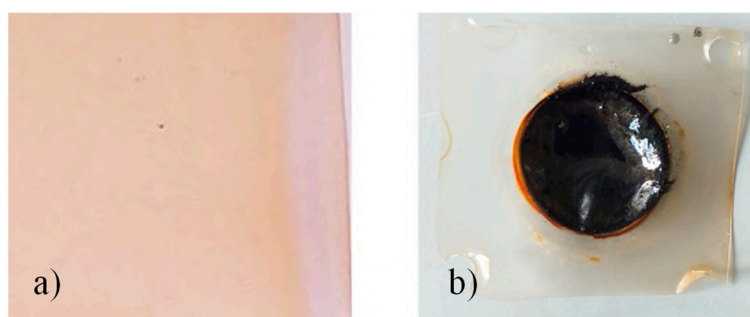

Figure 2. Nafion membrane at (**a**) day 0 and (**b**) after 30 days of operation.

Lower OLR in MFC2, despite lower energy production, contributed to more efficient and stable removal of organic compounds. In MFC1 (Figure 3a) the efficiency of COD removal ranged from 55 to 85% and averaged 65% at the end of the experiment. In MFC2, the COD removal efficiency increased from about 55% at the beginning of the experiment to 85% during the cell's stable operation and was significantly higher ($p = 0.03$, F = 7.17) than in MFC1. Higher COD removal in MFC2 with a

larger anode surface resulted from a higher biofilm mass (20.71 g/L) compared to MFC1 (10.85 g/L). The stable operation of the cell overlapped with the stabilization of the species composition of the microorganisms on the anode. The CE in both cases was low, indicating that only a limited fraction of organic matter was converted into electricity. In MFC2, a decrease in the CE value was noticeable during the experiment (Figure 3b). The highest CE was 0.024 and 0.028% in MFC1 and MFC2, respectively. Low CE could be caused by the consumption of electrons by microorganisms that do not transfer electrons to the electrode.
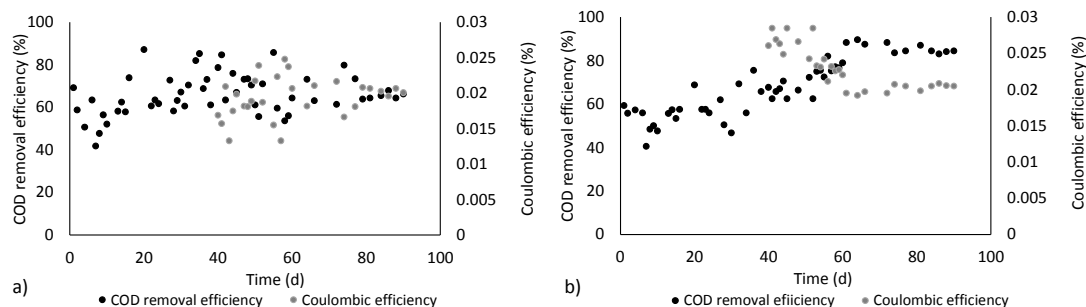
Figure 3. Chemical oxygen demand (COD) removal and coulombic efficiency in (**a**) MFC1 and (**b**) MFC2.

To conclude, while using VFAs to generate energy in MFCs, the cell should be designed to minimize the internal resistance and a rapid biofilm fouling. In the present study, more electricity was generated in MFC with a smaller anode, i.e., in MFC operated at the higher OLR. A large anode surface, although beneficial for the development of microorganisms and a more effective and stable decomposition of the complex substrate, was not conducive to energy generation. Larger anode surfaces can cause a large dispersion of electrons, some of which are consumed in other metabolic processes, which increases electron losses.

3.2. Microbial Community

Analysis of rarefaction curves indicated that in all samples the sequencing depth was sufficient (Figure S2). The results of NGS indicated that the number of operational taxonomic units (OTUs) did not differ significantly between MFC1 and MFC2 (Table 1). The largest difference in the number of OTUs was recorded on day 42, indicating a sharp decrease in the diversity of microorganisms in both MFCs. From this point, the Shannon index value increased in both MFCs reaching around 4.9 at the end of the study.

Principal Component Analysis (PCA) showed that the time of operation significantly affected the composition of microbial community in anode biofilm in MFCs (Figure 4). The most abundant groups of microorganisms throughout the entire experiment were *Rhodopseudomonas*, *Acidovorax*, *Acinetobacter*, *Clostridium*, *Methanobacterium* and *Leucobacter* (Figure 5). For both MFCs at the end of the study there was a large number of sequences that were not yet classified in databases. A high percentage of unclassified microorganisms indicates that the potential of microorganisms important for electricity generation in MFC powered with waste VFAs is still to be discovered.
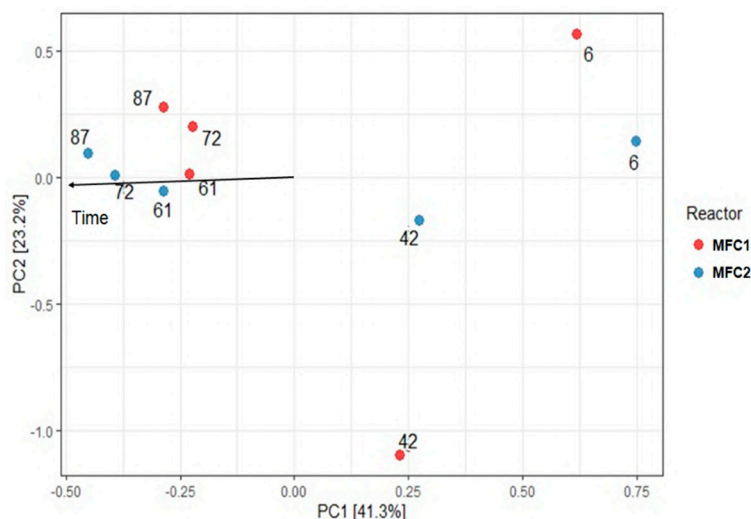
Figure 4. Results of PCA; numbers next to points indicate days of sampling during the MFC operation.

	6d	42d	61d	72d	87d	6d	42d	61d	72d	87d
Unclassified	19.5	8	23	22.8	28.1	21.3	16.8	26.6	20.6	17
Rhodopseudomonas	28.9	2.9	10.4	17	13.2	15.8	19.3	2	2.6	2
Acidovorax	18.3	17	5.3	1.7	1.6	5.2	12.2	7.9	5.1	3.3
Acinetobacter	1	18.9	11	7.3	3.7	0.1	3.1	5.6	7	2.6
Clostridium	1.6	1.4	5.5	4.9	5.9	5.2	5.3	5.7	5.5	6.4
Deftia	0.7	27.8	0.1	0	0	9.2	5.9	0.2	0.1	0.1
Methanobacterium	2.1	0.3	2.5	3.9	3.5	2.4	12.7	4.6	3.3	4.6
Leucobacter	0	1.7	3.7	4.5	3.9	0.1	0.8	3.8	7.2	11.5
Candidatus Competibacter	6.1	0	0.1	0.1	0	10.5	0	0	0	0
Phenylobacterium	0.1	0.3	1.4	1.6	2.5	0.1	0.8	1.4	3.5	4.8
No Hit	0.9	0.4	1.8	1.5	1.6	1	0.2	2.5	2.9	3.3
Pseudomonas	0.4	1.5	3.9	3.1	0.3	1.7	1.7	1.2	2.2	0.1
Frigoribacterium	0	0.6	1	1.4	1	0	0.5	1.5	3.4	5.2
Desulfobulbus	0.1	0	1.7	1.8	3.6	0	0.1	1.3	2	2.8
Stenotrophomonas	0	2.9	1.1	0.7	0.5	0.2	2.8	0.1	0.9	0.8
Legionella	0.2	0.1	2	1.2	0.9	0.2	0.3	0.4	1.2	2.7
Anaerovorax	0.5	0.2	0.8	1.1	1.3	0.7	1.4	1.2	1	0.8
Fusibacter	1	0.5	0.3	0.5	0.4	2.1	1	0.9	0.7	0.4
Rhizobium	0.4	0.2	0.7	0.7	1.4	2.1	0.1	0.2	0.4	1.4
Aminobacterium	0.3	0.2	1.5	1.5	1.6	0	0.2	0.4	0.9	0.8
Methanobrevibacter	0.3	0	0.6	0.6	0.4	0.1	0.3	2	1.5	0.8
Bacteroides	0.5	0.3	1.1	0.7	0.4	0.7	1.6	0.9	0.3	0.1
Thauera	0.3	0.3	0.1	0.1	0.3	0.2	0.1	4	0.8	0.1
Brevundimonas	0	0.7	0.2	0.2	0.2	0.3	3.1	0.2	0.5	0.8
Hydrogenophaga	1.2	0	0.6	0.4	0.2	0.6	0.1	1.6	1.1	0.2
Trichococcus	0.9	0	0.3	0.3	0.4	1.1	0.2	0.4	0.9	1.1
Fluviicola	0	5.5	0	0	0	0.2	0	0	0	0
Bifidobacterium	0.1	0	0.4	0.6	0.4	0.1	0	1.3	1.2	1.1
Lactobacillus	0.1	0	0.1	0.6	1.4	0.1	0	0.1	0.7	1.8
Pseudonocardia	1.5	0	0	0.1	0	2.5	0.1	0	0	0

Figure 5. Heatmap presenting the percentage of sequences belonging to particular taxa in MFC1 and MFC2; in the bottom row, days of MFC operation are given.

On day 42, in MFC1 high percentages of *Acidovorax* sp., *Acinetobacter* sp., *Deftia* sp. and *Fluviicola* sp. were observed. In contrast, in MFC2, next to *Acidovorax* sp., in the biofilm *Rhodopseudomonas* sp., *Methanobacterium* sp. and *Brevundimonas* sp. predominated (Figure 5). The high share of *Methanobacterium* sp. reaching 12.7% in MFC2 was unfavorable because methanogenesis may consume up to 26% of all electrons generated in the cell [33]. The hydrogen generated in the cell can also be used as an electron donor to produce methane in the oxidation of carbon dioxide to methane and water [34], lowering electricity generation. The results of molecular studies indicating a higher share of *Methanobacterium* sp. in MFC2 compared to MFC1 at the end of the study are in agreement with technological data indicating a lower cell power due to higher electron losses. In MFC1, the abundance of *Deftia* sp. reached 27.8% on day 42 and then this genus nearly disappeared in both MFCs (Figure 5). The presence of *Deftia* sp. is desirable because it is a potential exoelectrogen [35] capable of efficient generation of electricity in MFCs fed with organics such as sodium pyruvate [36]. Jangir

et al. [37] observed that after inoculation of MFC with *Deftia* sp., the anode current immediately rose above the typical background of 50 nA obtained for a sterile medium to about 400 nA after 11 h of testing. Percentage of *Acidovorax* sp. at day 42 was 17.0 and 12.2% in MFC1 and MFC2, respectively. This denitrifying bacterium is able to grow using fatty acids [38] and prefers lower operating temperatures of MFC [39]. Its high share in the initial stages of the experiment resulted from the fact that for inoculation of MFCs, denitrifying aerobic granular sludge was used. The higher decrease in the share of *Acidovorax* sp. in MFC1 indicated that this genus preferred lower OLR in MFC.

Rhodopseudomonas sp. predominated in biomass in MFC1, except from day 42, reaching 13.2% at the end of the study. In contrast, in MFC2 the share of *Rhodopseudomonas* sp. gradually decreased from 19.3% on day 42 to around 2% at the end of the study. *Rhodopseudomonas* sp. can produce electricity using a wide range of substrates at higher power densities than mixed cultures in the same device [40] and can also generate hydrogen. Generation of hydrogen by this genus is well documented. According to previous studies, hydrogen production by *Rhodopseudomonas* sp. from acetate and butyrate was 318.9 and 468.3 mL H_2/g COD, respectively [41] while wild strain *Rhodopseudomonas palustris* WP3-5 produced up to 1053.6 mL H_2/g acetate [42]. *Rhodopseudomonas* sp. share in biomass in MFC operated with acetate and glucose can reach over 60% [43]. *Acinetobacter* sp. that use hydrogen as an electron donor [44,45] were abundant in both MFCs and at the end of the experiment, their percentage was 3.7 and 2.6% in MFC1 and MFC2, respectively. *Acinetobacter* sp. is involved not only in the transfer of electrons to the anode, but also in a reduction of oxygen on the biocathode [9,46]. The share of *Acinetobacter* sp. in biomass on biocathode can reach as much as 57.81% [47]. In the presented study, the coexistence in the anode biofilm of hydrogen-consuming exoelectrogens belonging to *Acinetobacter* sp. with hydrogen-producing exoelectrogens of *Rhodopseudomonas* sp. could have resulted in a high current density.

In the present study, in MFCs powered by waste VFAs, different bacterial groups able to metabolize a very broad range of organic substrates were identified. *Clostridium* sp. was present in both reactors. Its participation in biomass in MFC1 increased from 1.4 to 1.6% at the beginning of the study to 5.9% at the end of the study. In MFC2, operated at the lower OLR, its share reached 6.4% at the end of the experiment. *Clostridium* sp. participate in decomposition of both simple and complex organic compounds, such as cellulose [48], producing butyrate, acetate, lactate, capronate (hexanoate), butanol, acetone, acetoin, and ethanol [49]. *Desulfobulbus* sp. constituted 3.6 and 2.8% of biomass in MFC1 and MFC2 at the end of the study, respectively. *Desulfobulbus* sp. can metabolize organic acids such as propionate, lactate and pyruvate [50], however, electron transfer to the anode resulting from metabolism of these acids is relatively inefficient; only about 25% of the available electrons are transferred to the electrode surface [51]. This inefficient electron transfer by *Desulfobulbus* sp. may have negatively affected electricity generation in MFCs in our study. Microorganisms from the genera *Bifidobacterium*, *Lactobacillus* and *Aminobacterium* constituted a small percentage of biomass at the beginning of the experiment, however, their number increased at the end of the experiment. The abundance of *Lactobacillus* sp. that ferments lactose to VFAs [52,53] was similar in both MFCs. The percentage of *Aminobacterium* sp., capable of protein degradation to monomeric by-products [54,55] was nearly two times higher in MFC1 than in MFC2; this indicated that these microorganisms preferred higher OLRs. The increase in *Aminobacterium* sp. abundance can be explained by the composition of the anolyte—proteins comprise about 30% of volatile suspended solids in a primary sludge [56].

The lower OLR in MFC2 favored the growth of *Phenylobacterium* sp., *Frigoribacterium* sp., *Leucobacter* sp., and *Bifidobacterium* sp. (Figure 5), that metabolize very diverse substrates, including hardly degradable ones. *Phenylobacterium* sp. use e.g., chloridazone, antipyrin, pyramidone for growth and simple compounds such as sugars, alcohols, amino acids or carboxilic acids are not used by them [57]. *Frigoribacterium* sp. are mainly involved in transformations of sugars such as N-acetyl-D-glucosamine, L-arabinose, p-arbutin, D-fructose or D-cellobiose, while with organic acids they use only citrate and fumarate [58]. Abundance of *Leucobacter* sp. increased over time; at the end of the study, *Leucobater* sp. constituted 3.9 and 11.5% of biomass in MFC1 in MFC2, respectively. Generally, *Leucobacter* sp.

show poor substrate utilization with a limited ability to assimilate many carbohydrates and carbon sources [59]. The abundance of these aerobic bacteria in MFC is, however, desirable. In MFCs powered with sodium acetate, glucose and ethanol in which air was introduced to the anode compartment during a start-up period, the presence of aerobic *Leucobacter* sp. in the anode biofilm increased electricity generation [60].

4. Conclusions

The use of waste VFAs from AD in MFCs favors energy recovery in wastewater treatment plants and is in line with assumptions of a circular economy. To optimize the operation of MFCs powered with waste substrates, knowledge of the effect of MFC operation and microbiological composition on energy production should be broadened. In this study, it was shown that the higher OLR in MFC1 favored growth of exoelectrogens from *Rhodopseudomonas* sp. (13.2%) resulting in a higher and more stable electricity production in comparison with MFC2. At a lower OLR in MFC2, the abundance of genera *Leucobacter, Frigoribacterium* and *Phenylobacterium* increased which resulted in the efficient decomposition of organics favoring high and stable COD removal. Independent of the anode size, *Clostridium* sp. and exoelectrogens belonging to genera *Desulfobulbus* and *Acinetobacter* were abundant in MFCs powered with waste VFAs. Future work will focus on a possibility of increasing electricity generation by increasing the surface area of PEM.

Supplementary Materials: The following are available online at http://www.mdpi.com/1996-1073/13/18/4712/s1, Figure S1: Design of a dual-chamber MFC reactor, Figure S2: Rarefaction curves obtained for biomass samples collected from MFC1 and MFC2 during the experiment (in Sample_ID the name of MFC and the day of sampling are given).

Author Contributions: Conceptualization, A.C.-K. and D.N.; methodology, A.C.-K.; formal analysis, D.N., A.C.-K.; investigation, D.N.; resources, A.C.-K.; data curation, D.N.; writing—original draft preparation, D.N.; writing—review and editing, A.C.-K.; visualization, A.C.-K. and D.N.; supervision, A.C.-K.; project administration, A.C.-K.; funding acquisition, A.C.-K. All authors have read and agreed to the published version of the manuscript.

Conflicts of Interest: The authors declare no conflict of interest.

References

1. Logan, B.E.; Hamelers, B.; Rozendal, R.; Schröder, U.; Keller, J.; Freguia, S.; Aelterman, P.; Verstraete, W.; Rabaey, K. Microbial fuel cells: Methodology and technology. *Environ. Sci. Technol.* **2006**, *40*, 5181–5192. [CrossRef] [PubMed]

2. Kumar, R.; Singh, L.; Zularisam, A.W.; Hai, F.I. Microbial fuel cell is emerging as a versatile technology: A review on its possible applications, challenges and strategies to improve the performances. *Int. J. Energy Res.* **2018**, *42*, 369–394. [CrossRef]

3. Tan, Y.C.; Kharkwal, S.; Chew, K.K.W.; Alwi, R.; Mak, S.F.W.; Ng, H.Y. Enhancing the robustness of microbial fuel cell sensor for continuous copper(II) detection against organic strength fluctuations by acetate and glucose addition. *Bioresour. Technol.* **2018**, *259*, 357–364. [CrossRef]

4. Christwardana, M.; Frattini, D.; Accardo, G.; Yoon, S.P.; Kwon, Y. Optimization of glucose concentration and glucose/yeast ratio in yeast microbial fuel cell using response surface methodology approach. *J. Power Sources* **2018**, *402*, 402–412. [CrossRef]

5. Mateo, S.; Cañizares, P.; Rodrigo, M.A.; Fernandez-Morales, F.J. Driving force behind electrochemical performance of microbial fuel cells fed with different substrates. *Chemosphere* **2018**, *207*, 313–319. [CrossRef] [PubMed]

6. Foudhaili, T.; Rakotonimaro, T.V.; Neculita, C.M.; Coudert, L.; Lefebvre, O. Comparative efficiency of microbial fuel cells and electrocoagulation for the treatment of iron-rich acid mine drainage. *J. Environ. Chem. Eng.* **2019**, *7*, 103149. [CrossRef]

7. Xin, X.; Ma, Y.; Liu, Y. Electric energy production from food waste: Microbial fuel cells versus anaerobic digestion. *Bioresour. Technol.* **2018**, *255*, 281–287. [CrossRef]

8. Hassan, S.H.A.; el Nasser, A.; Zohri, A.; Kassim, R.M.F. Electricity generation from sugarcane molasses using microbial fuel cell technologies. *Energy* **2019**, *178*, 538–543. [CrossRef]

9. Pepè Sciarria, T.; Arioli, S.; Gargari, G.; Mora, D.; Adani, F. Monitoring microbial communities' dynamics during the start-up of microbial fuel cells by high-throughput screening techniques. *Biotechnol. Rep.* **2019**, *21*, e00310. [CrossRef]

10. Freguia, S.; Teh, E.H.; Boon, N.; Leung, K.M.; Keller, J.; Rabaey, K. Microbial fuel cells operating on mixed fatty acids. *Bioresour. Technol.* **2010**, *101*, 1233–1238. [CrossRef]

11. Chen, C.-Y.; Cheng, C.-Y.; Chen, C.-K.; Hsieh, M.-C.; Lin, S.-T.; Ho, K.-Y.; Li, J.-W.; Lin, C.-P.; Chung, Y.-C. Hexavalent chromium removal and bioelectricity generation by *Ochrobactrum* sp. YC211 under different oxygen conditions. *J. Environ. Sci. Health Part A* **2016**, *51*, 502–508. [CrossRef] [PubMed]

12. Chae, K.J.; Choi, M.J.; Lee, J.W.; Kim, K.Y.; Kim, I.S. Effect of different substrates on the performance, bacterial diversity, and bacterial viability in microbial fuel cells. *Bioresour. Technol.* **2009**, *100*, 3518–3525. [CrossRef] [PubMed]

13. Freguia, S.; Rabaey, K.; Yuan, Z.; Keller, J. Syntrophic processes drive the conversion of glucose in microbial fuel cell anodes. *Environ. Sci. Technol.* **2008**, *42*, 7937–7943. [CrossRef] [PubMed]

14. Costerton, J.W. Control of all Biofilm Strategies and Behaviours. In *The Biofilm Primer*; Springer: Berlin/Heidelberg, Germany, 2007; pp. 85–105. [CrossRef]

15. Jiang, Y.B.; Zhong, W.H.; Han, C.; Deng, H. Characterization of electricity generated by soil in microbial fuel cells and the isolation of soil source exoelectrogenic bacteria. *Front. Microbiol.* **2016**, *7*. [CrossRef] [PubMed]

16. Kondaveeti, S.; Lee, S.H.; Park, H.D.; Min, B. Specific enrichment of different Geobacter sp. in anode biofilm by varying interspatial distance of electrodes in air-cathode microbial fuel cell (MFC). *Electrochim. Acta* **2020**, *331*, 135388. [CrossRef]

17. Almatouq, A.; Babatunde, A.O.; Khajah, M.; Webster, G.; Alfodari, M. Microbial community structure of anode electrodes in microbial fuel cells and microbial electrolysis cells. *J. Water Process Eng.* **2020**, *34*, 101140. [CrossRef]

18. Asefi, B.; Li, S.L.; Moreno, H.A.; Sanchez-Torres, V.; Hu, A.; Li, J.; Yu, C.P. Characterization of electricity production and microbial community of food waste-fed microbial fuel cells. *Process Saf. Environ. Prot.* **2019**, *125*, 83–91. [CrossRef]

19. Peixoto, L.; Rodrigues, A.L.; Martins, G.; Nicolau, A.; Brito, A.B.; Silva, M. Flat microbial fuel cell in small and deconcentrated applications: Performance and optimization. *Environ. Technol.* **2013**, *34*, 1947–1956. [CrossRef]

20. Chen, S.; Patil, S.A.; Brown, R.K.; Schröder, U. Strategies for optimizing the power output of microbial fuel cells: Transitioning from fundamental studies to practical implementation. *Appl. Energy* **2019**, *233–234*, 15–28. [CrossRef]

21. Lanas, V.; Ahn, Y.; Logan, B.E. Effects of carbon brush anode size and loading on microbial fuel cell performance in batch and continuous mode. *J. Power Sources* **2014**, *247*, 228–234. [CrossRef]

22. Rossi, R.; Evans, P.J.; Logan, B.E. Impact of flow recirculation and anode dimensions on performance of a large scale microbial fuel cell. *J. Power Sources* **2019**, *412*, 294–300. [CrossRef]

23. Świątczak, P.; Cydzik-Kwiatkowska, A. Performance and microbial characteristics of biomass in a full-scale aerobic granular sludge wastewater treatment plant. *Environ. Sci. Pollut. Res.* **2018**, *25*, 1655–1669. [CrossRef] [PubMed]

24. APHA. *Standard Methods for the Standard Methods for the Examination of Water and Wastewater*, 18th ed.; American Public Health Association (APHA), American Water Works Association (AWWA), Water Pollution Control Federation (WPCF): Washington, DC, USA, 1992.

25. Watson, V.J.; Logan, B.E. Analysis of polarization methods for elimination of power overshoot in microbial fuel cells. *Electrochem. Commun.* **2011**, *13*, 54–56. [CrossRef]

26. R Development Core Team. *A Language and Environment for Statistical Computing*; R Foundation for Statistical Computing: Vienna, Austria, 2019.

27. *RStudio Team RStudio: Integrated Development for R*, Computer Software v0.98.1074; RStudio, Inc.: Boston, MA, USA, 2015.

28. Hill, M.O. Diversity and evenness: A unifying notation and its consequences. *Ecology* **1973**, *54*, 427–432. [CrossRef]

29. Choi, J.-d.-r.; Chang, H.N.; Han, J.-I. Performance of microbial fuel cell with volatile fatty acids from food wastes. *Biotechnol. Lett.* **2011**, *33*, 705–714. [CrossRef]

30. Tardy, G.M.; Lóránt, B.; Lóka, M.; Nagy, B.; László, K. Enhancing substrate utilization and power production of a microbial fuel cell with nitrogen-doped carbon aerogel as cathode catalyst. *Biotechnol. Lett.* **2017**, *39*, 993–999. [CrossRef]

31. Revelo Romo, D.M.; Hurtado Gutiérrez, N.H.; Ruiz Pazos, J.O.; Pabón Figueroa, L.V.; Ordóñez Ordóñez, L.A. Bacterial diversity in the Cr(VI) reducing biocathode of a Microbial Fuel Cell with salt bridge. *Rev. Argent. Microbiol.* **2019**, *51*, 110–118. [CrossRef]

32. Oh, S.E.; Logan, B.E. Proton exchange membrane and electrode surface areas as factors that affect power generation in microbial fuel cells. *Appl. Microbiol. Biotechnol.* **2006**, *70*, 162–169. [CrossRef]

33. Tandukar, M.; Huber, S.J.; Onodera, T.; Pavlostathis, S.G. Biological chromium(VI) reduction in the cathode of a microbial fuel cell. *Environ. Sci. Technol.* **2009**, *43*, 8159–8165. [CrossRef]

34. Boone, D.R.; Genus, I. Methanobacterium. In *Bergey's Manual of Systematic Bacteriology*; George, M.G., Ed.; Springer: New York, NY, USA, 2001; pp. 215–218.

35. Chen, C.Y.; Chen, T.Y.; Chung, Y.C. A comparison of bioelectricity in microbial fuel cells with aerobic and anaerobic anodes. *Environ. Technol.* **2014**, *35*, 286–293. [CrossRef]

36. Leiva-Aravena, E.; Leiva, E.; Zamorano, V.; Rojas, C.; Regan, J.M.; Vargas, I.T. Organotrophic acid-tolerant microorganisms enriched from an acid mine drainage affected environment as inoculum for microbial fuel cells. *Sci. Total Environ.* **2019**, *678*, 639–646. [CrossRef] [PubMed]

37. Jangir, Y.; French, S.; Momper, L.M.; Moser, D.P.; Amend, J.P.; El-Naggar, M.Y. Isolation and characterization of electrochemically active subsurface *Delftia* and *Azonexus* species. *Front. Microbiol.* **2016**, *7*. [CrossRef] [PubMed]

38. Heylen, K.; Lebbe, L.; de Vos, P. *Acidovorax caeni* sp. nov., a denitrifying species with genetically diverse isolates from activated sludge. *Int. J. Syst. Evol. Microbiol.* **2008**, *58*, 73–77. [CrossRef] [PubMed]

39. Mei, X.; Xing, D.; Yang, Y.; Liu, Q.; Zhou, H.; Guo, C.; Ren, N. Adaptation of microbial community of the anode biofilm in microbial fuel cells to temperature. *Bioelectrochemistry* **2017**, *117*, 29–33. [CrossRef] [PubMed]

40. Xing, D.; Zuo, Y.; Cheng, S.; Regan, J.M.; Logan, B.E. Electricity generation by *Rhodopseudomonas palustris* DX-1. *Environ. Sci. Technol.* **2008**, *42*, 4146–4151. [CrossRef] [PubMed]

41. Wu, X.; Wang, X.; Yang, H.; Guo, L. A comparison of hydrogen production amog three photosynthetic baterial strains. *Int. J. Hydrog.* **2010**, *35*, 7194–7199. [CrossRef]

42. Yang, C.F.; Lee, C.M. Enhancement of photohydrogen production using phbC deficient mutant Rhodopseudomonas palustris strain M23. *Bioresour. Technol.* **2011**, *102*, 5418–5424. [CrossRef]

43. Zheng, W.; Cai, T.; Huang, M.; Chen, D. Comparison of electrochemical performances and microbial community structures of two photosynthetic microbial fuel cells. *J. Biosci. Bioeng.* **2017**, *124*, 551–558. [CrossRef]

44. Gross, R.; Simon, J. The *hydE* gene is essential for the formation of *Wolinella succinogenes* NiFe-hydrogenase. *FEMS Microbiol. Lett.* **2003**, *227*, 197–202. [CrossRef]

45. Iino, T.; Mori, K.; Uchino, Y.; Nakagawa, T.; Harayama, S.; Suzuki, K.I. *Ignavibacterium album* gen. nov., sp. nov., a moderately thermophilic anaerobic bacterium isolated from microbial mats at a terrestrial hot spring and proposal of *Ignavibacteria classis* nov., for a novel lineage at the periphery of green sulfur bacteria. *Int. J. Syst. Evol. Microbiol.* **2010**, *60*, 1376–1382. [CrossRef] [PubMed]

46. Liu, X.W.; Li, W.W.; Yu, H.Q. Cathodic catalysts in bioelectrochemical systems for energy recovery from wastewater. *Chem. Soc. Rev.* **2014**, *43*, 7718–7745. [CrossRef]

47. Cao, X.; Liang, P.; Song, X.S.; Wang, Y.H.; Qiu, Y.; Huang, X. Trickling filter in a biocathode microbial fuel cell for efficient wastewater treatment and energy production. *Sci. China Technol. Sci.* **2019**, *62*, 1703–1709. [CrossRef]

48. Rismani-Yazdi, H.; Christy, A.D.; Dehority, B.A.; Morrison, M.; Yu, Z.; Tuovinen, O.H. Electricity generation from cellulose by rumen microorganisms in microbial fuel cells. *Biotechnol. Bioeng.* **2007**, *97*, 1398–1407. [CrossRef] [PubMed]

49. Tracy, B.P.; Jones, S.W.; Fast, A.G.; Indurthi, D.C.; Papoutsakis, E.T. Clostridia: The importance of their exceptional substrate and metabolite diversity for biofuel and biorefinery applications. *Curr. Opin. Biotechnol.* **2012**, *23*, 364–381. [CrossRef] [PubMed]

50. El Houari, A.; Ranchou-Peyruse, M.; Ranchou-Peyruse, A.; Dakdaki, A.; Guignard, M.; Idouhammou, L.; Bennisse, R.; Bouterfass, R.; Guyoneaud, R.; Qatibi, A.I. *Desulfobulbus oligotrophicus* sp. Nov., a sulfate-reducing and propionate-oxidizing bacterium isolated from a municipal anaerobic sewage sludge digester. *Int. J. Syst. Evol. Microbiol.* **2017**, *67*, 275–281. [CrossRef]

51. Holmes, D.E.; Bond, D.R.; Lovley, D.R. Electron Transfer by *Desulfobulbus propionicus* to Fe(III) and Graphite Electrodes. *Appl. Environ. Microbiol.* **2004**, *70*, 1234–1237. [CrossRef]

52. Vilas Boas, J.; Oliveira, V.B.; Marcon, L.R.C.; Pinto, D.P.; Simões, M.; Pinto, A.M.F.R. Effect of operating and design parameters on the performance of a microbial fuel cell with *Lactobacillus pentosus*. *Biochem. Eng. J.* **2015**, *104*, 34–40. [CrossRef]

53. Wenzel, J.; Fuentes, L.; Cabezas, A.; Etchebehere, C. Microbial fuel cell coupled to biohydrogen reactor: A feasible technology to increase energy yield from cheese whey. *Bioprocess Biosyst. Eng.* **2017**, *40*, 807–819. [CrossRef]

54. Zhao, Z.; Zhang, Y.; Ma, W.; Sun, J.; Sun, S.; Quan, X. Enriching functional microbes with electrode to accelerate the decomposition of complex substrates during anaerobic digestion of municipal sludge. *Biochem. Eng. J.* **2016**, *111*, 1–9. [CrossRef]

55. Kumar, S.S.; Malyan, S.K.; Basu, S.; Bishnoi, N.R. Syntrophic association and performance of *Clostridium, Desulfovibrio, Aeromonas* and *Tetrathiobacter* as anodic biocatalysts for bioelectricity generation in dual chamber microbial fuel cell. *Environ. Sci. Pollut. Res.* **2017**, *24*, 16019–16030. [CrossRef]

56. Jimenez, J.; Vedrenne, F.; Denis, C.; Mottet, A.; Déléris, S.; Steyer, J.P.; Cacho Rivero, J.A. A statistical comparison of protein and carbohydrate characterisation methodology applied on sewage sludge samples. *Water Res.* **2013**, *47*, 1751–1762. [CrossRef] [PubMed]

57. Lingens, F.; Blecher, R.; Blecher, H. *Phenylobacterium immobile* gen. nov., sp. nov., a gram-negative bacterium that degrades the herbicide chloridazon. *Int. J. Syst. Bacteriol.* **1985**, *35*, 26–39. [CrossRef]

58. Kämpfer, P.; Nurmiaho Lassila, E.L.; Ulrych, U.; Busse, H.J.; Weiss, N.; Mikkola, R.; Salkinoja-Salonen, M. Frigoribacterium. In *Bergey's Manual of Systematics of Archaea and Bacteria*; John Wiley & Sons, Ltd.: Chichester, UK, 2000; pp. 1–8.

59. Takeuchi, M.; Weiss, N.; Schumann, P.; Yokota, A. *Leucobacter komagatae* gen. nov., sp. nov., a new aerobic gram-positive, nonsporulating rod with 2,4-diaminobutyric acid in the cell wall. *Int. J. Syst. Bacteriol.* **1996**, *46*, 967–971. [CrossRef]

60. Quan, X.; Quan, Y.; Tao, K.; Jiang, X. Comparative investigation on microbial community and electricity generation in aerobic and anaerobic enriched MFCs. *Bioresour. Technol.* **2013**, *128*, 259–265. [CrossRef] [PubMed]

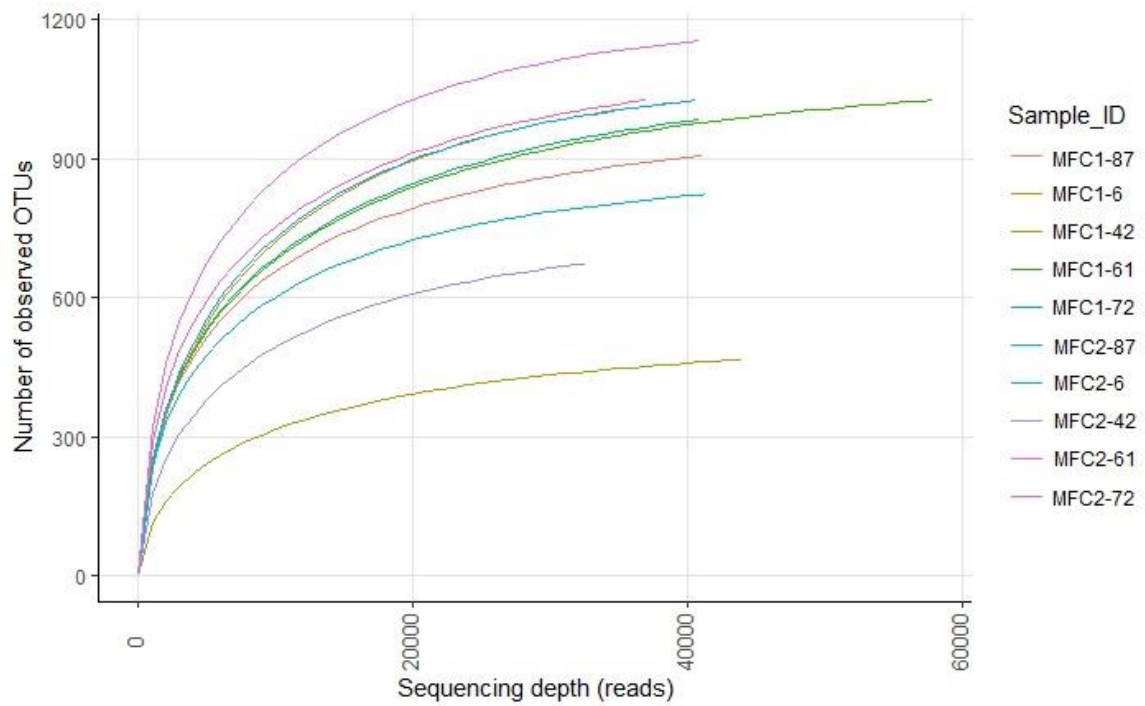# Microbial structure and energy generation in microbial fuel cells powered with waste anaerobic digestate

Dawid Nosek*, Agnieszka Cydzik-Kwiatkowska

University of Warmia and Mazury in Olsztyn, Department of Environmental Biotechnology, 10-709 Olsztyn, Słoneczna 45 G, Poland
*Corresponding author: dawid.nosek@uwm.edu.pl, tel. +48 89 5234144 fax: +48 89 523 41 31

Figure 1 SM. Design of a dual-chamber MFC reactor, where A- anode chamber, K- cathode chamber and M- PEM membrane.

Figure 2 SM. Rarefaction curves obtained for biomass samples collected from MFC1 and MFC2 during the experiment (in Sample_ID the name of MFC and the day of sampling are given).

mgr inż. Dawid Nosek

(imię i nazwisko)

Przewodniczący Rady Naukowej Dyscypliny

prof. dr hab. inż. Marcin Dębowski

Uniwersytetu Warmińsko-Mazurskiego w Olsztynie

OŚWIADCZENIE

kandydata

Oświadczam, że w pracy pod tytułem:

Nosek D., Cydzik-Kwiatkowska A. (2020). Microbial structure and energy generation in microbial fuel cells powered with waste anaerobic digestate. Energies 13(18), 4712, mój wkład merytoryczny w jej przygotowanie polegał na: zaplanowaniu koncepcji pracy, przeglądzie literatury pozyskaniu, opracowaniu i interpretacji wyników technologicznych, graficznym opracowaniu wyników oraz przygotowaniu pierwszej wersji manuskryptu.

Dawid Nosek

(podpis)

Olsztyn, 21.08.2024

(miejscowość, data)

prof. zw. dr hab. inż. Agnieszka Cydzik-Kwiatkowska

(imię i nazwisko)

Przewodniczący Rady Naukowej Dyscypliny

prof. dr hab. inż. Marcin Dębowski

Uniwersytetu Warmińsko-Mazurskiego w Olsztynie

OŚWIADCZENIE
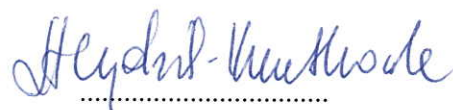
współautora

Oświadczam, że w pracy pod tytułem:

Nosek D., Cydzik-Kwiatkowska A. (2020). Microbial structure and energy generation in microbial fuel cells powered with waste anaerobic digestate. Energies 13(18), 4712, mój wkład merytoryczny w jej przygotowanie polegał na: opracowaniu koncepcji i metodyki pracy, wizualizacji uzyskanych wyników technologicznych, recenzowaniu i edycji tekstu, merytorycznym nadzorze pracy i pozyskaniu środków finansowych.

Jednocześnie wyrażam zgodę na przedłożenie w/w pracy przez Pana Dawida Noska jako część rozprawy doktorskiej w formie spójnego tematycznie zbioru artykułów naukowych opublikowanych w czasopismach naukowych. Oświadczam, iż samodzielna i możliwa do wyodrębnienia część ww. pracy wykazuje indywidualny wkład kandydata Pana Dawida Noska polegający na:

udziale w zaplanowaniu koncepcji pracy, pozyskaniu, opracowaniu i interpretacji wyników technologicznych, graficznym opracowaniu wyników oraz przygotowaniu pierwszej wersji manuskryptu.

(podpis)

85:6905983772

Praca nr 3

Nosek D., Samel O., Pokój T., Cydzik-Kwiatkowska A.

Waste volatile fatty acids as a good electron donor in microbial fuel cell with iron-modified anode.

International Journal of Environmental Science and Technology

2020

ORIGINAL PAPER

Waste volatile fatty acids as a good electron donor in microbial fuel cell with the iron-modified anode

D. Nosek[1] · O. Samsel[1] · T. Pokój[1] · A. Cydzik-Kwiatkowska[1]

Abstract

The commercialization of microbial fuel cell technology is limited by high operating costs and low electricity production due to poor electron transfer to the anode. Operational costs can be lowered by utilizing waste materials, and cell performance can be improved by anode modification. This study investigated how anode modification with iron compounds changed the efficiency of energy generation and the microbiome of microbial fuel cells fueled with waste volatile fatty acids from a full-scale anaerobic digestion. Anode modification with 2.5 g Fe_2O_3/m^2 increased the power density, current density, and voltage by 3.6-fold, 1.8-fold, and 1.4-fold, respectively. In the microbial fuel cell influent, propionic, enanthic, and iso-caproic acids predominated (60, 15, and 13% of all volatile fatty acids, respectively); in the outflow, propionic (71%) and valeric acids (17%) predominated. In anodic biofilms, *Acidovorax* sp. were most abundant; they have a great capacity for volatile fatty acids decomposition, and their abundance doubled in the microbial fuel cell with an iron-modified anode. The presence of iron significantly increased the abundance of the genera *Pseudomonas* and *Geothrix*, which were mainly responsible for electricity production. These results indicate that anode modification with iron changes the anode microbiome, favoring efficient volatile fatty acids metabolism and a greater abundance of electrogens in the biofilm, which ensures better electricity generation.

Keywords Anode modification · Microbial fuel cell · Microbiome · Iron · Volatile fatty acids

Introduction

In response to increased energy demand and out of concern for the natural environment, microbial fuel cells (MFCs) are of great interest to researchers. These cells, in addition to their main function of generating electricity, can also contribute to wastewater treatment (Liang et al. 2018). To generate electricity, microorganisms capable of biocatalysis can transform the organic compounds contained in wastewater (Ghasemi et al. 2011).

Carbon electrodes are commonly used electron acceptors in MFC. They can take various forms, such as brushes, rods, felts, and structures such as canvases. The most important characteristic of these electrodes is that they should have the largest possible number of microchannels to allow the penetration and flow of substances into the electrode (Greenman et al. 2021). Additionally, low resistance, high electrical conductivity, and a large specific surface area are also desirable (Zhou et al. 2011). It has been shown that increases in the efficiency of energy production by a microbial cell are closely related to increases in coverage of the anode with microorganisms. Electron transport at the anode is improved by the growth of a biofilm (Cornejo et al. 2015). The coverage of the electrode with microorganisms can be improved by increasing the specific surface area and reducing the charge transfer resistance by the applications of different anode materials and modifying the electrodes, e.g., with metal oxides (Nosek et al. 2020). These oxides significantly improve the efficiency of electron transport in an MFC by serving as electrical conductors inside biological membranes or by accumulating on the surface of bacterial cells (Karn et al. 2009). The presence of iron oxides in the environment increases the expression of genes encoding type-c cytochromes (Kato et al. 2013), which intensifies electron transfer processes in the anode regions. Iron (III) oxide in a nano-colloidal form created a network of

✉ D. Nosek
dawid.nosek@uwm.edu.pl

1 Department of Environmental Biotechnology, University of Warmia and Mazury in Olsztyn, Słoneczna 45 G, 10-709 Olsztyn, Poland

connections between organisms, increasing their mutual adhesion, which raised the power generated in the cell by up to 50-fold (Savla et al. 2020). Zheng et al. (2022) investigated the effect of iron added to the medium to improve the efficiency of MFC. The experiment was conducted in a single-chamber MFC with a carbon brush as an anode. The cell achieved the highest power of 391.11 ± 9.4 mW/m^2 at the lowest dose of magnetite Fe$_3$O$_4$ of 4.5 g/L. Yu et al. (2019) modified the graphite felt with Fe$_3$O$_4$ by bonding it to the surface with a polytetrafluoroethylene emulsion. This modification improved the power density in soil MFC by 1.7 times compared to the control. Tripathi et al. (2022) used dots coated with different doses (0.25, 0.5, 0.75, and 1 mg/cm^2) of iron (II, III) oxide (Fe$_3$O$_4$) as an anode. The anodes were synthesized using a hydrothermal-assisted probe sonication method. The maximum power density (440.01 mW/m^2) was observed in the MFC at the highest Fe$_3$O$_4$ dose of 1 mg/cm^2—it was about 1.5 times higher than that of the MFC with an anode made of pure graphite sheet. Up to now, mainly pure substrates have been used in MFCs, such as glycerol (Tremouli et al. 2016), glucose (Christwardana et al. 2018), or acetate (Ullah and Zeshan 2020), which ensured successful electricity production. Recently, waste substances have started to be used, including municipal wastewater, landfill leachate, and volatile fatty acids (VFAs) from primary sludge treatment; this approach offers the benefit of energy recovery from waste products.

From an engineering point of view, combining technologies like anaerobic digestion (AD) and MFC to generate energy from waste is beneficial. When organic compounds are decomposed in AD, VFAs are formed, which can serve as a carbon source for MFC microorganisms to simultaneously generate electricity. For example, Hou et al. (2020) used a digestion tank as the anodic chamber for an MFC process (AD-MFC) to treat food waste. They found that a combined AD-MFC system supported with algae in the cathode chamber produced biogas with a methane content twice as high as that produced by AD alone and 34% higher than that produced by AD-MFC. Additionally, the algae-supported MFC maintained a high voltage of 490 mV for 20 days. Combining AD and an MFC in one system can help with the early detection of VFA concentrations that are too high for the AD process. Schievano et al. (2018) reported that when the concentration of VFAs in the chamber increased to 4000 mg acetate/L, the voltage dropped, which was associated with the inhibition of the activity of microorganisms. Another study used a continuous process with hydrogen/VFA generation in the first stage and electricity generation in an MFC in the second. The combined system was able to reduce COD by 90%, and the maximum power density achieved with the system was 22.26 mW/m^2 (Pant et al. 2013). Choi et al. (2011) used VFA from the fermentation of food waste in a two-chamber

and a single-chamber MFC. They observed that acetic acid and propionic acid were consumed most rapidly and that the voltage and power density reached 533 mV and 240 mW/m^2, respectively. When only butyrate and valerate were present in the cell, the voltage dropped to 390 mV, indicating that electron deposition with these VFAs was lower in comparison with the deposition with VFAs with shorter chain lengths. Acetate alone was removed more rapidly than acetate in a mixture with other VFAs, suggesting that the other VFAs may have inhibited acetate degradation. In another study by Freguia et al. (2010), a synthetic VFA mixture based on the composition of digested sludge from domestic wastewater treatment was used. For power generation from the VFAs, mainly acetate and propionate were utilized, while butyrates, valerates, and caproic acids were utilized to a lesser extent. To the best of the authors' knowledge, no studies were conducted with real VFA in MFCs with Fe-modified anodes.

Energy generation in an MFC is closely related to the species composition of the anode biofilm. Typically, mixed cultures make good synergistic consortiums because each species plays a specific role in the degradation of complex organic compounds. Some bacteria are responsible for breaking down complex compounds into simple ones and others for protecting the biofilm from environmental stress (Costerton 2007). Xin et al. (2019) tested the use of food waste hydrolysate as an electron donor in an MFC. They found that the main genera were *Rummeliibacillus*, *Burkholderia*, *Enterococcus*, and *Clostridium* and that the electrogenesis efficiency (0.977 kWh/kg COD) was higher than that of a single carbon source MFC. Syntrophic interactions between fermentation species and exoelectrogens played a key role in the generation of electricity by the anode biofilm. He et al. (2021) used sludge fermentation liquid (SFL) and fruit waste extracts (FWE) in MFC. The mixture of SFL and FWE promoted the presence of the genera *Clostridium*, *Alicycliphilus*, *Thermomonas*, *Geobacter*, *Paludibaculum*, *Pseudomonas*, *Taibaiella*, and *Comamonas*, which collaborated to degrade COD and generate electricity. Analysis of the VFAs in the wastewater of the MFC fed FWE indicated that synergistic interactions of microorganisms led to substrate bioconversion and bioelectricity production. In studies using the PCR-DGGE technique, in which real or synthetic VFAs were used in MFCs, microorganisms of the genera *Geobacter, Comammonas, Pseudomonas, Xanthomonas, Sphingobacterium*, and *Pelobacter* were present in the biofilm that developed on unmodified electrodes (Freguia et al. 2010, Choi et al. 2011). However, their percent abundance in the biomass could not be determined, due to the limitations of the method. To ensure an in-depth analysis of the microbial community, the most advanced molecular techniques, such as next-generation sequencing, should be

used that allow determining the percentages of all bacteria in the community even those that are present in low numbers, but can be of great importance for the process efficiency (Dubey et al. 2022). These advanced methods have not been used to investigate how modifying the anode with iron affects the relationships between organic degraders and electrogens in the anodic biofilm of MFCs fed with real VFAs.

Even though energy can be efficiently produced in MFC by using pure, quickly metabolized substrates such as glucose or acetate, the economic aspects of the process should be improved. Using complex waste substrates does not involve the costs associated with pure substrates and is in line with the assumptions of a circular economy. However, these substrates tend to reduce the efficiency and energy generation potential of the process. A potential means of offsetting these reductions is the use of modified anodes. It is also important to determine which microorganisms guarantee effective energy production under these conditions. So far no studies were presented on the use of VFA in MFC with MFC coated with iron oxide, none were the metabolism of VFA and microbial structure of anodic consortium analyzed to focus on how the substrates from waste VFAs are used in MFC and indicate the main players involved in the metabolism of real mixed organic compounds and energy generation. Therefore, the objectives of this study were to assess the possibility of using VFAs from the full-scale AD of primary sludge for electricity generation in an MFC with an iron-modified anode and to investigate the influence of iron on the microbial composition of the anodic biofilm and VFA removal.

This study was carried out in northeastern Poland from September 2021 to March 2022.

Materials and methods

MFC configuration

The tests were performed in two separate reactors made of transparent acrylic glass (Fig. 1). Each of them contained anode and cathode chambers (active volume 1 L), which were connected by a transverse, cylindrical conductor in which a Nafion N-117 proton exchange membrane (Alfa Aesar) was placed. The membrane area was 8.5 cm^2. Before use, the membrane was rinsed for half an hour in acetone and then rinsed with distilled water, soaked in 1 M HCl for 30 min, and rinsed with distilled water. Due to membrane clogging, once a week, the membrane was cleaned in 1 M HCl and rinsed with distilled water (for details, see Nosek and Cydzik-Kwiatkowska 2020). The electrodes were made of 10×10 cm carbon felt (CGT Carbon GmbH). The external electrical circuit was made of stainless steel wire and connected to a 4.7 kΩ resistor. The cathode chamber was filled with a catholyte containing 1.5 mg of NaCl and 38 mL of phosphate buffer in 1 L of distilled water. The cathode chamber was continuously aerated with an airflow rate (20 mL/min).

Anode modification

The control reactor (MFC$_{control}$) was operated with an unmodified anode (pure carbon felt). In the second reactor (MFC$_{Fe}$), an anode made of carbon felt was modified by the deposition of 0.05 g of iron (III) oxide (Chempur, Poland). For modification, a suspension containing 0.05 g of metal oxide and 100 mL of distilled water was prepared. The suspension was placed in an ultrasonic bath for 15 min, the carbon felt was immersed in the slurry and autoclaved (Prestige Medical, 1.1 bar, and 121 °C). After autoclaving

Fig. 1 Scheme of the MFC rector
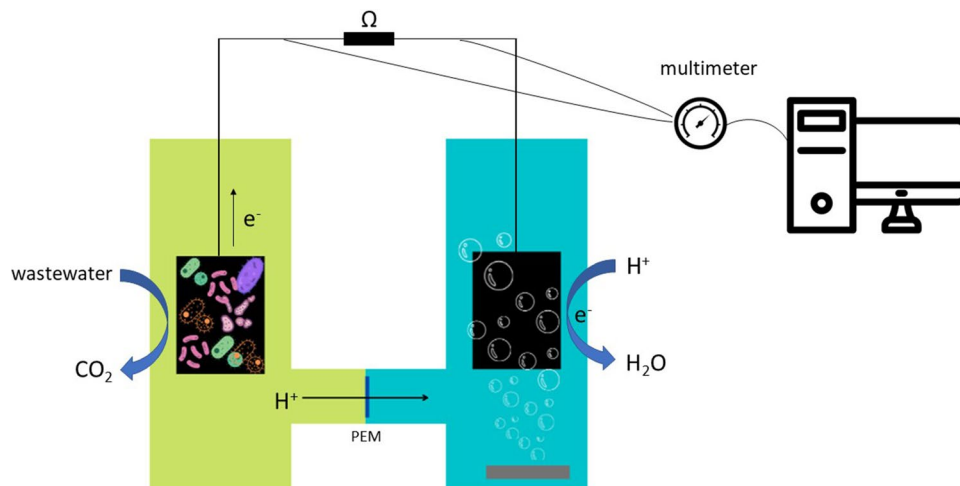
for 1 h, the anode was dried at 80 °C. If it was determined that the iron deposition on the electrode was less than 95%, the procedure was repeated.

The degree of Fe deposition on the anode (n) was determined by measuring the Fe concentration using the Hach Lange LCK 320 cuvette test, and then subtracting the final concentration of Fe in the liquid (after deposition) from the initial concentration, according to the following formula (Eq. 1):

$$n = \frac{Fe0 - Fe1}{Fe0} \cdot 100\% \tag{1}$$

where Fe0 is the initial concentration of Fe, and Fe1 is the concentration of iron remaining in the liquid after deposition.

MFC operation

The anode chambers in both MFCs were inoculated with 50 mL of anaerobic sludge from the digestion chambers of the "Łyna" wastewater treatment plant in Olsztyn (20°29'E 53°47'N). As a substrate, a mixture of volatile fatty acids (VFAs) from the digestion of primary sludge in the wastewater treatment plant was used. The VFA mixture was poured through a 2 mm sieve to remove large suspensions and stored at 4 °C. The VFA mixture was characterized by 2298 mg COD/L; 788 mg CH_3COOH/L; 35.5 mg N-NH_4/L. The VFA mixture was diluted to 400 mg COD/L and adjusted to pH 7 with 1 M HCl (anolyte). The anolyte was replaced daily and the volumetric exchange rate was 50%. After a two-week acclimatization period of MFCs, the experiment was carried out for 18 cycles.

Physico-chemical analyses

In samples taken from the anode chamber, the following values were determined: COD (dichromate method), VFA (direct distillation), N-NH_4 (direct Nesslerization) according to APHA (1992), and pH and alkalinity (TitroLine, Donserv). The voltage produced in the MFC was measured with a multimeter (True-RMS). The 6600 Counts PC-LINK program was used to save the data; changes in the generated voltage were recorded every minute. The current intensity was calculated using Ohm's law on the basis of the external resistance. The power curves were determined by changing the external resistance in the range of 0–27 000 Ω. The VFA composition was determined using a Varian CP-3800 chromatograph (Bułkowska et al. 2021). Spectroscopic characterization of the surface of pure carbon felt after sonication in the ultrasound batch and carbon felts modified with a dose of Fe_2O_3 was performed using a Quanta FEG

250 Scanning Electron Microscope (SEM/EDX, Quanta FEG 250, FEI).

Abiotic test of iron release

To monitor iron release from the carbon felt, a biomass-free test was performed. For this purpose, an anode modified as described above was placed in a measuring vessel with a volume of 1 L. As a substrate, synthetic wastewater (Coelho et al. 2000) without iron was used; the pH was adjusted to match the pH of the VFA mixture. The measuring vessel was sealed to maintain anaerobic conditions. The experiment was carried out for 18 cycles, in parallel to the operation of both MFCs used in the study. After each cycle, 0.5 L of wastewater was removed and replaced with fresh substrate. The iron content in the collected supernatant was determined using the Hach Lange LCK320 cuvette test using a Hach Lange DR 3900 spectrophotometer (Hach Lange, Germany).

Microbial analyses

FastDNA SPIN Kit for Soil (MP Biomedicals) was used to isolate DNA from inoculum and 100 μg of biofilm scratched from the anodes at the end of the experiment. Isolations were performed in duplicate and DNAs from each repetition were mixed. The quality and quantity of the DNA were assessed using NanoDrop spectrometer (Thermo Scientific). For amplification of the DNA, a primer set 515F/806R (5'- GTG CCAGCMGCCGCGGTAA-3'/5'—GGACTACHVGGG TWTCTAAT-3') targeting the hypervariable region (V4) of bacterial and archaeal 16S rDNA genes was used (Caporaso et al. 2011). The amplicons were sequenced at Research and Testing Laboratory (USA) using the MiSeq platform. The sequences were analyzed as described in Świątczak and Cydzik-Kwiatkowska (2018). The raw sequences were deposited in the NCBI Sequence Read Archive (SRA) as BioProject PRJNA834909.

Statistical analyses

For statistical analysis, Statistica (13.3, StatSoft) was used. For the analysis of COD and NH_4-N, results from the whole experimental period were taken. The voltages were analyzed for the seven cycles obtained during the experiment. For analysis of variance, one-way ANOVA was used followed by Tukey's test (HSD). Molecular data were analyzed using MicrobiomeAnalyst (Dharival et al. 2017, Chong et al. 2020). The number of reads was not normalized, because in the complex microbial communities, bacteria with a low abundance may be of great importance (McMurdie and Holmes 2014).

The Shannon index of diversity is calculated according to the formula (Eq. 2):
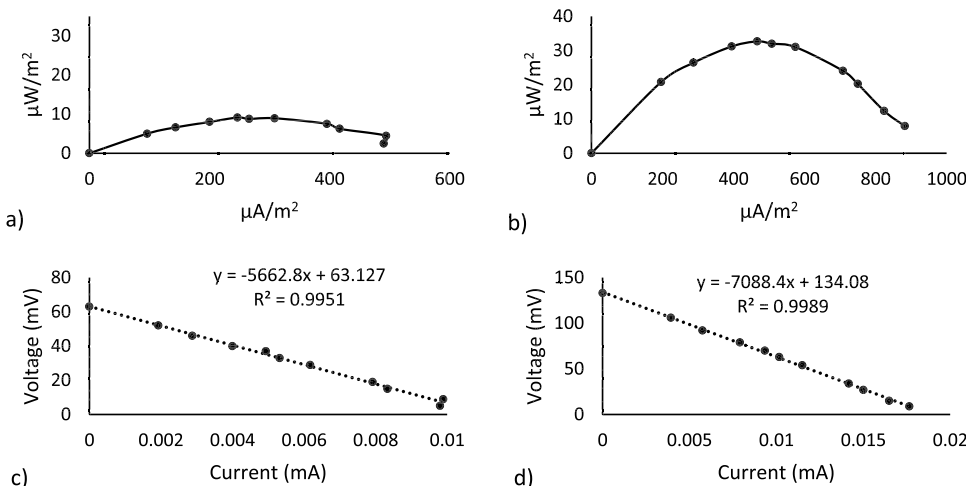
$$H = - \sum (p \cdot \ln(p)) \qquad (2)$$

where p—the proportion of the entire community made up of species. $\ln(p)$—natural logarithm from p (Shannon 1948).
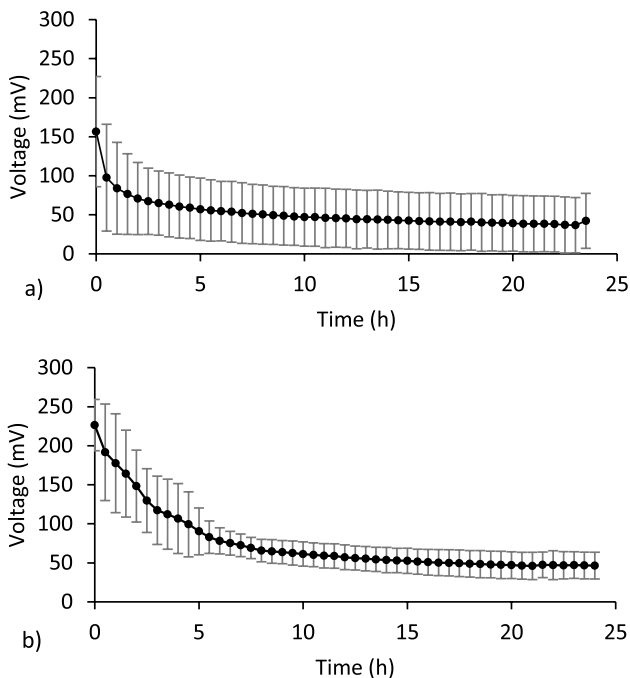
Fig. 2 The averaged voltages that were recorded during the cycle in **a** $MFC_{control}$ and **b** MFC_{Fe} (average from the last seven cycles of the experiment). Vertical whiskers represent the standard deviation of the mean ($n = 7$)

Results and discussion

Abiotic test of iron release

The amount of iron deposited on the anode was 50 mg Fe_2O_3, which corresponds to 34.9 mg of iron. The iron release test carried out without the presence of biofilm on the anode showed that only divalent iron was present in the effluent, which indicates the reducing conditions in the measuring vessel. The total amount of iron released from the electrode and removed with wastewater after 18 cycles was 2.46 mg Fe. It means that after the experiment, 7.05% of all iron that was used for the anode modification was removed. However, it should be noted that the calculated amount of iron removed is only an estimate, as the amount of iron released from the abiotic anode may differ from that released from the inhabited anode.

Electricity generation

The deposition of iron (III) oxide on the carbon felt was verified with an electron microscope. Both SEM (Fig. 1 SM) images and EDS analyses (Fig. 2SM) showed that iron oxide was successfully and regularly deposited on the electrode. The degree of iron deposition on the electrode was 99.1%.

In both MFCs, the voltage surges were observed at the beginning of each new cycle (Fig. 2) to on average 150 ± 68 mV and 226 ± 32 mV in the $MFC_{control}$ and MFC_{Fe}, respectively. In the $MFC_{control}$, the voltage gradually decreased to about 57 ± 39 mV after 5 h. In this reactor, a less stable generation of electricity was observed, as evidenced by the standard deviations. The average value of the

Fig. 3 Power curves for **a** $MFC_{control}$ and **b** MFC_{Fe} and polarization curves for **c** MFC_{contol} and **d** MFC_{Fe}

91:5423425267

output voltage from the cell for all cycles was 52 ± 20 mV. In MFC_{Fe}, the voltage decreased gradually for about 10 h and then stabilized at about 40–50 mV. The average value of the voltage in the MFC_{Fe} was 75 ± 41 mV. The voltages recorded in the MFC_{Fe} were significantly higher (ANOVA–Tukey's HSD post hoc test, $p = 0.0006$) than in the $MFC_{control}$ (Fig. 3SM). The presence of iron on the anode not only improved electricity generation but also resulted in a more stable reactor operation in comparison with $MFC_{control}$ as can be concluded from the standard deviations. The previous study has shown that in the presence of Fe ions on the surface of the anode, Fe_3C is formed, which promotes the adsorption of flavin (Sun et al. 2022). Flavins mediate electron transfer between the substrate and cells. The direct contact of flavin with cell membrane proteins results in a strong direct electron transfer that stimulates mediation and direct electrochemical processes. This positive effect of iron is also observed for complex chemical compounds containing iron. The use of $MgFe_2O_4$ as a modifier of stainless steel anode in MFC designed to remove Congo red allowed to obtain 20% higher voltages than in the control reactor with the unmodified anode (Khan et al. 2021).

The power and polarization curves were determined in the stable period of operation of the MFCs (the fourth cycle of voltage measurements). Polarization curves were determined by changing the external resistance in the MFC and registering the voltage generated by the cell. Based on Ohm's law, the maximum power of the cell was obtained. In $MFC_{control}$, the maximum power was nearly four times lower (Fig. 3a) than the power obtained in the MFC_{Fe} (Fig. 3b). The positive effect of modification of anode with iron was also observed in the studies by Sayed et al. (2020) in which wastewater containing 700 mg COD/L was used as a substrate. In the case of a cell with an unmodified anode, a power density of 40 mW/m^2 and a current density of 71 mA/m^2 were obtained. After the anode was modified with iron, the power density and the current density doubled.
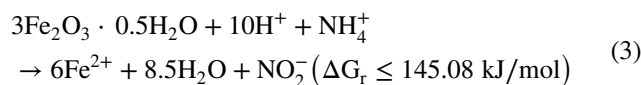
In our study, the low power densities can be related to the high internal resistances of the MFCs. The internal resistance of the MFC_{Fe} was 7088.4 Ω (Fig. 3d) and was 1.25 times higher than in $MFC_{control}$ (Fig. 3c). Internal resistance consists of ohmic losses, activation losses, bacterial metabolic losses, and concentration losses (Logan et al. 2006). A previous study on the effect of iron on the ohmic resistance of MFC has shown that the addition of 4.5 and 9.0 g Fe_3O_4/L of the substrate fed to MFC reduced the ohmic resistance 1.50 and 1.08 times, compared to the control. On the other hand, at the dose of 18.0 g/L, the resistance was increased because the excess iron negatively affected the adhesion of electrogens (Zheng et al. 2022).

Nevertheless, in our research, the MFC_{Fe} obtained higher power despite the higher internal resistance.

In general, the use of VFAs produced during fermentation increases the conductivity of the anolyte, which resulted in a reduction in the resistance of ion flow through the membrane and the flow of electrons through the anolyte (Raychaudhuri and Behera 2021). However, an important operating parameter of the MFC is also the concentration of the organics in the reactor. Our previous study has shown that high organic loadings favor membrane clogging and thus obstruct MFC operation (Nosek and Cydzik-Kwiatkowska 2020). Therefore, in our study, the concentration of COD in the MFC at the beginning of the cycle was low and averaged 0.26 ± 0.017 g COD/L. This allowed stable electricity generation without the necessity of often membrane cleaning. This low concentration caused, however, that the electricity obtained in MFCs was lower than in other studies. Chatzikonstantinou et al. (2018) tested the use of food residue biomass in the dual-chamber MFC by applying concentrations of organics as high as 14.0 g COD/L. The highest power density of 29.6 mW/m^2 and the corresponding current density of 88 mA/m^2 were observed for 6 g COD/L.

COD, VFA, and ammonium removal

COD concentrations in the MFC effluents fluctuated in the initial period of operation, reaching about 170 and 230 mg/L in $MFC_{control}$ and MFC_{Fe}, respectively. During the period of stable operation of the MFCs, the concentration of COD in the outflow ranged from 100 to 140 mg/L and the average COD removal efficiency was $54.3 \pm 9.8\%$ and $48.8 \pm 9.5\%$ for $MFC_{control}$ and MFC_{Fe}, respectively. No significant differences were observed in COD removal efficiency between the reactors (Fig. 4SM). The mean concentrations of ammonium in the outflow were $5.4 \pm 0.8\%$ and $4.4 \pm 0.8\%$ for $MFC_{control}$ and MFC_{Fe}, respectively. The ammonium concentrations in the MFC_{Fe} outflow were significantly lower (ANOVA–Tukey's HSD post hoc test, $p = 0.0025$) than in the $MFC_{control}$ showing a positive effect of iron presence on the ammonium metabolism (Fig. 5SM). In anaerobic environments, in the presence of Fe(III), NH_4^+ is an electron donor and is oxidized to NO_2^- by reduction in Fe(III) to Fe(II) according to the formula (Huang and Jaffé, 2015) (Eq. 3).
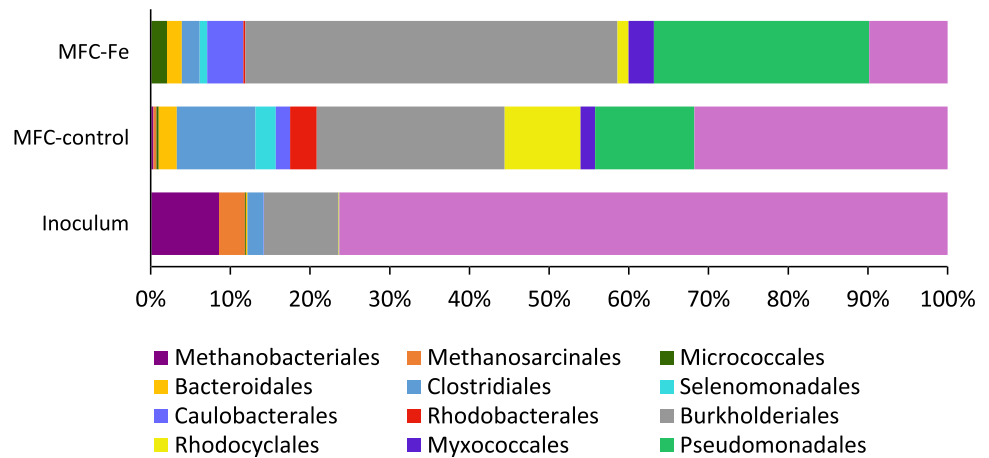
$$3Fe_2O_3 \cdot 0.5H_2O + 10H^+ + NH_4^+ \rightarrow 6Fe^{2+} + 8.5H_2O + NO_2^- \left(\Delta G_r \leq 145.08 \text{ kJ/mol} \right) \tag{3}$$

Fig. 4 VFA profile of anolyte added to MFCs and in the MFC effluents. Vertical whiskers represent the standard deviation of the mean ($n = 2$)
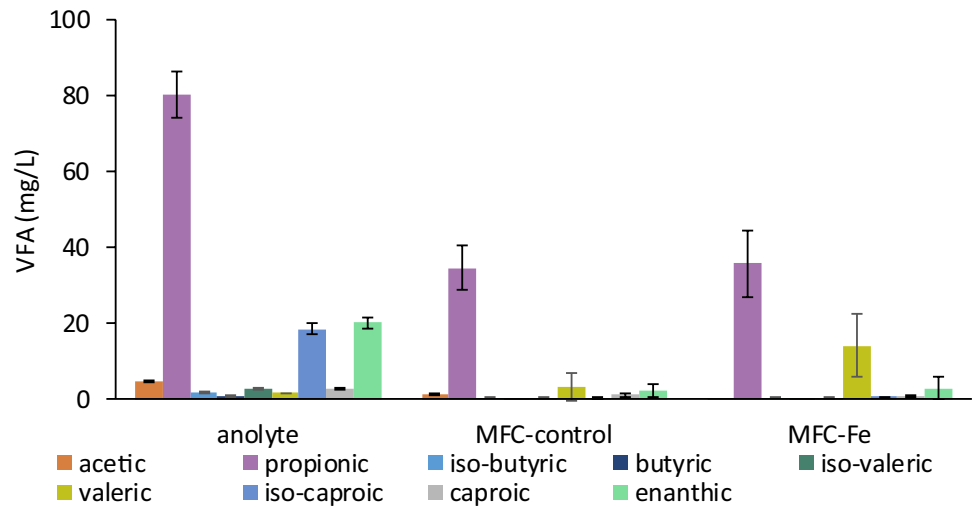
Fig. 5 Relative abundance of particular bacterial orders in the inoculum and anodic biofilm obtained from the MFCs

Zhu et al. (2022) tested the effect of five Fe (III) compounds (Fe_2O_3, Fe_3O_4, $Fe(OH)_3$, Fe-citrate, and pyrite) on the anaerobic ammonium oxidation. The highest improvement in ammonium removal efficiency was observed after the addition of 20 mM Fe_2O_3—the effluent ammonium concentration dropped drastically from 104.79 mg/L to 52.3 mg/L.

The VFA removal efficiency in both reactors was similar and remained at the level of $60.4 \pm 16.9\%$ and $50.2 \pm 26.3\%$, in $MFC_{control}$ and MFC_{Fe}, respectively. Analysis of the VFA profile in the inflow and outflow of the MFCs revealed that propionic acid was the major component (Fig. 4). Its share in anolyte and MFC_{Fe} outflow was 60–65%, while in the outflow from $MFC_{control}$, its share reached 80%. In the raw wastewater, a high proportion of iso-caproic and enanthic acids (15 and 14%, respectively) was observed, but in the MFC outflows, the proportion

Table 1 Alpha diversity indicators in all tested MFC reactors; OUT–Operational Taxonomic Unit, Shannon–biodiversity index

	OTU	Shannon	Number of reads
Inoculum	106	2.21	20,963
$MFC_{control}$	183	3.18	21,371
MFC_{Fe}	117	2.42	20,336

of these acids decreased to below 5%. The outflow from MFC_{Fe} showed a higher share of valeric acid (26%) compared to the outflow from $MFC_{control}$. In earlier studies regarding the fermentation of waste activated sludge, along with the increase in the dose of nano-zero valent iron in the feed in fermentation reactors, the share of individual acids in the production of VFA increased, while in the control reactor, acetic acid predominated (98%) (Luo

93:7812611474

et al. 2014). Our study confirms the positive effect of Fe on the synthesis of medium-chain length VFAs also in MFC reactors. The effluent from MFC reactors with Fe-modified anodes can be a valuable source of carbon for crucial processes in biological wastewater treatment. For example, Janczukowicz et al. (2013) reported that propionic acid and valeric acid can be effectively used for denitrifications of high concentrations of nitrates from wastewater (over 90% efficiency with an initial concentration of 15.2 mg/L). On the other hand, the efficiency of phosphorus removal was lower when propionic and valeric acids were used than when acetic acid was used. Propionic and valeric acids present in MFC effluent can be converted during fermentation to produce polyhydroxyvalerate (PHV) polymer (Carvalheira and Duque 2021).

Biofilm analyses

The anode biofilm from MFCs was subjected to molecular analysis. The total number of readings per both MFC samples and inoculum was over 20 000 (Tab. 1). The numbers of OTU and Shannon index indicate that anode modification with Fe lowered the diversity of anodic biofilm by over 20% in comparison with MFC$_{control}$. Similar results were obtained in studies, in which Fe (II) was directly added to the feed introduced to MFC reactors. The presence of 100 μM and 200 μM Fe in the anolyte decreased the Shannon index to 3.72, 4.71 in comparison with 5.21 observed in the control MFC (Liu et al. 2017). The lower microbial diversity in the MFC$_{Fe}$ biofilm may result from the fact that the presence of iron particles could be toxic to some microorganisms. The toxicity of metal oxides was recently described in a review by Niño-Martínez et al. (2019). The authors indicated that metals and metal oxides with small particle size showed greater antimicrobial activity and that their toxicity may result from both the electrostatic attraction of negatively charged pathogens and positively charged nanoparticles and the release of ions that are toxic to bacteria (Niño-Martínez et al. 2019). Apparently, in the present study, the interactions between the iron(III) oxide particles and microorganisms inhabiting the anode caused some of the microorganisms to disappear from the biofilm as a result of community adaptation.

In the inoculum, unclassified bacteria had the largest share (38%), followed by Methanobacteriales (9%) and Burkholderiales (9%). At the genus level, *Methanobacterium* sp. (9%), *Hydrogenophaga* sp. (9%), *Candidatus* Cloacimonas acidaminovorans (7%), and

Inoculum	MFC-contol	MFC-Fe	
8.5	0.1	0.0	*Methanobacterium*
0.6	0.0	0.0	*Methanolinea*
3.1	0.2	0.0	*Methanosaeta*
0.0	0.0	1.0	*Geothrix*
0.0	0.2	2.0	*Leucobacter*
0.1	1.2	0.8	*Bacteroides*
1.0	0.5	0.0	*Cytophaga*
7.2	0.1	0.0	*Candidatus* Cloacimonas
0.0	0.6	0.3	*Enterococcus*
1.5	5.2	1.3	*Clostridium*
0.0	0.6	0.0	*Acidaminobacter*
0.0	1.0	0.2	*Anaerovorax*
0.0	0.9	0.2	*Schwartzia*
0.0	0.9	4.3	*Brevundimonas*
0.0	0.7	0.2	*Phenylobacterium*
0.0	0.7	0.4	*Rhizobium*
0.0	23.1	46.3	*Acidovorax*
9.3	0.5	0.3	*Hydrogenophaga*
0.0	9.1	0.3	*Zoogloea*
0.0	0.7	0.1	*Desulfobulbus*
0.0	0.8	0.2	*Desulfomicrobium*
0.0	1.8	3.2	*Corallococcus*
0.0	1.7	7.8	*Acinetobacter*
0.0	9.4	18.2	*Pseudomonas*
0.0	1.3	0.4	*Pseudoxanthomonas*
0.0	0.1	0.8	*Prosthecobacter*

Fig. 6 Heatmap showing 26 of the most numerous genera in the inoculum and anodic biofilms from the investigated MFCs

Metanosaeta sp. (3%) were most abundant, but all these microorganisms disappeared from the anodic biofilm during the experiment. At the anodes in both MFCs, at the end of the study, the most abundant group of microorganisms at the class level were Betaproteobacteria, including Burkholderiales (24% in MFC$_{control}$ and 47% in MFC$_{Fe}$), and Gammaproteobacteria, including Pseudomonadales (12% in MFC$_{control}$ and 27% in MFC$_{Fe}$) (Fig. 5).

The presence of iron on the anode positively affected the abundance of Burkholderiales and Pseudomonadales in the microbiome, which was about two times higher in the MFC$_{Fe}$ than in the MFC$_{control}$ (Fig. 5). The higher abundance of Burkholderiales in MFC$_{Fe}$ could be due to the fact that some species of this order are metal persistent and participate in the biotransformation of metal oxides (e.g., Fe and Mn) and support biocorrosion (Beech and Gaylarde 1999). On the other hand, the results showed the sensitivity of Rhodocyclales and Clostridiales to the presence of Fe, because the share of those bacteria in MFC$_{Fe}$ was 10 and 5 times lower, respectively, than in the control.

The most numerous genus in anodic biofilms was *Acidovorax* followed by *Pseudomonas* and *Acinetobacter*

(Fig. 6). *Acinetobacter* sp. presence was not affected by the presence of Fe on the anode and remains at about 8%, but the abundance of the other two genera was higher on Fe-modified anodes. *Acidovorax* sp. could utilize different carbon sources such as ethanol, methanol, glucose, or sodium acetate (Nalcaci et al. 2011), and it was observed on biocathodes in MFCs (Sun et al. 2012). Members of the genus *Acidovorax* are facultative microorganisms, that reduce nitrate and oxidize iron most likely indirectly through the reactive nitrogen species produced during the denitrification process (Klueglein et al. 2015). The study on native rock samples indicated that there was a strong correlation between the abundance of *Acidovorax* sp. and Fe-containing pyrite. *Acidovorax* sp. colonies were attached to the rock samples and single cells were surrounded by exopolysaccharides containing ferric iron which may have enhanced the bio-oxidation of metallic sulfides (Escudero et al. 2020). Members of *Pseudomonas* sp. are also able to reduce Fe(III) and were proven to effectively utilize various hexose and pentose sugars through anode respiration (Ali et al. 2017). Both the ability to utilize various organics and preference toward Fe in the environment decided that in the present study, *Acidovorax* sp. and *Pseudomonas* sp. abundances increased twice in MCF with the Fe-modified anode. In the case of *Acidovorax* sp., it caused that they constituted nearly half of all bacteria in the biofilm on the Fe-modified anode. Members of *Pseudomonas* sp. hydrolyze sugars and generate VFAs. Previous studies in digesters indicate that the growth of *Pseudomonas* sp. in biomass was stimulated by the presence of peroxydisulfate and Fe(II) or zero valent iron (Luo et al. 2020).

The presence of iron on the anode significantly increased the number of microorganisms belonging to the genera *Brevundimonas*, *Geothrix,* and *Leucobacter zeae*. The increased presence of *Geothrix* sp. is advantageous for electricity generation because members of *Geothrix* sp. can secrete redox-active electron shuttles with separate redox potentials of − 0.2 V and 0.3 V. The compound with the lower midpoint potential was identified as riboflavin and it was responsible for 20 to 30% of electron transfer activity in MFC (Mehta-Kolte and Bond 2012). Better conditions for growth for *Geothrix* sp. on iron-modified anode can be also explained by the fact that they use iron in their metabolism. Coates et al. (1999) indicated that *Geothrix fermentans* was able to grow with VFA such as acetate, lactate, propionate, or fumarate as alternative electron donors using Fe(III) as the acceptor of electron and oxidized long-chain FA using Fe(III) as the sole electron acceptor. *Brevundimonas* sp. is a facultative anaerobic bacterium whose presence has been reported on the biocathode in the presence of Cr(VI) (Romo et al. 2019), but its role in MFC has not yet been elucidated. However, a positive effect of iron on selected metabolic changes in *Brevundimonas* sp. was observed. In some *Brevundimonas* strains, the efficiency of H_2 production from sugars increased in the reactor to which Fe(II) was dosed (Bao et al. 2013).

The abundance of *Zoogloea* sp. (Rhodocyclales order) decreased significantly in MFC with the iron-modified anode to below 0.3% in comparison with 9.14% in the control MFC. Earlier studies indicate that in aerobic conditions, *Zoogloea* sp. may be abundant in biomass despite high iron concentrations in the environment. For example, in the aerobic granules from the reactor operated at the Fe concentration in the wastewater at the level of 6 mg Fe(III)/L, *Zoogloea* sp. accounted for nearly 70% of all bacteria (Zou et al. 2021). In our research, the decrease in the share of *Zoogloea* sp. w MFC with modified anode indicates that this genus lost in competition with facultative, Fe-oxidizing bacteria that predominated in the biofilm.

Conclusion

In this study, waste VFA from the fermentation of primary sludge was used in MFC with an iron-modified anode for electricity generation and the structure of the anode microbiome was determined. The study showed that the power obtained from MFC_{Fe} was 3.6 times higher than in $MFC_{control}$, and the efficiency of COD removal was 50%. The main VFA components in the MFC outflows were propionic acid; a high proportion of valeric acid was observed in the outflow from MFC_{Fe}. The presence of iron on the anode promoted the presence of electrogens such as *Pseudomonas* sp. and *Geothrix* sp. and VFA degrades such as *Acidovorax* sp. Moreover, the proportion of *Brevundimonas* sp. and *Leucobacter* sp. in MFC_{Fe} was significantly higher than in $MFC_{control}$. However, in MFC_{Fe}, *Zoogloea* sp. was replaced by other iron-reducing microorganisms. Research indicates that waste VFA can be effectively used to produce electricity, and the confluence of MFC with AD may give good results in bioenergy in the future.

and the Polish National Science Center (Grant Number 2016/21/B/NZ9/03627). The language correction of the manuscript was financially supported by the Minister of Education and Science under the program entitled "Regional Initiative of Excellence" for the years 2019–2023, Project No. 010/RID/2018/19, amount of funding 12.000.000 PLN.

Declarations

Conflict of interest The authors have no conflicts of interest to declare.

Human participants or animal This article does not contain any studies with human participants or animal performed by any of the authors.

Open Access This article is licensed under a Creative Commons Attribution 4.0 International License, which permits use, sharing, adaptation, distribution and reproduction in any medium or format, as long as you give appropriate credit to the original author(s) and the source, provide a link to the Creative Commons licence, and indicate if changes were made. The images or other third party material in this article are included in the article's Creative Commons licence, unless indicated otherwise in a credit line to the material. If material is not included in the article's Creative Commons licence and your intended use is not permitted by statutory regulation or exceeds the permitted use, you will need to obtain permission directly from the copyright holder. To view a copy of this licence, visit http://creativecommons.org/licenses/by/4.0/.

References

Ali N, Anam M, Yousaf S, Maleeha S, Bangash Z (2017) Characterization of the electric current generation potential of the *Pseudomonas aeruginosa* using glucose, fructose, and sucrose in double chamber microbial fuel cell. Iran J Biotechnol 15(4):216–223. https://doi.org/10.15171/ijb.1608

APHA (1992) Standard Methods for the Standard Methods for the Examination of Water and Wastewater, 18th ed.; American Public Health Association (APHA), American Water Works Association (AWWA), Water Pollution Control Federation (WPCF): Washington, DC, USA

Bao MD, Su HJ, Tan TW (2013) Dark fermentative bio-hydrogen production: effects of substrate pre-treatment and addition of metal ions or L-cysteine. Fuel 112:38–44. https://doi.org/10.1016/j.fuel.2013.04.063

Beech IB, Gaylarde CC (1999) Recent advances in the study of biocorrosion: an overview. Rev Argent Microbiol 30(3):117–190. https://doi.org/10.1590/S0001-37141999000300001

Bułkowska K, Mikucka W, Pokój T (2021) Enhancement of biogas production from cattle manure using glycerine phase as a co-substrate in anaerobic digestion. Fuel 317:123456. https://doi.org/10.1016/j.fuel.2022.123456

Caporaso JG, Lauber CL, Walters WA, Berg-Lyons D, Lozupone CA, Turnbaugh PJ, Fierer N, Knight R (2011) Global patterns of 16S rRNA diversity at a depth of millions of sequences per sample. Proc Natl Acad Sci USA 108(Supplement 1):4516–4522. https://doi.org/10.1073/pnas.1000080107

Carvalheira M, Duque AF (2021) From food waste to volatile fatty acids towards a circular economy. In: Laranjo M (ed) Fermentation-Processes, Benefits and Risks. IntechOpen, United Kingdom, pp 165–185

Chatzikonstantinou D, Tremouli A, Papadopoulou K, Kanellos G, Lampropoulos I, Lyberatos G (2018) Bioelectricity production from fermentable household waste in a dual-chamber microbial fuel cell. Waste Manag Res 36(11):1037–1042. https://doi.org/10.1177/0734242X18796935

Choi J, Chang HN, Han J-I (2011) Performance of microbial fuel cell with volatile fatty acids from food wastes. Biotechnol Letter 33:705–714. https://doi.org/10.1007/s10529-010-0507-2

Chong J, Liu P, Zhou G, Xia J (2020) Using microbiomeanalyst for comprehensive statistical, functional, and meta-analysis of microbiome data. Nat Protoc 15(3):799–821. https://doi.org/10.1038/s41596-019-0264-1

Christwardana M, Frattini D, Accardo G, Yoon SP, Kwon Y (2018) Optimization of glucose concentration and glucose/yeast ratio in yeast microbial fuel cell using response surface methodology approach. J Power Sources 402:402–412. https://doi.org/10.1016/j.jpowsour.2018.09.068

Coates JD, Ellis DJ, Gaw CV, Lovley DR (1999) *Geothrix fermentans* gen. nov., sp. Nov., a novel Fe(III)-reducing bacterium from a hydrocarbon-contaminated aquifer. Int J Syst Bacteriol 49(4):1615–1622. https://doi.org/10.1099/00207713-49-4-1615. (**PMID: 10555343**)

Coelho MAZ, Russo C, Araujo OQF (2000) Optimization of a sequencing batch reactor for biological nitrogen removal. Water Res 34(10):2809–2817. https://doi.org/10.1016/S0043-1354(00)00010-5

Cornejo JA, Lopez C, Babanova S, Santoro C, Artyushkova K, Ista L, Chuler AJ, Atanassov P (2015) Surface modification for enhanced biofilm formation and electron transport in *Shewanella* anodes. J Electroche Soc 162(9):H597

Costerton JW (2007) The Biofilm Primer. Springer, Berlin-New York, p 70

Dhariwal A, Chong J, Habib S, King I, Agellon LB, Xia J (2017) MicrobiomeAnalyst—a web-based tool for comprehensive statistical, visual and meta-analysis of microbiome data. Nucleic Acids Res 45(W1):W180–W188. https://doi.org/10.1093/nar/gkx295

Dubey A, Malla MA, Kumar A (2022) Role of Next-generation sequencing (NGS) in understanding the microbial diversity. In: Kumar A, Choudhury B, Dayanandan S, Khan ML (eds) Molecular genetics and genomics tools in biodiversity conservation. Springer, Singapore, pp 307–328

Escudero C, del Campo A, Ares JR, Sánchez C, Martínez JM, Gómez F, Amils R (2020) Visualizing microorganism-mineral interaction in the iberian pyrite belt subsurface: the *Acidovorax* case. Front Microbiol 11:572104. https://doi.org/10.3389/fmicb.2020.572104

Freguia S, The EH, Boon N, Leung KM, Keller J, Rabaey K (2010) Microbial fuel cells operating on mixed fatty acids. Bioresour Technol 101(4):1233–1228. https://doi.org/10.1016/j.biortech.2009.09.054

Ghasemi M, Shahgaldi S, Ismail M, Kim BH, Yaakob Z, Daud WRW (2011) Activated carbon nanofibers as an alternative cathode catalyst to platinum in a two-chamber microbial fuel cell. Int J Hydrog Energy 36(21):13746–13752. https://doi.org/10.1016/j.ijhydene.2011.07.118

Greenman J, Gajda I, You J, Mendis BA, Obata O, Pasternak G, Ieropoulos I (2021) Microbial fuel cells and their electrified biofilms. Biofilm 3:100057. https://doi.org/10.1016/j.bioflm.2021.100057

He J, Xin X, Pei Z, Chen L, Chu Z, Zhao M, Wu X, Li B, Tang X, Xiao X (2021) Microbial profiles associated improving bioelectricity generation from sludge fermentation liquid via microbial fuel cells with adding fruit waste extracts. Bioresour Technol 337:125452. https://doi.org/10.1016/j.biortech.2021.125452

Hou Q, Yang Z, Chen S, Pei H (2020) Using an anaerobic digestion tank as the anodic chamber of an algae-assisted microbial fuel cell to improve energy production from food waste. Water Res 170:115305. https://doi.org/10.1016/j.watres.2019.115305

Huang S, Jaffé PR (2015) Characterization of incubation experiments and development of an enrichment culture capable of ammonium oxidation under iron-reducing conditions. Biogeosciences 12(3):769–779. https://doi.org/10.5194/bg-12-769-2015

Janczukowicz W, Rodziewicz J, Czaplicka K, Kłodowska I, Mielcarek A (2013) The effect of volatile fatty acids (VFAs) on nutrient removal in SBR with biomass adapted to dairy wastewater. J Environ Sci Health Part A 48(7):809–816. https://doi.org/10.1080/10934529.2013.744658

Karn B, Kuiken T, Otto M (2009) Nanotechnology and in situ remediation: a review of the benefits and potential risks. Environ Health Perspect 117(12):1813–1831. https://doi.org/10.1289/ehp.0900793

Kato S, Hashimoto K, Watanabe K (2013) Iron-oxide minerals affect extracellular electron-transfer paths of *Geobacter* spp. Microbes Environ. https://doi.org/10.1264/jsme2.ME12161

Khan N, Anwer AH, Khan MD, Azam A, Ibhadon A, Khan MZ (2021) Magnesium ferrite spinels as anode modifier for the treatment of Congo red and energy recovery in a single chambered microbial fuel cell. J Hazard Mater 410:124561. https://doi.org/10.1016/j.jhazmat.2020.124561

Klueglein N, Picardal F, Zedda M, Zwiener C, Kappler A (2015) Oxidation of Fe (II)-EDTA by nitrite and by two nitrate-reducing Fe (II)-oxidizing *Acidovorax* strains. Geobiology 13:198–207. https://doi.org/10.1111/gbi.12125

Liang P, Duan R, Jiang Y, Zhang X, Qiu Y, Huang X (2018) One-year operation of 1000-L modularized microbial fuel cell for municipal wastewater treatment. Water Res 141:1–8. https://doi.org/10.1016/j.watres.2018.04.066

Liu Q, Liu B, Li W, Zhao X, Zuo W, Xing D (2017) Impact of ferrous iron on microbial community of the biofilm in microbial fuel cells. Front Microbiol 8:920. https://doi.org/10.3389/fmicb.2017.00920

Logan BE, Hamelers B, Rozendal R, Schröder U, Keller J, Freguia S, Aelterman P, Verstraetate W, Rabaey K (2006) Microbial fuel cells: methodology and technology. Environ Sci Technol 40(17):5181–5192. https://doi.org/10.1021/es0605016

Luo J, Feng L, Chen Y, Li X, Chen H, Xiao N, Wang D (2014) Stimulating short-chain fatty acids production from waste activated sludge by nano zero-valent iron. J Biotechnol 187:98–105. https://doi.org/10.1016/j.jbiotec.2014.07.444

Luo J, Huang W, Zhu Y, Guo W, Yibing L, Wu L, Zhang Q, Wu Y, Fang F, Cao J (2020) Influences of different iron forms activated peroxydisulfate on volatile fatty acids production during waste activated sludge anaerobic fermentation. Sci Total Environ 705:135878. https://doi.org/10.1016/j.scitotenv.2019.135878

McMurdie PJ, Holmes S (2014) Waste not, want not: why rarefying microbiome data is inadmissible. PLoS Comput Biol 10(4):e1003531. https://doi.org/10.1371/journal.pcbi.1003531

Mehta-Kolte MG, Bond DR (2012) *Geothrix fermentans* secretes two different redox-active compounds to utilize electron acceptors across a wide range of redox potentials. Appl Environ Microbiol 78(12):6987–6995. https://doi.org/10.1128/AEM.01460-12

Nalcaci OO, Böke N, Ovez B (2011) Potential of the bacterial strain *Acidovorax avenae* subsp. avenae LMG 17238 and macro algae *Gracilaria verrucosa* for denitrification. Desalination 274(1–3):44–53. https://doi.org/10.1016/j.desal.2011.01.067

Niño-Martínez N, Salas Orozco MF, Martínez-Castañón GA, Torres Méndez F, Ruiz F (2019) Molecular mechanisms of bacterial resistance to metal and metal oxide nanoparticles. Int J Mol Sci 20(11):2808. https://doi.org/10.3390/ijms20112808

Nosek D, Cydzik-Kwiatkowska A (2020) Microbial structure and energy generation in microbial fuel cells powered with waste anaerobic digestate. Energies 13(18):4712. https://doi.org/10.3390/en13184712

Nosek D, Jachimowicz P, Cydzik-Kwiatkowska A (2020) Anode modification as an alternative approach to improve electricity generation in microbial fuel cells. Energies 13(24):6596. https://doi.org/10.3390/en13246596

Pant D, Arslan D, Van Bogaert G, Gallego YA, De Wever H, Diels L, Vanbroekhoven K (2013) Integrated conversion of food waste diluted with sewage into volatile fatty acids through fermentation and electricity through a fuel cell. Environ Technol 34(13–14):1935–1945. https://doi.org/10.1080/09593330.2013.828763

Raychaudhuri A, Behera M (2021) Enhancement of bioelectricity generation by integrating acidogenic compartment into a dual-chambered microbial fuel cell during rice mill wastewater treatment. Process Biochem 105:19–26. https://doi.org/10.1016/j.procbio.2021.03.003

Romo DMR, Gutiérrez NHH, Pazos JOR, Figueroa LVP, Ordóñez LAO (2019) Bacterial diversity in the Cr (VI) reducing biocathode of a microbial fuel cell with salt bridge. Rev Argent Microbiol 51(2):110–118. https://doi.org/10.1016/j.ram.2018.04.005

Savla N, Anand R, Pandit S, Prasad R (2020) Utilization of nanomaterials as anode modifiers for improving microbial fuel cells performance. J Renew Mater 8(12):1581–1605

Sayed ET, Alawadhi H, Elsaid K, Olabi AG, Adel AM, Bin Tamim ST, Alafranji GHM, Abdelkareem MA (2020) A carbon-cloth anode electroplated with iron nanostructure for microbial fuel cell operated with real wastewater. Sustainability 12(16):6538. https://doi.org/10.3390/su12166538

Schievano A, Colombo A, Cossettini A, Goglio A, D'Ardes V, Trasatti S, Cristiani P (2018) Single-chamber microbial fuel cells as on-line shock-sensors for volatile fatty acids in anaerobic digesters. Waste Manage 71:785–791. https://doi.org/10.3390/su12166538

Shannon CE (1948) A mathematical theory of communication. The Bell Syst Techn J 27(3):379–423

Sun Y, Wei J, Liang P, Huang X (2012) Microbial community analysis in biocathode microbial fuel cells packed with different materials. AMB Expr 2:21. https://doi.org/10.1186/2191-0855-2-21

Sun X, Wu X, Shi Z, Li X, Qian S, Ma Y, Sun W, Guo C, Li CM (2022) Electrospinning iron-doped carbon fiber to simultaneously boost both mediating and direct biocatalysis for high-performance microbial fuel cell. J Power Sources 530:231277. https://doi.org/10.1016/j.jpowsour.2022.231277

Świątczak P, Cydzik-Kwiatkowska A (2018) Performance and microbial characteristics of biomass in a full-scaleaerobic granular sludge wastewater treatment plant. Environ Sci Pollut Res 25:1655–1669. https://doi.org/10.1007/s11356-017-0615-9

Tremouli A, Vlassis T, Antonopoulou G, Lyberatos G (2016) Anaerobic degradation of pure glycerol for electricity generation using a MFC: the effect of substrate concentration. Waste Biomass Valorization 7(6):1339–1347. https://doi.org/10.1016/j.jpowsour.2022.231277

Tripathi B, Pandit S, Sharma A, Chauhan S, Mathuriya AS, Dikshit PK, Gupta PK, Singh RC, Sahni M, Pant K, Singh S (2022) Modification of graphite sheet anode with iron (II, III) oxide-carbon dots for enhancing the performance of microbial fuel cell. Catalysts 12(9):1040. https://doi.org/10.3390/catal12091040

Ullah Z, Zeshan S (2020) Effect of substrate type and concentration on the performance of a double chamber microbial fuel cell. Water

Sci Technol 81(7):1336–1344. https://doi.org/10.2166/wst.2019.387

Xin X, Hong J, Liu Y (2019) Insights into microbial community profiles associated with electric energy production in microbial fuel cells fed with food waste hydrolysate. Sci Total Environ 670:50–58. https://doi.org/10.1016/j.scitotenv.2019.03.213

Yu B, Li Y, Feng L (2019) Enhancing the performance of soil microbial fuel cells by using a bentonite-Fe and Fe_3O_4 modified anode. J Hazard Mater 377:70–77. https://doi.org/10.1016/j.jhazmat.2019.05.052

Zheng X, Hou S, Amanze C, Zeng Z, Zeng W (2022) Enhancing microbial fuel cell performance using anode modified with Fe_3O_4 nanoparticles. Bioprocess Biosyst Eng 45:877–890. https://doi.org/10.1007/s00449-022-02705-z

Zhou M, Chi M, Luo J, He H, Jin T (2011) An overview of electrode materials in microbial fuel cells. J Power Sources 196(10):4427–4435. https://doi.org/10.1016/j.jpowsour.2011.01.012

Zhu TT, Lai WX, Zhang YB, Liu YW (2022) Feammox process driven anaerobic ammonium removal of wastewater treatment under supplementing Fe (III) compounds. Sci Total Environ 804:149965. https://doi.org/10.1016/j.jcis.2006.09.011

Zou J, Yu F, Chen J, Mannina G, Li Y (2021) Influence of ferric iron dosing on aerobic granular sludge: granule formation, nutrient removal and microbial community. J Chem Technol Biotechnol 96:1277–1284. https://doi.org/10.1002/jctb.6640

Supplementary materials

Title : Waste volatile fatty acids as a good electron donor in microbial fuel cell with the iron-modified anode

Dawid Nosek*, Oliwia Samsel, Tomasz Pokój, Agnieszka Cydzik-Kwiatkowska

University of Warmia and Mazury in Olsztyn, Department of Environmental Biotechnology, 10-709 Olsztyn, Słoneczna 45 G

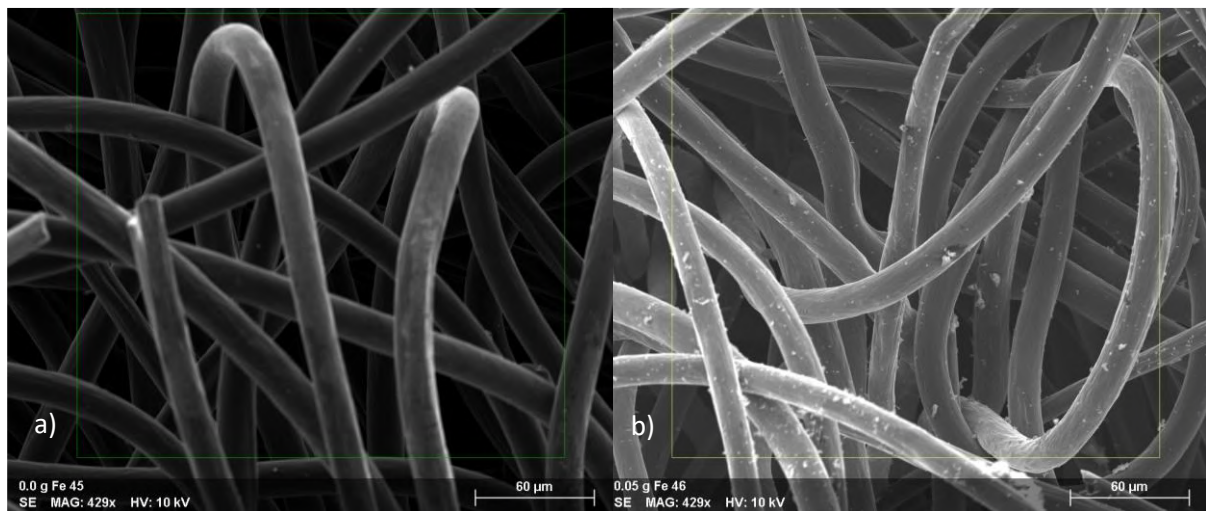Corresponding author: dawid.nosek@uwm.edu.pl, tel. +48 89 5234144

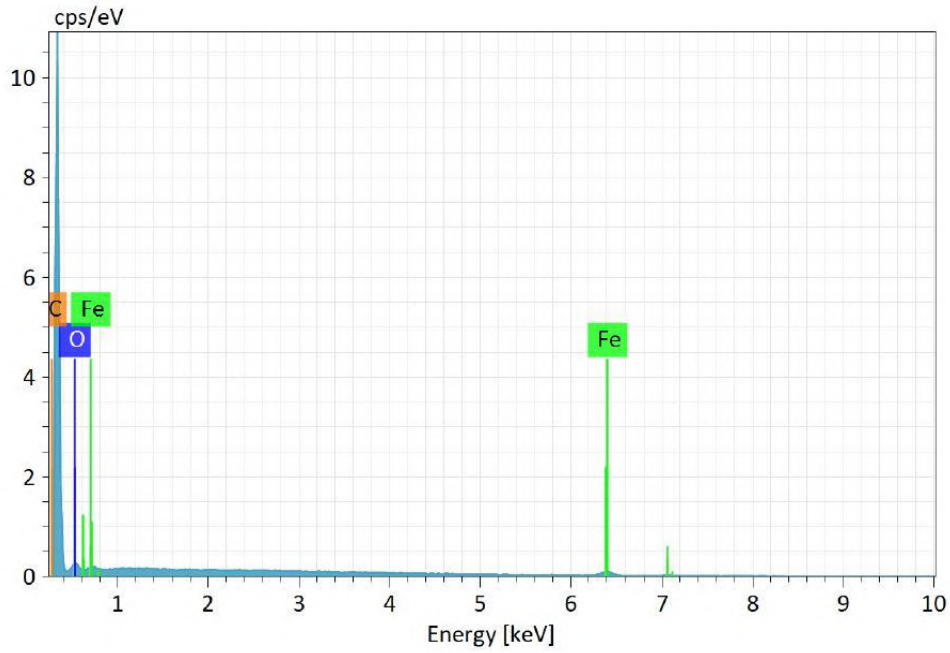Fig. 1SM. SEM analyses of anodes' surfaces a) pristine, b) with 0.05 g Fe_2O_3

Fig. 2SM. EDS analysis for carbon felt coated with iron (III) oxide.
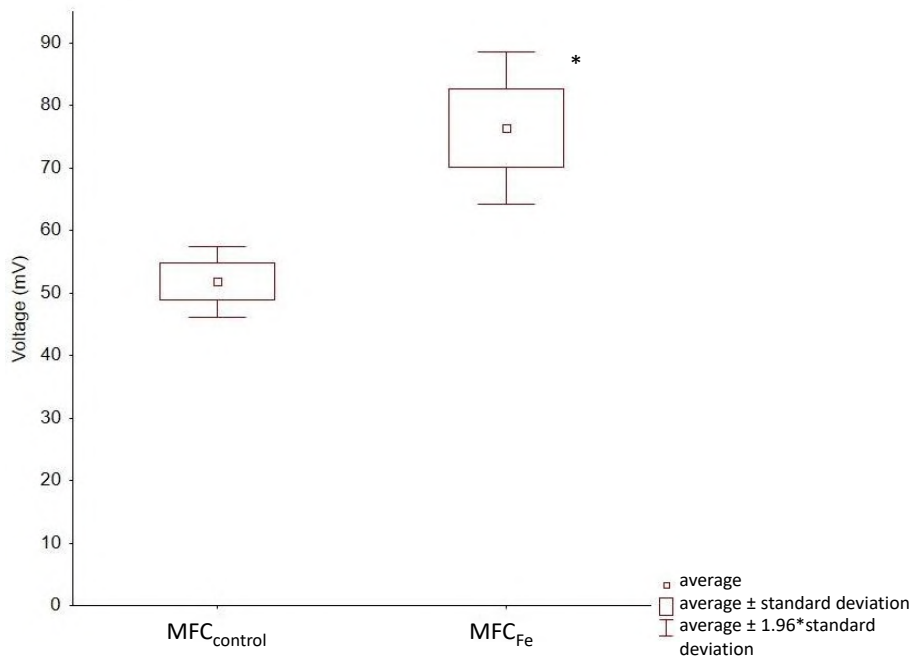
Fig. 3SM. Statistical differences in the voltages obtained in the individual reactors (ANOVA – Tukey's HSD post-hoc test), $p<0.05$; * - significantly higher than in the remaining $MFC_{control}$
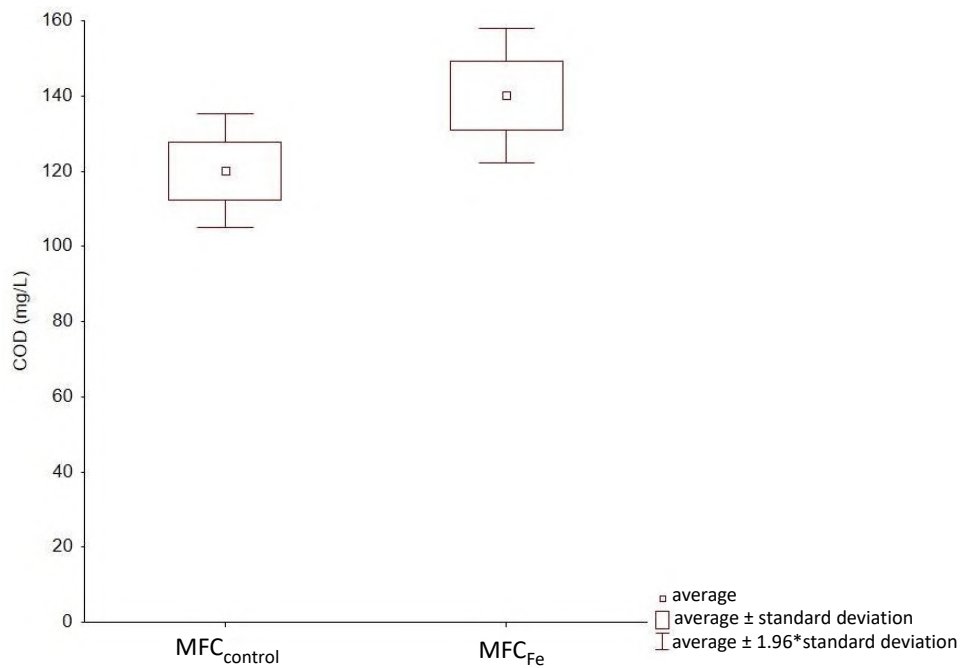
Fig. 4SM. Lack of significant differences in the COD concentration in the effluents from MFC reactors (ANOVA – Tukey's HSD post-hoc test), p<0.05.
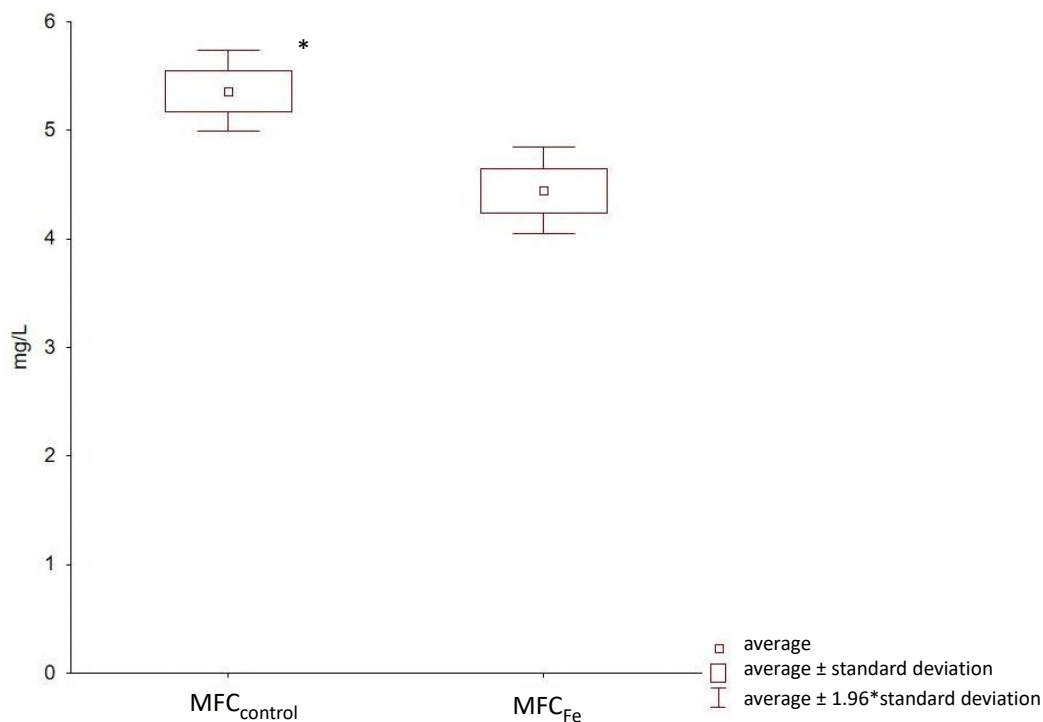
Fig. 5SM. Statistical differences in the N-NH$_4$ concentration in the effluents from MFC reactors (ANOVA – Tukey's HSD post-hoc test), p<0.05; * - significantly higher than in the remaining MFC$_{Fe}$

mgr inż. Dawid Nosek

(imię i nazwisko)

Przewodniczący Rady Naukowej Dyscypliny

prof. dr hab. inż. Marcin Dębowski

Uniwersytetu Warmińsko-Mazurskiego w Olsztynie

OŚWIADCZENIE

kandydata

Oświadczam, że w pracy pod tytułem:

Nosek D., Samel O., Pokój T., Cydzik-Kwiatkowska A. (2023). Waste volatile fatty acids as a good electron donor in microbial fuel cell with iron-modified anode. International Journal of Environmental Science and Technology 20, 13021–13032., mój wkład merytoryczny w jej przygotowanie polegał na: zaplanowaniu koncepcji pracy, pozyskaniu, opracowaniu i interpretacji wyników technologicznych, graficznym opracowaniu wyników oraz przygotowaniu pierwszej wersji manuskryptu.

(podpis)

Olsztyn, 21.08.2024

(miejscowość, data)

Oliwia Samel

(imię i nazwisko)

Przewodniczący Rady Naukowej Dyscypliny

prof. dr hab. inż. Marcin Dębowski

Uniwersytetu Warmińsko-Mazurskiego w Olsztynie

OŚWIADCZENIE

współautora

Oświadczam, że w pracy pod tytułem:

Nosek D., Samel O., Pokój T., Cydzik-Kwiatkowska A. (2023). Waste volatile fatty acids as a good electron donor in microbial fuel cell with iron-modified anode. International Journal of Environmental Science and Technology 20, 13021–13032., mój wkład merytoryczny w jej przygotowanie polegał na: pozyskaniu wyników technologicznych oraz częściowym przygotowaniu pierwszej wersji artykułu.

Jednocześnie wyrażam zgodę na przedłożenie w/w pracy przez Pana Dawida Noska jako część rozprawy doktorskiej w formie spójnego tematycznie zbioru artykułów naukowych opublikowanych w czasopismach naukowych. Oświadczam, iż samodzielna i możliwa do wyodrębnienia część ww. pracy wykazuje indywidualny wkład kandydata Pana Dawida Noska polegający na:

udziale w zaplanowaniu koncepcji pracy, pozyskaniu, opracowaniu i interpretacji wyników technologicznych, graficznym opracowaniu wyników oraz przygotowaniu pierwszej wersji manuskryptu.

Samel Olivia

(podpis)

103:1084416337

dr hab. inż. Tomasz Pokój, prof. UWM

(imię i nazwisko)

Przewodniczący Rady Naukowej Dyscypliny

prof. dr hab. inż. Marcin Dębowski

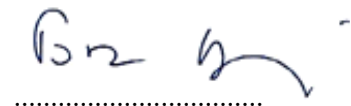**Uniwersytetu Warmińsko-Mazurskiego w Olsztynie**

OŚWIADCZENIE

współautora

Oświadczam, że w pracy pod tytułem:

Nosek D., Samsel O., Pokój T., Cydzik-Kwiatkowska A. (2023). Waste volatile fatty acids as a good electron donor in microbial fuel cell with iron-modified anode. International Journal of Environmental Science and Technology 20, 13021–13032., mój wkład merytoryczny w jej przygotowanie polegał na: pozyskaniu części wyników technologicznych oraz edycji tekstu pierwszej wersji artykułu.

Jednocześnie wyrażam zgodę na przedłożenie w/w pracy przez Pana Dawida Noska jako część rozprawy doktorskiej w formie spójnego tematycznie zbioru artykułów naukowych opublikowanych w czasopismach naukowych. Oświadczam, iż samodzielna i możliwa do wyodrębnienia część ww. pracy wykazuje indywidualny wkład kandydata Pana Dawida Noska polegający na:

udziale w zaplanowaniu koncepcji pracy, pozyskaniu, opracowaniu i interpretacji wyników technologicznych, graficznym opracowaniu wyników oraz przygotowaniu pierwszej wersji manuskryptu.

....

(podpis)

prof. dr hab. inż. Agnieszka Cydzik-Kwiatkowska

(imię i nazwisko)

Przewodniczący Rady Naukowej Dyscypliny

prof. dr hab. inż. Marcin Dębowski

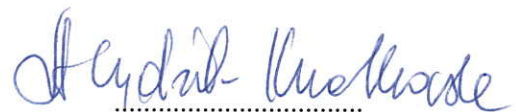**Uniwersytetu Warmińsko-Mazurskiego w Olsztynie**

OŚWIADCZENIE

współautora

Oświadczam, że w pracy pod tytułem:

Nosek D., Samsel O., Pokój T., Cydzik-Kwiatkowska A. (2023). Waste volatile fatty acids as a good electron donor in microbial fuel cell with iron-modified anode. International Journal of Environmental Science and Technology 20, 13021–13032., mój wkład merytoryczny w jej przygotowanie polegał na: udziale w zaplanowaniu koncepcji pracy, recenzowaniu i edycji tekstu, merytorycznym nadzorze pracy i pozyskaniu środków finansowych.

Jednocześnie wyrażam zgodę na przedłożenie w/w pracy przez Pana Dawida Noska jako część rozprawy doktorskiej w formie spójnego tematycznie zbioru artykułów naukowych opublikowanych w czasopismach naukowych. Oświadczam, iż samodzielna i możliwa do wyodrębnienia część ww. pracy wykazuje indywidualny wkład kandydata Pana Dawida Noska polegający na:

udziale w zaplanowaniu koncepcji pracy, pozyskaniu, opracowaniu i interpretacji wyników technologicznych, graficznym opracowaniu wyników oraz przygotowaniu pierwszej wersji manuskryptu.

(podpis)

105:1100397861

Praca nr 4

Nosek D., Mikołajczyk T., Cydzik-Kwiatkowska A.

Anode modification with Fe_2O_3 affects the anode microbiome and improves energy generation in microbial fuel cells powered by wastewater.

International Journal of Environmental Research and Public Health

2023

Article

Anode Modification with Fe$_2$O$_3$ Affects the Anode Microbiome and Improves Energy Generation in Microbial Fuel Cells Powered by Wastewater

Dawid Nosek [1,*], Tomasz Mikołajczyk [2] and Agnieszka Cydzik-Kwiatkowska [1]

1. Department of Environmental Biotechnology, University of Warmia and Mazury in Olsztyn, Słoneczna 45 G, 10-709 Olsztyn, Poland
2. Department of Chemistry, University of Warmia and Mazury in Olsztyn, plac Łódzki 4, 10-721 Olsztyn, Poland
* Correspondence: dawid.nosek@uwm.edu.pl; Tel.: +48-89-5234144

Abstract: This study investigated how anode electrode modification with iron affects the microbiome and electricity generation of microbial fuel cells (MFCs) fed with municipal wastewater. Doses of 0.0 (control), 0.05, 0.1, 0.2, and 0.4 g Fe$_2$O$_3$ per the total anode electrode area were tested. Fe$_2$O$_3$ doses from 0.05 to 0.2 g improved electricity generation; with a dose of 0.10 g Fe$_2$O$_3$, the cell power was highest (1.39 mW/m^2), and the internal resistance was lowest (184.9 Ω). Although acetate was the main source of organics in the municipal wastewater, propionic and valeric acids predominated in the outflows from all MFCs. In addition, Fe-modification stimulated the growth of the extracellular polymer producers *Zoogloea* sp. and *Acidovorax* sp., which favored biofilm formation. Electrogenic *Geobacter* sp. had the highest percent abundance in the anode of the control MFC, which generated the least electricity. However, with 0.05 and 0.10 g Fe$_2$O$_3$ doses, *Pseudomonas* sp., *Oscillochloris* sp., and *Rhizobium* sp. predominated in the anode microbiomes, and with 0.2 and 0.4 g doses, the electrogens *Dechloromonas* sp. and *Desulfobacter* sp. predominated. This is the first study to holistically examine how different amounts of Fe on the anode affect electricity generation, the microbiome, and metabolic products in the outflow of MFCs fed with synthetic municipal wastewater.

Keywords: MFC; iron; anode modification; internal resistance; microbiome

1. Introduction

Microbial fuel cells (MFCs) convert energy from biomass into electricity using electroactive bacteria (electrogens, EEs). To date, most research has been conducted at the laboratory scale because of the cells' low power output, making it challenging to transfer MFC technology to commercial-scale systems [1]. As far as the authors know, the largest MFC tested to date had a volume of 1200 L [2].

The most important factor for the efficiency of MFCs is the electrode material. Carbon materials that possess good electrical conductivity, such as carbon felt (CF), carbon fabric, or carbon paper, are most commonly used [3]. In recent years, the focus has been on improving these materials by coating their surfaces with metal oxides, which increases the surface roughness, thereby improving the adhesion of bacteria and increasing electron transfer at the anode [4,5]. Iron oxide, for example, improves the power output of MFCs by stimulating the activity of microorganisms and by improving electrical conductivity. Iron oxide (III) is an attractive material for anode electrode modification because of its properties to improve the surface structure of the anode and generate electrical energy in the MFC. Studies report that modifying the anode electrode with Fe$_2$O$_3$ changes the surface from smooth to rough, improving the microorganisms' attachment [6]. Additionally, the hydrophobic carbon surface can be hydrophilized by coating with Fe$_2$O$_3$ due to the hydrogen bond formed between the Fe$_2$O$_3$ oxygen and the water molecule [7]. The advantages of choosing this

material are its easy availability, chemical stability, and low cost. Furthermore, insoluble Fe_2O_3 has a high affinity for type C cytochromes (OmcA and MtrC) [8], which influences the increased electron transfer; thus, it is often used as a modifier in MFC layouts. Studies show that the presence of Fe(III) oxide increases the proportion of electroactive bacteria such as Pseudomonas sp. and *Geobacter* sp. on the anode [9]. Yamashita et al. [10] tested a flame-oxidized (FO) stainless steel (SS) anode in a single-chamber MFC compared to SS and CC anodes without treatment. The tests showed that the flame oxidation produced spots on the anode consisting mainly of Fe_2O_3, which increased the power density by 184 and 24% over untreated SS and CC. *Geobacter* sp. bacteria were more numerous on the FO–SS anode (8.8–9.2%) than on SS and CC (0.7–1.4%). Another study tested the addition of Fe_2O_3 to sediment MFC (SMFC). The TOC and DOC removal rates were 2.6 and 1.82 times higher in SMFC with iron oxide (III), respectively than in open-cycle reactors without the addition of Fe(III). The presence of Fe(III) increased the proportion of *Pseudomonas* sp. and *Desulfobacterium* sp. in biofilm about two-fold [11]. In another study, a composite anode SS with ultracapacitor powdered activated carbon (UAC) was tested with Fe_2O_3. The MFC with Fe_2O_3 showed a faster start-up time than the anode without the addition of Fe_2O_3. It was found that the Fe_2O_3-modified anode showed the highest repeatable voltage of 550 mV. Tafel's electrochemical extrapolation technique showed that MFC anode oxidation activation was stronger when Fe_2O_3 was added. The authors attribute the increase in kinetic activity to the facilitated extracellular electron transfer from the cell to the bacteria, showing that the rate of anode electron transfer can be increased by the addition of Fe_2O_3 [12]. Sayed et al. [13] found that a carbon cloth (CC) anode covered with Fe nanostructures had a lower potential than an unmodified anode (-0.01 and 0.16 V vs. Ag/AgCl, respectively). The high roughness and the nano-layer structure of the Fe-CC anode provided a greater surface area for growth and electron transfer between the microorganisms and the anode surface, increasing the MFC's maximum power and current density.

Similarly, Sekar et al. [14] synthesized copper-doped iron oxide nanoparticles with the use of *Amaranthus blitum* phytochemicals and found that they showed good hydrophilic properties on the anode surface. Modification of the anode with copper-doped iron oxide increased peak power density to 161.5 mW/m^2, decreased ohmic resistance by 98%, decreased charge transfer resistance by 95%, and increased the power density of the cell 1.3 times. Wang et al. [15] used anodes modified with α-Fe_2O_3 in conjunction with polyelectrolytes for energy generation in MFCs. The highest power density was observed in an MFC with a CC anode covered with four double layers of polydimethyl diallyl ammonium chloride, poly sodium-p-styrene sulfonate, and one layer of α-Fe_2O_3. The use of this anode ensured the lowest internal resistance of the MFC, and the high roughness and large surface area of the anode were beneficial for microbial growth.

In MFCs, iron-reducing EEs, such as *Geobacter* sp. and *Shewanella* sp., play significant roles. As iron compounds are insoluble at pH 7–8, these bacteria reduce Fe either via direct contact with their outer membranes' cytochromes or with conductive pili [16]. For example, in an MFC with a CF anode modified with graphene oxide/Fe_2O_3 that was supplied with pure acetate, the maximum stable voltage was 590 ± 5 mV, and the presence of iron increased the abundance of EEs belonging to *Desulfovibrio* sp. [17].

Fe addition can not only increase the output of MFCs, but it can also improve wastewater treatment. In a bioelectrochemical system, the use of Fe-carbon electrodes increased the activities of denitrifying enzymes such as nitrite reductase, nitric oxide reductase, and nitrous oxide reductase [18]. Dosing Fe(III) during wastewater treatment favors the removal of micropollutants via the adsorption of compounds on the surface of iron sulfide (FeS), followed by their biodegradation [19]. Moreover, Fe addition also prevents methane production under redox conditions [20], a common problem in MFCs.

The effect of anode modification with Fe depends on the anode material. Mohamed et al. [6] modified CF, CC, and graphite (G) anodes with Fe and found that the presence of Fe improved the wettability of the electrode surface, the rate of degradation of organic compounds and the adhesion of microorganisms to the electrode surface, and it decreased

the electron transfer resistance. After modification, the power generated in the MFC increased by 385%, 170%, and 130% for the CF-, CC-, and G-based electrodes, respectively. In addition, in the MFCs with modified electrodes, over 80% of organic compounds were removed from the effluent.

Although adding Fe promotes the formation of the anode's biofilm and accelerates MFC start-up, high doses of Fe may reduce cell efficiency. Zheng et al. [21] investigated how different doses of Fe_3O_4 in a medium affect energy generation and the anodic microbiome in an MFC. A dose of 4.5 g/L provided the highest power (391.11 ± 9.4 mW/m^2) and the highest share of electroactive bacteria of the genus *Geobacter* sp. in the microbiome. In a different study, 100 μM $FeSO_4$ improved the performance of an MFC so that it produced a maximum voltage of 0.55 V, but higher doses reduced the voltage to 0.47 V. Iron salts at a dose of 200 μM decreased *Geobacter* sp. abundance from 49.3% to 24.4% [22]. Similarly, another study found that 200 μM Fe(III) increased an MFC's electrochemical activity and current efficiency and decreased the anode overpotential. However, excess amounts of Fe(III) (1000 and 2000 μM) competed with the anode for electrons and inhibited the electrochemical activity of biofilms, thus lowering the power density [23]. Mechanistic investigations showed that Fe_3O_4 increased the conductivity of the fermented sludge, providing a better conductive environment for the anaerobic microbes. A Fe(II)/Fe(III) redox cycle was present in the fermentation system with Fe_3O_4, which likely increased electron transfer (ET) efficiency [24].

An important aspect of the large-scale use of MFC is the durability of the anode electrodes. Since they come into contact with the water environment and microorganisms, which may cause them to swell, materials with hydrophobic properties should be used. The surface of the anode electrodes should be rough enough to increase the adhesion of organisms, but not too rough so as not to cause the growth of pollutants resulting from the prolonged use of the electrodes [25]. Yaquoob et al. [26] studied the durability of composite graphene oxide (GO) electrodes made from biomass and the same GO with TiO_2. The longevity of the fabricated electrodes was 85 days. The increasing voltage on both electrodes indicated stable colonization of bacterial species on the surface of the anodes. Later, the voltage suddenly dropped due to cell death. The second cycle with fresh inoculum also showed an increasing voltage trend to 170 mV, which was due to the fresh inoculum source and organic substrate enhancing the bacterial respiration process to actively oxidize the substrate. The introduction of TiO_2 nanoparticles increased the lifetime of the composite anode, resulting in better interaction between bacterial cells and anode, smooth anode surface, and higher anode conductivity. In addition, a visualization test was performed after the completion of the reaction (85 days), and the electrodes were found to be mechanically stable and in excellent condition. Gnana Kumar et al. [27] tested a CC composite anode with reduced graphene oxide (rGO), poly(3,4-ethylenedioxythiophene) (PEDOT), and iron oxide (Fe_3O_4) nanorods. The authors analyzed electrode lifetime in an open circuit voltage (OCV) as a function of time under a constant load mode with an external resistance of 510 Ω. Bare CC had a lower lifetime due to the reduction of the exposed surface after repeated cycles, due to the large number of water particles on the surface as well as the bare mass CC. The composite of rGO and Fe_3O_4 prevented shrinkage of the active sites during repeated cycles and provided rapid stability of rGO/Fe_3O_4/CC parameters. Among the tested catalysts, the rGO/PEDOT/Fe_3O_4 composite was characterized by high physical and electrochemical strength and high electrical conductivity, which effectively prevented the destruction of the electrocatalytic activities due to strong π-π interactions and Fe-S coordination bonds between the active carbon support and the conductive polymer and the conductive polymer and Fe_3O_4 nanorods, respectively. The maximum OCV of 0.45 V was maintained for 200 h, and the concrete OCV was maintained for 600 h in three cycles.

Introducing Fe into an MFC system, as in the studies cited above, requires regular monitoring of Fe concentration in the effluent and carries the risk of elevated Fe concentrations in the MFC effluents. In contrast, covering the anode with Fe not only ensures direct

Int. J. Environ. Res. Public Health **2023**, *20*, 2580

4 of 21

contact between the microorganisms and Fe, but the fact that the biofilm covers the anode minimizes the risk of Fe contamination of the wastewater.

Therefore, the objective of this study was to holistically determine the influence of an MFC's anode modification with different doses of Fe_2O_3 on the power generation, the microbiome, and the conversion of organic matter. The use of a low-cost method for anode modification and the use of wastewater make this proposed solution economical, thus increasing its potential for implementation. Furthermore, the molecular results obtained greatly expand the knowledge of which microorganisms play a key role in biofilm formation and electricity generation when Fe is present on the anode.

2. Materials and Methods

2.1. Experimental Set-Up

The dual-chamber MFCs were made of plexiglass. The anode and cathode chambers had active volumes of 2 L. An 8×8 cm Nafion 117 proton-exchange membrane (PEM) (Dupont) was used as a separator between the chambers. Before the membranes were placed in the MFCs, they were soaked in acetone for 15 min, then rinsed in distilled water, soaked in 1M HCl for 30 min, and rinsed again with distilled water. Because of membrane clogging, the membranes were cleaned in 1M HCl and rinsed with distilled water once per week (for details, see Nosek and Cydzik-Kwiatkowska [28]).

The anodes were made of carbon felt ($10 \times 20 \times 0.3$ cm) connected to a stainless-steel wire. Before use, the carbon felt was sonicated in an ultrasonic bath (InterSonic, 15 min) to remove impurities. An MFC with an unmodified anode was used as a control ($MFC_{control}$). In the remaining MFCs, Fe_2O_3 was deposited on the anode in doses of 0.05 g ($MFC_{0.05Fe}$, 1.25 g Fe_2O_3/m^2), 0.1 g ($MFC_{0.1Fe}$, 2.5 g Fe_2O_3/m^2), 0.2 g ($MFC_{0.2Fe}$, 5 g Fe_2O_3/m^2), and 0.4 g ($MFC_{0.4Fe}$, 10 g Fe_2O_3/m^2). For deposition, Fe_2O_3 (Chempur) was suspended in 100 mL of distilled water in an ultrasonic bath for 15 min. Next, the anode was placed in a crystallizer, quenched with a Fe_2O_3 slurry, autoclaved (121 °C, 1.1 Bar, Classic Prestige Medical 210001), and dried at 80 °C.

The anode chambers were inoculated with 100 mL of a 1:1 (v/v) mixture of fermentation sludge from the municipal wastewater treatment plant in Olsztyn (Poland) and a laboratory methane fermentation reactor. The MFCs were supplied with synthetic municipal wastewater [29], and sodium acetate was used as a source of organics in the amount of 400 mg COD/L. The anode chamber was sealed to prevent air access, and the chamber contents were mixed at a speed of 100 rpm/min. The cathode chamber was aerated by an air diffuser (20 mL/min). The composition of the catholyte was 75 mL of phosphate buffer and 3 g of NaCl in 2 L of distilled water, and it was replaced once per week.

Initially, the MFCs were left for 3 days in open circuit mode to adapt the biomass to the environmental conditions in the MFCs and to support microbial colonization of the electrodes [30]. After 3 days, the contents of the anode chambers were replaced with fresh portions of wastewater. After this time, the MFCs were operated with an external resistance of 1200 Ω. This value was chosen based on preliminary experiments [31]. The operational cycle of the MFCs was 48 h; after this time, half of the anode chamber volume was replaced. The experiment was conducted for 18 cycles (36 days), and stable MFC operation was observed after 5 cycles. In the effluent, the concentration of COD, NH_4-N, volatile fatty acids (VFAs) [32], pH, and alkalinity (TitroLine, Donserv) were determined. The VFA composition was determined using a Varian CP-3800 chromatograph [33]. For spectroscopic characterization of the surfaces of pure carbon felt after sonication in the ultrasound batch and carbon felts modified with different doses of Fe_2O_3, a Quanta FEG 250 Scanning Electron Microscope (SEM) equipped with Bruker XFlash 6010 Energy-dispersive X-ray spectrometer (EDX) was used.

2.2. Electrochemical Analyses

The polarization and power curves were determined according to Watson and Logan [34] using a True-RMS multimeter, varying the external resistance of the cell in the range

of 75–7200 Ω. Voltage changes were recorded every minute using a 6600 Counts PC-LINK data acquisition unit. The current was calculated from the external resistance using Ohm's law. Cyclic voltammetry (CV) was performed with a three-electrode system: an anode as a working electrode, a platinum countercurrent electrode, and an Ag/AgCl reference electrode with a constant potential of 0.197 mV (Gammry Instrument Interface 1010E). CV measurements were conducted at a scan rate of 20 mV/s. The electrochemical behavior of the biofilm–anode system was tested in the 14th cycle of MFC operation, 25 h after reactor feeding (stable current generation) with the catholyte present in the cathode chamber. The MFCs were operated, and the measurements were performed at room temperature.

2.3. Molecular Analyses

Genomic DNA was extracted from 100 μg of inoculum and biomass from the anode surface using a FastDNA SPIN Kit for Soil (MP Biomedicals). Samples from the anode surface were collected in the experiment's 3rd, 10th, and 18th cycles. The purity and concentration of the DNA were measured using a NanoDrop spectrometer (Thermo Scientific). The DNA was amplified using a 515F/806R primer set (5′-GTGCCAGCMGCCGCGGTAA-3′/5′-GGACTACHVGGGTWTCTAAT-3′) targeting the hypervariable V4 region of bacterial and archaeal 16S rDNA genes [35]. The amplicons were sequenced using the MiSeq platform (Illumina) at Research and Testing Laboratory (USA). The reads were analyzed bioinformatically [36] and deposited in the NCBI Sequence Read Archive (BioProject PRJNA822890).

2.4. Statistical Analyses

The results from each MFC's last five cycles of operation were statistically analyzed ($p < 0.05$ considered significant, Statistica 13.3, StatSoft). One-way analysis of variance (ANOVA) was used, followed by Tukey's test (HSD). For statistical and metagenomic analysis of microbiome data, MicrobiomeAnalyst [37,38] was used ($p < 0.05$). Due to the fact that, in complex microbial communities, bacteria with a low abundance may be of great importance, the number of reads was not normalized before the calculation of diversity indices [39].

3. Results and Discussion

3.1. Analysis of the Electrode Surface

The photos show a pure carbon felt that was subjected to sonication (Figure 1a) and Fe_2O_3-modified anodes (Figure 1b–e). The mass fractions of iron that were detected (by means of a combined SEM/EDX methodology) on the electrodes were 5.5%, 6.9%, 10.7%, and 14.2% when Fe_2O_3 was dosed on the carbon felt in amounts of 0.05, 0.1, 0.2, and 0.4 g, respectively. Small differences in weight percentages of Fe between electrodes may be caused by limitations in the SEM/EDX technique, as this analysis shows only information on the surface of the electrode. Thus, this method was used as a qualitative confirmation of the Fe deposition, not the quantitative one. Analysis of SEM shows that iron has been deposited on the GF anode electrodes. The photos (Figure 1b–e and Figure S1) show Fe_2O_3 particles deposited on GF fibers. Compared to the bare electrode (Figure 1a), the fibers have a rougher surface, which significantly increases the specific surface area of the electrodes [40] and enhances and prolongs the bioadhesion of microorganisms to the surface of modified anode materials [41].
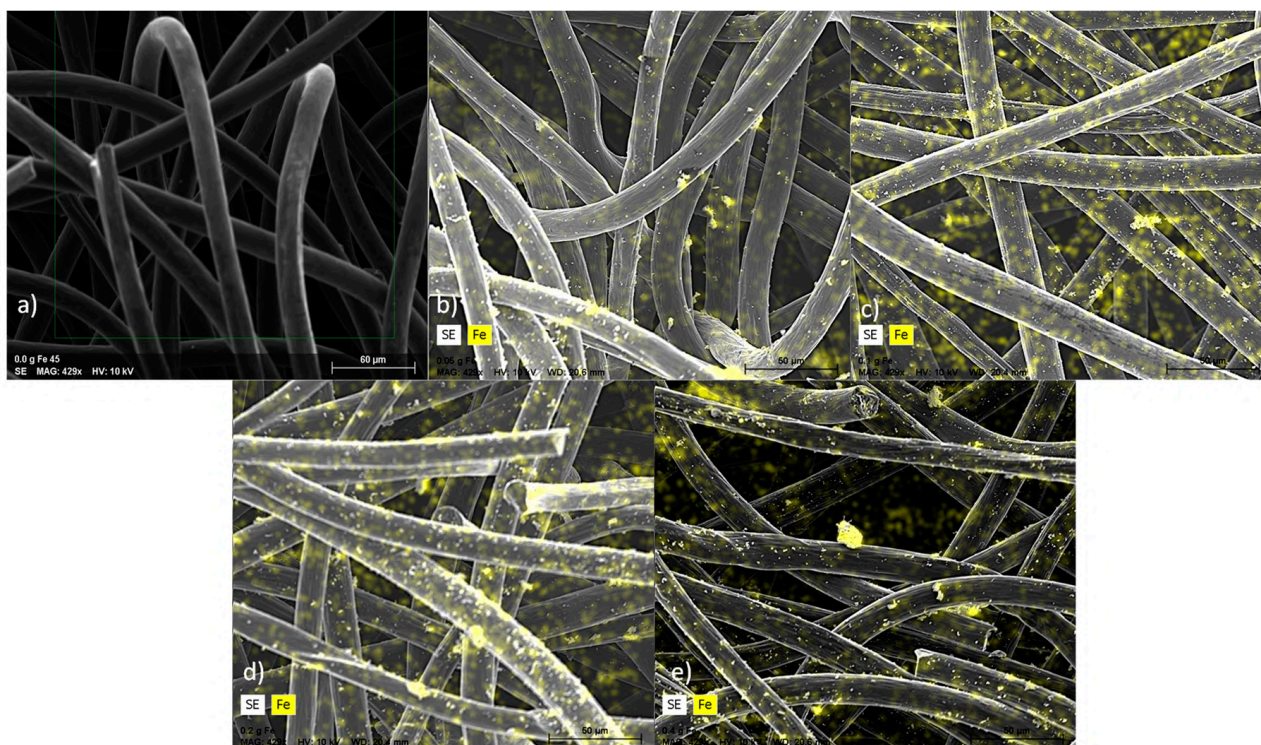
Figure 1. SEM/EDS analyses of anodes' surfaces for an acceleration voltage of 15 kV (**a**) pristine, (**b**) with 0.05 g Fe2O3, (**c**) with 0.1 g Fe2O3, (**d**) with 0.2 g Fe2O3, and (**e**) with 0.4 g Fe2O3.

3.2. Electricity Generation

In all tested MFCs, regardless of the iron dose, the voltage was generated from the first cycle of operation. The highest voltages were obtained immediately after the addition of the substrate, which may have resulted from rapid proton flow through the membrane, but during the first 2–3 h, the voltages dropped rapidly. In $MFC_{0.05Fe}$ (Figure 2b) and $MFC_{0.1Fe}$ (Figure 2c), the voltage decreased until c.a. 24 h of the cycle and increased afterward. The highest average voltages in the cycle (125 ± 48.5 mV) were observed in $MFC_{0.05Fe}$ and were about 3 times higher than in the control. The average voltages obtained in $MFC_{0.05Fe}$ and $MFC_{0.1Fe}$ were significantly higher than those in the other MFCs (Figure S2). In the control, $MFC_{0.2Fe}$, and $MFC_{0.4Fe}$, the voltage gradually decreased during the cycle to 20–50 mV at the cycle end (Figure 2). The voltage was lowest in $MFC_{control}$, and was also the least stable, as indicated by large standard deviations. Zheng et al. [21] added Fe_3O_4 to MFC with a medium. Their studies showed that the output voltage at the highest dose of 18 g/L was the lowest of all MFC tested. This suggests that the voltage shifts at higher doses could be due to the accumulation of Fe occupying the attachment site of electroactive bacteria. SEM/EDX analysis showed that the anode electrodes with higher iron doses had greater roughness. High electrode surface roughness increases the likelihood of polymerization and fouling of the electrode surface as well as electrode poisoning after prolonged use [25], which can lead to lower output voltages. High Fe concentrations can have an inhibitory effect on energy generation by reducing substrate biodegradation [23,42] or by increasing internal resistance of MFC, which was confirmed in our studies (internal resistance was higher at doses of 0.2 and 0.4 than at 0.05 and 0.1 g Fe_2O_3/the entire surface of the electrode). Power output over 18 cycles is shown in Supplementary Materials Figure S3.

*Int. J. Environ. Res. Public Health* **2023**, 20, 2580

7 of 21
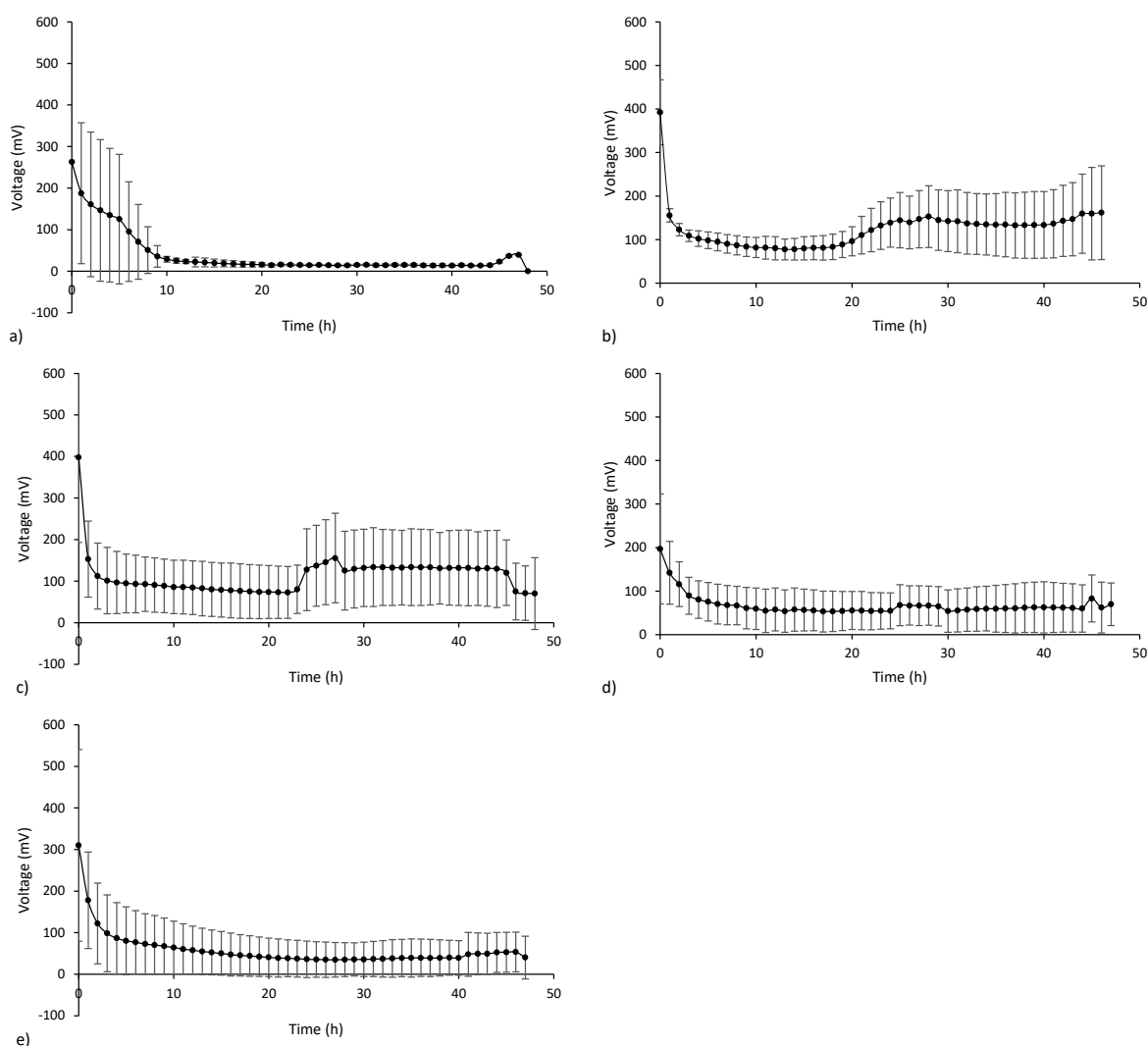
Figure 2. Averaged voltages (*n* = 5) from the last 5 cycles for (**a**) MFCcontrol, (**b**) MFC0.05Fe, (**c**) MFC0.1Fe, (**d**) MFC0.2Fe, and (**e**) MFC0.4Fe.

The electrochemical behavior of the control and Fe-modified electrodes with and without biofilm was tested by cyclic voltammetry in a working solution. Figure S4 shows the cyclic voltammograms recorded for all examined electrodes over a potential range of -0.50 to 0.50 V vs. SCE, which were obtained at room temperature with a sweep rate of 20 mV/s. The voltammograms of Fe-modified electrodes without biofilm did not exhibit any well-defined cathodic and anodic features related to iron behavior. However, the current of the cathodic peak corresponding to the hydrogen evolution reaction increased slightly with the addition of Fe. Nevertheless, the current increase was not strictly correlated with the amount of added iron, which could be caused by insufficient electric contact between the base electrode and the deposited iron oxide. On the other hand, after biofilm formation, the current density of the Fe-modified electrodes was significantly higher than that of the control with biofilm and the Fe-modified electrodes without biofilm. Additionally, the current values positively correlated with the amount of Fe that was deposited (188, 152, 51, and 43 mA with 0.4, 0.2, 0.1 and 0.05 g of Fe).

Furthermore, the CV profiles of the electrodes with 0.4 and 0.2 g of Fe_2O_3 exhibited two broad reversible features centered at -0.32 and 0.38 V vs. SCE. Therefore, those anodic peaks are most likely related to the process of iron oxidizing to Fe(II) and (III), while the cathodic peaks are associated with the reduction of those oxidized species [43]. Therefore, the changes observed after biofilm formation are most likely due to the following phenomena:

Int. J. Environ. Res. Public Health **2023**, *20*, 2580

8 of 21

a better electrical connection between iron oxide particles and the base electrode provided by the biofilm and the increased biofilm formation at higher doses of Fe. The areas under the CV curves (Figure S2b obtained in $MFC_{0.2Fe}$ and $MFC_{0.4Fe}$) were larger than in the other MFCs, which may indicate a higher charge capacity. This may be due to the fact that the charge capacity of the electrode is proportional to the electrode surface, which indicates that the surface area increases after modification [44], which is also visible in SEM images.

Figure 3a shows the power curves from the 14th cycle of MFC operation. The highest power density of 1.39 mW/m^2 was obtained in $MFC_{0.1Fe}$ and $MFC_{0.2Fe}$. This power density was 2.8 times higher than that obtained in $MFC_{control}$, and 1.7 and 5.8 times higher, respectively, than the values obtained in $MFC_{0.05Fe}$ and $MFC_{0.4Fe}$. Yang et al. [45] studied an anode with a carbonized *Shewanella* sp. biomass that produced a nanocomposite iron oxide/carbon catalyst. Their results showed that coating the anode with the nanocomposite increased the cell's power 3.5 times compared to that of a cell with a pure CF anode. The power was higher in the cell with the modified anode because, compared to the control, the surface roughness of the anode was higher with lower charge transfer resistance. Liu et al. [23] found that, in an MFC fed with sodium acetate and increasing iron doses in the substrate, the cell power density decreased from 0.95 W/m^2 at 200 µM Fe(III) to 0.59 W/m^2 at 2000 µM Fe(III). In $MFC_{0.4Fe}$ in our study, with the highest dose of Fe_2O_3 used for anode modification, the highest power achieved in the cell was two-fold lower than the value achieved with the control anode. The low power in $MFC_{0.4Fe}$ could be due to an excess of iron at the anode that decreased the quality of the anode. Yang et al. [45] observed that Fe(III) aggregated on the anode can compete for electrons with the anode and inhibit the electrochemical activity of biofilms.
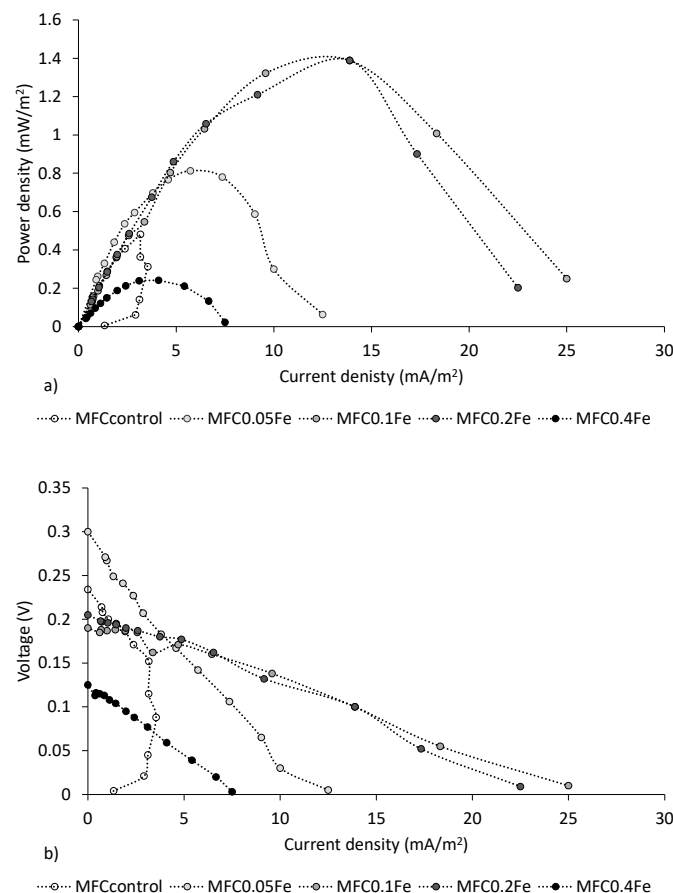

Figure 3. Power curves (**a**) and polarization curves (**b**) for all MFCs.

The polarization curves showed that modification of the anode with iron reduced the cell's internal resistance, most likely via better electron transfer due to the presence of iron
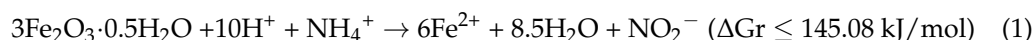
particles. The highest internal resistance of 1029 Ω was recorded in MFC$_{control}$, while the lowest internal resistance (184.9 Ω) was recorded in MFC$_{0.1Fe}$ (Figure 3). Increasing the iron dose used for anode modification from 0.1 to 0.4 g gradually increased the internal resistance of the cell to 397 Ω in MFC$_{0.4Fe}$. In a study by Mohamed et al. [6], electrode position of iron (200 mM FeCl$_3$ working solution) on CF, G, and CC electrodes caused the total internal resistance of an MFC to decrease by 2.0, 1.9, and 1.4 times, respectively. In addition, electrolytic deposition improved the wettability and increased the porosity and biocompatibility of the surfaces.

3.3. COD Removal

The elimination of organic compounds in the MFC is carried out by their microbial decomposition, the products of which are carbon dioxide, hydrogen protons, and electrons, the acceptor of which is the electrode. The decomposition of organic compounds can be illustrated by the example of acetic acid as follows:

$$C_2H_4O_2 + 2H_2O \rightarrow 2CO_2 + 8H^+ + 8e^-$$
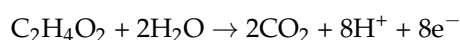
Complex organic compounds must be converted to monosaccharides or other low-molecular-weight compounds [46]. Therefore, the high biodiversity of microorganisms is important in MFC systems using complex effluents. Organic nitrogen in wastewater is converted to NH$_4$-N, which is removed in the MFC mainly by migration through the EMF and volatilization in the cathode chamber [47] or by precipitation in the form of struvite, cattiite ((Mg$_3$(PO$_4$)$_2$·22H$_2$O)) or in the presence of iron-vivianite (Fe$_3$(PO$_4$)$_2$·8H$_2$O) [48]. In anaerobic environments, in the presence of Fe(III), NH$_4^+$ is an electron donor and is oxidized to NO$_2^-$ by reduction of Fe(III) to Fe(II) according to the formula [49] (Equation (1))

$$3Fe_2O_3 \cdot 0.5H_2O + 10H^+ + NH_4^+ \rightarrow 6Fe^{2+} + 8.5H_2O + NO_2^- \quad (\Delta Gr \leq 145.08 \text{ kJ/mol}) \quad (1)$$

The average COD removal efficiency was above 70% for all reactors, indicating that the anaerobic biofilm on the anode was well developed and active. Low iron dosages favored more stable and effective COD removal compared to MFC$_{control}$ (Figure 4a). In MFC$_{0.05Fe}$ and MFC$_{0.1Fe}$, COD was stably removed with efficiencies of 83.96 ± 10.1% and 85.5 ± 14%, respectively (Figure 4b,c). The mean COD concentrations in the treated wastewater from MFC$_{0.05Fe}$ and MFC$_{0.1Fe}$ were 29.5 ± 14.9 and 30.8 ± 7.6 mg COD/L, respectively, and were significantly lower than concentrations in the other MFCs. Better COD removal can be explained by the iron-modified anode having a higher surface area, which results in better biocompatibility and adhesion of microorganisms [4,50]. However, our results suggest that if the Fe dose is too high, the stability of COD removal decreases (Figure 4d,e). For example, in MFC$_{0.4Fe}$, the range of COD in wastewater was between 29 and 141 mg/L. Mohamed et al. [51] reported that Fe(III) at a dose of 40 mg/L in wastewater treatment systems decreases COD's removal efficiency. At high concentrations of Fe(III) in the environment, Fe(III) penetrates bacterial cells in large numbers and reduces enzyme activity or generates toxic free radicals that damage cell structures [52,53].

The addition of iron facilitated the maintenance of a neutral pH in the MFCs. The mean pH of the effluent from MFC$_{control}$ (pH 8.3) was significantly higher than that of the MFCs with iron-modified anodes (pH 7.7, 7.9, 7.8, and 7.8, for MFC$_{0.05Fe}$, MFC$_{0.1Fe}$, MFC$_{0.2Fe}$, and MFC$_{0.4Fe}$, respectively). Although the pH was lower in the MFCs with iron-modified anodes, it increased during the cycle, indicating that the rate of transport of protons through the PEM was slower than the rate of their production in the anode chamber. The efficiency of an MFC is optimal when a constant pH is achieved in the anode chamber, and the rate of proton production in the anode chamber is equal to the rate of their consumption at the cathode [54]. At the same time, the effluents from MFC$_{0.2Fe}$ and MFC$_{0.4Fe}$ had significantly lower alkalinity than that from MFC$_{control}$. The oxidation of organic compounds usually produces more protons than bicarbonate ions, which lowers the pH and alkalinity and may harm the anode biofilm [55]. The lower alkalinity that

was observed in the MFCs modified with the highest Fe doses may decrease conductivity, increase internal resistance, and decrease the efficiency of electricity generation [56].
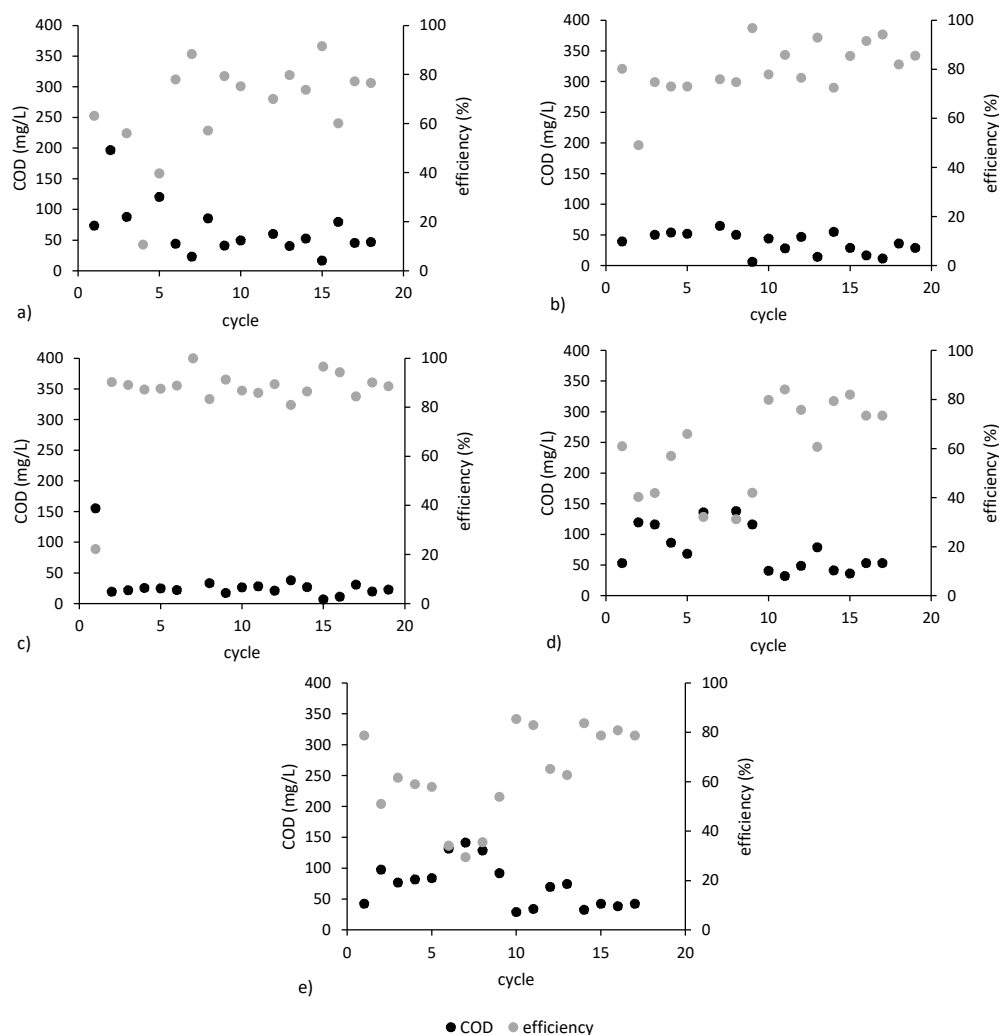
Figure 4. COD concentration in the effluent and COD removal efficiency in (**a**) $MFC_{control}$, (**b**) $MFC_{0.05Fe}$, (**c**) $MFC_{0.1Fe}$, (**d**) $MFC_{0.2Fe}$, and (**e**) $MFC_{0.4Fe}$.

The efficiency of NH_4-N removal in all MFCs was about 37%, and the NH_4-N concentrations in the effluents did not differ significantly.

3.4. Chromatographic Analyses of VFAs

In our study, the differences in the effluent compositions indicated that the presence of Fe on the anode affected the metabolic conversions in the MFC. To illustrate the changes in VFA composition during wastewater treatment in MFCs, chromatographic analyses were performed (Figure 5). Acetic acid comprised the largest share of VFAs in the substrate (86%), while the remaining 14% were other acids, mostly propionic acid (7%). Yu et al. [57] investigated the influence of various substrates on energy production and did not note any changes in the VFA profile in an acetate-fed rector—acetic acid was the only VFA in the effluent. In our study, in contrast, acetic acid was present only in small amounts (from 0.2% in $MFC_{0.1Fe}$ to 3.0% in $MFC_{control}$), while propionic and valeric acid proportions significantly increased in comparison to their proportions in the raw wastewater. In the outflow from $MFC_{control}$, propionic and valeric acids constituted 58% and 23% of VFAs, respectively, while hexanoic and iso-hexanoic acids accounted for 12%. As the iron dose was increased, the proportion of propionic acid also increased, while the proportions of valeric,

Int. J. Environ. Res. Public Health **2023**, 20, 2580

11 of 21

caproic, and iso-caproic acids decreased. Some microorganisms are able to form storage compounds in the form of polyhydroxyalkanoate (PHA) during the anaerobic degradation of organic compounds, especially VFA. Under aerobic conditions, PHAs are used as a carbon source, e.g., during biological phosphorus removal [58]. Wang et al. [59] proposed an anaerobic pathway for the synthesis and degradation of PHAs. The type of VFA determines the composition of stored PHA, which in turn affects the types of VFA produced during PHA degradation. Polyhydroxybutyrate (one of the forms of PHA) is degraded to acetate and butyrate, and polyhydroxyvalerate (PHV) is degraded to propionate, acetate, and valerate. In our study, in the biofilm microorganisms such as *Zooglea* sp., *Dechloromonas* sp., *Acidovorax* sp., and *Hydrogenophaga* sp. (see Section 3.5), capable of PHA accumulation, were observed. Due to the prevailing anaerobic conditions, it is possible that they converted them to organic acids present in the wastewater, i.e., mainly propionic and valeric acids, which would indicate that the reserve substance was stored mainly in the form of PHV.
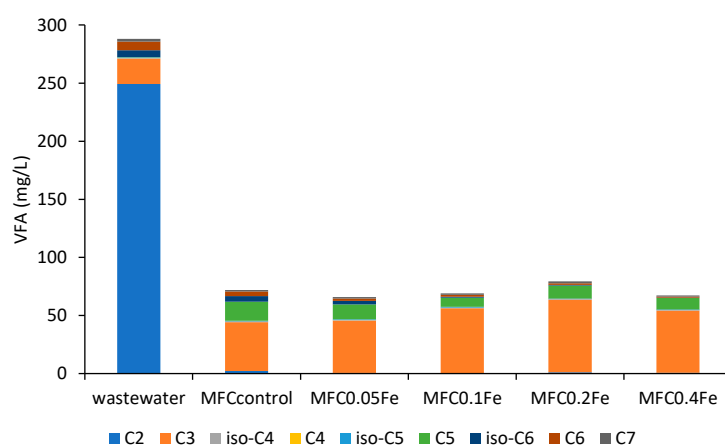
Figure 5. Profile of VFA concentration in raw wastewater and the effluents from all MFCs (average of $n = 5$), where C_2—acetic acid, C_3—propionic acid, C_4—butyric acid, C_5—valeric acid, C_6—caproic acid, and C_7—enanthic acid.

These results indicate that microbial metabolism in MFCs leads to the formation of VFAs other the acetic acid; this process has been observed, for example, during acetate conversion under anaerobic conditions [60]. Moreover, propionic acid that is present in wastewater may not be metabolized in MFCs. During anaerobic fermentation, the conversion of butyric acid and propionic acid to acetic acid does not occur spontaneously, due to the high Gibbs free energy of the reaction, resulting in an accumulation of the two acids [61]. The presence of propionate as a metabolic product of wastewater conversion in MFCs inhibits the activity of acidogenic bacteria and methanogens [62], which can eliminate electron loss during methane fermentation in MFCs.

3.5. Microbial Structure of Inoculum and Anode Biofilm in the MFCs

A total number of 498,906 readings was obtained after sequencing. The lowest number of readings was recorded in $MFC_{0.4Fe}$ in the 10th cycle of MFC operation, and the highest in $MFC_{0.1Fe}$ in the 10th cycle of operation (Table 1). The flattening of the rarefaction curves (Figure S6) indicates that the depth of the sequencing was sufficient. However, the OTU number for the tested samples was quite low and varied from 66 to 117. For comparison, the average number of OTUs for biofilms from the anode modified with Fe_2O_3 in an acetate-fed dual-chamber MFC was about 600 [63]. In our study, many unclassified microorganisms were detected, which may explain the low number of OTUs.

Int. J. Environ. Res. Public Health **2023**, *20*, 2580

12 of 21

Table 1. Alpha diversity indicators in all MFC reactors; the number after the reactor name indicates the cycle in which sampling was performed; OUT—operational taxonomic unit, Chao1—richness estimator, Shannon—biodiversity index, ACE—abundance-based coverage estimator.

Reactor—Cycle Number	OTU	Chao1	Shannon	ACE	Total Read Counts
Inoculum	91	91.5	2.51	92.7	26,877
MFC$_{control}$—3	103	103.6	3.14	103.6	25,053
MFC$_{control}$—10	108	108.5	2.97	108.2	29,183
MFC$_{control}$—18	112	114.3	2.85	114.8	28,548
MFC$_{0.05Fe}$—3	108	108.5	2.85	108.3	35,811
MFC$_{0.05Fe}$—10	105	108.0	1.51	108.1	38,831
MFC$_{0.05Fe}$—18	111	111.0	2.77	111.3	24,160
MFC$_{0.1Fe}$—3	109	110.6	1.47	111.1	43,390
MFC$_{0.1Fe}$—10	101	101.6	1.23	102.8	49,705
MFC$_{0.1Fe}$—18	117	117.9	2.69	118.5	33,249
MFC$_{0.2Fe}$—3	66	69.0	1.72	68.5	24,281
MFC$_{0.2Fe}$—10	101	101.5	3.14	103.5	28,223
MFC$_{0.2Fe}$—18	118	122.7	2.57	122.5	30,545
MFC$_{0.4Fe}$—3	64	65.3	1.45	66.8	28,970
MFC$_{0.4Fe}$—10	103	104.1	3.21	105.3	17,967
MFC$_{0.4Fe}$—18	111	111.8	2.56	113.0	34,113

The ACE index in MFC$_{control}$ and the MFCs operated with the two lower iron doses increased with time, but in the reactors with modified anodes, the diversity slightly decreased during the 10th cycle of reactor operation (Table 1). In MFC$_{0.2Fe}$ and MFC$_{0.4Fe}$, the ACE changed more dynamically, indicating that the presence of Fe changed the metabolism and biodiversity of the anode biofilm. In the third cycle of reactor operation (In MFC$_{0.2Fe}$ and MFC$_{0.4Fe}$), the ACE dropped significantly from 92 in the inoculum to about 70. However, the species diversity then increased with time, and at the end of the experiment, it was nearly two times higher than during the third cycle of MFC operation.

Throughout the experiment, Proteobacteria predominated in the microbial communities in the individual MFCs. The share of Proteobacteria increased in relation to the dose of iron used for the anode modification (Figure 6), reaching a value above 75% of all identified microorganisms in MFC$_{0.4Fe}$. Proteobacteria members are electroactive bacteria crucial for extracellular electron transport [64]. They are involved in sludge hydrolysis and short-chain fatty acid production and are the main consumers of acetate, propionate, and butyrate during fermentation [65], which explains their high abundance in MFCs fed with acetate-containing wastewater. In a study in which Fe$_3$O$_4$ was dosed to the medium in a single-chamber MFC, the numbers of Proteobacteria in the biomass were also high, followed by Desulfobacterota and Bacteroidota [21]. The second most abundant group in the present study was Bacteroidetes (up to 11% in MFC$_{0.05}$). A high percentage of unclassified bacteria (up to 44% in MFC$_{0.05}$) indicated that many yet undiscovered bacteria played an important role in energy production in MFCs.

A common feature of the microbiome in all MFCs was the presence of *Acidovorax* sp. during reactor start-up (Figure 7). Its share ranged from 3 to 18.5% depending on the MFC, and then, in subsequent cycles, it decreased to <0.5%; only in the control did its share amount to 1.3% in the 18th cycle. *Acidovorax* sp. are capable of efficient extracellular polymeric substances (EPS) production (over 150 mg/L in R2A agar medium [66]), and probably participated in anode colonization and the formation of an anode biofilm in the initial stage of MFC operation.
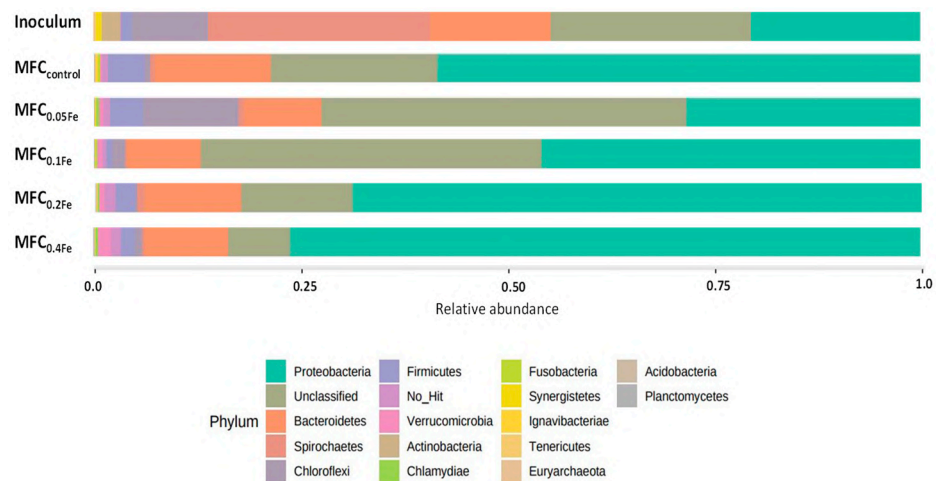
Figure 6. Relative abundance of particular phyla in the inoculum and anodic biomass obtained from all MFCs.
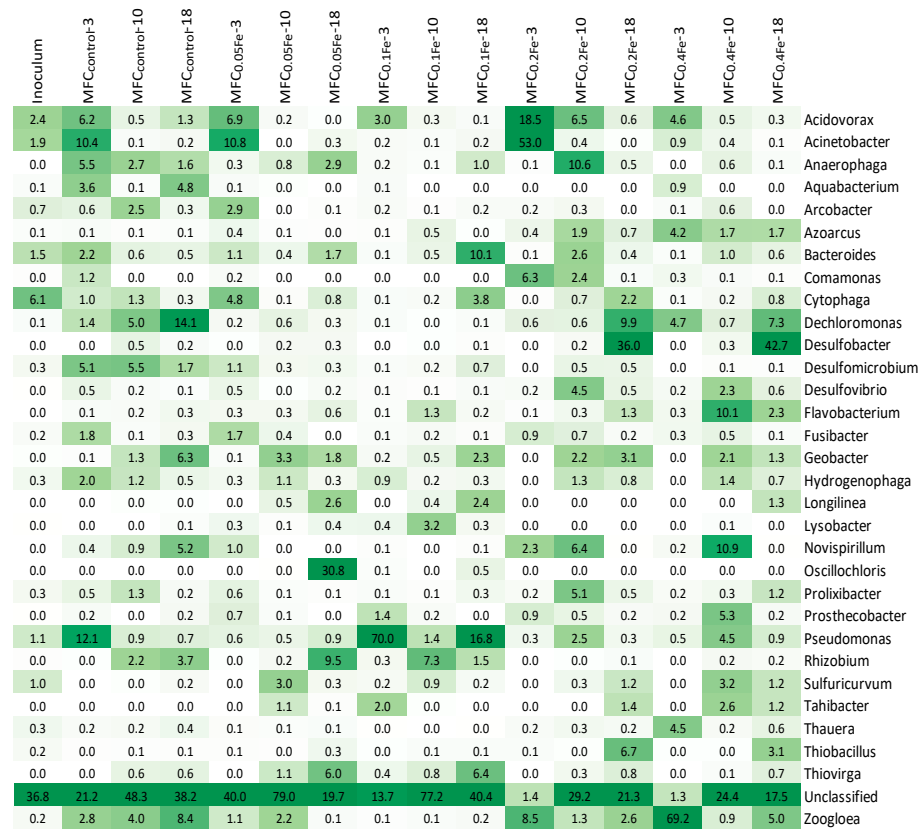

Figure 7. Heatmap showing 30 of the most numerous genera in the investigated MFCs, the number after the reactor name indicates the cycle in which sampling was performed.

One of the most frequently identified EEs is *Geobacter* sp., which is able to convert energy from the decomposition of organic compounds with electron transfer to the anode using nanowires [67]. Liu et al. [22] observed a decrease in the share of *Geobacter* sp. in the bacterial community with an increasing concentration of $FeCl_3$ in a medium from 200 to 1000 μM. Zheng et al. [21] investigated the effect of Fe_3O_4 added to the medium in a single-chamber MFC. Their results show that the lowest tested dose of 4.5 g/L led to an enrichment of the anode biofilm in *Geobacter* sp. (17.4% for control and 31.5% for MFC with the tested Fe_3O_4 dose), but higher doses decreased their share. Our study

Int. J. Environ. Res. Public Health **2023**, 20, 2580

14 of 21

shows that *Geobacter* sp. was present in all tested MFCs, with the highest proportion (6.3%) being observed in the MFC$_{control}$. In the remaining MFCs, the share of *Geobacter* sp. ranged from 1.3 to 3.3%. The results indicate that the percentage of *Geobacter* sp. in the biofilm did not directly translate into energy production in MFCs, which was highest in MFC$_{0.1Fe}$. The numerical abundance of microorganisms in biofilms cannot be assumed a priori to correlate to the capacities of these species to produce power [68]. In MFCs with lower *Geobacter* sp. abundances, a greater role was played by the synergistic interactions between microorganisms. In co-cultures with EE microbes, other bacteria may facilitate the current generation by removing chemicals or by producing a substrate for the current generation [69]. The lower proportion of *Geobacter* sp. in the presence of iron ions may result from the fact that these microorganisms do not appear to significantly reduce crystalline forms of Fe(III) [70]. Growing these microorganisms in media with crystalline forms of Fe(III) led to the enrichment of methane-producing cultures, while the addition of weakly crystalline Fe(III) resulted in the successful enrichment of *Geobacter* sp. [67]. The other study focused on the analysis of protein expression in *Geobacter sulfurreducens* showed that in the presence of Fe(III) oxide, about 76% of proteins were less abundant than in the presence of Fe(III) citrate due to the slower rate of bacterial metabolism and growth with an insoluble electron acceptor. Most of these proteins were involved in metabolic processes such as electron transport (13 c-type cytochromes) or were structural proteins for electrically conductive pili (PilA, [71]).

As environmental conditions in MFCs with iron-modified anodes did not favor *Geobacter* sp., in these MFCs, electricity generation was supported by other microorganisms. At two lower doses of iron on the anodes, EEs belonging to the genera *Pseudomonas* and *Oscillochloris* were identified in large numbers. *Oscillochloris* sp. is a type of filamentous bacteria, classified as anoxygenic phototrophs, that binds carbon through the reductive pentose phosphate cycle [72]. Phototrophic bacteria of various types are capable of generating energy [73–75]. In the MFC$_{0.1Fe}$, *Pseudomonas* sp. comprised up to 70% of bacteria in the anode biofilm. *Pseudomonas* sp. produces several electrochemically active phenazine derivatives, such as phenazines-1-carboxylic acid, pyocyanin, oxychlororaphin, and pyorubin, which can act as redox mediators in the MFC [76]. The high abundance of *Pseudomonas* sp. in MFC$_{0.1Fe}$ may explain the high power obtained in this cell because electrons produced by other bacteria could be transferred to the anode via mediators produced by *Pseudomonas* sp. In high concentrations, the mediators produced by *Pseudomonas* sp. can be toxic to other species, thus giving *Pseudomonas* sp. an environmental advantage in competition with other bacterial species [69]. The energy production by pure cultures of *Pseudomonas* sp. is lower than that of biofilms with a high proportion of *Geobacter* sp.; however, this lower energy production by Pseudomonas sp. may be compensated by their high abundance in biofilm. Moreover, competition in biofilms involves many factors, and the ability to conduct current may not be the only or main reason for the predominance of high-power-producing bacteria. For example, some EEs bacteria in a mixed culture of the anode in MFC are capable of higher power production than after isolation from this biofilm and cultivation in the pure culture [68].

In MFC$_{0.05Fe}$ and MFC$_{0.1Fe}$, *Rhizobium* sp., *Thiovirga* sp., *Longilinea* sp., and *Bacteroides* sp. occurred in the anode biofilm, which all have been reported to be involved in energy generation in MFCs. The *Rhizobium anhuiense* strain is an effective EE and generated a maximum voltage of 635 mV and output power of 1.07 mW/m^2 in a glucose-fed dual-chamber MFC operated in an open circuit [77]. *Thiovirga* sp. is a type of chemolithoautotrophic bacteria, and in MFCs, they play an essential role in sulfide metabolism and COD removal [78]. *Thiovirga* sp. shows good resistance to high metal concentrations; however, our study indicates that, although Fe presence favors *Thiovirga* sp. growth in anodic biofilm, this genus prefers lower Fe concentrations in the environment [79,80]. *Longilinea* sp. decomposes hydrocarbon into acetate and H$_2$ [81]. Yang et al. [82] reported that the presence of Fe$_2$O$_3$ at the anode promoted the reproduction of *Longilinea* sp., which could release intracellular electrons through the metabolism of substrates or intermediates [83]. *Bacteroides* sp. were

one of the main bacteria producing electricity in the constructed wetland MFC [84]. It efficiently produced electricity by degradation of organic substances, preferably acetate [85], as well as by transferring electrons that reduce Fe(III) [86].

At the two highest doses of iron at the end of the study, biomass was mostly occupied by *Desulfobacter* sp., *Dechloromonas* sp., and *Thiobacillus* sp. *Dechloromonas* sp. have been reported to both generate electricity in MFCs [87,88] and play an important role in the conversion of ferrous ions in Fe-contaminated soils or waters [89,90]. Li et al. [91] observed that during municipal wastewater treatment in MFC coupled with an up-flow in denitrification biofilter abundance of *Dechloromonas* sp. ranged from 1.29% to 9.52%. The authors reported a negative correlation between the abundances of *Dechloromonas* sp. and *Geobacter* sp., which play a predominant role in denitrification and anodic respiration. This observation indicates their similar respiring and metabolizing processes and, thus, potential competing relationships. Our studies indicate that their abundance also depends on the iron content in the environment. *Desulfobacter* sp. are a type of EE [92] using acetate as an electron donor and sulfate, sulfite, and thiosulfate as final electron acceptors [93]. *Desulfobacter* sp. generated electric power of 370–1400 mW/m^2 in the concentration range from 550 to 1270 mg COD/(L·h) [94]. *Thiobacillus* sp. was present in both the anode and cathode biofilm [95,96] with abundances in anode biofilms as high as 24.5% during the treatment of wastewater with high sulfur content [97].

In MFC$_{0.4Fe}$ at the beginning of the experiment, Proteobacteria constituted as much as 96% of the entire bacterial community, and the *Zoogloea* sp. share was close to 70%. The predominance of *Zoogloea* sp. in the biofilm from MFC$_{0.4Fe}$ may result from the fact that these microorganisms can produce large amounts of EPS. Production of protein- and polysaccharide-rich EPS plays a vital role in cell protection under metal stress conditions [98,99], as functional groups from EPS form complexes with metal ions protecting the cell surface [100]. Metal ions may also be sorbed on the cell surface of *Zoogloea* sp. by electrostatic interactions such as van der Waals forces [101,102]. A decrease in the abundance of *Zoogloea* sp. in the course of the experiment indicated bacterial succession maturation of the anodic biofilm. Another bacterial group that preferred high iron concentrations was *Flavobacterium* sp. (up to 10.1% of the bacterial community in MFC$_{0.4Fe}$). Previous research indicated that *Flavobacterium* sp. predominated in acetate-fed MFC [103] and was an important player in electricity production [104,105].

The presence of Fe$_2$O$_3$ on the anode was positively correlated with the abundances of *Methylovresatilis* sp. and *Fluviicola* sp., whose share on the MFC$_{0.4Fe}$ anode reached 1.2% and 1.5%, respectively (Figure S5). *Methyloversatilis* sp. is a type of facultative methylotroph that can grow on a variety of C$_1$ and multi-carbon compounds [106] and has been reported in MFCs [107]. Our study indicated for the first time that the presence of *Methyloversatilis* sp. in the environment is stimulated by increasing Fe concentrations. It may be explained by the important role of Fe-containing enzymes in *Methyloversatilis* sp. [108] as well as by the involvement of this genus in iron conversions in the environment [109]. The positive effect of the addition of ferrous ions (FeII) on *Fluviicola* sp. abundance was observed in up-flow anaerobic sludge blanket digestion reactors in which these bacteria conducted NO$_2$ reduction together with Fe(II) [110].

4. Conclusions

Bioelectrochemical systems that recover energy from wastewater and waste can play an important role in the energy industry's future. In this study, to improve electrical power generation in MFCs, various doses of Fe$_2$O$_3$ were used to modify the anode surface. In MFC$_{0.1Fe}$, the power and cell resistances were the best, 2.8 times higher and 5.6 times lower than in the control. Organics removal from wastewater was more stable in MFCs with anodes modified with lower Fe$_2$O$_3$ doses. Although the main source of carbon in wastewater was acetate, propionic and valeric acids predominated among the VFAs in the MFC effluents; the proportion of propionic acid to other VFAs increased with increasing iron dose. EPS producers, such as *Zoogloea* sp. and *Acidovorax* sp., were abundant during

reactor start-up, facilitating microbial colonization of the anode and the development of anode biofilms. The addition of iron increased the diversity of the bacterial community. Our study indicated that EE composition was strongly affected by the presence of iron on the anode. The abundance of EE *Geobacter* sp. was 2–3% on the anodes modified with Fe_2O_3 in comparison with 6% in the control MFC. At the two lower doses of Fe_2O_3, the abundance of EEs belonging to *Oscillochloris* sp. and *Pseudomonas* sp. increased, while at the two highest Fe_2O_3 doses, EEs belonging to *Dechloromonass* sp. and *Desulfobacter* sp. predominated in the biofilm. To improve the operation of the MFC, more research is needed to evaluate the effects of iron dose on the anode electrode, because too much iron can negatively affect the current generation and the anode biofilm, and researchers often focusing on the modification itself, ignoring the microbiological aspect. This research could help scientists further develop MFCs through low-cost methods, but more resistant materials need to be developed for industrial applications, as the technologies need to work in the long term.

Supplementary Materials: The following are available online at https://www.mdpi.com/article/10.3390/ijerph20032580/s1, Figure S1. SEM/EDS analyses of anodes' surfaces for an acceleration voltage of 15 kV: (a) pristine, (b) with 0.05 g Fe_2O_3, (c) with 0.1 g Fe_2O_3, (d) with 0.2 g Fe_2O_3, (e) with 0.4 g Fe_2O_3. Figure S2. Statistical differences in the voltages obtained in the individual reactors (ANOVA; Tukey's HSD post hoc test), $p < 0.05$, * significantly higher than in the remaining MFCs. Figure S3. Power output within 18 cycles for (a) $MFC_{control}$, (b) $MFC_{0.05Fe}$, (c) $MFC_{0.1Fe}$, (d) $MFC_{0.2Fe}$, (e) $MFC_{0.4Fe}$. Figure S4. CV for (a) abiotic anodes, (b) with biofilm. Figure S5. Refraction curves; the number after the reactor name indicates the cycle in which sampling was performed. Figure S6. Top 25 genera with abundances most strongly correlated with the dose of Fe_2O_3 used for anode modification.

Author Contributions: Conceptualization: D.N. and A.C.-K.; data curation: D.N.; formal analysis: D.N., T.M. and A.C.-K.; funding acquisition: A.C.-K.; investigation: D.N.; methodology: D.N.; resources: D.N. and A.C.-K.; software: D.N. and T.M.; supervision: A.C.-K.; validation: D.N.; visualization: D.N. and T.M.; writing—original draft: D.N.; writing—review and editing: D.N., T.M. and A.C.-K. All authors have read and agreed to the published version of the manuscript.

Institutional Review Board Statement: Not applicable.

Informed Consent Statement: Not applicable.

Data Availability Statement: The datasets used and/or analyzed during the current study are available from the corresponding author upon reasonable request.

Conflicts of Interest: The authors declare that they have no conflict of interest.

References

1. Jadhav, D.A.; Mungray, A.K.; Arkatkar, A.; Kumar, S.S. Recent advancement in scaling-up applications of microbial fuel cells: From reality to practicability. *Sustain. Energy Technol. Assess.* **2021**, *45*, 101226. [CrossRef]
2. Mohamed, A.; Zmuda, H.M.; Ha, P.T.; Coats, E.R.; Beyenal, H. Large-scale switchable potentiostatically controlled/microbial fuel cell bioelectrochemical wastewater treatment system. *Bioelectrochemistry* **2021**, *138*, 107724. [CrossRef] [PubMed]
3. Nosek, D.; Jachimowicz, P.; Cydzik-Kwiatkowska, A. Anode modification as an alternative approach to improve electricity generation in microbial fuel cells. *Energies* **2020**, *13*, 6596. [CrossRef]
4. Pandit, S.; Khilari, S.; Roy, S.; Pradhan, D.; Das, D. Improvement of power generation using Shewanella putrefaciens mediated bioanode in a single chambered microbial fuel cell: Effect of different anodic operating conditions. *Bioresour. Technol.* **2014**, *166*, 451–457. [CrossRef] [PubMed]
5. Harshiny, M.; Samsudeen, N.; Kameswara, R.J.; Matheswaran, M. Biosynthesized FeO nanoparticles coated carbon anode for improving the performance of microbial fuel cell. *Int. J. Hydrogen Energy* **2017**, *42*, 26488–26495. [CrossRef]
6. Mohamed, H.O.; Obaid, M.; Poo, K.M.; Abdelkareem, M.A.; Talas, S.A.; Fadali, O.A.; Kim, H.Y.; Chae, K.J. Fe/Fe_2O_3 nanoparticles as anode catalyst for exclusive power generation and degradation of organic compounds using microbial fuel cell. *Chem. Eng. J.* **2018**, *349*, 800–807. [CrossRef]

7. Gao, X.; Qiu, S.; Lin, Z.; Xie, X.; Yin, W.; Lu, X. Carbon-based composites as anodes for microbial fuel cells: Recent advances and challenges. *ChemPlusChem* **2021**, *86*, 1322–1341. [CrossRef]

8. Beliaev, A.S.; Saffarini, D.A.; McLaughlin, J.L.; Hunnicutt, D. MtrC, an outer membrane decahaem c cytochrome required for metal reduction in Shewanella putrefaciens MR-1. *Mol. Microbiol.* **2001**, *39*, 722–730. [CrossRef]

9. Sharafat, I.; Ali, J.; Hussain, A.; Torres, C.I.; Ali, N. Trivalent iron shaped the microbial community structure to enhance the electrochemical performance of microbial fuel cells inoculated with soil and sediment. *J. Environ. Chem. Eng.* **2022**, *10*, 107790. [CrossRef]

10. Yamashita, T.; Ishida, M.; Asakawa, S.; Kanamori, H.; Sasaki, H.; Ogino, A.; Katayose, Y.; Hatta, T.; Yokoyama, H. Enhanced electrical power generation using flame-oxidized stainless steel anode in microbial fuel cells and the anodic community structure. *Biotechnol. Biofuels* **2016**, *9*, 62. [CrossRef]

11. Xu, X.; Zhao, Q.; Wu, M.; Ding, J.; Zhang, W. Biodegradation of organic matter and anodic microbial communities analysis in sediment microbial fuel cells with/without Fe (III) oxide addition. *Bioresour. Technol.* **2017**, *225*, 402–408. [CrossRef] [PubMed]

12. Peng, X.H.; Chu, X.Z.; Huang, P.F.; Shan, K. Improved power performance of activated carbon anode by Fe_2O_3 addition in microbial fuel cells. *Appl. Mech. Mater.* **2015**, *700*, 170–174. [CrossRef]

13. Sayed, E.T.; Sayed, E.T.; Alawadhi, H.; Elsaid, K.; Olabi, A.G.; Adel Almakrani, M.; Bin Tamim, S.T.; Alafranji, G.H.M.; Abdelkareem, M.A. A carbon-cloth anode electroplated with iron nanostructure for microbial fuel cell operated with real wastewater. *Sustainability* **2020**, *12*, 6538. [CrossRef]

14. Sekar, A.D.; Sekar, A.D.; Jayabalan, T.; Muthukumar, H.; Chandrasekaran, N.I.; Mohamed, S.N.; Matheswaran, M. Enhancing power generation and treatment of dairy waste water in microbial fuel cell using Cu-doped iron oxide nanoparticles decorated anode. *Energy* **2019**, *172*, 173–180. [CrossRef]

15. Wang, M.; Wang, M.; Wang, Z.; Hu, F.; Fan, L.; Zhang, X. Polyelectrolytes/α-Fe_2O_3 modification of carbon cloth anode for dealing with food wastewater in microbial fuel cell. *Carbon Resour. Convers.* **2020**, *3*, 76–81. [CrossRef]

16. Ahmed, M.; Lin, O.; Saup, C.M.; Wilkins, M.J.; Lin, L.S. Effects of Fe/S ratio on the kinetics and microbial ecology of an Fe (III)-dosed anaerobic wastewater treatment system. *J. Hazard. Mater.* **2019**, *369*, 593–600. [CrossRef]

17. Fu, L.; Wang, H.; Huang, Q.; Song, T.; Xie, J. Modification of carbon felt anode with graphene/Fe_2O_3 composite for enhancing the performance of microbial fuel cell. *Bioprocess Biosyst. Eng.* **2020**, *43*, 373–381. [CrossRef] [PubMed]

18. Qian, G.; Qian, G.; Ye, L.; Li, L.; Hu, X.; Jiang, B.; Zhao, X. Influence of electric field and iron on the denitrification process from nitrogen-rich wastewater in a periodic reversal bio-electrocoagulation system. *Bioresour. Technol.* **2018**, *258*, 177–186. [CrossRef]

19. Kulandaivelu, J.; Kulandaivelu, J.; Gao, J.; Song, Y.; Shrestha, S.; Li, X.; Li, J.; Doederer, K.; Keller, J.; Yuan, Z.; et al. Removal of pharmaceuticals and illicit drugs from wastewater due to ferric dosing in sewers. *Environ. Sci. Technol.* **2019**, *53*, 6245–6254. [CrossRef]

20. Lovley, D.R.; Phillips, E.J. Organic matter mineralization with reduction of ferric iron in anaerobic sediments. *Appl. Environ. Microbiol.* **1986**, *51*, 683–689. [CrossRef]

21. Zheng, X.; Hou, S.; Amanze, C.; Zheng, Z.; Weimin, Z. Enhancing microbial fuel cell performance using anode modified with Fe_3O_4 nanoparticles. *Bioprocess Biosyst. Eng.* **2022**, *45*, 877–890. [CrossRef] [PubMed]

22. Liu, Q.; Liu, Q.; Liu, B.; Li, W.; Zhao, X.; Zuo, W.; Xing, D. Impact of ferrous iron on microbial community of the biofilm in microbial fuel cells. *Front. Microbiol.* **2017**, *8*, 920. [CrossRef] [PubMed]

23. Liu, Q.; Yang, Y.; Mei, X.; Liu, B.; Chen, C.; Xing, D. Response of the microbial community structure of biofilms to ferric iron in microbial fuel cells. *Sci. Total Environ.* **2018**, *631*, 695–701. [CrossRef]

24. Luo, T.; Xu, Q.; Wei, W.; Sun, J.; Dai, X.; Ni, B.J. Performance and mechanism of Fe_3O_4 improving biotransformation of waste activated sludge into liquid high-value products. *Environ. Sci. Technol.* **2022**, *56*, 3658–3668. [CrossRef]

25. Gnana Kumar, G.; Sarathi, V.S.; Nahm, K.S. Recent advances and challenges in the anode architecture and their modifications for the applications of microbial fuel cells. *Biosens. Bioelectron.* **2013**, *43*, 461–475. [CrossRef]

26. Yaqoob, A.A.; Ibrahim, M.N.M.; Umar, K. Biomass-derived composite anode electrode: Synthesis, characterizations, and application in microbial fuel cells (MFCs). *J. Environ. Chem. Eng.* **2021**, *9*, 106111. [CrossRef]

27. Gnana Kumar, G.; Kirubaharan, C.J.; Yoo, D.J.; Kim, A.R. Graphene/poly (3, 4-ethylenedioxythiophene)/Fe_3O_4 nanocomposite–An efficient oxygen reduction catalyst for the continuous electricity production from wastewater treatment microbial fuel cells. *Int. J. Hydrogen Energy* **2016**, *41*, 13208–13219. [CrossRef]

28. Nosek, D.; Cydzik-Kwiatkowska, A. Microbial structure and energy generation in microbial fuel cells powered with waste anaerobic digestate. *Energies* **2020**, *13*, 4712. [CrossRef]

29. Coelho, M.A.Z.; Russo, C.; Araujo, O.Q.F. Optimization of a sequencing batch reactor for biological nitrogen removal. *Water Res.* **2000**, *34*, 2809–2817. [CrossRef]

30. Lobato, J.; Cañizares, P.; Fernández, F.J.; Rodrigo, M.A. An evaluation of aerobic and anaerobic sludges as start-up material for microbial fuel cell systems. *New Biotechnol.* **2012**, *29*, 415–420. [CrossRef]

31. Nosek, D.; Cydzik-Kwiatkowska, A. Anode modification with reduced graphene oxide–iron oxide improves electricity generation in microbial fuel cell. *J. Ecol. Eng.* **2022**, *23*, 147–153. [CrossRef]

32. APHA. *Standard Methods for the Standard Methods for the Examination of Water and Wastewater*, 18th ed.; American Public Health Association (APHA), American Water Works Association (AWWA), Water Pollution Control Federation (WPCF): Washington, DC, USA, 1992.

Int. J. Environ. Res. Public Health **2023**, *20*, 2580

18 of 21

33. Bułkowska, K.; Mikucka, W.; Pokój, T. Enhancement of biogas production from cattle manure using glycerine phase as a co-substrate in anaerobic digestion. *Fuel* **2022**, *317*, 123456. [CrossRef]

34. Watson, V.J.; Logan, B.E. Analysis of polarization methods for elimination of power overshoot in microbial fuel cells. *Electrochem. Commun.* **2011**, *13*, 54–56. [CrossRef]

35. Caporaso, J.G.; Lauber, C.L.; Walters, W.A.; Berg-Lyons, D.; Lozupone, C.A.; Turnbaugh, P.J.; Fierer, N.; Knight, R. Global patterns of 16S rRNA diversity at a depth of millions of sequences per sample. *Proc. Nat. Acad. Sci. USA* **2011**, *108* (Suppl. S1), 4516–4522. [CrossRef]

36. Świątczak, P.; Cydzik-Kwiatkowska, A. Performance and microbial characteristics of biomass in a full-scale aerobic granular sludge wastewater treatment plant. *Environ. Sci. Pollut. Res.* **2018**, *25*, 1655–1669. [CrossRef]

37. Dhariwal, A.; Chong, J.; Habib, S.; King, I.L.; Agellon, L.B.; Xia, J. MicrobiomeAnalyst—A web-based tool for comprehensive statistical, visual and meta-analysis of microbiome data. *Nucleic Acids Res.* **2017**, *45*, W180–W188. [CrossRef]

38. Chong, J.; Liu, P.; Zhou, G.; Xia, J. Using Microbiome Analyst for comprehensive statistical, functional, and meta-analysis of microbiome data. *Nat. Protoc.* **2020**, *15*, 799–821. [CrossRef]

39. McMurdie, P.J.; Holmes, S. Waste not, want not: Why rarefying microbiome data is inadmissible. *PLoS Comput. Biol.* **2014**, *10*, e1003531. [CrossRef]

40. Fan, L.; Xi, Y. Effect of polypyrrole-Fe_3O_4 composite modified anode and its electrodeposition time on the performance of microbial fuel cells. *Energies* **2021**, *14*, 2461. [CrossRef]

41. O'Brien, F.J.; Harley, B.A.; Yannas, I.V.; Gibson, L.J. The effect of pore size on cell adhesion in collagen-GAG scaffolds. *Biomaterials* **2005**, *26*, 433–441. [CrossRef]

42. Wei, L.; Han, H.; Shen, J. Effects of temperature and ferrous sulfate concentrationson the performance of microbial fuel cell. *Int. J. Hydrogen Energy* **2013**, *38*, 11110–11116. [CrossRef]

43. Kuczyński, M.; Łuba, M.; Mikołajczyk, T.; Pierożyński, B.; Jasiecka-Mikołajczyk, A.; Smoczyński, L.; Sołowiej, P.; Wojtacha, P. Electrodegradation of acid mixture dye through the employment of Cu/Fe macro-corrosion galvanic cell in Na_2SO_4 synthetic wastewater. *Molecules* **2021**, *26*, 4580. [CrossRef] [PubMed]

44. Pareek, A.; Shanthi Sravan, J.; Venkata Mohan, S. Graphene modified electrodes for bioelectricity generation in mediator-less microbial fuel cell. *J. Mater. Sci.* **2019**, *54*, 11604–11617. [CrossRef]

45. Yang, Q.; Yang, S.; Liu, G.; Zhou, B.; Yu, X.; Yin, Y.; Yang, J.; Zhao, H. Boosting the anode performance of microbial fuel cells with a bacteria-derived biological iron oxide/carbon nanocomposite catalyst. *Chemosphere* **2021**, *268*, 128800. [CrossRef]

46. Ren, Z.; Steinberg, L.M.; Regan, J.M. Electricity production and microbial biofilm characterization in cellulose-fed microbial fuel cells. *Water Sci. Technol.* **2008**, *58*, 617–622. [CrossRef]

47. Paucar, N.E.; Sato, C. Microbial fuel cell for energy production, nutrient removal and recovery from wastewater: A review. *Processes* **2021**, *9*, 1318. [CrossRef]

48. Baby, M.G.; Ahammed, M.M. Nutrient removal and recovery from wastewater by microbial fuel cell-based systems–A review. *Water Sci. Technol.* **2022**, *86*, 29–55. [CrossRef]

49. Huang, S.; Jaffé, P. Characterization of incubation experiments and development of an enrichment culture capable of ammonium oxidation under iron-reducing conditions. *Biogeosciences* **2015**, *12*, 769–779. [CrossRef]

50. Bose, S.; Hochella, M.F., Jr.; Gorby, Y.A.; Kennedy, D.W.; McCready, D.E.; Madden, A.S.; Lower, B.H. Bioreduction of hematite nanoparticles by the dissimilatory iron reducing bacterium *Shewanella oneidensis* MR-1. *Geochim. Cosmochim. Acta* **2009**, *73*, 962–976. [CrossRef]

51. Zhang, L.; Zhang, M.; You, S.; Ma, D.; Zhao, J.; Chen, Z. Effect of Fe^{3+} on the sludge properties and microbial community structure in a lab-scale A^2O process. *Sci. Total Environ.* **2021**, *780*, 146505. [CrossRef]

52. Cao, J.; Xie, Y.; Fang, F.; Hu, H. Influences of Fe^{3+} on phosphorus removal and microbial products in denitrifying phosphorus removal system. *Res. Environ. Sci.* **2015**, *28*, 125–133. [CrossRef]

53. Mena, N.P.; Bulteau, A.L.; Salazar, J.; Hirsch, E.C.; Núñez, M.T. Effect of mitochondrial complex I inhibition on Fe–S cluster protein activity. *Biochem. Biophys. Res. Commun.* **2011**, *409*, 241–246. [CrossRef]

54. Jadhav, G.S.; Ghangrekar, M.M. Performance of microbial fuel cell subjected to variation in pH, temperature, external load and substrate concentration. *Bioresour. Technol.* **2009**, *100*, 717–723. [CrossRef]

55. Franks, A.E.; Nevin, K.P.; Jia, H.; Izallalen, M.; Woodard, T.L.; Lovley, D.R. Novel strategy for three-dimensional real-time imaging of microbial fuel cell communities: Monitoring the inhibitory effects of proton accumulation within the anode biofilm. *Energy Environ. Sci.* **2009**, *2*, 113–119. [CrossRef]

56. Wu, S.; Zou, S.; Yang, Y.; Qian, G.; He, Z. Enhancing the performance of an osmotic microbial fuel cell through self-buffering with reverse-fluxed sodium bicarbonate. *Chem. Eng. J.* **2018**, *349*, 241–248. [CrossRef]

57. Yu, J.; Park, Y.; Kim, B.; Lee, T. Power densities and microbial communities of brewery wastewater-fed microbial fuel cells according to the initial substrates. *Bioprocess Biosyst. Eng.* **2015**, *38*, 85–92. [CrossRef] [PubMed]

58. Arun, V.; Mino, T.; Matsuo, T. Biological mechanism of acetate uptake mediated by carbohydrate consumption in excess phosphorus removal systems. *Water Res.* **1988**, *22*, 565–570. [CrossRef]

59. Wang, R.; Li, Y.; Chen, W.; Zou, J.; Chen, Y. Phosphate release involving PAOs activity during anaerobic fermentation of EBPR sludge and the extension of ADM1. *J. Chem. Eng.* **2016**, *287*, 436–447. [CrossRef]

60. Barcenilla, A.; Barcenilla, A.; Pryde, S.E.; Martin, J.C.; Duncan, S.H.; Stewart, C.S.; Henderson, C.; Flint, H.J. Phylogenetic relationships of butyrate-producing bacteria from the human gut. *Appl. Environ. Microbiol.* **2000**, *66*, 1654–1661. [CrossRef]

61. Ye, W.; Lu, J.; Ye, J.; Zhou, Y. The effects and mechanisms of zero-valent iron on anaerobic digestion of solid waste: A mini-review. *J. Clean. Prod.* **2021**, *278*, 123567. [CrossRef]

62. Barredo, M.S.; Evison, L. Effect of propionate toxicity on methanogen-enriched sludge, *Methanobrevibacter smithii*, and *Methanospirillum hungatii* at different pH values. *Appl. Environ. Microbiol.* **1991**, *57*, 1764–1769. [CrossRef]

63. Liu, Y.; Zhang, X.; Li, H.; Peng, L.; Qin, Y.; Lin, X.; Zheng, L.; Li, C. Porous α-Fe_2O_3 nanofiber combined with carbon nanotube as anode to enhance the bioelectricity generation for microbial fuel cell. *Electrochim. Acta* **2021**, *391*, 138984. [CrossRef]

64. Schilirò, T.; Tommasi, T.; Armato, C.; Hidalgo, D.; Traversi, D.; Bocchini, S.; Cilli, C.F.; Pirri, C.F. The study of electrochemically active planktonic microbes in microbial fuel cells in relation to different carbon-based anode materials. *Energy* **2016**, *106*, 277–284. [CrossRef]

65. Luo, J.; Feng, L.; Chen, Y.; Sun, H.; Shen, Q.; Li, X.; Chen, H. Alkyl polyglucose enhancing propionic acid enriched short-chain fatty acids production during anaerobic treatment of waste activated sludge and mechanisms. *Water Res.* **2015**, *73*, 332–341. [CrossRef] [PubMed]

66. Chen, G.Q.; Chen, G.Q.; Wu, Y.H.; Chen, Z.; Luo, L.W.; Wang, Y.H.; Tong, X.; Bai, Y.; Wang, H.B.; Xu, Y.Q.; et al. Enhanced extracellular polymeric substances production and aggravated membrane fouling potential caused by different disinfection treatment. *J. Membr. Sci.* **2022**, *642*, 120007. [CrossRef]

67. Lovley, D.R.; Ueki, T.; Zhang, T.; Malvankar, N.; Shrestha, P.M.; Flanagan, K.A.; Aklujkar, M.; Butler, J.E.; Giloteaux, L.; Rotaru, A.E.; et al. *Geobacter*: The microbe electric's physiology, ecology, and practical applications. *Adv. Microb. Physiol.* **2011**, *59*, 1–100. [CrossRef]

68. Kiely, P.D.; Call, D.F.; Yates, M.D.; Regan, J.R.; Logan, B.E. Anodic biofilms in microbial fuel cells harbor low numbers of higher-power producing bacteria than abundant genera. *Appl. Microbiol. Biotechnol.* **2010**, *88*, 371–380. [CrossRef]

69. Logan, B.E.; Rossi, R.; Ragab, A.; Saikaly, P.E. Electroactive microorganisms in bioelectrochemical systems. *Nat. Rev. Microbiol.* **2019**, *17*, 307–319. [CrossRef]

70. Phillips, E.J.; Lovley, D.R.; Roden, E.E. Composition of non-microbially reducible Fe (III) in aquatic sediments. *Appl. Environ. Microbiol.* **1993**, *59*, 2727–2729. [CrossRef] [PubMed]

71. Ding, Y.H.R.; Hixson, K.K.; Aklujkar, M.A.; Lipton, M.S.; Smith, R.D.; Lovley, D.R.; Mester, T. Proteome of *Geobacter sulfurreducens* grown with Fe(III) oxide or Fe(III) citrate as the electron acceptor. *Biochim. Biophys. Acta (BBA)-Proteins Proteom.* **2008**, *1784*, 1935–1941. [CrossRef]

72. DiLoreto, Z.A.; Bontognali, T.R.; Al Disi, Z.A.; Al-Kuwari, H.A.S.; Williford, K.H.; Strohmenger, C.J.; Sadooni, F.; Palermo, C.; Rivers, J.M.; McKenzie, J.A.; et al. Microbial community composition and dolomite formation in the hypersaline microbial mats of the Khor Al-Adaid sabkhas, Qatar. *Extremophiles* **2019**, *23*, 201–218. [CrossRef] [PubMed]

73. Hasan, K.; Reddy, K.V.R.; Eßmann, V.; Górecki, K.; Conghaile, P.Ó.; Schuhmann, W.; Leech, D.; Hägerhäll, C.; Gorton, L. Electrochemical communication between electrodes and *Rhodobacter capsulatus* grown in different metabolic modes. *Electroanalysis* **2015**, *27*, 118–127. [CrossRef]

74. Wong, M.T.; Cheng, D.; Wang, R.; Hsing, I.M. Modifying the endogenous electron fluxes of *Rhodobacter sphaeroides* 2.4. 1 for improved electricity generation. *Enzym. Microb. Technol.* **2016**, *86*, 45–51. [CrossRef]

75. Zheng, W.; Cai, T.; Huang, M.; Chen, D. Comparison of electrochemical performances and microbial community structures of two photosynthetic microbial fuel cells. *J. Biosci. Bioeng.* **2017**, *124*, 551–558. [CrossRef] [PubMed]

76. Price-Whelan, A.; Dietrich, L.E.; Newman, D.K. Rethinking 'secondary' metabolism: Physiological roles for phenazine antibiotics. *Nat. Chem. Biol.* **2006**, *2*, 71–78. [CrossRef] [PubMed]

77. Žalnèravičius, R.; Paškevičius, A.; Samukaitė-Bubnienė, U.; Ramanavičius, S.; Vilkienė, M.; Mockevičienė, I.; Ramanavičius, A. Microbial fuel cell based on nitrogen-fixing *Rhizobium anhuiense* bacteria. *Biosensors* **2022**, *12*, 113. [CrossRef] [PubMed]

78. Wang, H.; Fu, B.; Xi, J.; Hu, H.Y.; Liang, P.; Huang, X.; Zhang, X. Remediation of simulated malodorous surface water by columnar air-cathode microbial fuel cells. *Sci. Total Environ.* **2019**, *687*, 287–296. [CrossRef]

79. Whaley-Martin, K.; Jessen, G.L.; Nelson, T.C.; Mori, J.F.; Apte, S.; Jarolimek, C.; Warren, L.A. The potential role of *Halothiobacillus* spp. in sulfur oxidation and acid generation in circum-neutral mine tailings reservoirs. *Front. Microbiol.* **2019**, *10*, 297. [CrossRef]

80. Miettinen, H.; Bomberg, M.; Le, T.M.K.; Kinnunen, P. Identification and metabolism of naturally prevailing microorganisms in zinc and copper mineral processing. *Minerals* **2021**, *11*, 156. [CrossRef]

81. Yamada, T.; Sekiguchi, Y.; Hanada, S.; Imachi, H.; Ohashi, A.; Harada, H.; Kamagata, Y. *Anaerolinea thermolimosa* sp. nov., *Levilinea saccharolytica* gen. nov., sp. nov. and *Leptolinea tardivitalis* gen. nov., sp. nov., novel filamentous anaerobes, and description of the new classes Anaerolineae classis nov. and Caldilineae classis nov. in the bacterial phylum Chloroflexi. *Int. J. Syst. Evol. Microbiol.* **2006**, *56*, 1331–1340. [CrossRef]

82. Yang, C.; Xiao, N.; Chang, Z.A.; Huang, J.J.; Zeng, W. Biodegradation of TOC by nano-Fe_2O_3 modified SMFC and its potential environmental effects. *ChemistrySelect* **2021**, *6*, 5597–5602. [CrossRef]

83. Zhang, D.; Shen, J.; Shi, H.; Su, G.; Jiang, X.; Li, J.; Liu, J.; Mu, Y.; Wang, L. Substantially enhanced anaerobic reduction of nitrobenzene by biochar stabilized sulfide-modified nanoscale zero-valent iron: Process and mechanisms. *Environ. Int.* **2019**, *131*, 105020. [CrossRef]

84. Zhang, K.; Wu, X.; Luo, H.; Li, X.; Chen, W.; Chen, J.; Mo, Y.; Wang, W. CH$_4$ control and associated microbial process from constructed wetland (CW) by microbial fuel cells (MFC). *J. Environ. Manag.* **2020**, *260*, 110071. [CrossRef] [PubMed]

85. Iigatani, R.; Ito, T.; Watanabe, F.; Nagamine, M.; Suzuki, Y.; Inoue, K. Electricity generation from sweet potato-shochu waste using microbial fuel cells. *J. Biosci. Bioeng.* **2019**, *128*, 56–63. [CrossRef]

86. Wang, A.; Liu, L.; Sun, D.; Ren, N.; Lee, D.J. Isolation of Fe(III)-reducing fermentative bacterium Bacteroides sp. W7 in the anode suspension of a microbial electrolysis cell (MEC). *Int. J. Hydrogen Energy* **2010**, *35*, 3178–3182. [CrossRef]

87. Wang, J.; Song, X.; Wang, Y.; Abayneh, B.; Li, Y.; Yan, D.; Bai, J. Nitrate removal and bioenergy production in constructed wetland coupled with microbial fuel cell: Establishment of electrochemically active bacteria community on anode. *Bioresour. Technol.* **2016**, *221*, 358–365. [CrossRef] [PubMed]

88. Kisková, J.; Perháčová, Z.; Vlčko, L.; Sedláková, J.; Kvasnová, S.; Pristaš, P. The bacterial population of neutral mine drainage water of Elizabeth's shaft (Slovinky, Slovakia). *Curr. Microbiol.* **2018**, *75*, 988–996. [CrossRef]

89. Li, X.; Zhang, W.; Liu, T.; Chen, L.; Chen, P.; Li, F. Changes in the composition and diversity of microbial communities during anaerobic nitrate reduction and Fe(II) oxidation at circumneutral pH in paddy soil. *Soil Biol. Biochem.* **2016**, *94*, 70–79. [CrossRef]

90. Drewniak, L.; Krawczyk, P.S.; Mielnicki, S.; Adamska, D.; Sobczak, A.; Lipinski, L.; Burec-Drewniak, W.; Sklodowska, A. Physiological and metagenomic analyses of microbial mats involved in self-purification of mine waters contaminated with heavy metals. *Front. Microbiol.* **2016**, *7*, 1252. [CrossRef]

91. Li, Z.L.; Zhu, Z.L.; Lin, X.Q.; Chen, F.; Li, X.; Liang, B.; Huang, C.; Zhamg, Y.M.; Sun, K.; Zhou, A.A.; et al. Microbial fuel cell-upflow biofilter coupling system for deep denitrification and power recovery: Efficiencies, bacterial succession and interactions. *Environ. Res.* **2021**, *196*, 110331. [CrossRef]

92. Varanasi, J.L.; Sinha, P.; Das, D. Maximizing power generation from dark fermentation effluents in microbial fuel cell by selective enrichment of exoelectrogens and optimization of anodic operational parameters. *Biotechnol. Lett.* **2017**, *39*, 721–730. [CrossRef] [PubMed]

93. Kuever, J.; Rainey, F.A.; Widdel, F. Desulfobacter. In *Bergey's Manual of Systematics of Archaea and Bacteria*; Wiley Online Library: Hoboken, NJ, USA, 2015; pp. 1–7. [CrossRef]

94. Nicolova, M.; Groudev, S.; Spasova, I.; Groudeva, V.; Georgiev, P. Electricity generation by means of microorganisms from different physiological groups. *Industry 4.0* **2018**, *3*, 80–81.

95. Tang, R.; Wu, D.; Chen, W.; Feng, C.; Wei, C. Biocathode denitrification of coke wastewater effluent from an industrial aeration tank: Effect of long-term adaptation. *Biochem. Eng. J.* **2017**, *125*, 151–160. [CrossRef]

96. Zhang, Z.; Zhang, K.; Ouyang, H.; Li, M.K.; Luo, Z.; Li, Y.; Chen, C.; Yang, X.; Shao, Z.; Yan, D.Y. Simultaneous PAHs degradation, odour mitigation and energy harvesting by sediment microbial fuel cell coupled with nitrate-induced biostimulation. *J. Environ. Manag.* **2021**, *284*, 112045. [CrossRef] [PubMed]

97. Sangcharoen, A.; Niyom, W.; Suwannasilp, B.B. A microbial fuel cell treating organic wastewater containing high sulfate under continuous operation: Performance and microbial community. *Process Biochem.* **2015**, *50*, 1648–1655. [CrossRef]

98. Mohite, B.V.; Koli, S.H.; Patil, S.V. Heavy metal stress and its consequences on exopolysaccharide (EPS)-producing *Pantoea agglomerans*. *Appl. Biochem. Biotechnol.* **2018**, *186*, 199–216. [CrossRef] [PubMed]

99. Ibrahim, I.M.; Konnova, S.A.; Sigida, E.N.; Lyubun, E.V.; Muratova, A.Y.; Fedonenko, Y.P.; Elbanna, K. Bioremediation potential of a halophilic *Halobacillus* sp. strain, EG1HP4QL: Exopolysaccharide production, crude oil degradation, and heavy metal tolerance. *Extremophiles* **2020**, *24*, 157–166. [CrossRef]

100. Giese, E.C. Evidences of EPS-iron (III) ions interactions on bioleaching process mini-review: The key to improve performance. *Orbital-Electron. J. Chem.* **2019**, *11*, 200–204. [CrossRef]

101. Sag, Y.; Kutsal, T. Determination of the biosorption heats of heavy metal ions on *Zoogloea ramigera* and *Rhizopus arrhizus*. *Biochem. Eng. J.* **2000**, *6*, 145–151. [CrossRef] [PubMed]

102. Perpetuo, E.A.; Souza, C.B.; Nascimento, C.A.O. Engineering Bacteria for Bioremediation. *Prog. Mol. Biol. Transl. Sci.* **2011**, *28*, 605–632. [CrossRef]

103. Mei, X.; Guo, C.; Liu, B.; Tang, Y.; Xing, D. Shaping of bacterial community structure in microbial fuel cells by different inocula. *RSC Adv.* **2015**, *5*, 78136–78141. [CrossRef]

104. Lee, J.; Phung, N.T.; Chang, I.S.; Kim, B.H.; Sung, H.C. Use of acetate for enrichment of electrochemically active microorganisms and their 16S rDNA analyses. *FEMS Microbiol. Lett.* **2003**, *223*, 185–191. [CrossRef]

105. Alatraktchi, F.A.A.; Zhang, Y.; Angelidaki, I. Nanomodification of the electrodes in microbial fuel cell: Impact of nanoparticle density on electricity production and microbial community. *Appl. Energy* **2014**, *116*, 216–222. [CrossRef]

106. Kalyuzhnaya, M.G.; De Marco, P.; Bowerman, S.; Pacheco, C.C.; Lara, J.C.; Lidstrom, M.E.; Chistoserdova, L. *Methyloversatilis universalis* gen. nov., sp. nov., a novel taxon within the Betaproteobacteria represented by three methylotrophic isolates. *Int. J. Syst. Evol.* **2006**, *56*, 2517–2522. [CrossRef]

107. Ramanaiah, S.V.; Cordas, C.M.; Matias, S.C.; Reddy, M.V.; Leitao, J.H.; Fonseca, L.P. Bioelectricity generation using long-term operated biocathode: RFLP based microbial diversity analysis. *Biotechnol. Rep.* **2021**, *32*, e00693. [CrossRef] [PubMed]

108. Cheng, R.; Weitz, A.C.; Paris, J.; Tang, Y.; Zhang, J.; Song, H.; Naowarojna, N.; Li, K.; Qiao, L.; Lopez, J.; et al. OvoAMtht from *Methyloversatilis thermotolerans* ovothiol biosynthesis is a bifunction enzyme: Cysteine dioxygenase and sulfoxide synthase activities. *Chem. Sci.* **2022**, *13*, 3589–3598. [CrossRef] [PubMed]

Int. J. Environ. Res. Public Health **2023**, *20*, 2580

21 of 21

109. Issayeva, A.U.; Pankiewicz, R.; Otarbekova, A.A. Bioleaching of metals from wastes of phosphoric fertilizers production. *Pol. J. Environ. Stud.* **2020**, *29*, 4101–4108. [CrossRef]

110. Zhang, Y.B.; Wang, Y.L.; Li, W.H.; Bao, L.N.; Wang, L.H.; Huang, X.H.; Huang, B. Biogas emission from an anaerobic reactor. *Aerosol Air. Qual. Res.* **2018**, *18*, 1493–1502. [CrossRef]
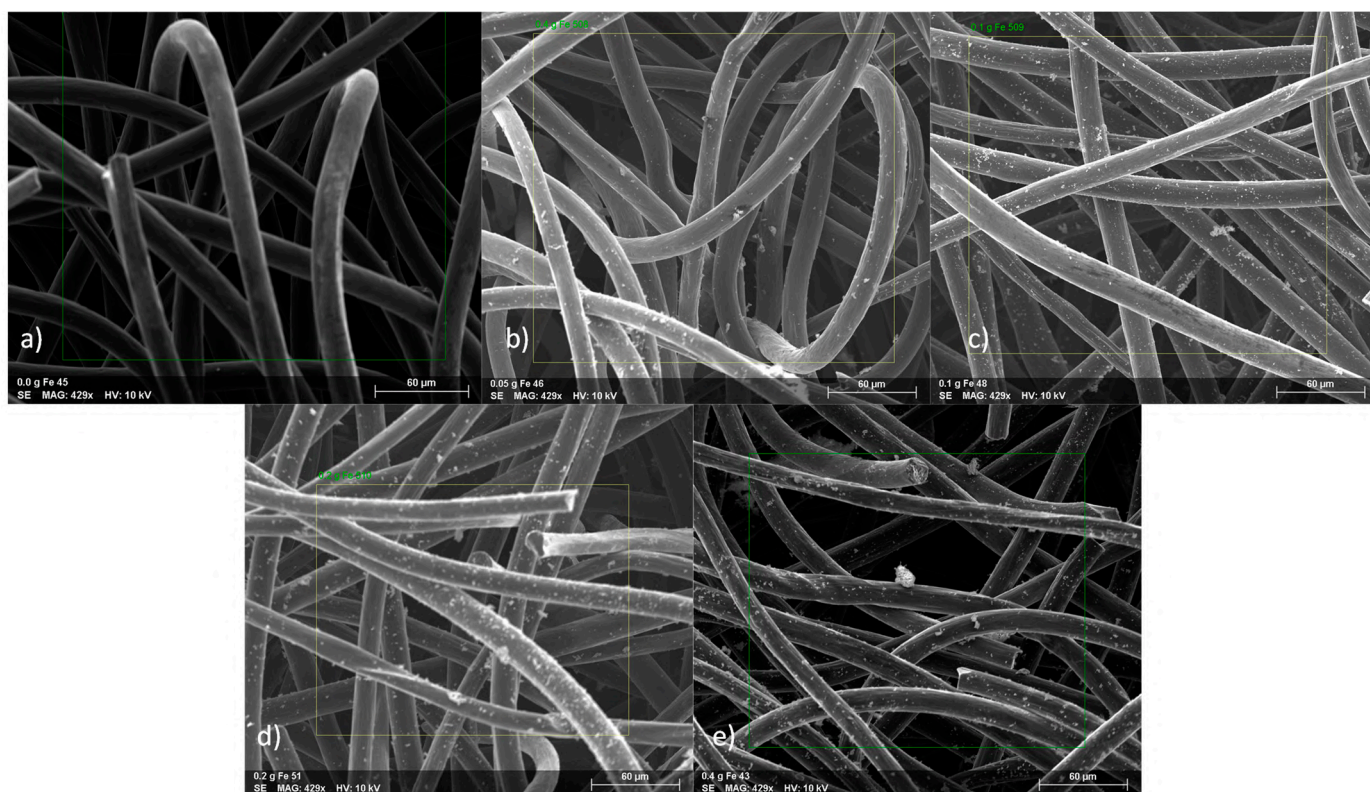
Anode Modification with Fe₂O₃ Affects the Anode Microbiome and Improves Energy Generation in Microbial Fuel Cells Powered by Wastewater

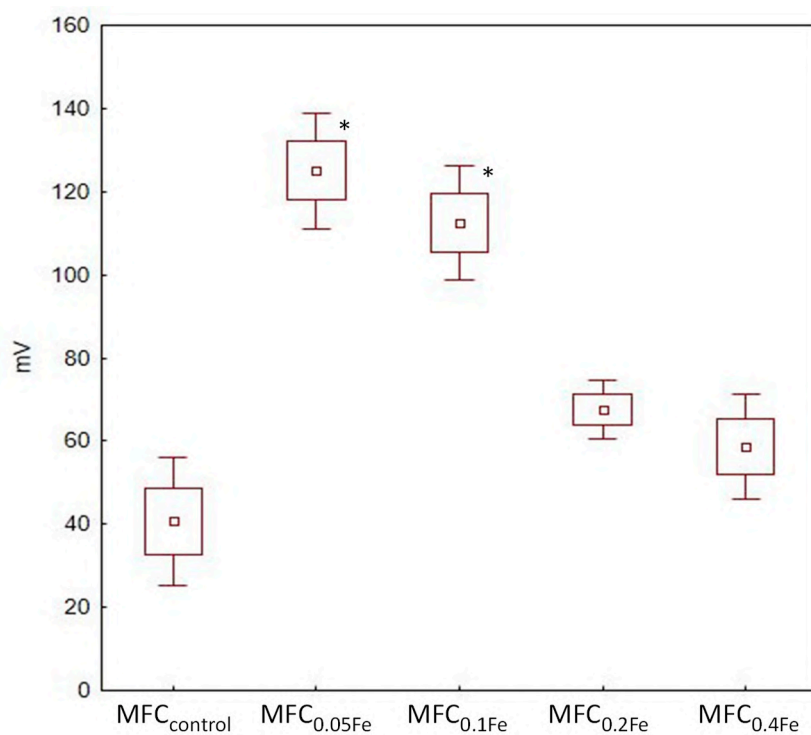**Dawid Nosek [1,*], Tomasz Mikołajczyk [2] and Agnieszka Cydzik-Kwiatkowska [1]**

[1] Department of Environmental Biotechnology, University of Warmia and Mazury in Olsztyn, Słoneczna 45 G, 10-709 Olsztyn, Poland

[2] Department of Chemistry, University of Warmia and Mazury in Olsztyn, plac Łódzki 4, 10-721 Olsztyn, Poland
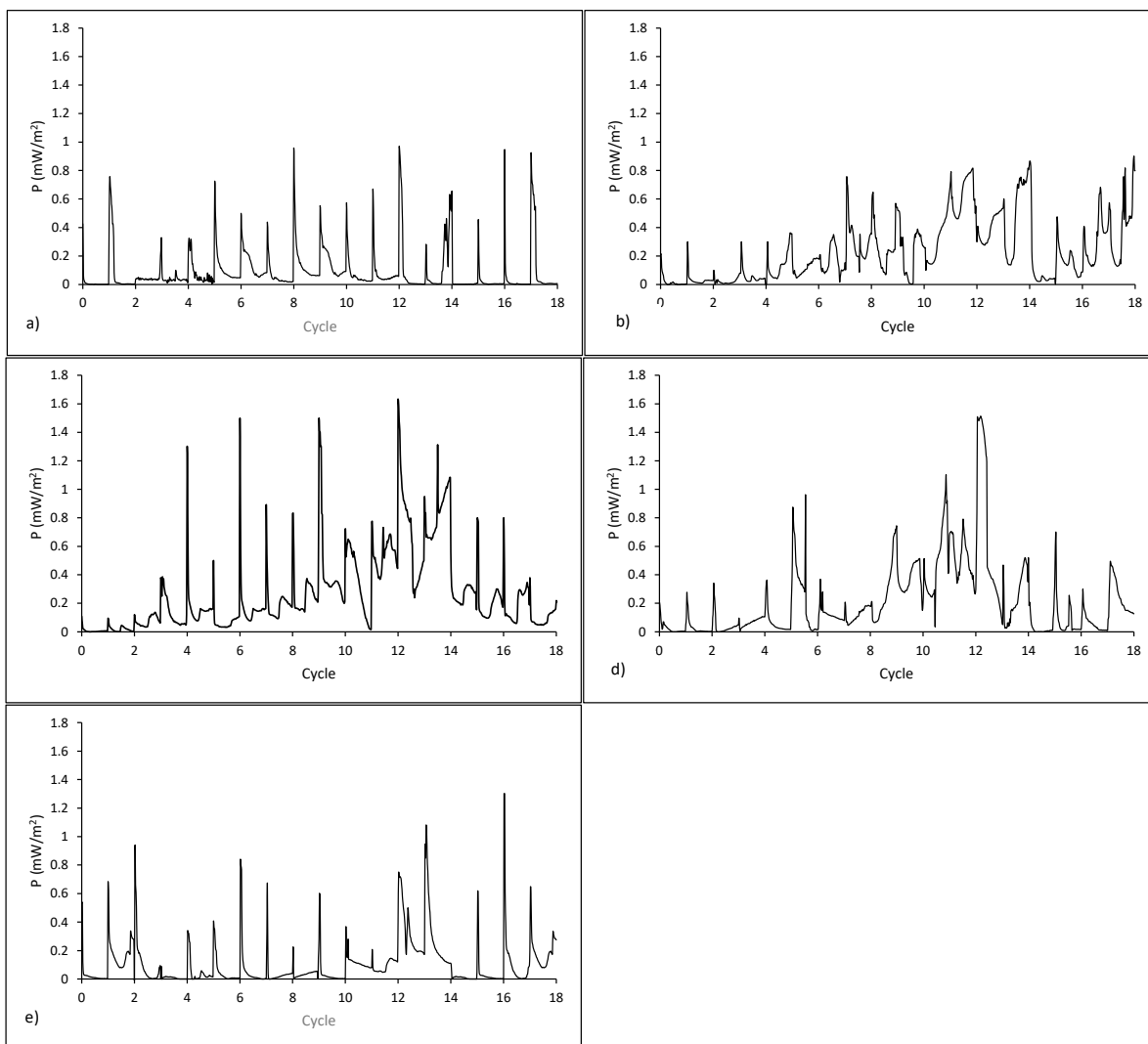
[*] Correspondence: dawid.nosek@uwm.edu.pl; Tel. +48-89-5234144

Figure S1. SEM/EDS analyses of anodes' surfaces for an acceleration voltage of 15 kV: (a) pristine, (b) with 0.05 g Fe2O3, (c) with 0.1 g Fe2O3, (d) with 0.2 g Fe2O3, (e) with 0.4 g Fe2O3.

Figure S2. Statistical differences in the voltages obtained in the individual reactors (ANOVA; Tukey's HSD post hoc test), $p < 0.05$, * significantly higher than in the remaining MFCs

Figure S3. Power output within 18 cycles for (a) $MFC_{control}$, (b) $MFC_{0.05Fe}$, (c) $MFC_{0.1Fe}$, (d) $MFC_{0.2Fe}$, (e) $MFC_{0.4Fe}$.

Figure S4. CV for (a) abiotic anodes, (b) with biofilm

Figure S5. Refraction curves; the number after the reactor name indicates the cycle in which sampling was performed.

Figure S6. Top 25 genera with abundances most strongly correlated with the dose of Fe_2O_3 used for anode modification.

Olsztyn, 21.08.2024

(miejscowość, data)

mgr inż. Dawid Nosek

(imię i nazwisko)

Przewodniczący Rady Naukowej Dyscypliny

prof. dr hab. inż. Marcin Dębowski

Uniwersytetu Warmińsko-Mazurskiego w Olsztynie

OŚWIADCZENIE

kandydata

Oświadczam, że w pracy pod tytułem:

Nosek D., Mikołajczyk T., Cydzik-Kwiatkowska A. (2023). Anode modification with Fe2O3 affects the anode microbiome and improves energy generation in microbial fuel cells powered by wastewater. International Journal of Environmental Research and Public Health 20(3), 2580, mój wkład merytoryczny w jej przygotowanie polegał na: zaplanowaniu koncepcji pracy, pozyskaniu, opracowaniu i interpretacji wyników technologicznych, graficznym opracowaniu wyników oraz przygotowaniu pierwszej wersji manuskryptu.

(podpis)

Olsztyn, 21.08.2024

(miejscowość, data)

dr inż. Tomasz Mikołajczyk

(imię i nazwisko)

Przewodniczący Rady Naukowej Dyscypliny

prof. dr hab. inż. Marcin Dębowski

Uniwersytetu Warmińsko-Mazurskiego w Olsztynie

OŚWIADCZENIE

współautora

Oświadczam, że w pracy pod tytułem:

Nosek D., Mikołajczyk T., Cydzik-Kwiatkowska A. (2023). Anode modification with Fe_2O_3 affects the anode microbiome and improves energy generation in microbial fuel cells powered by wastewater. International Journal of Environmental Research and Public Health 20(3), 2580, mój wkład merytoryczny w jej przygotowanie polegał na: pozyskaniu, analizie i graficznym opracowaniu wyników oraz edycji tekstu pierwszej wersji manuskryptu.

Jednocześnie wyrażam zgodę na przedłożenie w/w pracy przez Pana Dawida Noska jako część rozprawy doktorskiej w formie spójnego tematycznie zbioru artykułów naukowych opublikowanych w czasopismach naukowych. Oświadczam, iż samodzielna i możliwa do wyodrębnienia część ww. pracy wykazuje indywidualny wkład kandydata Pana Dawida Noska polegający na:

udziale w zaplanowaniu koncepcji pracy, pozyskaniu, opracowaniu i interpretacji wyników technologicznych, graficznym opracowaniu wyników oraz przygotowaniu pierwszej wersji manuskryptu.

(podpis)

134:8368165014

prof. dr hab. inż. Agnieszka Cydzik-Kwiatkowska

(imię i nazwisko)

Przewodniczący Rady Naukowej Dyscypliny

prof. dr hab. inż. Marcin Dębowski

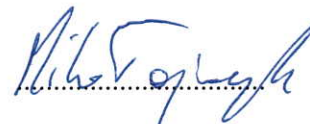**Uniwersytetu Warmińsko-Mazurskiego w Olsztynie**

OŚWIADCZENIE

współautora

Oświadczam, że w pracy pod tytułem:

Nosek D., Mikołajczyk T., Cydzik-Kwiatkowska A. (2023). Anode modification with Fe_2O_3 affects the anode microbiome and improves energy generation in microbial fuel cells powered by wastewater. International Journal of Environmental Research and Public Health 20(3), 2580, mój wkład merytoryczny w jej przygotowanie polegał na: udziale w zaplanowaniu koncepcji pracy, recenzowaniu i edycji tekstu, merytorycznym nadzorze pracy i pozyskaniu środków finansowych.

Jednocześnie wyrażam zgodę na przedłożenie w/w pracy przez Pana Dawida Noska jako część rozprawy doktorskiej w formie spójnego tematycznie zbioru artykułów naukowych opublikowanych w czasopismach naukowych. Oświadczam, iż samodzielna i możliwa do wyodrębnienia część ww. pracy wykazuje indywidualny wkład kandydata Pana Dawida Noska polegający na:

udziale w zaplanowaniu koncepcji pracy, pozyskaniu, opracowaniu i interpretacji wyników technologicznych, graficznym opracowaniu wyników oraz przygotowaniu pierwszej wersji manuskryptu.

....

(podpis)

135:4627851213

Praca nr 5

Nosek D., Mikołajczyk T., Cydzik-Kwiatkowska A.

Enhancing microbial fuel cell performance: anode modification with reduced graphene oxide and iron(III) for improved electricity generation.

Clean Technology and Environmental Policy

2024

ORIGINAL PAPER

Enhancing microbial fuel cell performance: anode modification with reduced graphene oxide and iron(III) for improved electricity generation

Dawid Nosek[1] · Tomasz Mikołajczyk[2] · Agnieszka Cydzik-Kwiatkowska[1]

Abstract

Microbial fuel cells (MFCs) are a promising technology for energy recovery from wastewater. To improve energy generation, reduced graphene oxide (rGO) and composites of rGO and Fe(III) in two doses (34 mg and 68 mg) were electrochemically deposited on graphite felt anodes in a dual-chamber MFC fueled with wastewater. The power density (8.55 mW/m^2) and voltage (342.7 ± 72.8 mV) were higher in the MFC with the anode modified with rGO/68 mg Fe composite than in the other variants. The total internal resistance of this cell was about 4 times lower and the load transfer resistance was 2 times lower than with the control. The double-layer capacitances of the modified anodes at 900 mV were higher than those of the MFC-control (up to 3.7 times in the case of the MFC with anode modified with rGO and 68 mg Fe). Our study identified 12 bacterial species (such as *Pseudoxanthomonas* sp., *Dechloromonas* sp., *Stenotrophomonas* sp., *Microcystis* sp.) that supported the generation of voltage, current, and power in the MFC. Analysis of the metabolic potential of anodic biofilms indicated that electricity production was mainly related to the citrate cycle. In MFC with the anode modified with rGO/34 mg Fe composite, the metabolic potential for energy production and conversion, defense mechanisms, replication, recombination, and repair was highest. This is the first study to holistically investigate how rGO and iron affect power generation, microbiome composition, and bacterial metabolism in municipal wastewater-fed MFCs.
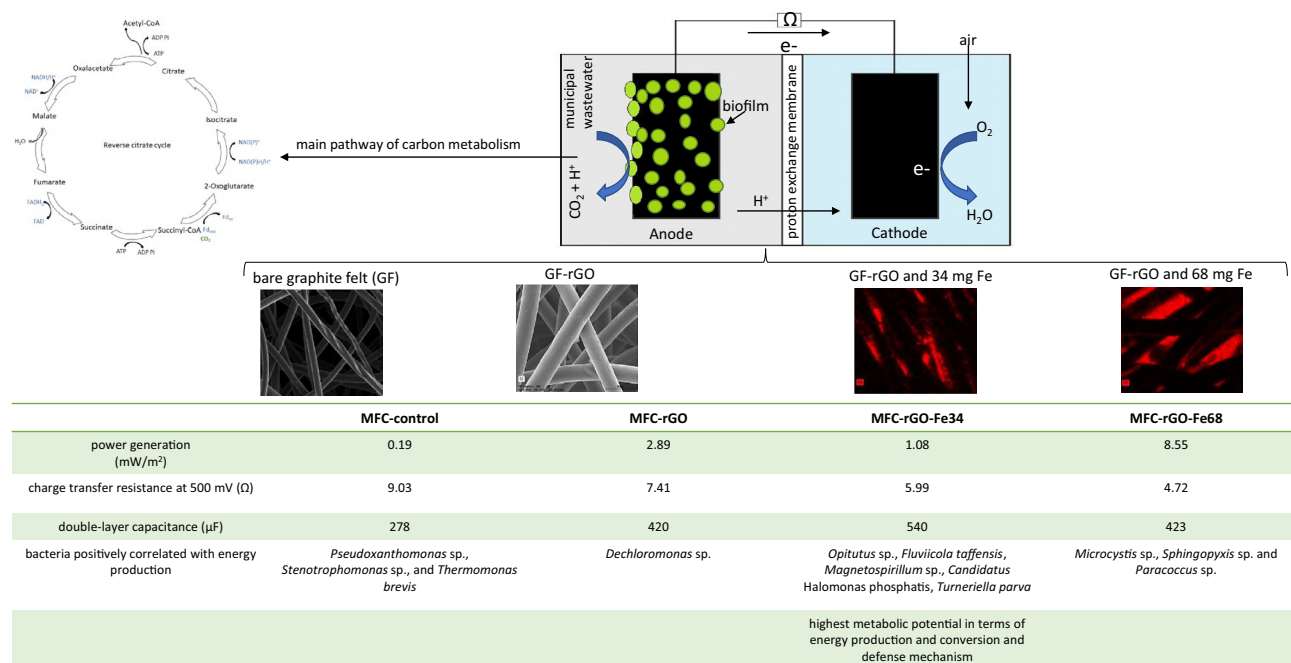
✉ Dawid Nosek
dawid.nosek@uwm.edu.pl

1 Department of Environmental Biotechnology, University of Warmia and Mazury in Olsztyn, Słoneczna 45 G, 10-709 Olsztyn, Poland

2 Department of Chemistry, University of Warmia and Mazury in Olsztyn, Plac Łódzki 4, 10-721 Olsztyn, Poland

🖄 Springer

Graphical abstract

	MFC-control	MFC-rGO	MFC-rGO-Fe34	MFC-rGO-Fe68
power generation (mW/m^2)	0.19	2.89	1.08	8.55
charge transfer resistance at 500 mV (Ω)	9.03	7.41	5.99	4.72
double-layer capacitance (µF)	278	420	540	423
bacteria positively correlated with energy production	*Pseudoxanthomonas* sp., *Stenotrophomonas* sp., and *Thermomonas brevis*	*Dechloromonas* sp.	*Opitutus* sp., *Fluviicola taffensis*, *Magnetospirillum* sp., *Candidatus* Halomonas phosphatis, *Turneriella parva*	*Microcystis* sp., *Sphingopyxis* sp. and *Paracoccus* sp.
			highest metabolic potential in terms of energy production and conversion and defense mechanism	

Keywords Microbial fuel cell · Anode modification · Reduced graphene oxide · Iron · Microbiome · Metabolic potential

Introduction

Microbial fuel cells (MFCs) continue to be of great interest to scientists as an environmentally friendly technology for wastewater treatment and biodegradation while simultaneously generating electricity. The environmental aspect is the main factor contributing to the popularity of this technology; however, the power output remains low with increasing reactor size, which limits the transfer of this technology to a large scale (Tabassum et al. 2021). The insufficient charge transport capacity and high internal resistance have led scientists to attempt to improve the kinetics of the reactions occurring at the anode by developing better electrode materials (Banerjee et al. 2022).

Anode electrodes should have a large specific surface area, roughness, and biocompatibility to allow better bacteria to colonize the anode (Nosek et al. 2020). To achieve these properties, carbon nanomaterials have been used to modify electrodes, due to their good electrical properties (Ni and Li 2016). Graphene (G) is one such material, and it offers several advantages over graphite: it has higher durability, a two-dimensional molecule structure, and better electrical properties. G is considered the thinnest material with a unique combination of properties that offer potential applications for future technology development (Wu et al. 2007). The range of measured values for the single-layer thickness

of G was between 0.4 and 1.7 nm (Shearer et al. 2016). The particular form of G that is more commonly used in MFCs is reduced graphene oxide (rGO). rGO sheets are obtained by thermal, hydrothermal, or chemical reduction in GO, and rGO has a good electrical conductivity value of 6000 S/cm (Du et al. 2008).

Recently, attempts have been made to further improve MFC by combining carbon nanomaterials, e.g., rGO, with metal oxide nanoparticles. Metal oxide nanomaterials are advantageous due to their excellent structural dynamics, large surface area, porosity environmental friendliness, non-toxicity, and availability (Aiswaria et al. 2022). They have unpaired *d*-orbital electrons in their structure, which enables good electrochemical catalytic activity in MFC (Dessie and Tandesse 2021). Most current research on the use of rGO in combination with metal oxides in MFC is mainly concerned with the effects of electrode modifications often using pure bacterial cultures, e.g., *Rhodobacter sphaeroides* spp. (Islam et al. 2020) or *Shewanella oneidensis* MR-1 (Li et al. 2018). Studies with pure cultures are useful to identify the mechanisms involved in the process. Still, they are impractical for large-scale processes due to the higher cost of maintaining this culture in reactors. A small amount of research has focused on microbiological analysis of mixed biofilms formed on anodes modified with G compounds. The selection of technological parameters for MFC operation,

such as the type of substrate (Gezginci and Uysal 2016) or organic load (Nosek and Cydzik-Kwiatkowska 2019), the method of modifying the anode surface (Xiao et al. 2020), allows to shape the microbial community and stimulate the development of specific microorganisms. Knowing the species responsible for energy production allows the use of bio-augmentation to accelerate the development of the biofilm and the stable operation of the MFC.

Bioelectrochemical systems can be used as a good technology for decolorization and wastewater treatment (Kong et al. 2022). The use of municipal wastewater or landfill leachate in MFC has a twofold advantage. First, the wastewater is purified, reducing organic carbon to a large extent, and second, electricity is generated with low CO_2 production. This energy can be used in the future, for example, to aerate the biological basins or to light the operational buildings of the treatment plant. Therefore, it makes sense to fulfill the assumptions of the circular economy and to use waste materials as a valuable energy source.

Table 1SM (Supplementary Materials) presents the results of the research on anode modification using rGO. To date, most research has focused on the electrochemical aspects of the MFC itself, i.e., the deposition of rGO and nanoparticles on the electrode and the electrical behavior of the modified electrode. Many studies have concluded that electrode modification with rGO increases current response and charge storage capacity, reduces charge transfer resistance, and that higher open-circuit potentials indicate higher electrogenic activity and reaction rates at the anode (Pareek et al. 2019). In addition, Shao et al. (2010) reported that rGO exhibits exceptionally high electrochemical capacitance and cyclic stability, far exceeding that of carbon nanotubes. However, the information on the electrochemical behavior of modified anodes alone may prove to be insufficient in the future. Knowledge of the species composition of the anode biofilms is also an important aspect of MFC operation to identify the species that are directly and indirectly responsible for the current generation and that contribute to substrate decomposition. To the authors' knowledge, no molecular studies have been performed in MFC with anodes modified with iron oxide and rGO and inhabited by a mixed microbial community fed with wastewater. Therefore, the objective of the present study was not merely to verify the effect of modification of carbon felt with rGO in combination with iron (III) on electricity generation, but, most importantly, to describe the species composition of the anode biofilm, which is the main factor in energy generation in MFCs. Our research has shown that anode modification with rGO alone can lead to voltage reversal, which is not common in single MFCs, and that the presence of iron helps to overcome this phenomenon. An additional novel aspect of this study was the use of Phylogenetic Investigation of Communities by Reconstruction of Unobserved States (PICRUSt) analysis

based on the Kyoto Encyclopedia of Genes and Genomes (KEGG) database to predict the potential metabolic functions of anodic biofilm in the presence of rGO and iron (III). Metabolic functions in MFCs have not been widely discussed in the literature so far, and understanding the potential metabolic pathways in which organic compounds are removed and energy is produced is an important element in adapting MFCs to various types of substrates to use this technology most effectively in the future.

Materials and Methods

Experimental set-up

The dual-chamber MFCs were constructed using Plexiglas. The anode and cathode chambers had a volume of 2L each. An 8×8 cm Nafion 117 proton-exchange membrane (PEM) from Dupont was utilized as the separator between the chambers. Before inserting the membranes into the MFCs, they underwent a preparation process. The steps involved were as follows: soaking in acetone for 15 min to remove impurities, rinsing with distilled water to eliminate residual acetone, soaking in 1 M HCl for 30 min to further clean the membranes, rinsing with distilled water to remove any traces of acid. To prevent membrane clogging, a weekly cleaning procedure was performed: soaking in 1 M HCl, and rinsing with distilled water to ensure the removal of acid residues (Nosek and Cydzik-Kwiatkowska 2019).

Anodes preparation

The anodes made of carbon felt (CF) $(10 \times 20 \times 0.3$ cm) were connected to a stainless steel wire. Before use, the CF was subjected to treatment in an ultrasonic bath (InterSonic, 15 min) to remove impurities. An MFC with an unmodified anode was used as a control (MFC-control). rGO was electrodeposited on a CF electrode under oxygen-free conditions (the absence of oxygen ensured by using argon bubbles). The process involved 15 voltammetry cycles between -1.5 and 0.8 V versus an Ag/AgCl electrode (3 M) with a scan rate of 50 mV/s. The choice of the minimum potential of -1.5 V for the simultaneous reduction electrodeposition process aimed to maximize the reduction in the oxygen-based groups while minimizing the damage to the deposited rGO film due to hydrogen evolution. The CF was used as the working electrode (WE), while a platinized titanium mesh (10 cm $\times$ 15 cm, Goodfellow, UK) served as the counter electrode (CE). The electrolyte solution consisted of an aqueous solution containing 150 mM NaCl and 0.5 mg/mL rGO (Sigma-Aldrich). Subsequently, electrochemical deposition of iron on the rGO/CF samples was performed using an electrolytic bath containing the following components:

FeSO$_4$·7H$_2$O (99% purity, Sigma-Aldrich)—240 g/L; NaCl ($\geq$ 99.5%, Sigma-Aldrich)—40 g/L. The deposition process was carried out at a cathodic current density of 1 mA/cm^2 at room temperature for 2 and 4 min, resulting in a corresponding catalyst deposition of about 34 (rGO-Fe34) and 68 mg (rGO-Fe68), respectively.

MFCs inoculation and operation

The anode chambers were inoculated with 100 mL of a 1:1 (v/v) mixture of digested sludge from the municipal wastewater treatment plant in Olsztyn (Poland). The MFCs were fed with synthetic medium containing 4 g/L K$_2$HPO$_4$, 3.4 g/L KH$_2$PO$_4$, 0.15 g/L NH$_4$Cl, 0.1 g/L NaCl, 0.13 g/L KCl, 0.1 g/L MgSO$_4$·7H$_2$O, and sodium acetate as a carbon source in the amount of 200 mg COD/L (0.3 g/L CH$_3$COONa). The anode chamber was sealed to prevent access to air, and the chamber contents were mixed at a speed of 100 rpm. The cathode chamber was aerated with an air diffuser (20 mL/min). As a catholyte, phosphate buffer was used (4 g/L KH$_2$PO$_4$ and 3.4 g/L K$_2$HPO$_4$ in distilled water), which was replaced once a week. Initially, the MFCs were left in an open circuit for one day to allow the biomass to adapt to the environmental conditions in the MFCs and to support microbial colonization of the electrodes (Lobato et al. 2012). Following this period, the MFCs were operated with an external resistance of 1000 Ω, a value determined based on preliminary experiments conducted by Nosek and Cydzik-Kwiatkowska (2022). The MFCs were operated in cycles lasting 120 h, after which 300 mL of the anode chamber volume was replaced. The experiment was conducted for 40 days. During this time, in the effluent, chemical oxygen demand (COD), ammonium nitrogen (NH$_4$-N), and volatile fatty acids (VFAs) were measured according to APHA (2012). pH and alkalinity were measured using a TitroLine instrument (Donserv). In the MFC effluents from the 5th, 8th, and 10th cycles, nitrite and nitrate were measured using cuvette tests (Hach Lange, Germany).

Electrochemical analyses

The polarization and power curves were determined using a True-RMS multimeter (the external resistance of the cell varied in the range of 75–7200 Ω) according to Watson and Logan (2011). Voltage readings were recorded at one-minute intervals using a data acquisition device (6600 Counts PC-LINK). The current flowing through the cell was calculated using Ohm's law based on the external resistance. Cyclic voltammetry (CV) measurements were conducted using a three-electrode system. The working electrode was the anode, accompanied by a platinum counter electrode and an Ag/AgCl reference electrode with a constant potential of 0.197 mV (Gammry Instrument Interface 1010E). The

CV experiments were performed at a scan rate of 20 mV/s. Electrochemical impedance spectroscopy (EIS) was performed in a three-electrode system as described above (anode as a working electrode), in the frequency range of 10^6—0.1 Hz with an AC signal of 10 mV amplitude, in the DC range of 400–900 mV. The electrochemical behavior of the biofilm-anode system was tested in the 9th cycle of stable phase MFC operation with the catholyte present in the cathode chamber. All experiments were performed at room temperature.

To characterize the surfaces of pure CF after sonication in the ultrasound batch and CFs modified with rGO and rGO-Fe, a Quanta FEG 250 Scanning Electron Microscope (SEM/EDX, Quanta FEG 250, FEI) was applied. To identify the presence of rGO on the electrode, the Fourier transform infrared spectroscopy (FTIR) spectrometer IRSpirit-T (Shimadzu) equipped with an attenuated total reflection (ATR-FTIR) diamond crystal was used. The measurements were performed with a resolution of 4 cm^{-1} in wavenumber ranges from 4000 to 400 cm^{-1}.

Molecular analyses

For genomic DNA extraction, 100 μg of inoculum and biomass were processed from the anode surface using a FastDNA SPIN Kit for Soil (MP Biomedicals). Samples were collected from the anode surface during the 10th, 20th, and 30th days of the experiment. After DNA extraction, the purity and concentration of the obtained DNA samples were determined using a NanoDrop spectrometer (Thermo Scientific). For DNA amplification, a 515F/806R primer set (5'-GTGCCAGCMGCCGCGGTAA-3'/5'-GGACTACHVGGG TWTCTAAT-3') was used targeting the V4 region of bacterial and archaeal 16S rDNA genes (Caporaso et al. 2011). Amplicons were sequenced (the MiSeq platform, Illumina) in the Research and Testing Laboratory (USA). Reads were analyzed as described in Świątczak and Cydzik-Kwiatkowska (2018) and deposited in the NCBI Sequence Read Archive (BioProject PRJNA978387). The pipelines of the PICRUSt program were used to predict metagenomics information on microbial metabolic function using the KEGG and the Cluster of Orthologous Groups (COG) databases (Douglas et al. 2020).

Statistical analysis

The results from each MFC's last 5 cycles of operation were analyzed statistically ($p < 0.05$ considered significant, Statistica 13.3, StatSoft) using one-way analysis of variance (ANOVA), followed by Tukey's test (HSD). MicrobiomeAnalyst (Chong et al. 2020) was used for metagenomic and statistical analysis of microbiome data ($p < 0.05$). To account for the potential importance of low-abundance

bacteria within complex microbial communities, diversity indices were calculated without normalizing for the number of reads, following the approach described by McMurdie and Holmes (2014).

Results and discussion

Fe and rGO deposition

SEM analysis is used both to analyze the surface of materials and to characterize single cells of microorganisms (Ren et al. 2023). The SEM/EDS analysis showed that the iron was successfully deposited on the electrodes, which was also confirmed by mapping the iron on the carbon fibers. As a result of the iron deposition, the surface roughness of the electrode has increased. The presence of sulfur on the carbon fibers (Fig. 1) was due to the use of ferrous sulfate (III) as a modifier and oxygen from both ferrous sulfate (III) and rGO. Since it was difficult to determine the presence of rGO on the CF in the EDS analysis, FTIR spectra were used to identify the presence of rGO on the electrode (Fig. 1SM). The peak around 1600 cm^{-1} was caused by the graphite domain, confirming the presence of the sp^2 carbon structure in rGO (Krishnamoorthy et al. 2013). This peak was not observed at pure CF and only occurred for rGO and CF-rGO. A peak at 1250 cm^{-1} was also noticeable, indicating the presence

of C-O and C–OH groups, which confirms the deposition of rGO (Zhou et al. 2019).

COD and ammonia removal

The initial concentration of COD in the reactors was about 180 mg/L. The average COD concentrations in the reactor effluent were 90.1 ± 29.6, 61.8 ± 9.5, 77 ± 19.9, 70.3 ± 14.5 mg COD/L in MFC-control, MFC-rGO, MFC-rGO-Fe34, and MFC-rGO-Fe68, respectively; the differences were not significant. The mean COD removal efficiencies were $49.9 \pm 16.5\%$, $65.6 \pm 5.4\%$, $56.9 \pm 11.1\%$, and $60.9 \pm 8.1\%$, respectively. Zheng et al. (2022) report that the efficiency of COD removal with the addition of iron oxide directly into the anode chamber in the amount of 0.0, 4.5, 9.0, and 18.0 g Fe$_3$O$_4$/L was $85.8 \pm 2.8\%$, $95.0 \pm 2.1\%$, $92.8 \pm 2.4\%$ and $84.8\% \pm 4.0\%$, respectively, within a cycle lasting approximately 10 days. Wang et al. (2020) indicated that modification of carbon cloth anode using polyelectrolytes/α-Fe$_2$O$_3$ resulted in COD removal efficiency of 67–69% within 5 days. Mohamed et al. (2021) investigated the modification of CF anode using tungsten carbide and rGO. Despite the modifications, they did not notice any improvement in COD removal, but the efficiency was about 70% for all tested CF, electrodes. In our previous study, COD removal was greater than 70%, and the average COD removal efficiency decreased with the iron dose at the anode (Nosek et al. 2023). COD removal was lower in this
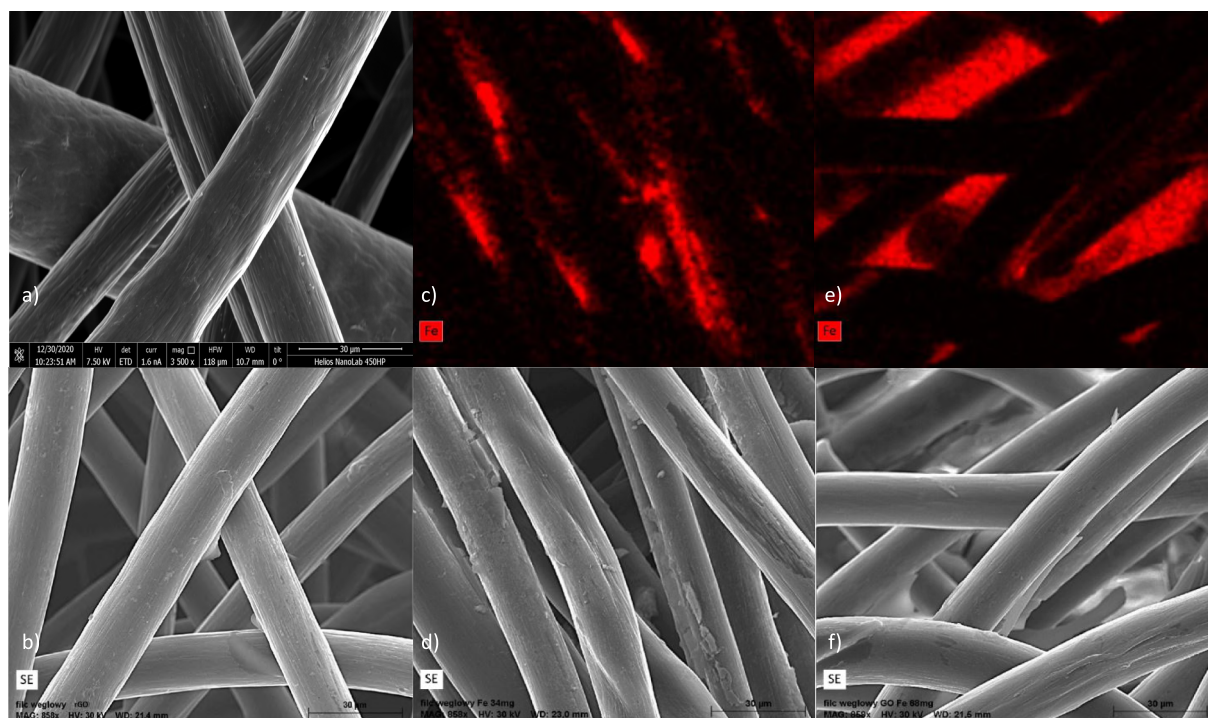
Fig. 1 SEM/EDS analyses of anodes' surfaces **a** pristine, **b** with rGO, **c** and **d** with rGO and 34 mg Fe, **e** and **f** with rGO and 68 mg Fe

study, possibly due to the longer cycle time that favored cell lysis (Wang et al. 2016).

The average concentration of ammonia in raw wastewater was 25.3 ± 2.3 mg/L. The ammonia removal efficiency was similar in all reactors (61–65%). MFC effluents were analyzed for the presence of nitrates and nitrites. Nitrate concentrations in the effluents did not differ between reactors and averaged 1.8 ± 1.2, 3.4 ± 1.1, 1.4 ± 1.5, and 2.01 ± 1.2 mg/L in MFC-control, MFC-rGO, MFC-rGO-Fe34, and MFC-rGO-Fe68, respectively. On the other hand, the highest average nitrate concentration was obtained in MFC-rGO-Fe34 (2.04 ± 2.09 mg/L). The MFCs were operated under anaerobic conditions, but some oxygen may have diffused from the cathode chamber. This oxygen can be used for both ammonium and organic matter oxidation. Liu and Logan (2004) reported that diffusion of oxygen through a Nafion membrane to a concentration of 0.05 mg/L may be responsible for the aerobic loss of 28% of 600 mg/L glucose added after 100 h of reactor operation.

Electricity generation

All tested reactors generated voltage from the first cycle of operation. The voltage fluctuations were lowest in MFC-rGO, but the voltage regularly reversed at the beginning of the cycle after the substrate change (Fig. 2b). After about 5 h of the cycle, the voltage started to increase, and after 20–25 h of the cycle, it was positive (+) again. The reversal voltage was observed in MFC with carbon nitride nanoparticles, G, and carbon nanotubes deposited on anodes; the cathode chambers were not aerated (Attia et al. 2022). Katuri et al. (2011) explained the lack of energy production during the first 60–80 h of their study by the fact that the greater part of the reducing equivalents from glucose oxidation were used for biosynthesis and biomass growth, while the remainder was used for power generation.

The voltage reversal in our study was due to an increase in the anode potential. Initially, the anode potential was -0.196 V; then it increased to a maximum value of 0.404 V—while the anode potential decreased, the cell voltage increased. In the stable phase of the cycle (plateaued voltage), the anode potential was -0.304 V. Solutes from chemical reactions and biological activity, as well as microbial attachments, can contaminate the membrane and interfere with proton transfer. Substrate flow into the cathodic chamber can reduce cathodic efficiency by lowering the potential below the thermodynamically predicted value (Rismani-Yazdi et al. 2008).

The nitrate concentrations in the MFC-rGO were higher than those in the other MFCs; thus, they might have affected the negative potentials of the cell. Marks et al. (2019) reported that the electrical output of an MFC was almost
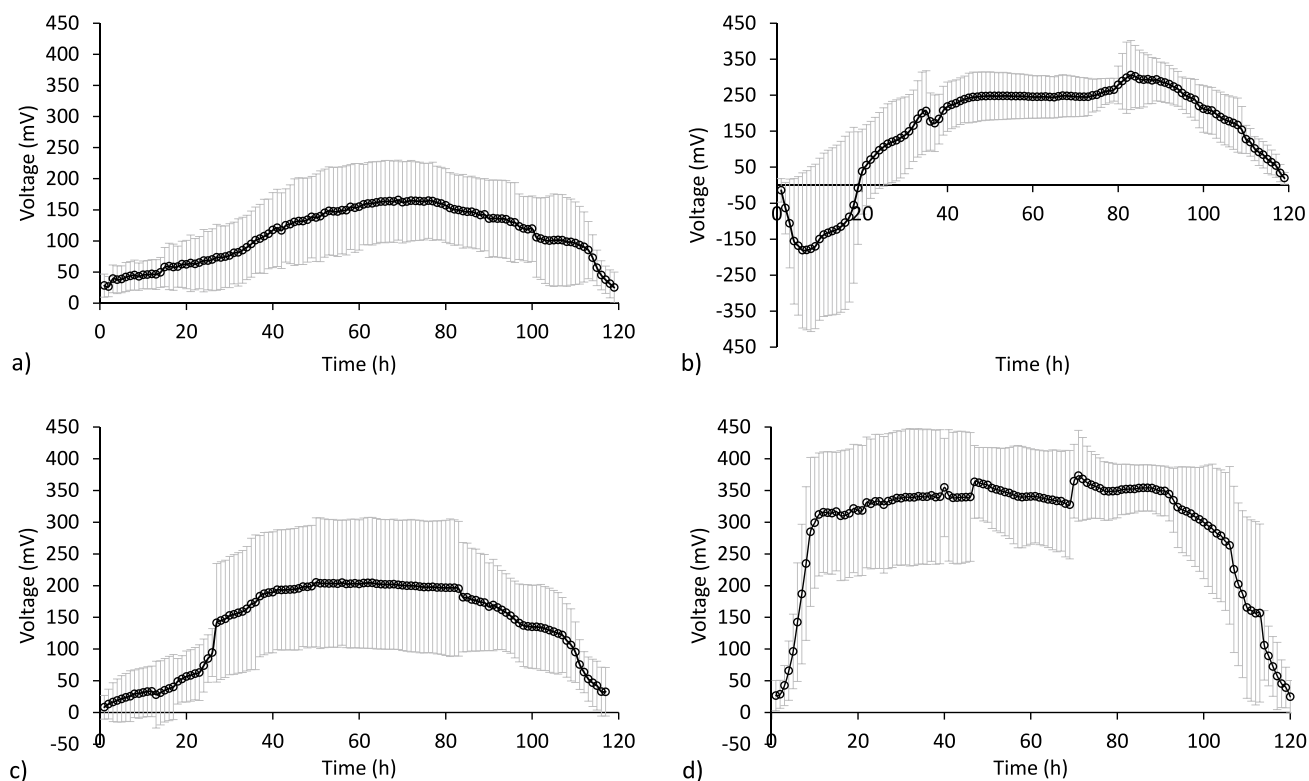
Fig. 2 Averaged voltages from the last 5 cycles (n = 5) for **a** MFC-control, **b** MFC-rGO, **c** MFC-rGO-Fe34, **d** MFC-rGO-Fe68

unchanged when the incoming nitrate concentration was below 0.9 mg/L. However, when nitrates were administered, limitations in mass transfer occurred, resulting from competition between electrogenic microorganisms and denitrifiers for the same substrate.

Our results suggest that the presence of Fe on the anode helps to overcome the voltage reversals observed when only rGO is used. The reversal voltage problem is not common in single MFCs, so this issue should be explored more deeply in future research. However, in our study, regular voltage reversal was only visible in MFC-rGO, while it did not occur in reactors with an anode modified with rGO-Fe, indicating a positive effect of iron on power generation in MFC. Studies prove that the deposition of FeO on the anode increases surface area and improves the conductivity of the CF electrode, and consequently, the effect of catalytic oxidation of the substrate (Yang et al. 2021). Fe(III) has a high affinity for c-type cytochromes (OmcA and MtrC) (Beliaev et al. 2001), resulting in increased electron transfer, which is why it is often used as a modifier in MFC circuits.

The best energy generation results were obtained when both rGO and Fe were used at the highest dose, indicating the validity of the proposed carbon anode modification. In MFC-rGO-Fe68, the voltages in the stable phase of the cycle (17 to 105 h) ranged from 250 to 445 mV, with an average of 342.7 ± 72.8 mV (Fig. 2d); these values were significantly higher than those in the other MFCs (Fig. 2SM). Fu et al. (2020) investigated anode modification of CF with GO and Fe_2O_3 in an MFC with anaerobically fermented biomass sludge and glucose as the carbon source. MFC with anode modified with GO and Fe_2O_3 achieved a maximum stable voltage of 590 ± 5 mV, while MFCs with GO-CF and CF exhibited maximum stable voltages of 555 ± 6 mV and 490 ± 6 mV, respectively. Ma et al. (2020) found that the incorporation of Fe_3O_4 nanospheres into rGO anodes increases their bio affinity, resulting in accelerated EET performance. Under the same operating conditions, the maximum power output of an MFC with rGO and Fe_3O_4-nanosphere anodes was higher than that of unmodified CP anodes, or anodes only with Fe_3O_4 nanospheres or rGO. The highest power of 8.55 mW/m^2 was obtained in MFC-rGO-Fe68 at a current density of 46.25 mA/m^2 (Fig. 3a). The power density of the MFC-rGO-Fe68 cell was 42.2-, 3.0-, and 7.9-fold higher than
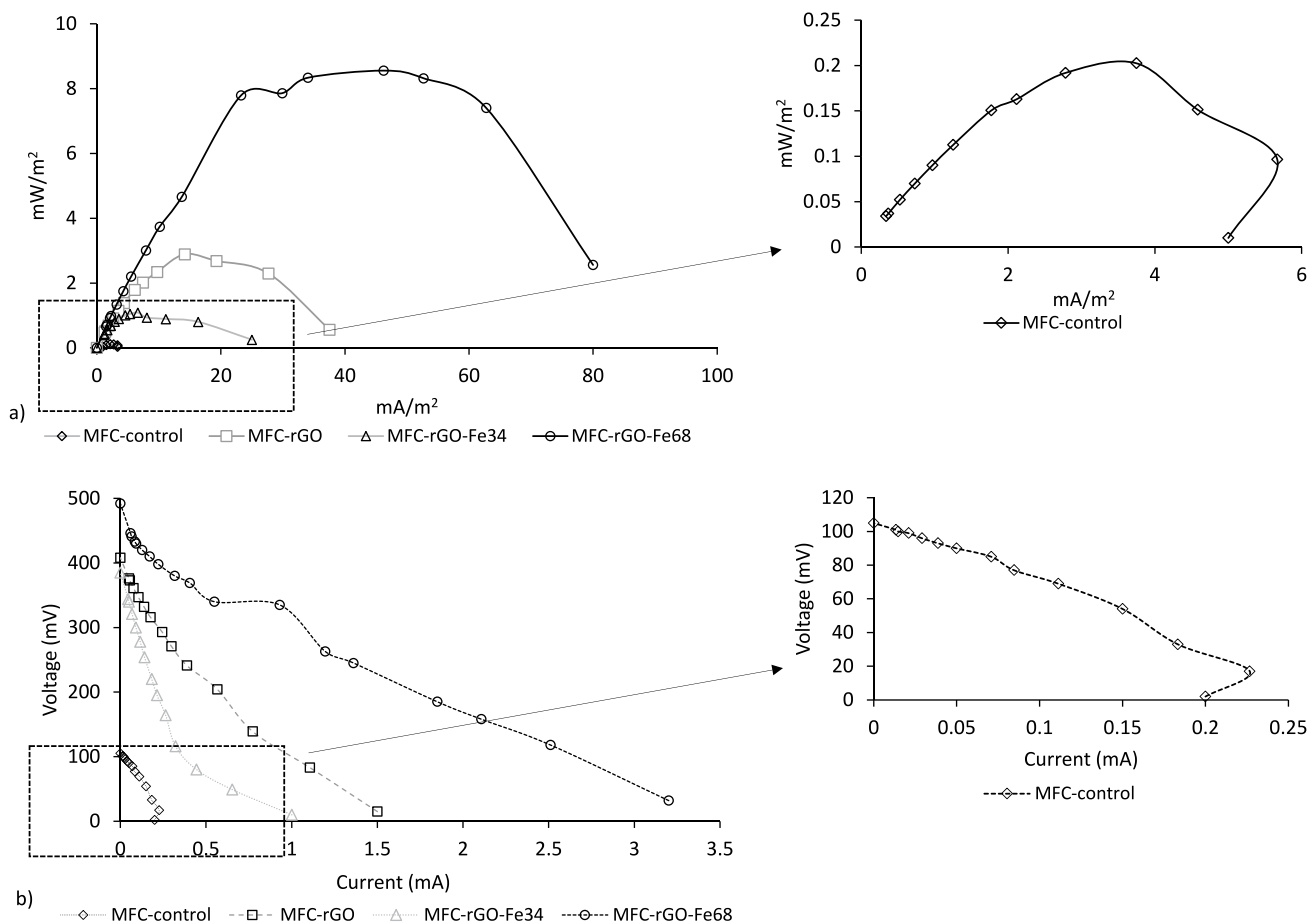
**Fig. 3** Power (**a**) and polarization (**b**) curves for all MFCs

that of the MFC-control, MFC-rGO and MFC-rGO-Fe34, respectively.

Modifying the anodes with rGO and Fe reduced the internal resistance, as calculated from the slope of the polarization curves (Fig. 3b). The internal resistance was 540 Ω in the MFC-control, 260 Ω in the MFC-rGO, 390 Ω in the MFC-rGO-Fe34, and 132 Ω in the MFC-rGO-Fe68 (Fig. 3SM). Although the internal resistance in MFC-rGO-Fe34 was higher than that in MFC-rGO, the value was still lower than that in the control, showing that the modification with rGO and Fe improved the efficiency of electron transfer from the biofilm to the electrodes. The resistance was reduced due to the good electrical conductivity and larger surface area of the deposited rGO and Fe, which improved the interfacial properties with the electrolyte (Chang et al. 2017). Ma et al. (2020) tested different ratios of Fe_3O_4 to rGO on a CP anode. Their study showed that a ratio of 1.5:1 gave the highest power of 3719.9 mW/m^2. Moreover, all tested MFCs with rGO-Fe showed much higher power than anodes with CP alone or with only rGO or Fe. Previous studies indicate that modification of the anode with G increases the specific surface area and electrical conductivity (Lawal 2018), which is due to better electron transfer efficiency, the capacitive properties of the electrode, and more electroactive regions on the anode (Zou et al. 2019).

Electrochemical characterization

CV was used to study the electrochemical behavior of the control and modified electrodes with biofilm in a working solution. Figure 4 shows the cyclic voltammograms of the electrodes in the potential range from −0.50 to 1.35 V versus the saturated calomel electrode (SCE). These measurements were performed at room temperature with a sweep rate of 20 mV/s. After rGO modification, the electrodes exhibited a remarkable increase in current densities compared to the control electrodes, ranging from 66 to 80 mA at 1.35 V. Subsequently, the addition of iron further increased the current densities to 82 and 136 mA at 1.35 V with iron deposits of 34 mg and 68 mg, respectively. Interestingly, the voltammograms of the rGO-Fe64 anode did not show the pronounced cathodic and anodic features associated with the behavior of iron. Except for a small oxidation peak corresponding to iron oxidation, these voltammogram profiles closely resembled those of the control and rGO electrodes within the potential range studied. In contrast, the rGO-Fe34 electrode showed well-defined anodic features (ranging from 0.2 to 0.8 V) related to the process of iron oxidation to Fe(II) and Fe(III). However, the cathodic peaks associated with the reduction in these oxidized species were not apparent. This discrepancy between Fe-modified electrodes may be attributed to higher biofilm formation (assessed based on the DNA recovery from biofilms, data not shown) on the rGO-Fe34 anode,

Fig. 4 CV for anodes with biofilm, using a three-electrode system with anode as a working electrode, with a scanning rate of 20 mV/s
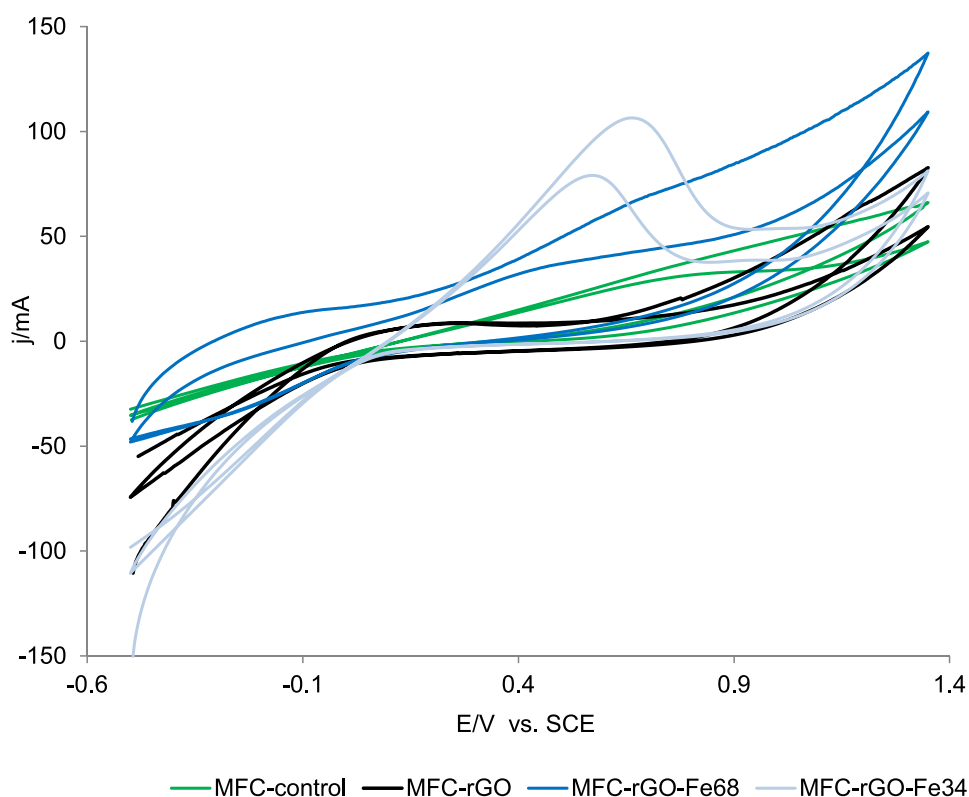
which may lead to greater oxidation of iron on the anode surface. It can be concluded that rGO modification of the electrodes increased current densities, indicating improved electrochemical performance. The addition of iron further increased the current density, (a potential synergistic effect between rGO and iron).

Figure 5 and Table 2SM show the EIS results for all studied electrodes, recorded at different potentials. The impedance response showed single and "depressed" semicircles at all potentials, indicating a one-step charge transfer response within the studied frequency range. Figure 6a shows examples of Nyquist impedance plots recorded at a potential of 900 mV against the Ag/AgCl electrode. The charge transfer resistance (R_{ct}) for the unmodified CF electrode ranged from about 9.0 Ω to about 7.7 Ω across the potentials studied. Modification of the electrode resulted in an overall decrease in charge transfer resistance, by about 1.2 times for the rGO electrode, 1.5 times for the rGO-Fe34 electrode, and 2 times for the rGO-Fe68 electrode at a working potential of 900 mV compared to the control electrode. These results are in agreement with the results of the CV experiments, where the electrode modification also improved the kinetics of the studied process.

In the MFC-control, the values recorded for the double-layer capacitance (C_{dl}) decreased from 263 µF at 400 mV to 88 µF at 900 mV. However, electrode modification caused a significant increase in the C_{dl} parameter for the rGO electrode compared to the CF electrode. Nevertheless, it also decreased with increasing potential, ranging from 420 µF at 500 mV to 95 µF at 900 mV. The deposition of iron caused a slight increase in the C_{dl} values compared to the MFC-rGO, but they were still 2.5× and 4.6× larger for a potential of 400 mV than those observed for the unmodified electrode.

The decrease in R_{ct} indicates improved electron transfer kinetics, while the increase in capacitance suggests an improved electrode–electrolyte interface for charge storage. These results highlight the potential of rGO and iron deposition as effective strategies to improve the electrochemical performance of MFCs. Further investigations could focus on optimizing the electrode modification process to achieve even better performance in terms of charge transfer and capacitance values.

Microbial structure and metabolism

After sequencing, a total of 1,045,303 reads were obtained; the number of reads for a single sample ranged from 63,651 to 93,660. Rarefaction curves showed that the sequencing depth was sufficient (data not shown). The number of OTUs for the tested samples ranged from 185 to 246 (Table 3SM). In comparison, the average number of OTUs for rGO-modified anode biofilms in a single-chamber glucose-fed MFC was approximately 7,539 (Rani and Kumar 2021). In our research, the lowest number of OTUs was recorded in the sludge used as inoculum and coming from a methane fermentation reactor operated on a technical scale. During the operation of the reactors, the number of OTUs increased to over 200 in all analyzed samples, which indicates that the community was enriched with new species after inoculation. The lower number of identified OTUs in our research can be
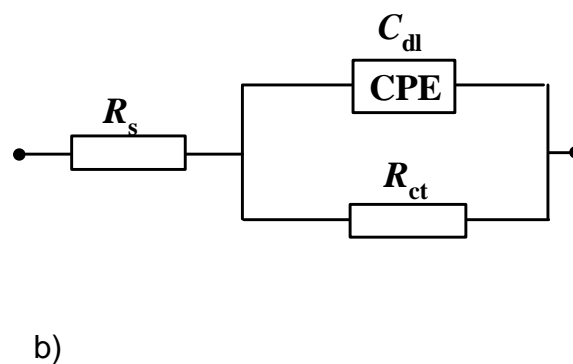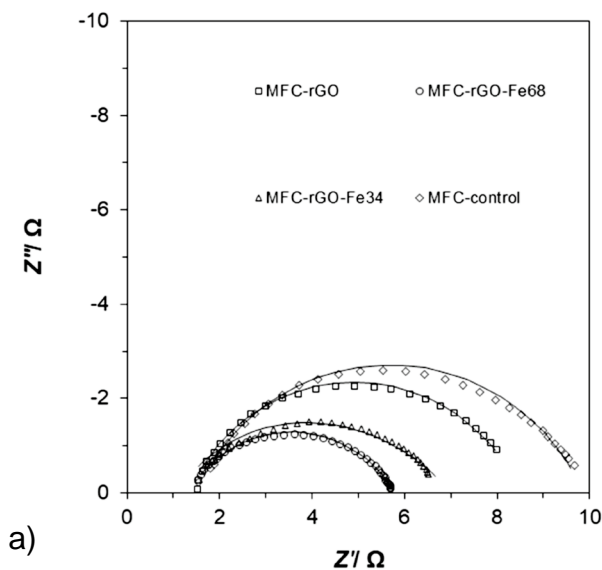
Fig. 5 a EIS plots recorded for the electrochemical behavior of all tested MFCs for a potential of 900 mV; **b** Equivalent circuit used to fit the impedance data, where Rct is the charge transfer resistance, and Cdl is the double-layer capacitance (capacitance parameter is CPE: constant phase element—modified), jointly in series with an uncompensated solution resistance, RS (the solid lines correspond to the representation of the data according to the equivalent circuit)
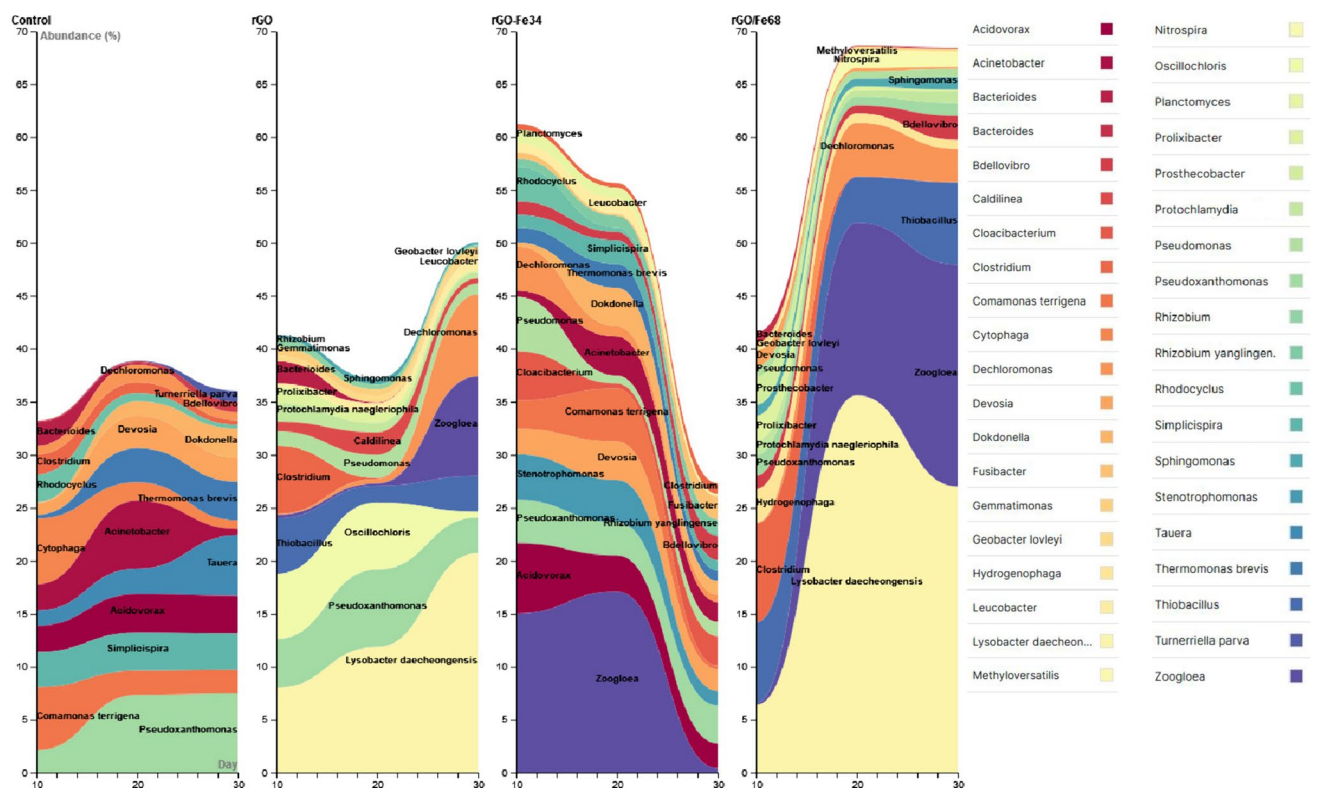
Fig. 6 Structure of the microbial community of different anode biofilms at the genus level, only genera with abundance > 1% in one of the MFC were analyzed

explained by the presence of many unclassified microorganisms in the conditions of dosing a complex substrate, which is municipal wastewater.

The Shannon index was slightly higher in all MFCs during the initial phase of operation relative to the inoculum, indicating that the microorganisms in the biomass were competing with each other. As the operation of the cells stabilized, the Shannon index values gradually decreased and reached values of 2.9–3.8 depending on the reactor, suggesting that the best-adapted microorganisms survived in the biofilm. The research showed that modification of the anode with iron oxides and rGO reduced the biodiversity of microorganisms in the anode biofilm. Statistical analysis showed significantly higher bacterial diversity in the MFC-control than in the MFC-rGO-Fe68, which may be due to the dominance of *Lysobacter daecheongensis* and *Zooglea* sp. in MFC-rGO-Fe68 during the experiment.

Proteobacteria predominated species in all samples (Fig. 4SM). Their percentage increased from 14.8% in the inoculum to 74.0% in the andic biofilm in MFC-rGO-Fe68 (day 30). The dominant classes were β-Proteobacteria and ϒ-Proteobacteria. Most of the known exoelectrogens belong to Proteobacteria, e.g., *Geobacter* sp*., Dechloromonas* sp*., Desulfovibrio* sp., and tend to be dominant in MFC anode biofilms (Xu et al. 2019). MFC-rGo-Fe68 (day 30) had the

highest proportion of *Verrucomicrobia* capable of oxidizing methane in association with the reduction of nitrates, nitrites, iron, manganese, sulfates, or humic substances as final electron acceptors (Guerrero-Cruz et al. 2021).

The best conditions for the development of Bacteroidetes were in MFC-rGO-Fe34; the percent abundance of this phylum reached 47.7% at the end of the study. Their number was not high in the reactors with anodes modified with rGO or rGO and iron at the highest dose, indicating these microbes' preferences regarding the concentration of iron (III) in the environment. Li et al. (2020), reported that in MFCs where zero-valent iron (Fe^0) was dosed, the abundance of this group was the highest with 0.1 g of Fe^0 and decreased as the dose was increased to 1 g Bacteroidetes. Zhang et al. (2021a) investigated the effect of ferric salts on wastewater treatment in an A2O system. In the anaerobic, anoxic, and aerobic zones, increasing the iron dose from 0 to 40 mg/L decreased the respective abundances of Bacteroidetes from 11.8% to 9.5%, 12.6% to 10.2%, and 10.9% to 9.9%. At the beginning of our experiment, the proportion of Bacteroidetes was similar in both reactors with an anode modified with rGO-Fe (approx. 15%). The order *Sphingobacteriales*, which belongs to the Bacteroidetes, could not be detected in MFC-rGO-Fe68 from the beginning, while in MFC-rGO-Fe34, unclassified bacteria of this order accounted for 31.6%

of all bacteria at the end of the experiment. Sun et al. (2023) reported that the presence of Fe ions has a positive effect on the growth of *Sphingobacteriales* and production EPS, but our study indicates that the higher dose of iron reduces their growth, which should be further investigated.

In our study, Firmicutes were an indicator of dynamic species changes in the early stages of anode biofilm formation. In the MFC-control, MFC-rGO and MFC-rGO-Fe68 Firmicutes accounted for 5.5, 9.2, and 11.2% of the community in the early stages, but their numbers decreased with time. Their important role in the biofilm formation phase may be due to their involvement in the hydrolytic processes that take place in the cell start-up phase (Salar-Garcia et al. 2020).

The presence of nitrates in our study resulted from the activity of nitrifying bacteria such as *Nitrosomonas* (0.2–0.6%) or *Nitrospira* (0.01–1.1%), and Anammox bacteria belonging to the Planctomycetes (Guo et al. 2020), whose percentage in MFC ranged from 0.2 to 2.6%. The highest nitrate concentrations were observed in MFC-rGO, where voltage reversal occurred (2.6%, 20th day), and the presence of nitrates led to competition for electrons between nitrates and the electrode (Marks et al. 2019). Once nitrates are depleted, denitrifying microorganisms use an anode as an electron acceptor (Sangchareon et al. 2015). Yang et al. (2023) tested electroactive nitrifying/denitrifying bacteria in a single-chamber MFC with an air cathode. The results showed disturbances in the output current due to short-term dosing of nitrates. A repeatable increase in current up to 0.76 A/m^3 was obtained when the cell was operated for extended periods in the presence of nitrates. The rapid decrease in COD with short-term nitrate addition confirmed competition for electron donors for heterotrophic denitrification. An increase in current and detection of nitrites without a concomitant decrease in COD indicate electroactive anodic nitrification. *Pseudoxanthomonas* sp., *Thauera* sp., and *Pseudomonas* sp. were enriched in the biofilm. Mixotrophic denitrification and electroactive anodic nitrification enabled energy recovery with high pollutant removal efficiency.

The most numerous bacteria in MFC-rGO and MFC-rGO-Fe68 was *Lysobacter daecheongensis* (Fig. 6), which accounted for 20.71% and 27.02%, respectively, at the end of the study. *Lysobacter* sp. are facultative autotrophic denitrifiers (Ding et al. 2019) and were detected in an anode biofilm in MFC in the presence of nitrates (Zhang et al. 2021b). *Acidovorax* sp. has been identified as an important electroactive denitrifier in MFC systems (Guo et al. 2020). In our study, *Acidovorax* sp. was abundant only in the MFC-control (2.48–3.62%) and MFC-rGO-Fe34 (2.33–6.65%). Their levels in MFC-rGO-68 ranged from 0.21–0.63%, indicating low tolerance to the presence of iron in the environment. Heterotrophic growth of *Acidovorax* sp. can be explained by the presence of O$_2$

entering from the cathode chamber or by the presence of nitrates produced by nitrifying bacteria (Park et al. 2017). *Pseudoxanthomonas* sp. was also sensitive to the presence of iron on the modified anode. In the MFC-control, *Pseudoxanthomonas* sp. accounted for over 7% of all identified sequences, whereas with the increase in Fe dose, its abundance in MFC-rGO-Fe34 and MFC-rGO-68 decreased to 3.59% and 0.73%, respectively.

EET in bacteria is carried out via polyheme cytochromes and some systems such as the metal reduction pathway (Mtr) in *Shewanella oneidensis*, the porin cytochrome pathway (Pcc) in *Geobacter sulfurreducens*, the metal oxidation pathway (Mto) in *Sideroxydans lithotrophicus*, and the phototrophic iron oxidation pathway (Pio) in *Rhodopseudomonas palustris*. Electron transfer across the outer membrane is facilitated by porin, which renders the membrane permeable to cytochromes, which in turn can release electrons through direct contact with extracellular compounds (Edwards et al. 2018).

The abundance of *Dechloromonas* sp. and *Zooglea* sp. were higher in MFCs with modified anodes than in the control. *Dechloromonas* sp. preferred rGO presence only reaching up to 7.73% in biofilm in MFC-rGO at the end of the study, while *Zooglea* sp. was the most abundant in the presence of Fe on the anodes. Both genera have the genomic potential for EET. Two multi-heme cytochromes were identified in *Dechloromonas* sp. one with four and one with eight heme binding sites. In addition, many proteins containing one or two heme cofactors were identified. Potential porins were also present, but none showed much similarity to porins previously described as involved in EET. The presence of homologs of the Mtr pathway in *Dechloromonas aromatica* (Shi et al. 2012) is an evidence that *Dechloromonas* spp. may be capable of EET (Berger et al. 2021). Berger et al. (2021) identified five genes in the *Zoogloea* sp. genome that could be associated with EET. The first gene of the cluster showed 73% amino acid sequence identity with MtrB/PioB, the porin protein that facilitates electron transport across the outer membrane. The second gene is a decaheme cytochrome that shows high similarity to the protein involved in extracellular dimethyl sulfoxide reduction in *Shewanella oneidensis* MR-1.

Comamonas terrigena was mainly present in the biofilm from MFC-control, reaching 5.94% on day 10 of the assay. The strain *Comamonas denitrificans* DX-4 was unable to respire using hydrated Fe(III) oxide, but produced 35 mW/m^2 using acetate as an electron donor in MFC (Xing et al. 2010), which could explain its low abundance on the modified anodes. Studies by Zhao and Kong (2018) have shown that with a very high percentage of *Comamonas* sp. (31.29%) on the anode with active-CF in a two-chamber MFC for the removal of p-nitrophenol, the cell reaches a voltage of 0.7 V. Even a small amount of *Comamonas* sp.

(1.46%) guaranteed efficient power generation in the MFC for oxyfluorfen removal (Zhang et al. 2018).

Devosia sp. produce electricity by autotrophic oxidation of nitrite to nitrate (Zhao et al. 2016) and was observed in all MFCs. *Devosia* sp., transport electrons to electrodes via *c*-type cytochromes on the outer surface, conducting pili, and secreted electron shuttles (Shen et al. 2020). *Geobacter* sp. is the most studied exoelectrogen in MFC and most publications show that the presence of Fe at the anode supports its abundance (Xu et al. 2018; Li et al. 2021). However, the results obtained do not indicate this. The presence of this exoelectrogen in the presence of iron at the anode did not exceed 0.8%. These results are consistent with our previous study, in which *Geobacter* sp. was more abundant in the anode biofilm of the control reactor than in the MFC with Fe_2O_3 on the anode (Nosek et al. 2023). The abundance of methanogens *Methanolinea, Methanosaeta*, and *Methanobacterium* in all anode biofilms was low (< 0.3%).

Generally, excess amounts of metals can be toxic to the microbial environment. Li et al. (2020) reported that the addition of only 0.5 g/L Fe^0 improved voltage generation in the MFC. Higher doses of Fe^0 in the presence of a small amount of oxygen in the anode reactor resulted in gradual oxidation of Fe^0, forming iron oxides deposited on the surface of the Fe^0. The release of excess iron ions had a toxic effect on exoelectrogens and inhibited their activity, consequently showing a rapid decrease in voltage. Our study is important because it confirms the fact that the dose of iron must be adjusted so it does not have a toxic effect on microorganisms.

Statistical correlation between voltage, current and electrical power, and the anode microbiome

Another aspect of the work was to analyze the relationship between the bacteria present in the MFC anode biofilms and the voltage, current, and performance of the cells (Table 4 SM). Only those microorganisms were selected for an analysis whose contribution to the anode microbiome at specific periods was > 0.1%.

Statistical analysis showed that the abundance of *Pseudoxanthomonas* sp., *Stenotrophomonas* sp., and *Thermomonas brevis* positively correlated with energy production in the MFC-control. *Stenotrophomonas* sp. was isolated from a two-chamber MFC that purified wastewater from seafood processing and produced a maximum voltage of 689 mV (Jayashree et al. 2016). *Thermomonas* sp., on the other hand, was able to produce extracellular proteases with high enzyme activity and was one of the most abundant bacteria (6.73%) of the anode biofilm in the MFC with an iron(III) chloride-modified anode (Watanabe, et al. 2011).

The abundance of *Dechloromonas* sp. in biofilm correlated positively with energy production in MFC-rGO. The highest number of bacteria which abundance positively correlated with energy production were identified in MFC-rGO-Fe34. These included *Opitutus* sp., *Fluviicola taffensis*, *Magnetospirillum* sp., *Candidatus* Halomonas phosphatis, *Turneriella parva*, and unclassified *Sphingobacteriales*, whose percentage in this MFC exceeded 31% at the end of the study. The presence of *Magnetospirillum* sp. facilitated power generation by anodic oxidation of the end products produced by fermentative bacteria during the purification of acidic food waste leachate in an MFC inoculated with wastewater and anaerobic sludge (Li et al. 2013).

In MFC-rGO-Fe68, statistical analysis showed that three species correlated with energy production, namely *Microcystis* sp., *Sphingopyxis* sp., and *Paracoccus* sp. *Microcystis* sp. belongs to the freshwater cyanobacteria. Lemos et al. (2021) reported that an increase in pH from 7.8 to 10.5 caused a sixfold increase in the current density of *Microcystis aeruginosa* to 30 mA/m². Previous studies have shown that a positive relationship exists between the presence of *Microcystis* sp. and *Sphingopyxis* sp. Ndayisenga et al. (2021) investigated the effect of microcystin-LRs (MC-LRs) isolated from *Microcystis aeruginosa* with sodium acetate as a co-substrate on energy production in an electroactive biofilm MFC. A sufficient supply of co-substrate (6.0 mM) eliminated the negative effect of MC-LR on the MFC performance; contributed to a 12.7% prolongation over electrical cycles; and produced a power density comparable to the corresponding control (acetate alone) and even 3.8% higher. The proportion of MC-degrading bacteria such as *Sphingopyxis* sp. was increased by up to 1800% at the anode. Jothinathan and Wilson (2018) used *Paracoccus homiensis* strain DRR-3 in MFC with CC, CP, and graphite plate anodes. Current generation was most effective in MFC with CP anode and Nafion 117 as a membrane (0.8 V and 0.12 mA).

Prediction of the potential bacterial function

Based on KEGG (Yuan et al. 2021), the metabolic potential and functions of the anode microbiomes were analyzed using PICRUSt (Fig. 7).

In all MFCs, based on 16S rRNA gene data general metabolism (14–16% of all functions presented) and translation of ribosomal structure and biogenesis (10.9–13.7%) predominated, but were lower relative to the inoculum (14.6%). The highest metabolic potential in terms of energy production and conversion (over 8% on average) and defense mechanism (1%) was observed in MFC-rGO-Fe34. It was significantly higher than the other reactors with modified anodes. MFC-rGO-Fe34 also had the highest replication, recombination, and repair among all MFCs. The obtained data suggest that the modified anode with rGO and a lower iron dose ensures a good metabolic potential of the anode community to cope with unfavorable environmental
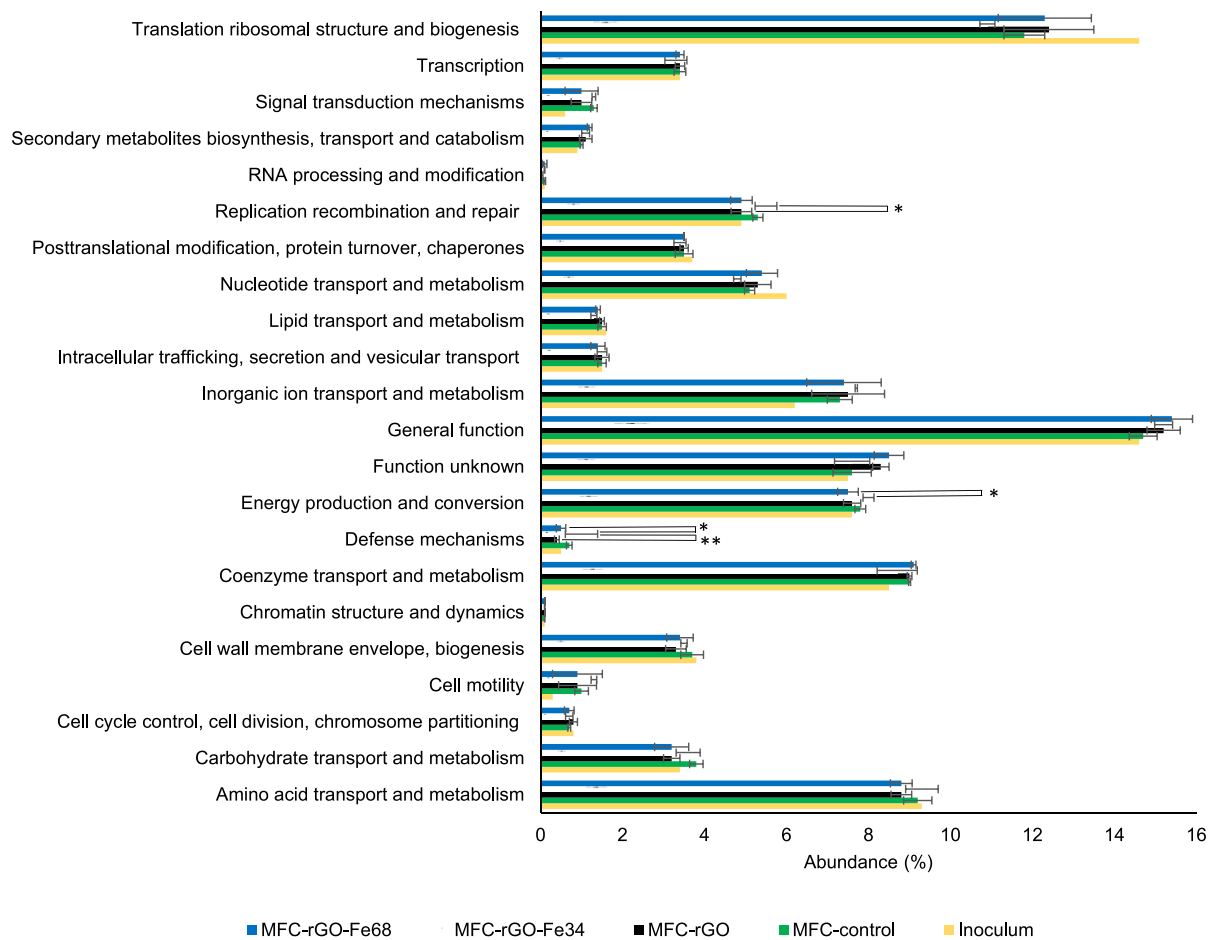
Fig. 7 KEGG metabolic characteristic analysis based on PICRUSt in MFC reactors. Horizontal whiskers represent the standard deviation of the mean of all samples from a particular MFC (n = 3) and "*" indicates a statistically significant difference between the selected reactors

conditions while providing the broadest range of potential metabolic pathways for energy production. The fact that such a range of metabolic pathways was not observed with rGO-Fe68 may indicate greater community specialization under conditions of higher iron presence, which could eliminate some Fe-sensitive microorganisms from the biofilm.

On average, cell motility increased 2.9-fold in all MFCs compared with the inoculum. Cell motility is associated with the presence of flagella and cilia on the bacterial surface. The fact that cell motility increases in the biofilm suggests that cilia and flagella are not primarily used for locomotion. The role of flagella and cilia is related to the adhesion of the biofilm to the anode and electron transfer. To investigate the role of flagella in the electroactive biofilm, Liu et al. (2019) tested *Geobacter sulfurreducens*, a strain without flagella and a strain with flagella. Their studies showed that the flagella-containing strain generated a maximum current density of about 1.24 ± 0.035 mA/cm^2 within 62 h, while the flagella-deficient strain generated only 0.37 ± 0.012 mA/cm^2 within 146 h. To suppress the expression of flagella

in the *Geobacter sulfurreducens* strain, *filC*, which encodes flagellar filament structural protein synthase, was deleted, resulting in the *Geobacter sulfurreducens* KN-$\Delta filC$ strain, which was unable to produce flagella but could produce pili normally. This KN-$\Delta filC$ strain produced a lower maximum current of about 0.91 ± 0.01 mA/cm^2 in 78 h. This means that the presence of flagella increases the thickness of the biofilm and causes an ordered arrangement of extracellular cytochromes. As a result, biofilms with many flagella can generate much more current than biofilms without flagella. The transition of microorganisms from free-floating to sedentary forms usually results in a decrease in target motility potential (Guttenplan and Kearns 2013). The ability to form cilia and flagella is characteristic of many members of the Proteobacteria (Xia et al. 2019) that predominated in anode biofilms in our study.

The metabolic functions with the highest percentage > 1% were also analyzed at KEGG level "ko" to identify individual metabolic pathways. The most developed metabolic pathways in all reactors were those related to amino

acid biosynthesis (ko01230, ca. 10%), carbon metabolism (ko01200, ca. 10%), methane metabolism (ko00680, 7–9%), and purine and pyrimidine metabolism (ko00230, ca. 5% and ko00240, ca. 4%, respectively) (Table 5 SM).

Carbon metabolism consisted mainly of the citrate cycle, carbohydrate glycolysis (Embden-Meyerhof pathway), glycolysis, pyruvate oxidation, and to a lesser extent photorespiration. In contrast, carbon metabolism associated with energy metabolism was based on the reductive citrate cycle (above 4%), the dicarboxylate-hydroxybutyrate cycle (2.5–3.5%), the incomplete reductive citrate cycle (3.5–4.4%), and the reductive pentose phosphate cycle (Calvin cycle, above 1.5%). In the case of the incomplete reductive citrate cycle, it was more pronounced in the control and in MFC-rGO, from which it can be concluded that the presence of iron did not support this metabolic pathway. The study by Feist et al. (2014) showed that the *Geobacter metallireducens* was able to grow in the presence of formate and Fe(III). Examination of the resulting flux distributions revealed that CO_2 from formate oxidation was reduced via a reductive citrate cycle to form acetyl-CoA, which was assimilated into the biomass. Electrons from formate oxidation were split between the reduced citrate cycle and Fe(III) reduction. The *Geobacter metallireducens* GS-15 genome encodes two of the six known carbon fixation pathways, while the pathways that were reconstructed in *Geobacter metallireducens* iAF987 are the reductive citric acid cycle and the dicarboxylate–hydroxybutyrate cycle (Berg et al. 2010). The above studies may suggest that although *Geobacter* sp. was not abundant in anode biofilms in our studies, other bacteria using these pathways may have been able to produce energy like *Geobacter* sp.

Methane metabolism (Ko00680 pathway) was more prevalent in the microbial community from reactors with modified anodes than in the control reactor. Methanogenesis from acetate and CO_2 accounted for the largest proportion (M00567 and M00357, respectively), which together accounted for 5.7–7.04% of the metabolic potential of the communities. Methane production in the MFC is undesirable due to substrate consumption. Analysis of metabolic data revealed that approximately 3% of bacteria can utilize methane as a substrate. The group that could utilize methane includes denitrifying anaerobic methane oxidation bacteria, which produce H^+ and electrons, leading to energy production (Su et al. 2021). *Verrucomicrobia* oxidizes methane under aerobic conditions (Dunfield et al. 2007), but studies by Guerrero-Cruz et al. (2021) show that the metabolic versatility of *Verrucomicrobia* allows them to oxidize methane under anaerobic conditions as well. The percentage of these bacteria reached as high as 6.8% in the anode biofilm in MFC-rGo-Fe68 (20 days). Most likely, methane monooxygenase from the *pmoA* family or canonical methane monooxygenase (Dalcin Martins et al. 2021) are involved in the process. Anaerobic oxidation of methane is combined with the reduction of nitrates, nitrites, iron, manganese, sulfates, and organic electron acceptors (e.g., humic substances) as terminal electron acceptors (Guerrero-Cruz et al. 2021).

The high proportion of metabolic pathways responsible for purine and pyrimidine metabolism (ko00230 and ko00240) can be explained by the fact that they provide the necessary energy and cofactors for microbial survival (Li et al. 2022; Sun et al. 2018) and are also involved in the transport of electrons when the cell is perturbed. Zhu et al. (2022) investigated the effects of electrical signaling disruption by the addition of tetraethylammonium (a potassium channel blocker) on the formation of electroactive biofilms in mixed cultures. Pyrimidine and purine metabolism increased significantly under tetraethylammonium dosing conditions compared to the control reactor.

The presence of rGO correlated with an increase in metabolic potential in terms of general function ($R = 0.58$) and biosynthesis of secondary metabolites, transport, and catabolism ($R = 0.58$). rGO was shown to increase anaerobic biomass activity. This may be because rGO has a much more efficient electron transfer capacity compared to, for example, coenzyme Q (Yin et al. 2015). Increasing the concentration of GO from 62.5 mg/L to 500 mg/L resulted in a decrease in proteins involved in lipid metabolism, coenzyme transport and metabolism, nucleotide transport, and metabolism in *Fusarium graminearum* (Wang et al. 2019). rGO promotes biofilm formation by modulating EPS secretion through transcriptional regulation and physical interactions—the presence of rGO resulted in the upregulation of genes involved in EPS production in *Citrifermentes bremense* (Meng et al. 2022). Guo et al. (2017) tested the effects of GO and rGO on the formation and development of biofilms in Luria–Bertani (LB) medium using *Escherichia coli* and *Staphylococcus aureus* as model organisms. rGO (≥ 50 mg/L) strongly inhibited cell growth and biofilm formation. However, the inhibitory effect of rGO (50 mg/L and 100 mg/L) was attenuated in the maturation phase (> 24 h) and abolished after 48 h. The level of reactive oxygen species (ROS) in the biofilm was significantly increased by rGO in the early phase, while it decreased to the same level as in the control in the mature phase, suggesting that oxidative stress contributed to the inhibitory effect of rGO on the bacterial biofilm. Therefore, it is possible that under stress conditions induced by the presence of rGO, the production of EPS increases the longer the biofilm is exposed to the material. In our study, the biofilm was well developed, especially on the modified electrodes, with a noticeable EPS layer. (Fig. 5SM). However, this issue should be further investigated in the future.

The prospect for future development of MFC technology in terms of anode modification

MFCs are still under development and many important challenges remain to be explored. Conventional carbon-based materials used to make electrodes can be improved by surface modification with advanced nanomaterials. However, this entails high costs and complicated modification processes. In this context, the electrochemical deposition of rGO and affordable iron(III) sulfate performed in this study seems to be a cheap and simple method of electrodeposition. Factors such as the presence of oxygen in the anode chamber, high nitrate content, membrane contamination associated with low cathodic efficiency, or mass transfer limitations may lead to reduced MFC performance or even voltage reversal phenomena. Our research also shows that the choice of modifying factors plays an important role when using modified anodes. Therefore, future research should take these factors into account and constantly monitor the operating conditions of the cell, with attention to the sealing of the reactor, the possible occurrence of oxidized forms of nitrogen, and regular cleaning of the membrane to avoid voltage reversal. rGO enables better immobilization of microorganisms on the electrode surface, effectively eliminating problems related to biofouling. In turn, the use of Fe particles improves electrical conductivity while overcoming voltage reversal problems.

Our previous study found that increased iron content at the anode reduces the removal of organic compounds from wastewater. Other authors have also reported that higher iron(III) concentrations in wastewater treatment systems lead to lower COD removal efficiency. However, the present study found that combining Fe(III) with rGO enables higher energy production and more stable COD removal, eliminating the negative effects previously reported with higher Fe doses. Therefore, future research can use this technique to increase the performance of the cells with iron doses without drastically reducing the efficiency of COD removal. To use an MFC system for wastewater treatment and power generation, the optimal iron levels deposited on the anodes should be determined for the proposed technology, e.g., with a certain dose of rGO deposited on the anode. The results presented here, including extensive metagenomic analyses, fill the knowledge gap regarding the effects of anode modification with rGO and Fe(III) on the structure of microbial communities and their metabolic potential.

Conclusion

Although much research has focused on the electrochemical aspects of the MFC itself, knowledge of the species composition of the anode biofilms is also an important aspect of MFC operation. Therefore, this study focused on the electrochemical, microbiological, and metabolic aspects of MFC. The modification of the electrodes resulted in a total reduction in the charge transfer resistance in relation to MFC-control, while the increase in capacitance of the modified electrodes suggests an improved electrode–electrolyte interface for charge storage. MFC voltage (342.7 ± 72.8 mV) and cell power (8.55 mW/m^2) were significantly higher when the composite of rGO and 68 mg Fe layer was deposited than in other variants. With the MFC-rGO-Fe68 composite, the total internal resistance of the cell was about 4 times lower and the load transfer resistance was 2 times lower than with the control. The main electrogenic bacteria in the MFCs were *Pseudoxanthomonas* sp., *Zoogloea* sp., and *Dechloromonas* sp. For each type of modifier, the microorganisms that played the most important role in electricity generation were identified. Electricity production was mainly related to the reverse citrate cycle and MFC-rGO-Fe34 had the widest range of potential metabolic pathways for efficient energy generation. To conclude, the selection of composites affects the species composition of the biofilm, which affects the cell's resistance to disturbances and the variety of energy generation pathways, thus enabling increased electricity production in the cell.

Author Contributions All authors contributed to the study's conception and design. Material preparation, data collection, and analysis were performed by DN and TM. The first draft of the manuscript was written by DN and Agnieszka Cydzik-Kwiatkowska, and all authors commented on previous versions of the manuscript. All authors read and approved the final manuscript.

Data availability Data will be made available on request.

Declarations

Competing interests The authors declare no competing interests.

References

Aiswaria P, Mohamed SN, Singaravelu DL, Brindhadevi K, Pugazhendhi A (2022) A review on graphene/graphene oxide supported electrodes for microbial fuel cell applications: Challenges and prospects. Chemosphere 296:133983. https://doi.org/10.1016/j.chemosphere.2022.133983

APHA (2012) Standard methods for examination of water and wastewater. American Public Health Association, Standard Methods, Washington. ISBN 978-087553-013-0

Attia YA, Samer M, Mohamed MSM, Moustafa E, Salah M, Abdelsalam EM (2022) Nanocoating of microbial fuel cell electrodes

for enhancing bioelectricity generation from wastewater. Biomass Conv Bioref 1:1–12. https://doi.org/10.1007/s13399-022-02321-7

Banerjee A, Calay RK, Mustafa M (2022) Review on material and design of anode for microbial fuel cell. Energies 15(6):2283. https://doi.org/10.3390/en15062283

Beliaev AS, Saffarini DA, McLaughlin JL, Hunnicutt D (2001) MtrC, an outer membrane decahaem c cytochrome required for metal reduction in *Shewanella putrefaciens* MR-1. Mol Microbiol 39(3):722–730. https://doi.org/10.1046/j.1365-2958.2001.02257.x

Berg IA, Kockelkorn D, Ramos-Vera WH, Say RF, Zarzycki J, Hügler M, Birgit EA, Fuchs G (2010) Autotrophic carbon fixation in archaea. Nat Rev Microbiol 8(6):447–460. https://doi.org/10.1038/nrmicro2365

Berger S, Shaw DR, Berben T, Ouboter HT, Frank J, Reimann J, Jetten MSM, Welte CU (2021) Current production by non-methanotrophic bacteria enriched from an anaerobic methane-oxidizing microbial community. Biofilm 3:100054. https://doi.org/10.1016/j.biofilm.2021.100054

Caporaso JG, Lauber CL, Walters WA, Berg-Lyons D, Lozupone CA, Turnbaugh PJ, Fierer N, Knight R (2011) Global patterns of 16S rRNA diversity at a depth of millions of sequences per sample. Proc Nat Acad Sci 108(Supplement 1):4516–4522. https://doi.org/10.1073/pnas.1000080107

Chang SH, Huang BY, Wan TH, Chen JZ, Chen BY (2017) Surface modification of carbon cloth anodes for microbial fuel cells using atmospheric-pressure plasma jet processed reduced graphene oxides. RSC Adv 7(89):56433–56439. https://doi.org/10.1039/C7RA11914C

Chong J, Liu P, Zhou G, Xia J (2020) Using MicrobiomeAnalyst for comprehensive statistical, functional, and meta-analysis of microbiome data. Nat Protoc 15(3):799–821. https://doi.org/10.1038/s41596-019-0264-1

Dalcin Martins P, de Jong A, Lenstra WK, van Helmond NA, Slomp CP, Jetten MS, Welte CU, Rasigraf O (2021) Enrichment of novel Verrucomicrobia, Bacteroidetes, and Krumholzibacteria in an oxygen-limited methane and iron-fed bioreactor inoculated with Bothnian Sea sediments. MicrobiologyOpen 10(1):e1175. https://doi.org/10.1002/mbo3.1175

Dessie Y, Tadesse S (2021) Nanocomposites as efficient anode modifier catalyst for microbial fuel cell performance improvement. J Chem Rev 3(4):320–344. https://doi.org/10.22034/JCR.2021.314327.1128

Ding X, Wei D, Guo W, Wang B, Meng Z, Feng R, Du B, Wei Q (2019) Biological denitrification in an anoxic sequencing batch biofilm reactor: Performance evaluation, nitrous oxide emission and microbial community. Bioresour Technol 285:121359. https://doi.org/10.1016/j.biortech.2019.121359

Douglas G, Maffei VJ, Zaneveld JR, Yurgel SN, Brown JR, Taylor CM, Huttenhower C, Langille MG (2020) PICRUSt2 for prediction of metagenome functions. Nat Biotechnol 38(6):685–688. https://doi.org/10.1038/s41587-020-0548-6

Du X, Skachko I, Barker A, Andrei EY (2008) Approaching ballistic transport in suspended graphene. Nat Nanotech 3:491–495. https://doi.org/10.1038/nnano.2008.199

Dunfield PF, Yuryev A, Senin P, Smirnova AV, Stott MB, Hou S, Ly B, Saw JH, Zhou Z, Ren Y, Wang J, Mountain BW, Crowe MA, Weatherby TM, Bodelier PLE, Liesack W, Feng L, Wang L, Alam M (2007) Methane oxidation by an extremely acidophilic bacterium of the phylum Verrucomicrobia. Nature 450:879–882. https://doi.org/10.1038/nature06411

Edwards MJ, White GF, Lockwood CW, Martel LMC, A, Harris G, Scott DJ, Richardson DJ, Butt JN, Clarke TA, (2018) Structural modeling of an outer membrane electron conduit from a metal reducing bacterium suggests electron transfer via periplasmic redox partners. J Biol Chem 293(21):8103–8112. https://doi.org/10.1074/jbc.RA118.001850

Feist AM, Nagarajan H, Rotaru AE, Tremblay PL, Zhang T, Nevin KP, Derek RL, Zengler K (2014) Constraint-based modeling of carbon fixation and the energetics of electron transfer in *Geobacter metallireducens*. PLoS Comput Biol 10(4):e1003575. https://doi.org/10.1371/journal.pcbi.1003575

Fu L, Wang H, Huang Q, Song TS, Xie J (2020) Modification of carbon felt anode with graphene/Fe$_2$O$_3$ composite for enhancing the performance of microbial fuel cell. Bioprocess Biosyst Eng 43:373–381. https://doi.org/10.1007/s00449-019-02233-3

Gezginci M, Uysal Y (2016) The effect of different substrate sources used in microbial fuel cells on microbial community. JSM Environ Sci Ecol 4(3): 1035. https://doi.org/10.47739/2333-7141/1035

Guerrero-Cruz S, Vaksmaa A, Horn MA, Niemann H, Pijuan M, Ho A (2021) Methanotrophs: discoveries, environmental relevance, and a perspective on current and future applications. Front Microbiol 12:678057. https://doi.org/10.3389/fmicb.2021.678057

Guo Y, Wang J, Shinde S, Wang X, Li Y, Dai Y, Ren J, Zhang P, Liu X (2020) Simultaneous wastewater treatment and energy harvesting in microbial fuel cells: an update on the biocatalysts. RSC Adv 10(43):25874–25887. https://doi.org/10.1039/D0RA05234E

Guo Z, Xie C, Zhang P, Zhang J, Wang G, He X, Ma X, Zhao B, Zhang Z (2017) Toxicity and transformation of graphene oxide and reduced graphene oxide in bacteria biofilm. Sci Total Environ 580:1300–1308. https://doi.org/10.1016/j.scitotenv.2016.12.093

Guttenplan SB, Kearns DB (2013) Regulation of flagellar motility during biofilm formation. FEMS Microbiol Rev 37(6):849–871. https://doi.org/10.1111/1574-6976.12018

Islam J, Chilkoor G, Jawaharraj K, Dhiman SS, Sani R, Gadhamshetty V (2020) Vitamin-C-enabled reduced graphene oxide chemistry for tuning biofilm phenotypes of methylotrophs on nickel electrodes in microbial fuel cells. Bioresour Technol 300:122642. https://doi.org/10.1016/j.biortech.2019.122642

Jayashree C, Tamilarasan K, Rajkumar M, Arulazhagan P, Yogalakshmi KN, Srikanth M, Banu JR (2016) Treatment of seafood processing wastewater using upflow microbial fuel cell for power generation and identification of bacterial community in anodic biofilm. J Environ Manage 180:351–358. https://doi.org/10.1016/j.jenvman.2016.05.050

Jothinathan D, Wilson RT (2018) Performance of *Paracoccus homiensis* DRR-3 in microbial fuel cell with membranes. Int J Ambient Energy 39(6):573–580. https://doi.org/10.1080/01430750.2017.1318779

Katuri KP, Scott K, Head IM, Picioreanu C, Curtis TP (2011) Microbial fuel cells meet with external resistance. Bioresour Technol 102(3):2758–2766. https://doi.org/10.1016/j.biortech.2010.10.147

Kong F, Ren HY, Liu D, Wang Z, Na J, Ren NQ, Fu Q (2022) Improved decolorization and mineralization of azo dye in an integrated system of anaerobic bioelectrochemical modules and aerobic moving bed biofilm reactor. Bioresour Technol 353:127147. https://doi.org/10.1016/j.biortech.2022.127147

Krishnamoorthy K, Kim GS, Kim SJ (2013) Graphene nanosheets: Ultrasound assisted synthesis and characterization. Ultrason Sonochem 20(2):644–649. https://doi.org/10.1016/j.ultsonch.2012.09.007

Lawal AT (2018) Progress in utilisation of graphene for electrochemical biosensors. Biosens Bioelectron 106:149–178. https://doi.org/10.1016/j.bios.2018.01.030

Lemos RV, Tsujimura S, Ledezma P, Tokunou Y, Okamoto A, Freguia S (2021) Extracellular electron transfer by *Microcystis aeruginosa* is solely driven by high pH. Bioelectrochemistry 137:107637. https://doi.org/10.1016/j.bioelechem.2020.107637

Li C, Zhou K, He H, Cao J, Zhou S (2020) Adding zero-valent iron to enhance electricity generation during MFC start-up. J Environ Res Public Health 17(3):806. https://doi.org/10.3390/ijerph17030806

Li R, Li T, Wan Y, Zhang X, Liu X, Li R, Pu H, Gao T, Wang X, Zhou Q (2022) Efficient decolorization of azo dye wastewater with

polyaniline/graphene modified anode in microbial electrochemical systems. J Hazard Mater 421:126740. https://doi.org/10.1016/j.jhazmat.2021.126740

Li X, Qian J, Guo X, Shi L (2018) One-step electrochemically synthesized graphene oxide coated on polypyrrole nanowires as anode for microbial fuel cell. 3 Biotech 8:1–8. https://doi.org/10.1007/s13205-018-1321-0

Li XM, Cheng KY, Selvam A, Wong JW (2013) Bioelectricity production from acidic food waste leachate using microbial fuel cells: effect of microbial inocula. Process Biochem 48(2):283–288. https://doi.org/10.1016/j.procbio.2012.10.001

Li Y, Liu J, Chen X, Yuan X, Li N, He W, Feng Y (2021) Tailoring spatial structure of electroactive biofilm for enhanced activity and direct electron transfer on iron phthalocyanine modified anode in microbial fuel cells. Biosens Bioelectron 191:113410. https://doi.org/10.1016/j.bios.2021.113410

Liu H, Logan BE (2004) Electricity generation using an air-cathode single chamber microbial fuel cell in the presence and absence of a proton exchange membrane. Environ Sci Technol 38(14):4040–4046. https://doi.org/10.1021/es0499344

Liu X, Zhuo S, Jing X, Yuan Y, Rensing C, Zhou S (2019) Flagella act as Geobacter biofilm scaffolds to stabilize biofilm and facilitate extracellular electron transfer. Biosens Bioelectron 146:111748. https://doi.org/10.1016/j.bios.2019.111748

Lobato J, Cañizares P, Fernández FJ, Rodrigo MA (2012) An evaluation of aerobic and anaerobic sludges as start-up material for microbial fuel cell systems. N Biotechnol 29(3):415–420. https://doi.org/10.1016/j.nbt.2011.09.004

Ma J, Shi N, Jia J (2020) Fe$_3$O$_4$ nanospheres decorated reduced graphene oxide as anode to promote extracellular electron transfer efficiency and power density in microbial fuel cells. Electrochim Acta 362:137126. https://doi.org/10.1016/j.electacta.2020.137126

Marks S, Makinia J, Fernandez-Morales FJ (2019) Performance of microbial fuel cells operated under anoxic conditions. Appl Energy 250:1–6. https://doi.org/10.1016/j.apenergy.2019.05.043

McMurdie PJ, Holmes S (2014) Waste not, want not: why rarefying microbiome data is inadmissible. PLoS Comput Biol 10(4):e1003531. https://doi.org/10.1371/journal.pcbi.1003531

Meng L, Xie L, Hirose Y, Nish Fiuchi T, Yoshida N (2022) Reduced graphene oxide increases cells with enlarged outer membrane of Citrifermentans bremense and exopolysaccharides secretion. Biosens Bioelectron 218:114754. https://doi.org/10.1016/j.bios.2022.114754

Mohamed HO, Talas SA, Sayed ET, Park SG, Eisa T, Abdelkareem MA, Fadali OA, Chae KJ, Castaño P (2021) Enhancing power generation in microbial fuel cell using tungsten carbide on reduced graphene oxide as an efficient anode catalyst material. Energy 229:120702. https://doi.org/10.1016/j.energy.2021.120702

Ndayisenga F, Yu Z, Yan G, Phulpoto IA, Li Q, Kumar H, Fu L, Zhou D (2021) Using easy-to-biodegrade co-substrate to eliminate microcystin toxic on electrochemically active bacteria and enhance bioelectricity generation from cyanobacteria biomass. Sci Total Environ 751:142292. https://doi.org/10.1016/j.scitotenv.2020.142292

Ni J, Li Y (2016) Carbon nanomaterials in different dimensions for electrochemical energy storage. Adv Energy Mater 6(17):1600278. https://doi.org/10.1002/aenm.201600278

Nosek D, Cydzik-Kwiatkowska A (2019) Microbial structure and energy generation in microbial fuel cells powered with waste anaerobic digestate. Energies 13(18):4712. https://doi.org/10.3390/en13184712

Nosek D, Cydzik-Kwiatkowska A (2022) Anode modification with reduced graphene oxide–iron oxide improves electricity generation in microbial fuel cell. J Ecol Eng 23(10):147–153. https://doi.org/10.12911/22998993/152440

Nosek D, Jachimowicz P, Cydzik-Kwiatkowska A (2020) Anode modification as an alternative approach to improve electricity generation in microbial fuel cells. Energies 13(24):6596. https://doi.org/10.3390/en13246596

Nosek D, Mikołajczyk T, Cydzik-Kwiatkowska A (2023) Anode modification with Fe$_2$O$_3$ affects the anode microbiome and improves energy generation in microbial fuel cells powered by wastewater. Int J Environ Res Public Health 20(3):2580. https://doi.org/10.3390/ijerph20032580

Pareek A, Sravan JS, Mohan SV (2019) Exploring chemically reduced graphene oxide electrode for power generation in microbial fuel cell. Mater Sci Technol 2(3):600–606. https://doi.org/10.1016/j.mset.2019.06.006

Park Y, Park S, Yu J, Torres CI, Rittmann BE, Lee T (2017) Complete nitrogen removal by simultaneous nitrification and denitrification in flat-panel air-cathode microbial fuel cells treating domestic wastewater. J Chem Eng 316:673–679. https://doi.org/10.1016/j.cej.2017.02.005

Rani R, Kumar S (2021) Microbial community dynamics of microbial fuel cell in response to NiWO4/rGO nanocomposites as electrocatalyst and its correlation with electrochemical properties. J Environ Chem Eng 9(1):104668. https://doi.org/10.1016/j.jece.2020.104668

Ren HY, Song X, Kong F, Song Q, Ren NQ, Liu BF (2023) Lipid production characteristics of a newly isolated microalga Asterarcys quadricellulare R-56 as biodiesel feedstock. Environ Sci Pollut Res 30:48339–48350. https://doi.org/10.1007/s11356-023-25728-9

Rismani-Yazdi H, Carver SM, Christy AD, Tuovinen OH (2008) Cathodic limitations in microbial fuel cells: an overview. J Power Sources 180(2):683–694. https://doi.org/10.1016/j.jpowsour.2008.02.074

Salar-Garcia MJ, Obata O, Kurt H, Chandran K, Greenman J, Ieropoulos IA (2020) Impact of inoculum type on the microbial community and power performance of urine-fed microbial fuel cells. Microorganisms 8:1921. https://doi.org/10.3390/microorganisms8121921

Sangcharoen A, Niyom W, Suwannasilp BB (2015) A microbial fuel cell treating organic wastewater containing high sulfate under continuous operation: performance and microbial community. Process Biochem 50(10):1648–1655. https://doi.org/10.1016/j.procbio.2015.06.013

Shao Y, Wang J, Engelhard M, Wang C, Lin Y (2010) Facile and controllable electrochemical reduction of graphene oxide and its applications. J Mater Chem 20(4):743748. https://doi.org/10.1039/B917975E

Shearer CJ, Slattery AD, Stapleton AJ, Shapter JG, Gibson CT (2016) Accurate thickness measurement of graphene. Nanotechnology 27(12):125704. https://doi.org/10.1088/0957-4484/27/12/125704

Shen J, Du Z, Li J, Cheng F (2020) Co-metabolism for enhanced phenol degradation and bioelectricity generation in microbial fuel cell. Bioelectrochemistry 134:107527. https://doi.org/10.1016/j.bioelechem.2020.107527

Shi L, Rosso KM, Zachara JM, Fredickson JK (2012) Mtr extracellular electron-transfer pathways in Fe(III)-reducing or Fe(II)-oxidizing bacteria: a genomic perspective. Biochem Soc Trans 40(6):1261–1267. https://doi.org/10.1042/BST20120098

Su C, Deng Q, Chen Z, Lu X, Huang Z, Guan X, Chen M (2021) Denitrifying anaerobic methane oxidation process responses to the addition of growth factor betaine in the MFC-granular sludge coupling system: Enhancing mechanism and metagenomic analysis. J Hazard Mater 416:126139. https://doi.org/10.1016/j.jhazmat.2021.126139

Sun L, Lin W, Li D, Xiao K, Chen D, Luo S, Huang X (2023) Significant insights of Cu and Fe as key metals to cause RO membrane

fouling under coal-mining wastewater treatment. Desalination 555:116517. https://doi.org/10.1016/j.desal.2023.116517

Sun Y, Guan Y, Wang D, Liang K, Wu G (2018) Potential roles of acyl homoserine lactone based quorum sensing in sequencing batch nitrifying biofilm reactors with or without the addition of organic carbon. Bioresour Technol 259:136–145. https://doi.org/10.1016/j.biortech.2018.03.025

Świątczak P, Cydzik-Kwiatkowska A (2018) Performance and microbial characteristics of biomass in a full-scale aerobic granular sludge wastewater treatment plant. Environ Sci Pollut Res 25:1655–1669. https://doi.org/10.1007/s11356-017-0615-9

Tabassum N, Islam N, Ahmed S (2021) Progress in microbial fuel cells for sustainable management of industrial effluents. Process Biochem 106:20–41. https://doi.org/10.1016/j.procbio.2021.03.032

Wang M, Wang Z, Hu F, Fan L, Zhang X (2020) Polyelectrolytes/α-Fe_2O_3 modification of carbon cloth anode for dealing with food wastewater in microbial fuel cell. Carbon Resour Convers 3:76–81. https://doi.org/10.1016/j.crcon.2020.02.004

Wang R, Li Y, Chen W, Zou J, Chen Y (2016) Phosphate release involving PAOs activity during anaerobic fermentation of EBPR sludge and the extension of ADM1. J Chem Eng 287:436–447. https://doi.org/10.1016/j.cej.2015.10.110

Wang X, Liu C, Li H, Zhang H, Ma R, Zhang Q, Yang F, Liao Y, Yuan W, Chen F (2019) Metabonomics-assisted label-free quantitative proteomic and transcriptomic analysis reveals novel insights into the antifungal effect of graphene oxide for controlling *Fusarium graminearum*. Environ Sci Nano 6(11):3401–3421. https://doi.org/10.1039/C9EN00981G

Watanabe K, Miyahara M, Shimoyama T, Hashimoto K (2011) Population dynamics and current generation mechanisms in cassette-electrode microbial fuel cells. Appl Microbiol Biotechnol 92:1307–1314. https://doi.org/10.1007/s00253-011-3598-3

Watson VJ, Logan BE (2011) Analysis of polarization methods for elimination of power overshoot in microbial fuel cells. Electrochem Commun 13:54–56. https://doi.org/10.1016/j.elecom.2010.11.011

Wu J, Pisula W, Müllen K (2007) Graphenes as potential material for electronics. Chem Rev 107(3):718–747. https://doi.org/10.1021/cr068010r

Xia T, Zhang X, Wang H, Zhang Y, Gao Y, Bian C, Wang X, Xu P (2019) Power generation and microbial community analysis in microbial fuel cells: A promising system to treat organic acid fermentation wastewater. Bioresour Technol 284:72–79. https://doi.org/10.1016/j.biortech.2019.03.119

Xiao N, Wu R, Huang JJ, Selvaganapathy PR (2020) Anode surface modification regulates biofilm community population and the performance of micro-MFC based biochemical oxygen demand sensor. Chem Eng Sci 221:115691. https://doi.org/10.1016/j.ces.2020.115691

Xing D, Cheng S, Logan BE, Regan JM (2010) Isolation of the exoelectrogenic denitrifying bacterium *Comamonas denitrificans* based on dilution to extinction. Appl Microbiol Biotechnol 85:1575–1587. https://doi.org/10.1007/s00253-009-2240-0

Xu H, Quan X, Xiao Z, Chen L (2018) Effect of anodes decoration with metal and metal oxides nanoparticles on pharmaceutically active compounds removal and power generation in microbial fuel cells. J Chem Eng 335:539–547. https://doi.org/10.1016/j.cej.2017.10.159

Xu H, Wang L, Wen Q, Chen Y, Qi L, Huang J, Tang Z (2019) A 3D porous NCNT sponge anode modified with chitosan and Polyaniline for high-performance microbial fuel cell. Bioelectrochemistry 129:144–153. https://doi.org/10.1016/j.bioelechem.2019.05.008

Yang N, Luo H, Liu M, Xiong X, Jin X, Zhan G (2023) Coupling mixotrophic denitrification and electroactive anodic nitrification by nitrate addition for promoting current generation and nitrogen removal. Sci Total Environ 856:159082. https://doi.org/10.1016/j.scitotenv.2022.159082

Yang Q, Yang S, Liu G, Zhou B, Yu X, Yin Y, Yang J, Zhao H (2021) Boosting the anode performance of microbial fuel cells with a bacteria-derived biological iron oxide/carbon nanocomposite catalyst. Chemosphere 268:128800. https://doi.org/10.1016/j.chemosphere.2020.128800

Yin X, Qiao S, Yu C, Tian T, Zhou J (2015) Effects of reduced graphene oxide on the activities of anammox biomass and key enzymes. J Chem Eng 276:106–112. https://doi.org/10.1016/j.cej.2015.04.073

Yuan H, Huang S, Yuan J, You Y, Zhang Y (2021) Characteristics of microbial denitrification under different aeration intensities: Performance, mechanism, and co-occurrence network. Sci Total Environ 754:141965. https://doi.org/10.1016/j.scitotenv.2020.141965

Zhang L, Zhang M, You S, Ma D, Zhao J, Chen Z (2021a) Effect of Fe^{3+} on the sludge properties and microbial community structure in a lab-scale A2O process. Sci Total Environ 780:146505. https://doi.org/10.1016/j.scitotenv.2021.146505

Zhang Q, Zhang L, Wang H, Jiang Q, Zhu X (2018) Simultaneous efficient removal of oxyfluorfen with electricity generation in a microbial fuel cell and its microbial community analysis. Bioresour Technol 250:658–665. https://doi.org/10.1016/j.biortech.2017.11.091

Zhang Z, Zhang K, Ouyang H, Li MK, Luo Z, Li Y, Chen C, Yang X, Shao Z, Yan DY (2021b) Simultaneous PAHs degradation, odour mitigation and energy harvesting by sediment microbial fuel cell coupled with nitrate-induced biostimulation. J Environ Manage 284:112045. https://doi.org/10.1016/j.jenvman.2021.112045

Zhao H, Kong CH (2018) Enhanced removal of p-nitrophenol in a microbial fuel cell after long-term operation and the catabolic versatility of its microbial community. J Chem Eng 339:424–431. https://doi.org/10.1016/j.cej.2018.01.158

Zhao H, Zhao J, Li F, Li X (2016) Performance of denitrifying microbial fuel cell with biocathode over nitrite. Front Microbiol 7:344. https://doi.org/10.3389/fmicb.2016.00344

Zheng X, Hou S, Amanze C, Zeng Z, Zeng W (2022) Enhancing microbial fuel cell performance using anode modified with Fe_3O_4 nanoparticles. Bioprocess Biosyst Eng 45:877–890. https://doi.org/10.1007/s00449-022-02705-z

Zhou S, Lin M, Zhuang Z, Liu P, Chen Z (2019) Biosynthetic graphene enhanced extracellular electron transfer for high performance anode in microbial fuel cell. Chemosphere 232:396–402. https://doi.org/10.1016/j.chemosphere.2019.05.191

Zhu Q, Hu J, Liu B, Liang S, Xiao K, Yu W, Yuan S, Yang J, Hou H (2022) Potassium channel blocker selectively enriched *Geobacter* from mixed-cultured electroactive biofilm: Insights from microbial community, functional prediction and gene expressions. Bioresour Technol 364:128109. https://doi.org/10.1016/j.biortech.2022.128109

Zou L, Huang Y, Wu X, Long ZE (2019) Synergistically promoting microbial biofilm growth and interfacial bioelectrocatalysis by molybdenum carbide nanoparticles functionalized graphene anode for bioelectricity production. J Power Sources 413:174–181. https://doi.org/10.1016/j.jpowsour.2018.12.041

Enhancing microbial fuel cell performance: anode modification with reduced graphene oxide and iron(III) for improved electricity generation

Dawid Nosek[a]*, Tomasz Mikołajczyk[b], Agnieszka Cydzik-Kwiatkowska[a]

[a] University of Warmia and Mazury in Olsztyn, Department of Environmental Biotechnology, 10-709 Olsztyn, Słoneczna 45 G

[b] University of Warmia and Mazury in Olsztyn, Department of Chemistry, 10-721 Olsztyn, plac Łódzki 4

*Corresponding author: dawid.nosek@uwm.edu.pl, tel. +48 89 5234144

	Modified anode	Effect of modification
Chen et al. (2020)	CC/rGO	reduction of the water contact angle from 134.13° to 94.63°; reduction of the ohmic resistance from 19.8 Ω to 18.1 Ω, of the charge transfer resistance from 178.3 Ω to 20.3 Ω, of the internal resistance of the MFC from 270.0 Ω to 20.5 Ω; increase of the electrical power density from 340 mW/m2 to 1258 mW/m^2.
Parek et al. 2020	CC/rGO and CC/GO	the shape of the CV curves obtained for rGO indicates a good electrochemical capacitive response of the rGO bilayer; a much smaller Nyquist diameter compared to the CC and GO electrodes; higher power density (6 mW/m^2 at 9.9 mA/m^2) compared to the CC anode (0.8 mW/m^2 at 8.6 mA/m^2) and GO (1.6 mW/m^2 at 10.8 mA/m^2).
Zhang et al. (2018)	CC/rGO and CC/GO	MFC with 0.4 g rGO improved the power density almost threefold. The GO proved to be better in this case, with a 6.86-fold increase in power compared to the control group. The addition of 0.4 g rGO contributed to a 48% reduction in the internal resistance of the MFC compared to the control group; the peak current of the electrodes in the 0.4 g GO-MFC and the 0.4 g rGO-MFC was 1.9 times and 1.4 times greater than that of the ordinary sludge- MFC, respectively
Mehdinia et al. 2014	CC/rGO/SnO$_2$	a power density of 1624 mW/m^2 in a two-chamber MFC with E. coli pure culture; the power was 2.8 and 4.8 times higher than the rGO-coated anode and the bare anode, respectively; the high conductivity and large surface area of the nanocomposites significantly improved biofilm formation and electron transfer
Ma et al. (2020)	CP/rGO/Fe$_3$O$_4$	the highest power density of 1837.4 mW/m^2 for Fe3O4/rGO (1.5:1) compared to the MFC control 689.7 mW/m^2; the redox peak currents increased with increasing Fe$_3$O$_4$ content from 0.5:1 to 1.5:1 and decreased with increasing Fe$_3$O$_4$ content from 1.5:1 to 2.5:1; the Fe$_3$O$_4$ nanosphere/rGO (1.5:1) anode had a lower charge transfer resistance than the rGO anode, indicating accelerated extracellular electron transfer (EET) kinetics
Isalm et al. (2020)	rGO/NF	the power and current density of rGO/NF anode (1200 mW/m^2 and 680 mA/m^2) were 220 and 540 times higher, respectively, than bare NF (5.50 mW/m^2 and 1.26 mA/m^2); rGO/NF suppressed the charge transfer resistance by 40 times compared to the control; the wetting contact angle (hydrophilicity improvement) of NF was reduced from 1280 to 00.
Cheng et al. (2018)	CF/rGO/Ag	3.2-fold higher power density of 33.7 W/m^3 at a current density of 69.4 A/m^3 with a 75% shorter start period compared to the control; gold nanoparticles,

		which anchored on graphene sheets, promise the relatively high electroactive sites and facilitate electron transfer from electricigens to the anode.
Geetanjali et al. (2019)	CC/NiWO$_4$/GO	increasing the abundance and diversity of microorganisms in the biofilm and *Trichococcus* sp. that can use the anode as an electron acceptor.
Fu et al. (2020)	CF/G/Fe$_2$O$_3$	decrease of the number of Proteobacteria from 85.1% with pure CF to 55.3% with anode G-CF; the hydrophobicity of G led to a decrease in the abundance of *Geobacter* sp.; *Desulfovibrio* sp. in the G/Fe$_2$O$_3$-CF group (6.3%) was significantly higher than in the biofilm on pure CF (2.6%) and G-CF (4.2%).

Table 1 SM A review of the literature on rGO – modified anodes with a presentation of the effect after modification, where: CC – carbon cloth, rGO – reduced graphene oxide, G – graphene, NF – nickel foam.
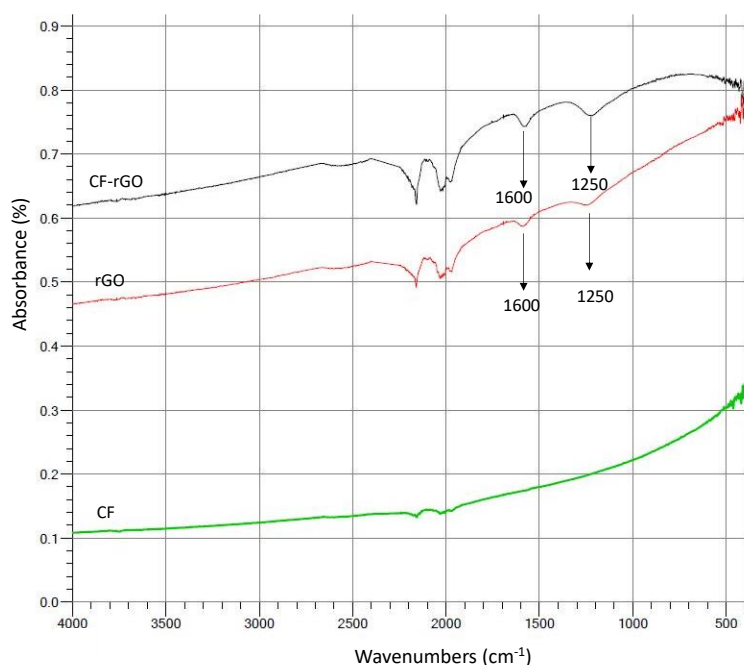
Fig. 1 SM FT-IR spectra for CF, rGO and CF-rGO.
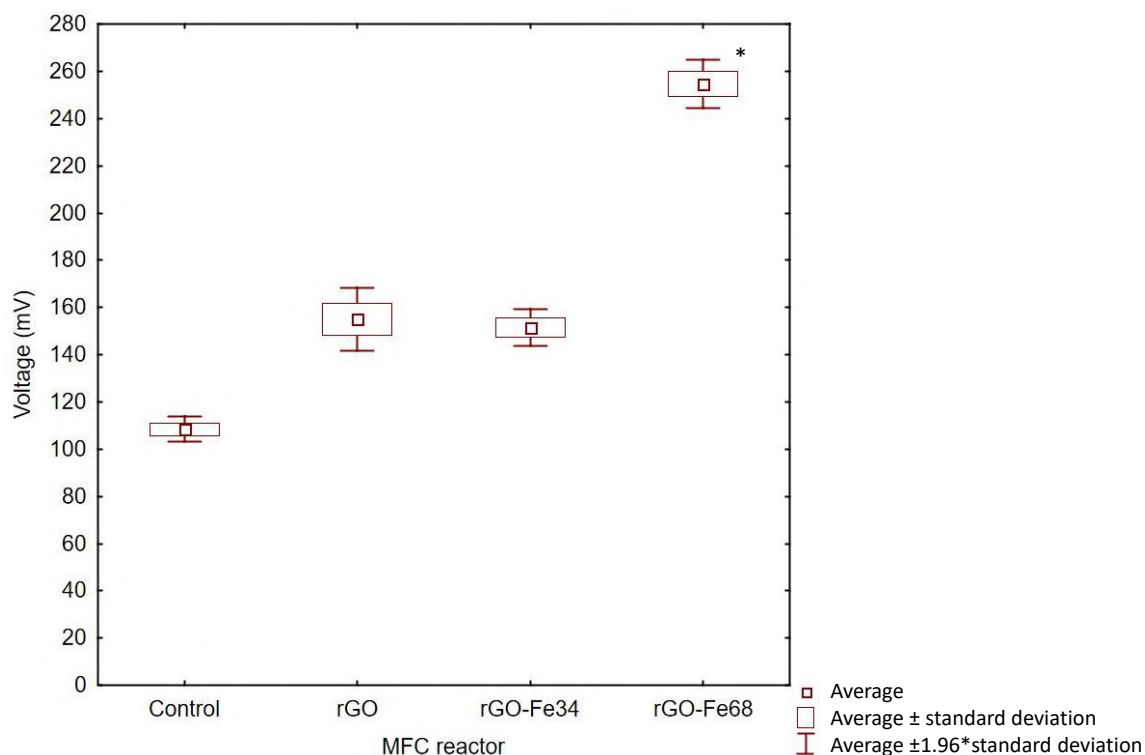
Fig. 2 SM Statistical differences in the voltages obtained in the individual reactors (ANOVA – Tukey's HSD post-hoc test), p<0.05, * – significantly higher than in the remaining MFCs
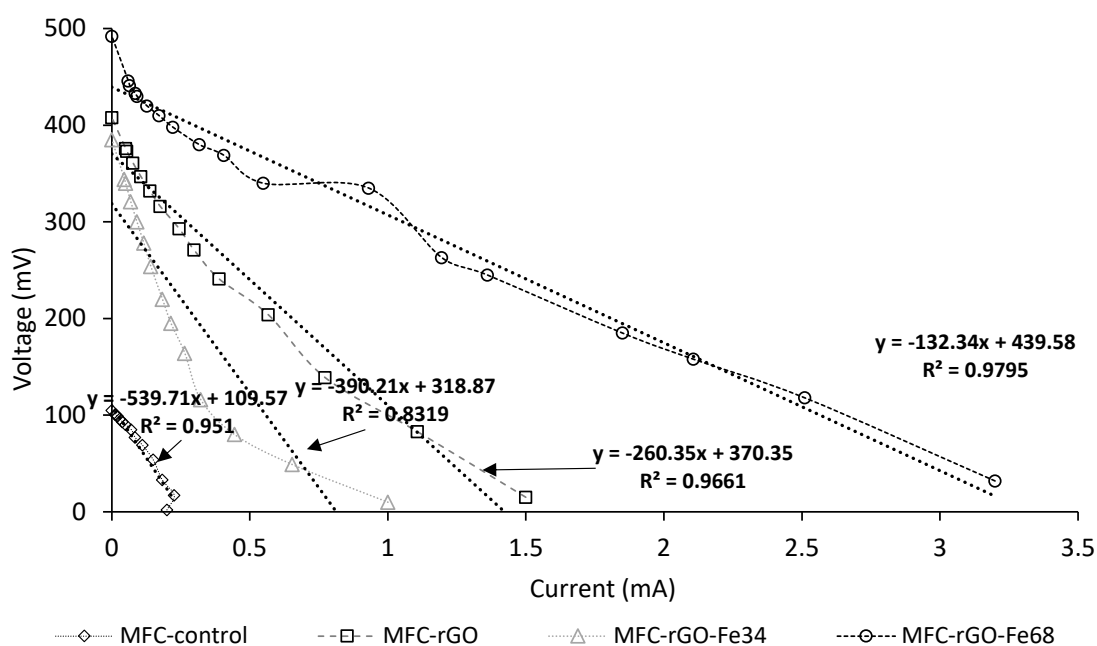
Fig. 3 SM Polarization curves with a trend line and an equation where the coefficient "a" from the formula y = ax+b determines the value of the internal resistance of MFCs.

| E/mV	R_{ct}/Ω	C_{dl}/μF
MFC-control		
400	8.49 ± 0.64	263 ± 19
500	9.03 ± 1.08	278 ± 33
600	8.07 ± 0.65	128 ± 10
700	8.03 ± 0.56	95 ± 7
800	7.73 ± 0.34	71 ± 3
900	8.12 ± 0.65	88 ± 7
MFC-rGO		
400	-	-
500	9.00 ± 0.91	420 ± 78
600	7.41 ± 0.38	330 ± 90
700	7.61 ± 0.84	362 ± 84
800	6.43 ± 0.07	171 ± 30
900	6.78 ± 0.13	95 ± 37
MFC-rGO-Fe34		
400	6.21 ± 0.68	558 ± 51
500	5.99 ± 1.10	540 ± 24
600	5.93 ± 0.89	553 ± 61
700	5.96 ± 0.86	483 ± 5
800	5.80 ± 0.76	291 ± 5
900	5.52 ± 0.97	221 ± 13
MFC-rGO-Fe68		
400	4.53 ± 0.68	472 ± 93
500	4.72 ± 0.36	423 ± 132
600	4.75 ± 0.53	378 ± 101
700	4.55 ± 0.77	448 ± 65
800	5.72 ± 0.90	407 ± 120
900	4.04 ± 0.45	329 ± 111

Table 2 SM Electrochemical parameters for the MFCs obtained in supporting solution. The results were recorded by fitting the CPE-modified Randles equivalent circuit (Fig. 6b) to the experimentally obtained impedance data (reproducibility usually below 10-15%, $\chi 2 = 2\times10^{-4}$ to 5×10^{-3}).
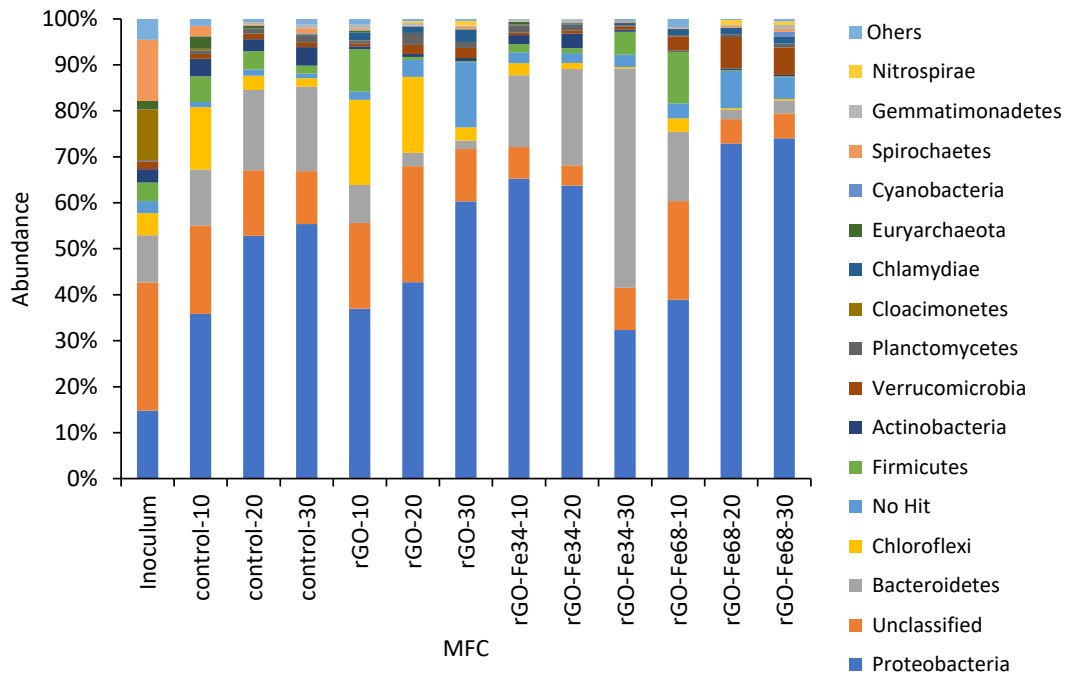
Fig. 4 SM Relative abundance of phyla in the inoculum and anodic biofilm obtained from MFCs. The number next to the reactor name corresponds with the day of the experiment.

Reactor - day number	OTU	Chao1	Shannon	Total read counts
Inoculum	185	232.4	3.1	63651
MFC-control – 10	234	236.5	3.7	74841
MFC-control – 20	246	246.0	3.8	82657
MFC-control – 30	231	232.0	3.8	66255
MFC-rGO – 10	213	234.7	3.5	88768
MFC-rGO – 20	210	218.6	3.3	82934
MFC-rGO – 30	213	216.0	3.1	77907
MFC-rGO-Fe34 – 10	218	219.3	3.6	75986
MFC-rGO-Fe34 – 20	212	212.7	3.4	85219
MFC-rGO-Fe34 – 30	201	203.3	3.2	93660
MFC-rGO-Fe68 – 10	211	224.5	3.4	69974
MFC-rGO-Fe68 – 20	201	207.0	2.6	92114
MFC-rGO-Fe68 – 30	203	212.6	2.9	88577

Table 3 SM Alpha diversity indicators in MFCs; the number after the reactor name indicates the cycle in which sampling was performed; OUT – Operational Taxonomic Unit, Chao1 – richness estimator, Shannon – biodiversity index

MFC reactor	Bacteria	Abundance (%)	R
MFC-control	*Pseudoxanthomonas* sp	2.1-7.27	0.99
	Stenotrophomonas sp.	0.40-0.70	0.99
	Thermomonas brevis	0.21-3.61	0.99
MFC-rGO	*Dechloromonas* sp.	0.07-7.73	0.99
MFC-rGO-Fe34	*Turneriella parva*	0-0.29	0.99
	Unclassified Sphingobacteriales	0.09-1.96	1.00
	Opitutus sp	0.01-0.12	0.99
	Candidatus Halomonas phosphatis	0.03-0.16	1.00
	Fluviicola taffensis	0.1-0.97	0.99
	Magnetospirillum sp.	0.01-0.18	1.00
MFC-rGO-Fe68	*Microcystis* sp	0.04-0.86	0.99
	Sphingopyxis sp	0.02-0.25	1.00
	Paracoccus sp	0.007-0.28	1.00

Table 4 SM Results of correlation between bacteria and voltage, current, and power generation in MFCs.

		MFC											
	Inoculum	control10d	control20d	control30d	rGO10d	rGO20d	rGO30d	rGOFe34-10d	rGOFe34-20d	rGOFe34-30d	rGOFe68-10d	rGOFe68-20d	rGOFe68-30d
ko00010	2.232556	2.387188	2.605982	2.611082	2.195035	2.764387	2.780813	2.5212	2.652286	2.29864	2.037634	2.818132	2.751043
ko00020	2.392526	2.226022	2.151763	2.184411	2.340217	2.410131	2.506591	2.024124	2.139509	1.80919	2.324303	2.431631	2.441796
ko00030	1.583182	1.608588	1.734343	1.746368	1.552451	1.670235	1.583013	1.708629	1.752219	1.635471	1.491153	1.658493	1.652147
ko00051	0.910303	0.990704	1.043154	1.033053	0.869874	1.04993	1.064192	1.032252	1.049484	0.980507	0.818278	1.077143	1.037522
ko00190	2.293731	1.986314	1.711314	1.713939	1.835229	1.723136	1.599361	1.809037	1.589038	2.102028	1.700744	1.565999	1.688265
ko00230	5.061129	4.736884	4.866443	5.000143	4.970607	4.847129	4.666195	4.713232	4.883796	4.450278	4.808408	4.772401	4.768109
ko00240	4.703223	4.245371	4.193186	4.299925	4.657223	4.122568	4.067234	4.114926	4.175558	4.045748	4.668264	4.076862	4.096048
ko00250	1.910844	1.838594	1.769325	1.795462	1.789063	1.750596	1.666472	1.793759	1.739713	1.863567	1.698287	1.68114	1.713861
ko00260	1.784264	1.610348	1.509211	1.523719	1.592379	1.49489	1.469809	1.522492	1.472529	1.584254	1.554565	1.461196	1.493348
ko00270	1.728597	1.66638	1.445574	1.449804	1.635587	1.583573	1.744523	1.461268	1.392808	1.546007	1.652981	1.618435	1.614127
ko00290	1.740006	1.694957	1.618788	1.616379	1.834329	1.65062	1.661433	1.60624	1.617824	1.603544	1.939994	1.635438	1.679304
ko00300	1.037965	1.027596	0.950893	0.947923	1.143136	1.017833	1.009495	0.924896	0.959107	0.830346	1.184007	0.98771	1.010026
ko00330	2.151464	2.222464	2.204178	2.195743	2.178639	2.181529	2.05439	2.271037	2.203178	2.369147	2.135403	2.088929	2.14314
ko00340	1.048095	1.066362	1.051886	1.054856	1.086812	1.055755	1.102295	1.042936	1.060401	1.00728	1.092403	1.083604	1.047706
ko00400	1.885322	1.974291	1.87609	1.881141	2.095439	1.959822	1.8608	1.903357	1.897095	1.890506	2.091002	1.850893	1.903618
ko00500	0.474502	0.919353	1.168758	1.14677	0.53045	0.82323	0.71278	1.126908	1.234342	0.889601	0.428236	0.909294	0.759981
ko00520	1.703566	1.81159	1.871783	1.862006	1.710685	1.739303	1.640168	1.822821	1.889741	1.623055	1.690959	1.739561	1.712163
ko00620	2.413771	2.335651	2.421458	2.434038	2.349797	2.626965	2.672648	2.3512	2.436527	2.233398	2.280247	2.646815	2.646354
ko00630	1.333219	1.414125	1.471562	1.468508	1.173806	1.196506	1.163384	1.422569	1.471848	1.295517	1.133571	1.271176	1.182931
ko00633	0.56597	0.565073	0.652748	0.659319	0.623038	0.883976	0.997081	0.624865	0.67636	0.577861	0.597522	0.926909	0.910972
ko00640	1.346103	1.205392	1.259292	1.293973	1.198753	1.466359	1.512092	1.16684	1.257923	1.012656	1.068003	1.483503	1.470061
ko00650	1.294862	1.299552	1.246459	1.250526	1.2644	1.401452	1.501398	1.214841	1.232421	1.17734	1.245393	1.434944	1.424709
ko00660	1.503566	1.38139	1.336699	1.349616	1.530911	1.37625	1.391144	1.297954	1.330274	1.270186	1.617158	1.371627	1.41181
ko00680	7.071801	7.75394	8.513704	8.380261	8.702532	8.5138	8.734905	8.720353	8.849028	9.008867	9.394292	8.682503	8.641675
ko00710	0.880699	0.970628	1.101401	1.106538	0.84004	1.154899	1.140153	1.074948	1.121729	1.012213	0.750986	1.172153	1.144316
ko00720	2.762726	2.701542	2.80284	2.820006	2.780201	3.277465	3.543005	2.745625	2.822227	2.72052	2.728442	3.37017	3.338511
ko00730	1.05075	1.074377	1.168114	1.181551	1.128219	1.160368	1.074763	1.121156	1.196455	1.004785	1.12107	1.133387	1.14581
ko00740	0.83408	0.771446	0.883476	0.902554	0.882733	0.859487	0.843561	0.830688	0.913761	0.688611	0.88307	0.88107	0.846611
ko00760	1.008311	0.948081	0.853679	0.855538	0.979629	0.980267	1.049442	0.858928	0.826912	0.903015	0.99472	0.979753	1.004663
ko00770	1.187264	1.241386	1.141511	1.123909	1.243439	1.109844	1.107458	1.183874	1.125782	1.265751	1.293933	1.088093	1.115462
ko00790	0.972511	0.933474	0.9794	0.996978	0.819336	0.947457	0.857696	0.955788	0.967124	0.928291	0.727967	0.916367	0.931408
ko00860	2.408361	2.847613	2.741401	2.668568	2.857165	2.732172	2.723289	2.780066	2.786786	2.736428	3.052701	2.716661	2.745544
ko00900	1.150824	1.075613	1.073508	1.099401	1.066237	1.011413	0.961313	1.05261	1.061658	1.018698	1.010368	0.994171	0.988029
ko01200	9.144091	9.659316	10.32422	10.2656	9.712252	10.16014	10.36487	10.4267	10.50601	10.62882	9.884518	10.40329	10.22478
ko01210	2.997543	2.940762	2.77401	2.752639	3.169198	2.803736	2.792736	2.829523	2.766209	2.95948	3.338077	2.736792	2.831835
ko01230	9.893735	10.12375	9.863734	9.851161	10.32937	9.791262	9.623329	9.863922	9.910827	9.648699	10.44122	9.657019	9.698411

Table. 5 SM Results of KEGG analysis for metabolism pathways.
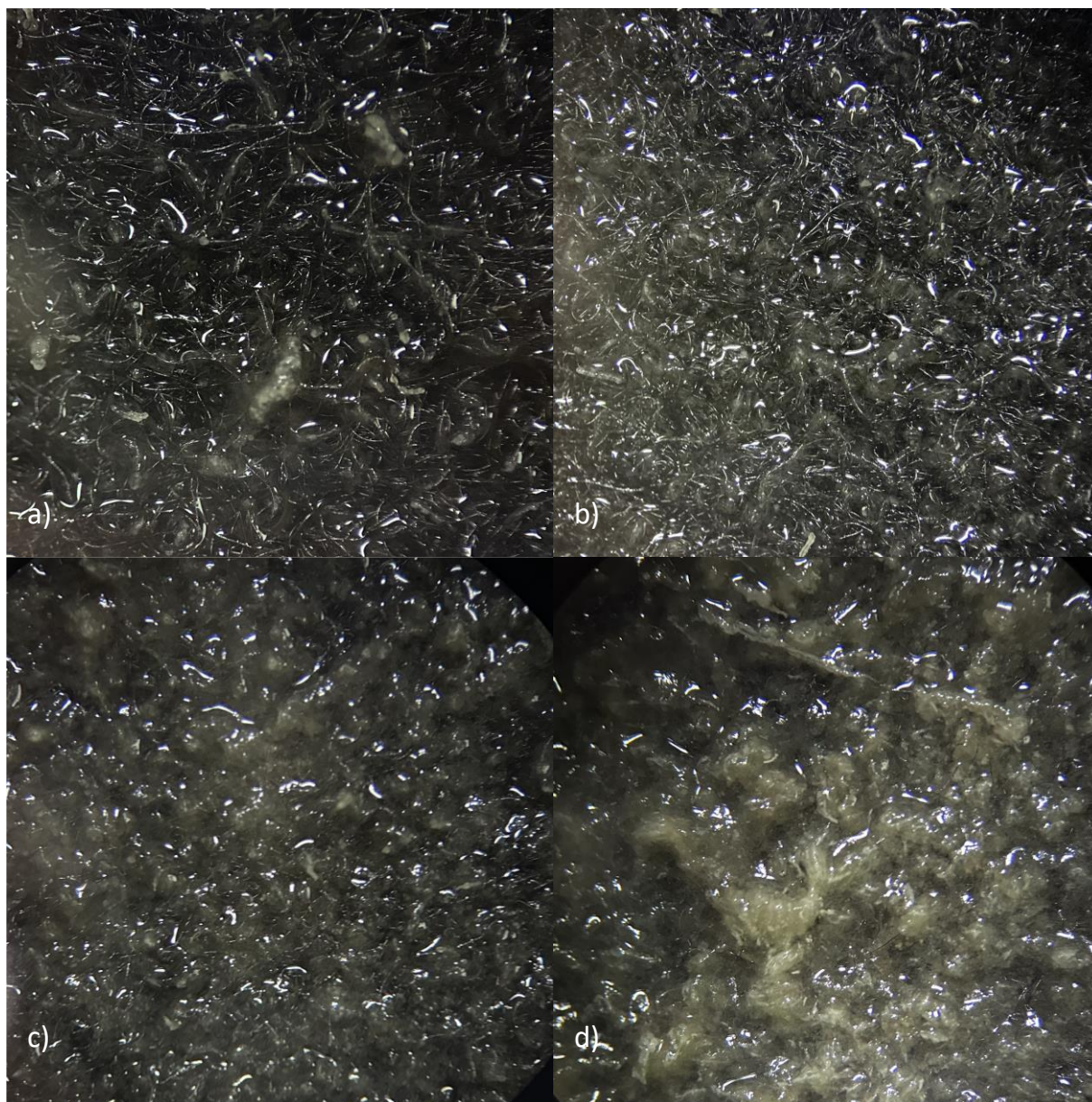
Fig. 5 SM Biofilm decomposition on the anodes of: a) unmodified CF, b) CF-rGO, c) CF-rGO-Fe34, d) CF-rGO-Fe68 (4x magnification).

References:

Chen X, Li Y, Yuan X, Li N, He W, Liu J (2020) Synergistic effect between poly (diallyldimethylammonium chloride) and reduced graphene oxide for high electrochemically active biofilm in microbial fuel cell. Electrochim Acta 359: 136949. https://doi.org/10.1016/j.electacta.2020.136949

Cheng Y, Mallavarapu M, Naidu R, Chen Z (2018) In situ fabrication of green reduced graphene-based biocompatible anode for efficient energy recycle. Chemosphere 193: 618-624. https://doi.org/10.1016/j.chemosphere.2017.11.057

Fu L, Wang H, Huang Q, Song TS, Xie J (2020) Modification of carbon felt anode with graphene/Fe_2O_3 composite for enhancing the performance of microbial fuel cell. Bioprocess Biosyst Eng 43: 373-381. https://doi.org/10.1007/s00449-019-02233-3

Geetanjali Rani R, Kumar S (2019) Enhanced performance of a single chamber microbial fuel cell using NiWO4/reduced graphene oxide coated carbon cloth anode. Fuel Cells 19(3): 299-308. https://doi.org/10.1002/fuce.201800120

Islam J, Chilkoor G, Jawaharraj K, Dhiman SS, Sani R, Gadhamshetty V (2020) Vitamin-C-enabled reduced graphene oxide chemistry for tuning biofilm phenotypes of methylotrophs on nickel electrodes in microbial fuel cells. Bioresour Technol 300: 122642. https://doi.org/10.1016/j.biortech.2019.122642

Ma J, Shi N, Jia J (2020) Fe_3O_4 nanospheres decorated reduced graphene oxide as anode to promote extracellular electron transfer efficiency and power density in microbial fuel cells. Electrochim Acta 362: 137126. https://doi.org/10.1016/j.electacta.2020.137126

Mehdinia A, Ziaei E, Jabbari A (2014) Facile microwave-assisted synthesized reduced graphene oxide/tin oxide nanocomposite and using as anode material of microbial fuel cell to improve power generation. Int J Hydrog Energy 39(20): 10724-10730. https://doi.org/10.1016/j.ijhydene.2014.05.008

Pareek A, Sravan JS, Mohan SV (2019) Exploring chemically reduced graphene oxide electrode for power generation in microbial fuel cell. Mater Sci Technol 2(3): 600-606. https://doi.org/10.1016/j.mset.2019.06.006

Zhang H, Da Z, Feng Y, Wang Y, Cai L, Cui H (2018) Enhancing the electricity generation and sludge reduction of sludge microbial fuel cell with graphene oxide and reduced graphene oxide. J Clean Prod 186: 104-112. https://doi.org/10.1016/j.jclepro.2018.02.159
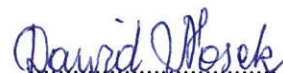
mgr inż. Dawid Nosek

(imię i nazwisko)

Przewodniczący Rady Naukowej Dyscypliny

prof. dr hab. inż. Marcin Dębowski

Uniwersytetu Warmińsko-Mazurskiego w Olsztynie

OŚWIADCZENIE

kandydata

Oświadczam, że w pracy pod tytułem:

Nosek D., Mikołajczyk T., Cydzik-Kwiatkowska A. (2024). Enhancing microbial fuel cell performance: anode modification with reduced graphene oxide and iron(III) for improved electricity generation. Clean Technology and Environmental Policy, doi.org/10.1007/s10098-024-02820-3, mój wkład merytoryczny w jej przygotowanie polegał na: zaplanowaniu koncepcji pracy, pozyskaniu, opracowaniu i interpretacji wyników technologicznych, graficznym opracowaniu wyników oraz przygotowaniu pierwszej wersji manuskryptu.

(podpis)

Olsztyn, 21.08.2024

(miejscowość, data)

dr inż. Tomasz Mikołajczyk

(imię i nazwisko)

Przewodniczący Rady Naukowej Dyscypliny

prof. dr hab. inż. Marcin Dębowski

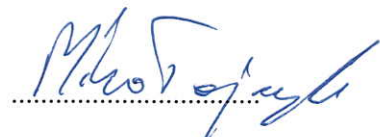**Uniwersytetu Warmińsko-Mazurskiego w Olsztynie**

OŚWIADCZENIE

współautora

Oświadczam, że w pracy pod tytułem:

Nosek D., Mikołajczyk T., Cydzik-Kwiatkowska A. (2024). Enhancing microbial fuel cell performance: anode modification with reduced graphene oxide and iron(III) for improved electricity generation. Clean Technology and Environmental Policy, doi.org/10.1007/s10098-024-02820-3, mój wkład merytoryczny w jej przygotowanie polegał na: przygotowaniu materiałów, analizie i graficznym opracowaniu części wyników i przygotowaniu pierwszej wersji manuskryptu.

Jednocześnie wyrażam zgodę na przedłożenie w/w pracy przez Pana Dawida Noska jako część rozprawy doktorskiej w formie spójnego tematycznie zbioru artykułów naukowych opublikowanych w czasopismach naukowych. Oświadczam, iż samodzielna i możliwa do wyodrębnienia część ww. pracy wykazuje indywidualny wkład kandydata Pana Dawida Noska polegający na:

udziale w zaplanowaniu koncepcji pracy, pozyskaniu, opracowaniu i interpretacji wyników technologicznych, graficznym opracowaniu wyników oraz przygotowaniu pierwszej wersji manuskryptu.

....

(podpis)

166:3549159989

prof. zw. dr hab. inż. Agnieszka Cydzik-Kwiatkowska

(imię i nazwisko)

Przewodniczący Rady Naukowej Dyscypliny

prof. dr hab. inż. Marcin Dębowski

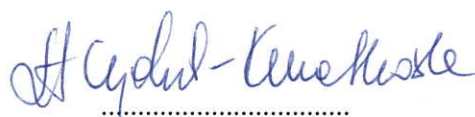**Uniwersytetu Warmińsko-Mazurskiego w Olsztynie**

OŚWIADCZENIE

współautora

Oświadczam, że w pracy pod tytułem:

Nosek D., Mikołajczyk T., Cydzik-Kwiatkowska A. (2024). Enhancing microbial fuel cell performance: anode modification with reduced graphene oxide and iron(III) for improved electricity generation. Clean Technology and Environmental Policy, doi.org/10.1007/s10098-024-02820-3, mój wkład merytoryczny w jej przygotowanie polegał na: przygotowaniu i edycji tekstu pierwszej wersji manuskryptu recenzowaniu i edycji tekstu, merytorycznym nadzorze pracy i pozyskaniu środków finansowych.

Jednocześnie wyrażam zgodę na przedłożenie w/w pracy przez Pana Dawida Noska jako część rozprawy doktorskiej w formie spójnego tematycznie zbioru artykułów naukowych opublikowanych w czasopismach naukowych. Oświadczam, iż samodzielna i możliwa do wyodrębnienia część ww. pracy wykazuje indywidualny wkład kandydata Pana Dawida Noska polegający na:

udziale w zaplanowaniu koncepcji pracy, pozyskaniu, opracowaniu i interpretacji wyników technologicznych, graficznym opracowaniu wyników oraz przygotowaniu pierwszej wersji manuskryptu.

....

(podpis)

167:1003642788